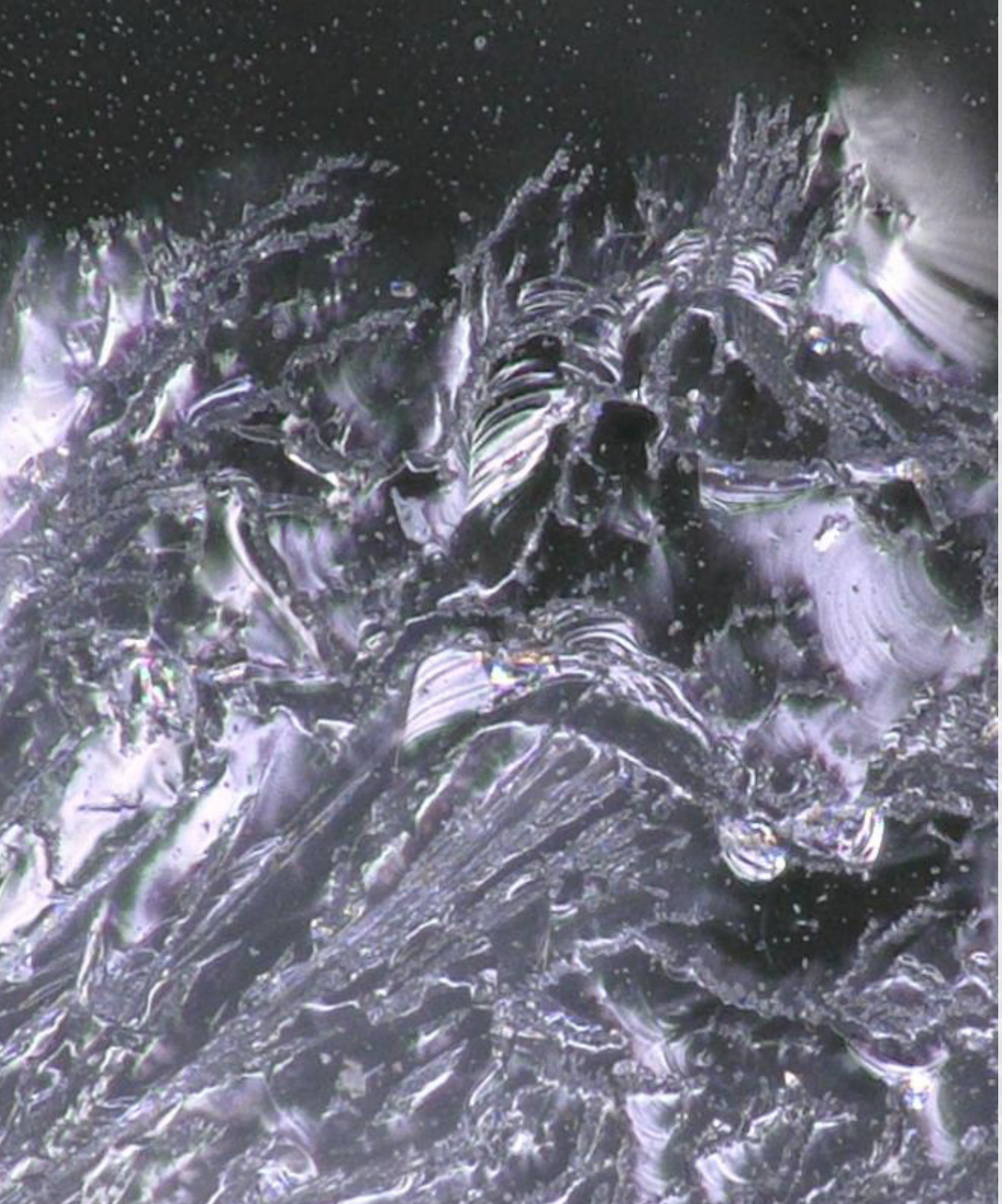

STRUCTURAL CAST GLASS-CERAMIC COMPONENTS

The potential of recycling soda-lime-silica glass into cast glass-ceramic components and its mechanical behaviour

MASTER'S THESIS

TU Delft

STRUCTURAL CAST GLASS-CERAMIC COMPONENTS

The potential of recycling soda-lime-silica glass into cast glass-ceramic components and its mechanical behaviour

by C.O.S. LEI

in partial fulfillment of the requirements for the degree of

Master of Science in Civil Engineering
at the Delft University of Technology

to be defended on Friday December 20th 2019 at 11:00am

Student number:	4290313	
Project duration:	March 2019- December 2019	
Thesis committee:	Prof. ir. R. Nijsse	TU Delft - Chairman
	Ir. T. Bristogianni	TU Delft - Supervisor
	Dr. ir. F.A. Veer	TU Delft
	Dr. ir. H.R. Schipper	TU Delft

TU Delft

Acknowledgement

This graduation research has been the final project of my specialization in Building Engineering of the Master program Civil Engineering of Delft University of Technology. I enjoyed the process of this research and am very glad to have done this research as a closure of my Master's program. More importantly, I am utmost grateful for the help, guidance and support I received throughout this period.

First of all, I would like to thank all the members of my graduation committee. Their patience, questions and knowledge have guided me through the process of this research in a subtle and smooth manner. Particularly my daily supervisor, who has been very caring and taught me all the necessities. Additionally, I am also very thankful for the exposure towards such interesting topics from the beginning of my Master's program. From the introductory tour to the glass lab in the first week of the Master's program to taking the course Structural Glass, their enthusiasm in the material glass had affected me deeply.

Other than my graduation committee, I would like to thank all the researchers that helped me in the lab or helped me performing certain analysis.

Lastly, I am very grateful for the support of friends and family. Especially to those who helped me collecting glass bottles for my melting experiments, those who gave me many tips and those who just blindly supported me.

Thank you.

Abstract

This master's graduation project researches the potential of upcycling waste glass into glass-ceramic components through casting techniques and thermal treatments.

To explore its potential and possibilities, the process of crystallization, the material glass-ceramic and influencing parameters are studied at first. A glass-ceramic is a glassy yet crystalline material consisting of inorganic and non-metallic compounds. A glass-ceramic can be produced through different controlled crystallization methods, whereas in this research heat treatment of casted components is applied. Upon heat treatment, crystallization occurs when the right temperatures are applied for the two-steps in crystallization; nucleation and crystal growth. Crystallization may occur spontaneously or along preferential sites, whereas this research makes use of the latter. Many parameters affect the crystallization process, whereas this research only focusses on glass composition, temperature and dwell time.

The parameters are set through literature study and trial and error of melting experiments. This research focusses on the crystallization of soda-lime-silica bottle glass, the results of each melting experiment show the effect of the parameters. Each glass from another manufacturing has another glass composition. The amounts of glass formers, modifiers and fluxes are various, resulting in diverse temperature curves and thus diverse melting temperatures and crystallization temperatures. Through the melting experiments are noticeable that the applied melting temperature were of bigger influence than the crystallization temperature. A melting temperature too low resulted in an undesired fused sample, while a too high melting temperature resulted in no or little preferential sites for crystallization to occur.
Through the results of the splitting experiment the mechanical characteristics could be observed, which are fracture toughness and fracture behaviour in this research. The fracture toughness seems better of samples with a higher quality crystal polymorph or with a higher amount of crystallinity or high amounts of glassy phases, whereby the material acts as one material upon loading rather than as a composite. While for samples with little and unconnected crystallization it does not seem to benefit its fracture toughness. The fracture propagation through glassy and crystalline phases is very different. A fracture propagation through a glassy phase is conchoidal, while the fracture propagation in the crystalline phase follows the crystalline structure, reaching its extremities or can be conchoidal, depending on the crystal polymorph. Observable from the fracture propagation from glassy to crystalline and from crystalline back to glassy is the discontinuity. The crystal or crystalline surface acts like an obstacle once the failure propagation reaches from the glassy phase. The failure does propagate but once it continues over to the glassy phase again, a change in energy and direction is noticeable.

All by all, there do is potential in upcycling waste glass into structural cast glass-ceramic components. Crystallization does influence the fracture toughness and fracture behaviour in a cast glass-ceramic component, but the effect is highly dependent on the amount and distribution of glassy and crystalline phases.

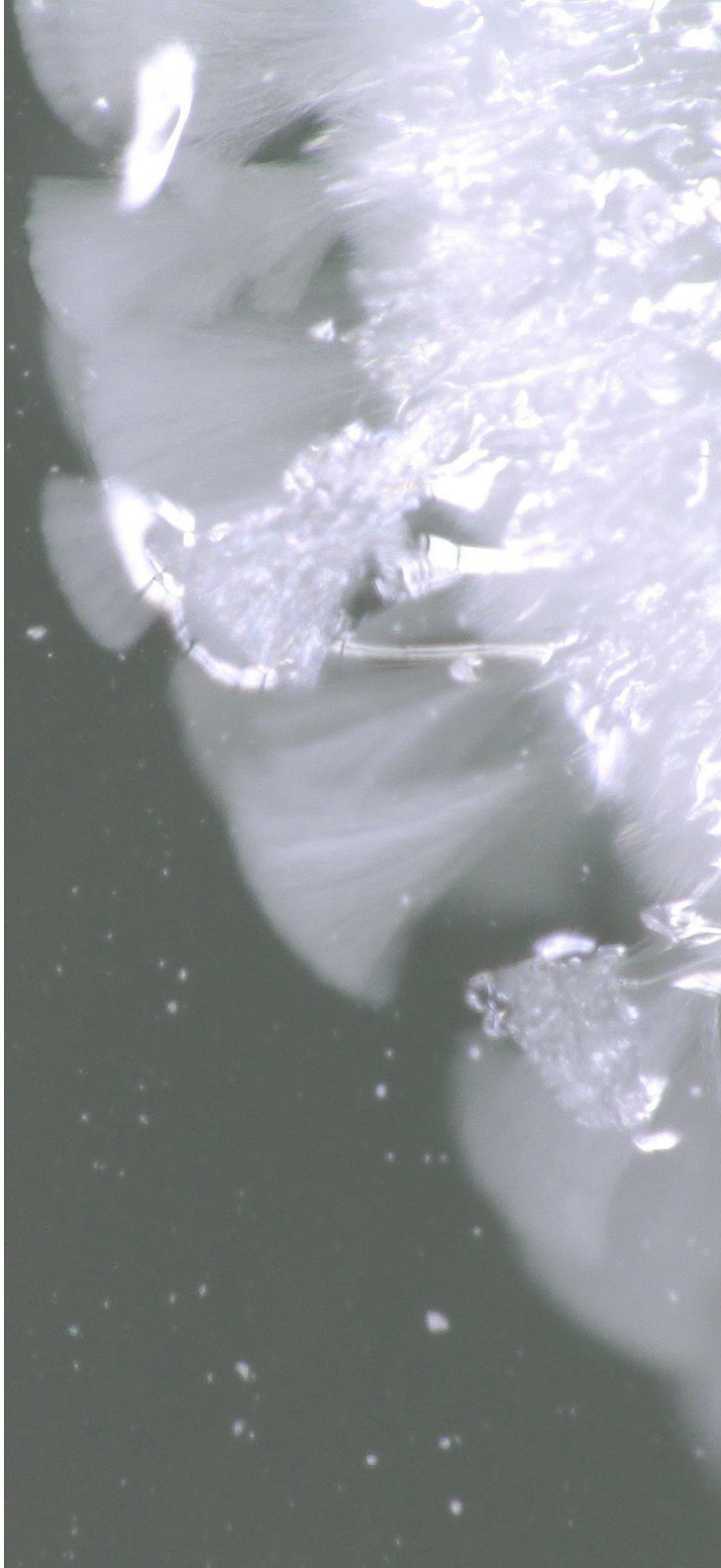

Table of Contents

PART III - LABORATORY TEST

PART IV - FINAL REMARKS

PART V - APPENDIX

Table of Figures

PART I - INTRODUCTION

PART II - LITERATURE STUDY

PART III - LABORATORY TEST

PART V - APPENDIX

Table of Tables

PART II - LITERATURE STUDY

PART III - LABORATORY TEST

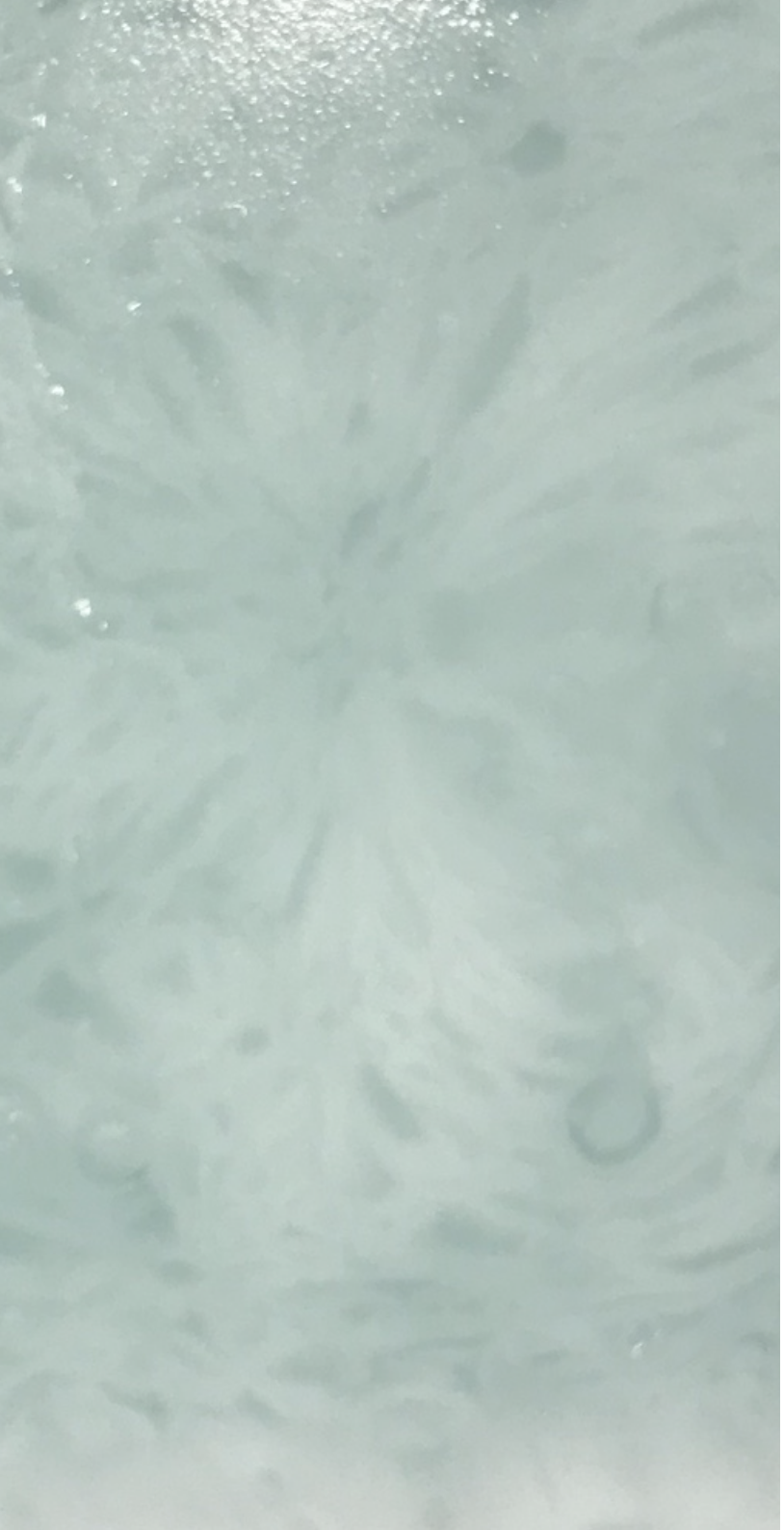

PART I - INTRODUCTION

Chapter 1 Introduction

1.1. Problem background

Glass is a widely used material, nowadays it can be found merely everywhere, thinking of glazing in the building industry, as packaging material in the food and beverage industry, as glassware in laboratories, as screens in the automotive and electronic industry or as a thin fine glass fibres with various of uses, for example as thermal building insulation or fibre reinforcing material and many more applications.

Yet, the lifespan of certain glass products ends at its initial purpose. The Netherlands have got recycle systems for packaging (food and beverage) glass and flat glass. Since roughly 40 years ago, households are able to recycle packaging glass through glasbakken (glass collecting containers) which are located at 15.000 locations through the country [40]. Recycling of packaging glass is a common phenomenon in the Netherlands, it is close to recycling all produced packaging glass, but still not 100%. The Afvalfonds Verpakkingen has set its goal for recycling packaging glass at 90% for 2018, which was 86% in 2017 compared to 84% in 2016 [02].

In 2002 the Stichting Vlakglas Recycling Nederland was established. The Stichting Vlakglas Recycling Nederland created a countrywide network of collection points for flat glass. Flat glass to be collected includes mirrors, window glazing (including insulated glazing), interior glass partitions, table glass, aquarium glass, etc. Small amounts of glass could be collected at glass companies, construction sites and milieustraten (Dutch naming of waste collection centers), while large amounts could be collected at certain storage/ transfer locations. The collected glass is transported from those collecting points to glass recyclers [48]. According to numbers from Vlakglas Recycling Nederland, about 80% of the flat glass waste is being collected, 10% goes directly from production waste to the flat glass plants and the last 10% is not collected separately and recycled [47].

Not all glass types can be recycled or be accepted for glass recycling collection. For both flat glass and packaging glass the glass may be contaminated till a certain acceptance level to be accepted by the glass recycler [24][25]. Resulting in a certain amount of waste glass unable to be recycled due to its level of contamination. Some glass types are not recyclable and are thrown away as general waste. Glass that cannot be collected and recycled include [06][12][42]:

- Crystal glass: contains lead oxide which is not permitted in glass packaging
- Ovenproof/ laboratory/ borosilicate glass: have a higher melting temperature than regular glass
- Opal glass (white): contains fluor

Another product consisting of glass, which have to be collected as chemical waste and cannot be used for recycling is:

- Light bulbs and fluorescent tubes: contain other materials apart from glass and contains hazardous substances (energy saving light bulbs and fluorescent tubes)

All by all, other than packaging glass and flat glass, many variants of glass products are ending up as general waste. From the numbers mentioned before can be concluded that a relatively high amount of packaging glass and flat glass is being collected and recycled. Waste glass passes waste glass collectors as waste glass, glass recyclers as raw material and glass producers as new product. Yet, still a small percentage is not being collected and/or recycled. Therefore, it is suggested to find a solution to increase the recyclability of different glass types or to find a way that contaminated glass can still be recycled in order to limit waste and to be considerate with the finite raw materials and energy consumptions. Whereas this research is a follow up of the paper “Structural cast glass components manufactured from waste glass: Diverting everyday discarded glass from the landfill to the building industry” by Bristogianni et al. 2018 [01].

1.2. State-of-the-art glass recycling

1.2.1. Glass recycling

Besides recycling collected glass into the same products as flat glass and packaging glass or letting collected glass end up as landfill, there are more recycling methods for glass created nowadays. Different companies have started creating new products from waste glass by mixing waste glass with other materials.

For example, 'Greenstone', a product created by the American company Realm of Design, that designs and creates architectural details. The Greenstone is a mixture of fly ash, recycled glass and some other renewable components. By recycling the glass and fly ash through this method, the materials are upcycled into the Greenstone. According to the creators of Greenstone, it is possible to replace standard concrete with Greenstone in virtually any project. Discarded alcohol bottles form the Las Vegas Strip has been used for the Greenstone for the construction of the Morrow Royal Pavilion in Las Vegas in 2012 [35].

Figure I.1 - end of life possibilities of waste glass

Similar to the Realm of Design, the African construction and brick manufacturing company Byiza Vuba Ltd. uses collected glass waste as a component for bricks, by partially replacing cement by crushed waste glass for the manufacturing of concrete [11].

Another example is the use of crushed glass, which would usually end up as dust for landfill, has found a new recycling path as wallboards. A British company, C2M created the material recycled glass hybrid (RGH), which can be combined with other another landfill regular, recycled plastic, to form new building components as wallboards. Those wallboards can be a eco-friendlier alternative to gypsum-based boards [05].

Therefore, besides recycling glass, it is also possible to upcycle glass into new building materials.

1.2.2. Glass-ceramics

A possible solution for re-using glass to make another product of 'glass' is to upcycle glass into glass-ceramics. Glass-ceramics have proven to have better thermal and mechanical properties [53]. Currently, glass-ceramics are only to be found in the building industry as different types of interior and exterior cladding.

The product Neopariés created by the Japanese Glass manufacturer Nippon Electric Glass is a crystallized glass material with a marble like appearance. Its appearance and enhanced material properties makes it an alternative to natural stone [41].

The German company Magna Glaskeramik manufactures similar glass-ceramic panels from glass waste, which are also 100% recycle at the end of its life cycle [23].

Nevertheless, from the fact that glass waste can already be used for the creation of glass-ceramic panels, there is expected to be a possibility of using glass waste to create different glass-ceramic products.

1.3. Research goal

Based on the aforementioned examples about turning glass into a different building material, it shows that glass indeed can be reused in diverse ways and even in ways where the glass does not have to be totally uncontaminated. Nevertheless, it will be still interesting and challenging to find an option to recycle glass in a manner whereby glass will be the main component of the new product and without losing its value. Therefore, an option to recycle different types of glass is to recycle it into cast glass components or even a step further, cast glass-ceramic components.

For cast glass the purity of the melt does not have to be as high as for flat glass or packaging glass, since the thickness of the component is higher, whereas the impurity over the thickness ratio is of lower impact compared to flat glass or packaging glass [01]. Previous studies have already shown that crystallization of glass results in a glass-ceramic material. Thereby, glass-ceramic components have proven to have enhanced mechanical and thermal properties compared to its parent glass [41][51]. Which is an attractive solution for structural building components. In addition, using waste glass to create glass-ceramics will be a more economic and sustainable solution than its conventional production. According to those theoretical advantages, cast glass-ceramic components are to be studied in this research.

Based on all above, this research focusses on the potential of structural cast glass-ceramic components, with the aim to create new possibilities for waste glass. The research will start with understanding the phenomenon crystallization and the materials glass and glass-ceramics, whereupon cast glass-ceramic components will be created and tested.

1.4. Problem definition

The research goal leads to the following main question, which will be answered through the sub questions:

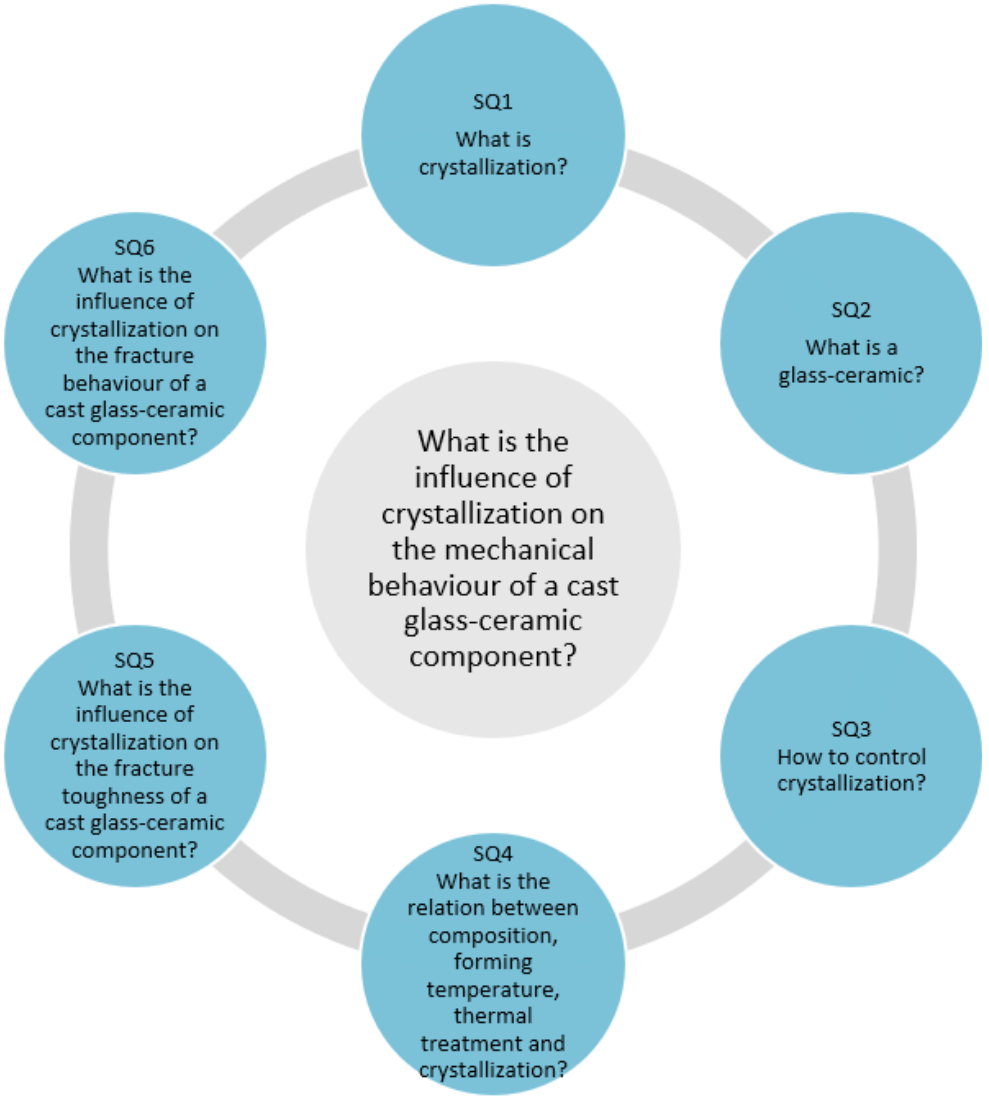

Figure I.2 - main research questions and sub questions (SQ)

1.5. Research methodology

The research is split into two parts, Part II - Literature study and Part III - Laboratory tests. The obtained knowledge from Part II functions as a base for the following experimental research in Part III.

The research methodology for Part II – Literature study is straightforwardly consulting and reviewing papers, documents and books about crystallization, glass-ceramics and relevant parameters in order to answer sub-question 1 to 3.

Part III – Laboratory tests consists of different experiments and is used to answer sub-question 4 to 6. Throughout trial and errors of melting experiments glass-ceramic samples have to be created and parameters have to be comprehended (SQ4). Selected parameters to be understood:

- glass type — what glass type should be used and crystallizes easily?
- glass size — what glass size is favourable for crystallization?
- temperatures — at what temperature does the glass melt and crystallize?
- dwell time — how long should glass dwell at a certain temperature (melting and crystallization)?

In addition, material tests as XRD and XRF analysis are performed to better understand the results of the melting experiments.
The splitting experiment is to test the fracture toughness (SQ5) of the glass-ceramic samples, which will thereupon be studied under the microscope to understand its fracture behaviour (SQ6).

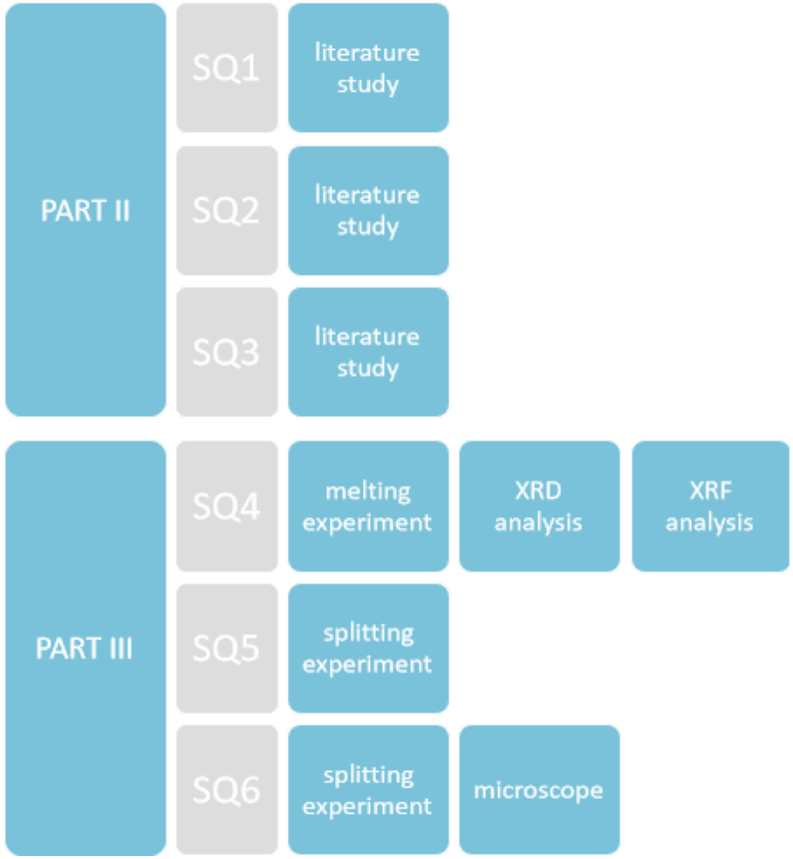

Figure I.3 - schematic overview of the research methodology

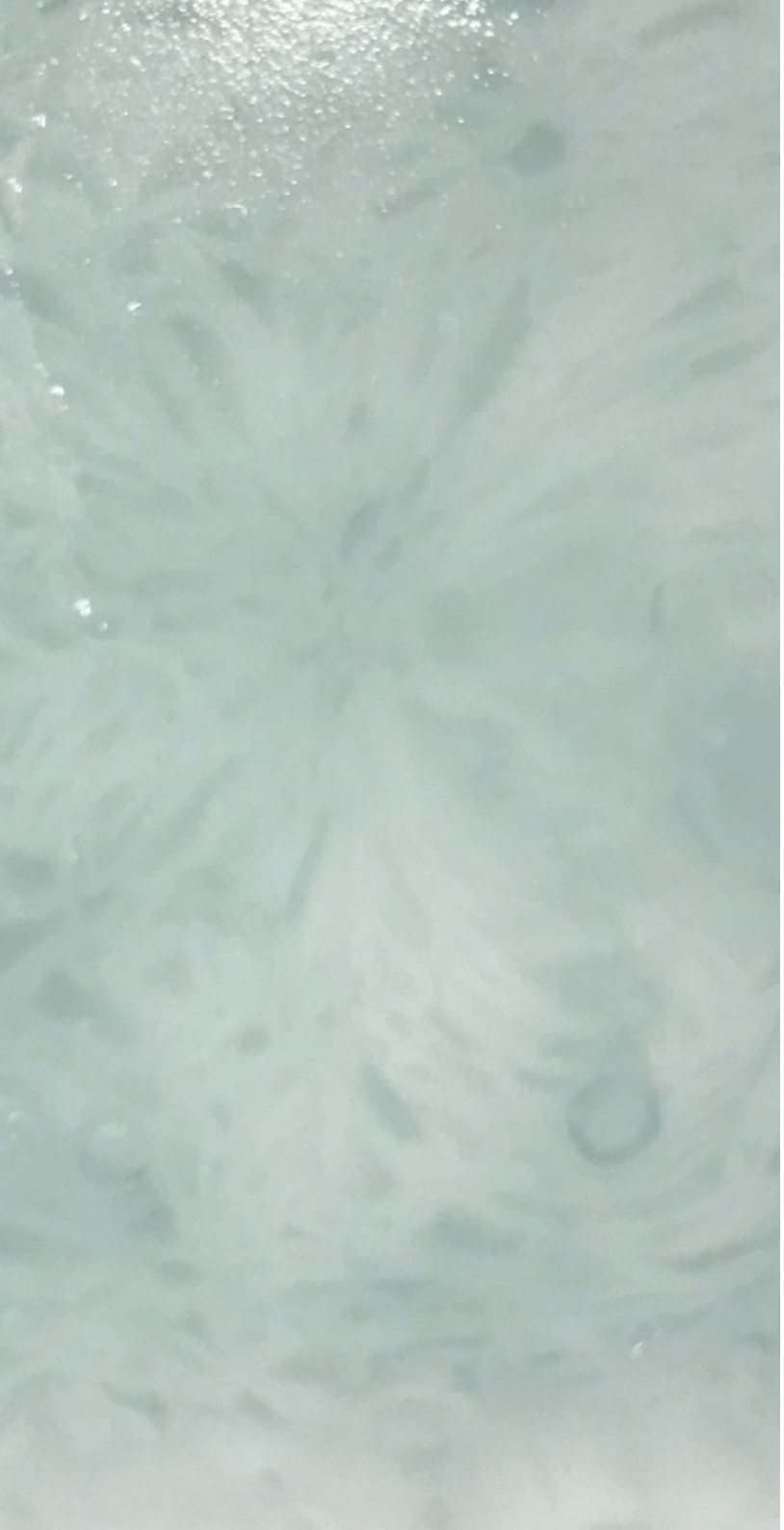

PART II - LITERATURE STUDY

Chapter 2 Glass-ceramics

2.1. Glass

2.1.1. Glass - the definition

The most common glass forming mechanism is through melting crystalline materials, the melted materials become a viscous fluid melt. This viscous melt cools down into a super-cooled liquid, and thereupon glass forms, Figure II.1. [49]

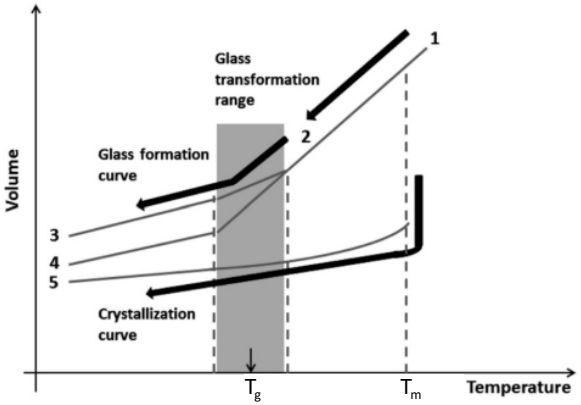

Figure II.1 - glass transformation graph [07]
1: liquid
2: supercooled liquid
3: glass on fast cooling
4: glass on slow cooling
5: crystal

Theoretically, glass can be obtained from any material, whereby no specific component or molecule compound is a prerequisite to form a glass. Using a melting procedure is a common but not a technical requirement to produce glass. For example, sol-gel, a process to obtain glassy or crystalline materials, which is formed by vapor deposition instead of melting. Thereby, glasses nowadays can be of organic, inorganic, non-metallic and metallic components, given an even wider range of possibilities to form a glass. [39]

Thus, glass can be obtained from any material and through diverse methods, as long as factors such as viscosity, temperature and cooling rate are in favour to form a glass. Since most commercial glasses are silica based and recycling waste glass is a priority of this research, therefore, transforming silica-based glass into glass-ceramics through casting will be the main focus of this research.

To define a material as a glass, two common characteristics have to be met. [39]

- The material should not consist of long range, periodic atomic arrangement.
  Resulting the glass to be a network of irregular atomic arrangements and therefor being an amorphous material.
- The material should consist of a time-dependent glass formation behaviour.
  This behaviour is dependent on the temperature curve, see Figure II.1 for the enthalpy-temperature diagram.

Concluding that glass can be formed from any material; inorganic, organic, metallic and non-metallic and by any glass transformation technique as long as it results in an amorphous solid with no long range, periodic atomic structure and it consists of a glass transformation region.

Even if it is theoretically possible to obtain glass from any material and through diverse techniques, (most) inorganic glasses (including soda-lime-silica glasses) do have a similarity. Those are the use of ceramic materials, and thus materials consisting of metallic and non-metallic elements (mainly oxygen).

Other relevant characteristics of silicate glasses are:

- Transparent [44]

  Electrons in glass are limited to certain energy levels, resulting in the restriction of the ability to absorb and reemit photons. Whereas light can pass through glass instead of being mainly reflected or absorbed, giving it its transparency.
- Strong [07][44]

  Glass is well known for its strength; its theoretical strength is estimated to be 14 to 35 gigapascals. The strength of commercial glasses on the other hand, are generally between 14 to 175 megapascals. The decrease of strength is the effect of imperfections such as flaws and scratches, which result in stress concentrations and thus weak spots.
- Hardness [21]

  Glass has a hardness of 5,4 to 6,6 on Mohs hardness scale.

2.1.2. Glass composition

According to Le Bourhis [21], glass forming is complex, yet, a few factors are in favour to the glass formation ability, which are:

- High viscosity
  Low movement rates of ions and atoms, hence small rearrangement rates and thus low crystallization rates.
- Avoid heterogenous nucleation
  The absence of impurities is till a certain degree controllable, removing impurities decreases the occurrence of heterogeneous nucleation.
- Systems with three or more elements of different atomic size, with a large crystal-liquid interfacial energy.
- Systems with large concentration change between liquid and crystal phase.

These factors can be obtained through the selection of the right compounds for a desirable glass composition. The composition of forming commercial oxide glasses are mainly the same. The batch materials can be distinguished into five categories; glass former, flux, property modifier, colorant and fining agent. [44]

- Glass formers
  Glass formers are network formers or so-called glass forming oxides, which function as the base of glass. The most common glass formers in commercial glasses are silica (SiO_2), boric oxide (B_2O_3) and phosphoric oxide (P_2O_5). Other possible glass formers for oxide glasses are molecule groups as GeO_2, Bi_2O_3, As_2O_3, Sb_2O_3, TeO_2, Al_2O_3, V_2O_5. [39]

- Fluxes
  Fluxes are used to decrease the processing temperature of the batch by decreasing its viscosity. The viscosity decreases through the breakage of bonds between atoms in the glassy network, Figure II.2. For example, if no flux was used in a silica-based batch, melting temperatures go up above 2000°C, while by adding a flux the melting temperature can be below 1600°C or even dropping to 800°C, depending on the amount of flux added. The most common fluxes in glass are alkali oxides as soda (Na_2O), lead (PbO) and potassium oxides (K_2O). A drawback of adding a flux is the degradation of properties, such as chemical durability and the viscosity. [21][27]

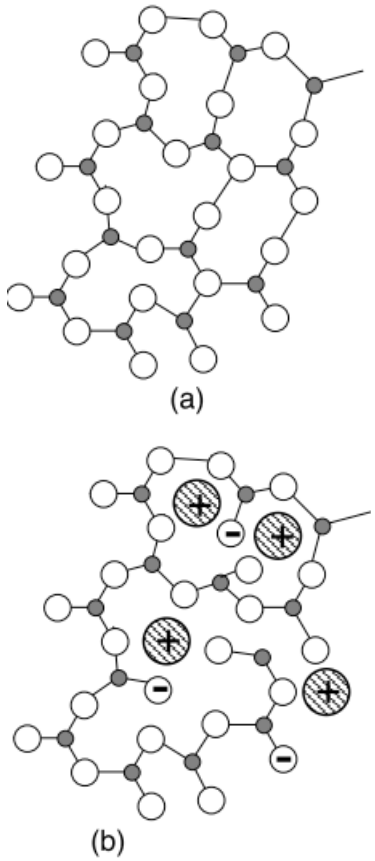

Figure II.2 - network of glass before (a) and after (b) adding a flux [27]

- Property modifiers

  Property modifiers can decrease the processing temperature and enhance other properties of the final glass. Yet it is used in smaller quantities than fluxes, it is used in controlled amounts to obtain the desired glass properties rather than aiming to lower the processing temperature. Possible property modifiers are alkaline earth oxides (as CaO, MgO), transition metal oxides and aluminium oxide. [21] The addition of molecule compounds as CaO and MgO reduces the solubility caused by soda in soda-lime-silica glass and enhances its hardness and chemical durability. As CaO and MgO, Al_2O_3 also enhances the chemical durability of glass. [07] Some molecule groups can show both behaviours, that of network former as well as property modifier, such as Al_2O_3 and other oxides (Ti, Zr, Be, Mg and Zn). [21][27]

- Colourants and decolourants

  Colourants and decolourants are used to control the desired colour of the final product. By adding ions of transition metals, it is possible to change the colour of the glass. The ions allow electronic excitation possibilities to visible light, resulting in a different colour to be observed. Examples of such are ions are Cr^{2+} for blue, Cr^{3+} for green, Co^{2+} for pink, Mn^{2+} for orange and Fe^{2+} for blue-green. [27]

- Fining agents

  Fining agents are used to chemically enhance the removal of bubbles in the melt, generally only an amount of 0.1 to 1wt% is used in the melt. Examples of fining agents are arsenic and antimony oxides, potassium and sodium nitrates, sodium chloride, or some fluorides and sulphates. Those fining agents result in a large amount of gas forming, creating large bubbles which rapidly rise to the surface. [39]

According to the patent of soda-lime-silica glass the composition of soda-lime-silica glass is generally as Table II.1.

Compound	Weight percentage	Preferable weight percentage	Category
SiO_2	68-75%	70-73,5%	Glass former
Al_2O_3	0-4%	0-3%	Glass former Property modifier
Na_2O	6-12,4%	9-12,2%	Flux
K_2O	0-3%	0-2%	Flux
CaO	10,2-17%	10,6-15%	Property modifer
MgO	0-5,5%	1-5%	Property modifer
Fe_2O_3	0-2%	-	Colorant
SO_3	0-0,5%	-	Fining agent

Table II.1 - soda-lime-silica glass composition and category of compound [02]

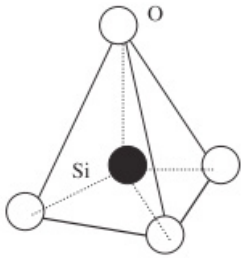

Figure II.3 - silicon- oxygen tetrahedron [21]

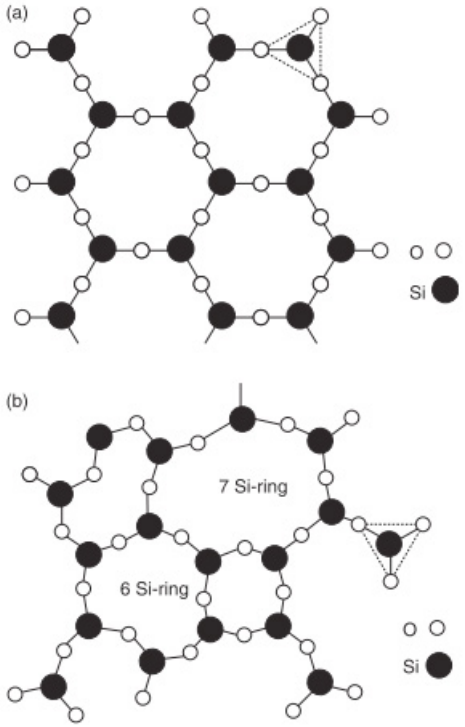

Figure II.4 - from crystalline to glassy structure [21]

2.1.3. Glass structure

Throughout the last century many theories for glass structures were defined. Such as comparing the structure of glass with that of fluids by Tammann. Through the high viscosity of the melt the structure of the fluid melt retains and remains fixed, resulting in the by Tammann's defined undercooled liquid. [49]

Another theory, by Goldschmidt, concluded that simple compounds easily solidify after fusion as a glass, but depending on the ratio of the sizes of its ions, whereby the ratio of the radii between the cations and anions of the principal glass formers have to be between 0,2 and 0,4. [49]

The random network theory by Zachariasen, was originally only based on property data, such as glass formation behaviour. The theory was later reinforced by Warren's X-ray investigations, which conclude that the glass is build-up of a network that consist of smaller building components, whereby tetrahedrons (e.g. SiO4) are the smallest building component, Figure II.3. [39] [49]

The structure of the base material quartz/sand for silica-based glasses consists a crystalline, well-ordered structure, Figure II.4a. To obtain a glass, the tetrahedra SiO_4 of the quartz/sand are broken upon the melting process. The crystal matrix breaks and strings and rings of tetrahedra in irregular patterns are formed, Figure II.4b. Through the high temperature the strings and rings will continue with degrouping and reforming, resulting in fluidity of the mass. Normally if the temperature of the melt gets below melting temperature the liquid transforms into a crystalline structure. However, if the liquid cools down without the formation of crystals, a supercooled liquid is formed. Thus, during cooling the SiO_2 will form groups again, resulting in a more viscous matter, allowing the glass to be shaped. Cooling down the matter even further results in lower kinetic energy and thus larger groupings of tetrahedra. When the temperature drops below the glass transformation temperature, it loses its fluidity, the viscosity becomes large enough and therefore no internal configurations will be done, and the structure is fixed. [27][39]

A glass has, therefore, no fixed structure regardless of the glass composition. According to Shelby [39], there do are elements that make a structural model for glasses, however, despite the required elements and fact that glass does not have just one single structure, it is required and/or simplifying to use an idealized structure for discussing glasses. Therefore, the random network theory of Zachariasen can be used.

According to Zachariasen the following rules apply:

Zachariasen's rules for glass formation in simple oxides

1. *Each oxygen is linked to no more than two cations.*
2. *The oxygen coordination number of the network cation is small.*
3. *Oxygen polyhedra share only corners and not edges or faces.*
4. *At least 3 corners of each oxygen polyhedron must be shared in order to form a 3-dimensional network.*

Modified rules for complex glasses

5. *The sample must contain a high percentage of network cations which are surrounded by oxygen tetrahedra or triangles.*
6. *The tetrahedra or triangles share only corners with each other.*
7. *Some oxygens are linked only to two network cations and do not form further bonds with any other cations.*

Structural models for oxide glasses mainly are derived from the models of vitreous silica and alkali silicate glasses and so is soda-lime silicate glass. The network consists of atoms of silicon bonded to oxygen atoms through covalent bonding. Other variants of structural models are not taken into account in this report.

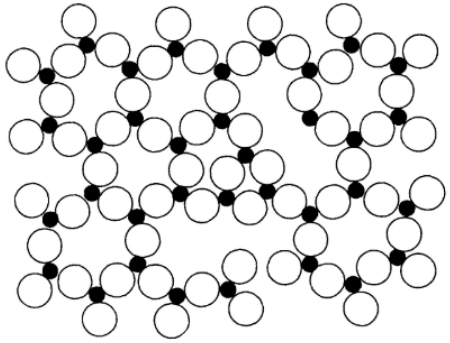

Figure II.5 - structural network of vitreous silica [39]

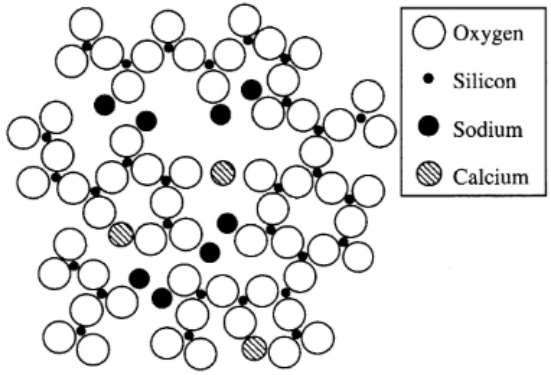

Figure II.6 - structural network of alkali (earth) silicate glass [39]

• Vitreous Silica

Vitreous silica is the purest form, made of only quartz sand and thus consisting of only silica. Figure II.5 shows a 2-dimensional structure of vitreous silica, a pure glass former. It consists of building blocks of silicon-oxygen tetrahedra (Figure II.3), each oxygen atom is bonded to two silicon atoms. Whereby each tetrahedron is linked at all four corners, creating a continuous 3-dimensional network. The disordered network is a result of diverse angles of Si-O-Si bonds connecting to an adjacent tetrahedron. In addition, rotational freedom of tetrahedra causes additional disorder. Besides, there are also regions with highly stressed bonds and defects. Such as Si-Si bonds through oxygen vacancies, Si-O-O-Si bonds through peroxy defects and defects caused by impurities, resulting in groups as SiOH and SiH.

• Alkali silicate glasses

Alkali silicate glasses consist of a large amount of alkali oxides, which is obtainable through melting silica with alkali carbonates or nitrates, giving a binary system. Thereby, glasses containing more than 10mol% of alkali oxides are easier to melt due to a lower viscosity. According to Shelby [39], the type of alkali oxide is of less importance, but depending on the amount of alkali oxide in the melt, the viscosity can reduce in many orders of magnitude and the glass transformation temperature can reduce up to circa 500°C. Also, the density, the refractive index, the electrical conductivity and the thermal expansion increases with an increased amount of alkali oxide. The enhancement of the material properties is due to the non-bridging oxygens. The alkali oxides cause bonds to break, whereby each non-bridging oxygen has an alkali ion in its surrounding to maintain local charge neutrality. Resulting in more broken chains compared to vitreous silica, see Figure II.6.

• Alkali/ Alkaline earth silicate glasses

A ternary glass containing alkaline earth oxides, alkali oxides and silica, primarily in the form of soda-lime-silica glasses. Soda-lime-silica glasses consists typically of 10-20mol% of alkali oxide (soda, Na_2O), 5-15mol% of alkaline earths (lime, CaO) and 70-75mol% of silica. Depending on the required properties of the final product small amounts of soda and lime can be replaced by other molecules. Small amounts of soda can also be replaced by other compounds such as K_2O and Li_2O. Lime can also be replaced by MgO, SrO and BaO. The 2-dimensional network of alkali earth silicate glasses is similar as alkali silicate glasses but including calcium ions.

2.2. Glass-ceramics

2.2.1. Glass-ceramics - the definition

Glass-ceramics are polycrystalline materials formed, among others, when glasses of suitable compositions are heat treated to a temperature range prone to crystallization.[08][21][34]

Even though glass is a material that tend to crystallize, it was not reported until the 1950's. The crystallization is hard to control, but the controllability do is required to produce glass-ceramic products. [21] Other than glass, which can be formed from organic, inorganic, metallic and non-metallic materials as mentioned in Chapter 2.1.1. The term glass-ceramics is only used for inorganic, non-metallic materials. Thereby, a glass-ceramic is a material with a combination of the properties of glass and a ceramic, it contains both glassy phases and crystalline phases. Originally, a glass-ceramic was defined if the crystalline phases account for 50 to 95vol%. [04]

However, in the past 60 years more glass-ceramic products were developed with lower amounts of crystalline phases, whereas the initial restraint does not specify the term glass-ceramic properly. Given the emerge of new restraints, according to Debeuner et al. [04]:

- a glass-ceramic is obtained by controlled crystallization of inorganic, non-metallic glasses;
- its microstructure consists of at least one functional crystal and one glassy fraction;
- a glass-ceramic is pore-free or it consists various levels of porosity, which can be engineered through adding additives;
- it is not mixed with other crystalline materials, such as ceramics, metals, semiconductors and polymers, if so, it is considered to be a composite rather than a glass-ceramic;
- it is not crystallized through only nucleating agents, since the desired functionality is typically not achievable through crystallization based on nucleating agents.

All by all, based on the original definition of Stookey and the new definition by Deubener et al., the following definition for a glass-ceramic arose [04]:
"Glass-ceramics are made by first melting and forming special glasses containing nucleating agents and then causing controlled crystallization of the glass". Whereby, *“Glass-ceramics are inorganic, non-metallic materials prepared by controlled crystallization of glasses via different processing methods. They contain at least one type of functional crystalline phase and a residual glass. The volume fraction crystallized may vary from ppm to almost 100vol%”.*

By comparing properties of glass with that of glass-ceramics, some advantages are created through crystallization. Mechanical properties as strength and toughness of controlled glass-ceramics are superior of that of the parent glass. [21]

The relevant properties:

- Transparency [38]

  Generally crystalline phases are used to be non-transparent. Yet transparent glass-ceramic products are nowadays available on the market.

- Strong [44]

  Glass-ceramics are well-known for their high strength characteristics. Since ceramics are generally stronger than glass, favourable glass-ceramics consist of a high strength capacity e.g. 100-200MPa bending strength and 500-1000MPa compressive strength for certain glass-ceramic products.

- Hardness [08]

  The hardness of glass-ceramic is theoretically superior compared of the hardness of its parent glass, whereas glass-ceramic should deform less compared to its parent glass. This can be the result of several factors, such as a reduction of defect size as a result of crystallization and reduction of glassy phases in the surface area together with the increase of crystalline phases in the surface area. However, the increase of hardness compared to its parent glass is not a linear relation. The hardness is dependent on the behaviour of particles of the residual glass, since the hardness is characterized through plasticity. Whereby the shear flow of the residual glass is significant, since the weakest phase in glass-ceramic is the residual glass. [08] As previous sub chapter showed, crystals are built of a discrete structure, which may cause deflection, branching or splintering of cracks according to Höland and Beall. The crystals may act as an obstruction of fracture propagation, whereas a finely crystallized glass may give a better structural reliability.

Each glass-ceramic product consists of different crystalline phases and crystal to glass ratio, which results in different properties. Hence, the properties and amounts of the crystalline phases are of major importance for determining the key properties of the resulting glass-ceramic.

2.2.2. *Crystalline silica structures*

Other than glass, where the glassy structure consists of short-ranged orders, creating a random and disordered network. Crystalline structures consist of more long-range orders which are repetitive and creating a periodical structure throughout the network.[21]

According to Höland and Beall crystalline structures of interest of silica-based glass-ceramics can be divided into six categories; nesosilicates, sorosilicates, cyclosilicates, inosilicates, phyllosilicates and tectosilicates, see Figure II.7.[08] [34]

Nesosilicates has the lowest polymerization and is therefore the least important mineral group within the glass-ceramics. It consists of isolated tetrahedra, with no sharing between the mineral groups and thus no solid nor strong structure. Whereas tectosilicates, the framework silicates, are the major mineral group in glass-ceramics. Those tectosilicates are high in SiO_2 and Al_2O_3, which are, as mentioned before (Chapter 2.1.2), main glass formers for oxide glasses.[08]

On the following page, Figure II.8 and Figure II.9, gives a glance of commercial glass-ceramic products and its crystalline phase and some examples of crystalline phases and its crystalline structure type.

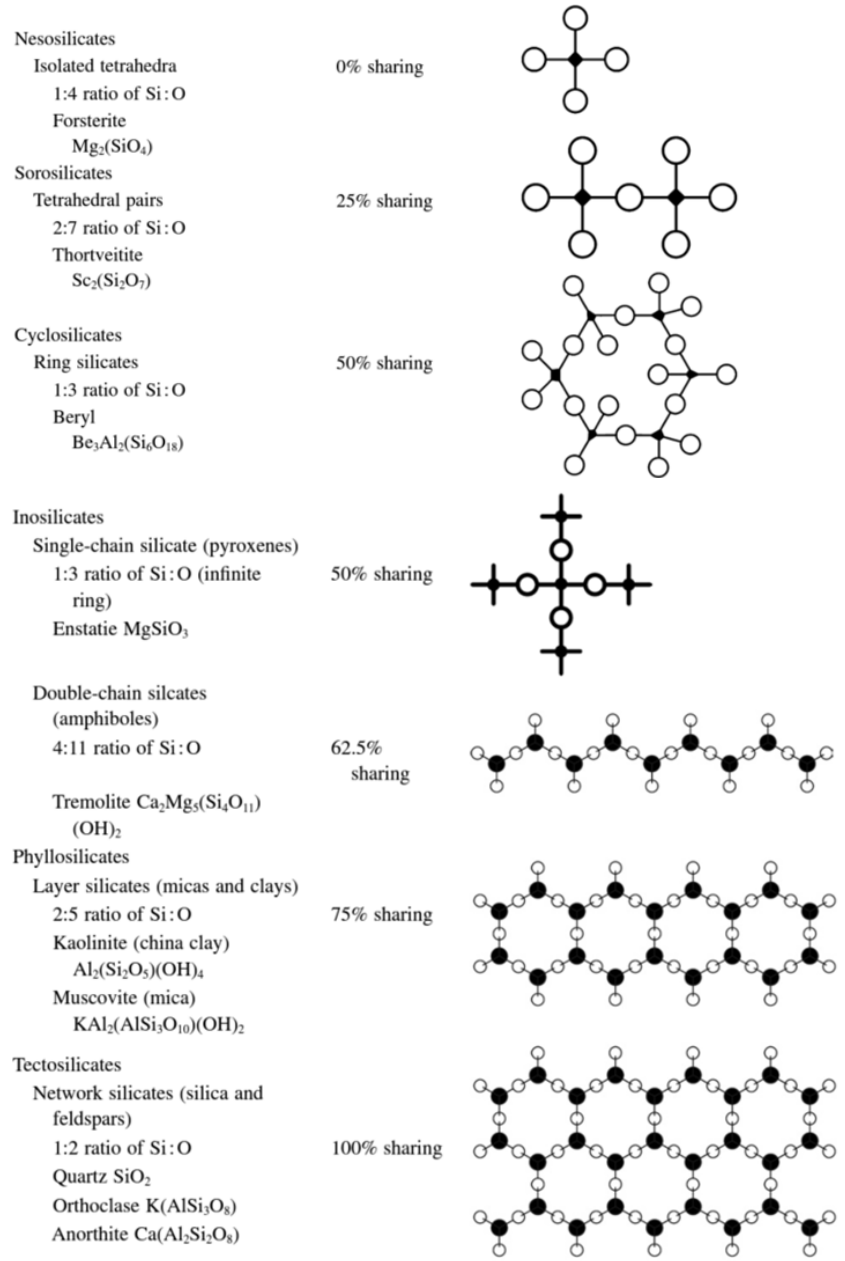

Figure II.7 - crystalline silicate structures [08]

Company	Products	Crystal type	Applications
SCHOTT, Germany	Foturan®	Lithium-silicate	Photosensitive and etched patterned materials
	Zerodur®	β-quartz ss	Telescope mirrors
	Ceran® / Robax®	β-quartz ss	Cookware, stovetops, cooktop and oven doors
	Nextrema®	Lithium Aluminosilicate	Fireproof windows and doors
Corning, USA	Pyroceram®	β-Spodumene ss	Cookware
	Fotoform® / Fotoceram®	Lithium silicate	Photosensitive and etched patterned materials
	Cercor®	β-Spodumene ss	Gas turbines and heat exchangers
	Centura®	Barium silicate	Microwave tableware
	Vision®	β-quartz ss	Cookware and cooktop
	9606®	Cordierite	Radomes
	MACOR®	Mica	Machinable glass-ceramic
	9664®	Spinel-enstatite	Magnetic memory disk substrate
	DICOR®	Mica	Dental restoration
Nippon Electric Glass, Japan	ML-05™	Lithium disilicate	Magnetic memory disk substrate
	Neoparies®	β-wollastonite	Architectural glass-ceramic
	Firelite™	β-quartz ss	Architectural fire-resistant windows
	Neoceram™ N-11	β-Spodumene ss	Cooktop and kitchenware
	Narumi®	β-quartz ss	Low thermal expansion GC
	Neoceram™ N-0	β-quartz ss	Color filter substrates for LCD panels

Figure II.8 - examples of crystalline silicate structures of commercial products [92]

	Name and formula	Structure type	Reference
1	α-Quartz (SiO_2)	Framework silicate	Levien et al. (1980)
2	β-Quartz (SiO_2)	Framework silicate	Wright and Lehmann (1981)
3	Cristobalite (SiO_2)	Framework silicate	Dowty (1999a)
4	Tridymite (SiO_2)	Framework silicate	Kihara (1977)
5	β-Eucryptite ($LiAlSiO_4$)	Framework silicate	Guth and Heger (1979)
6	β-Spodumene ($LiAlSi_2O_6$)	Framework silicate	Li and Peacor (1968)
7	Enstatite ($MgSiO_3$)	Chain silicate	Ghose et al. (1986)
8	Wollastonite ($CaSiO_3$)	Chain silicate	Ohashiy and Finger, (1978)
9	Diopside ($CaMgSi_2O_6$)	Chain silicate	Clark et al. (1969)
10	Fluorrichterite ($KNaCaMg_5Si_8O_{22}F_2$)	Chain silicate	Cameron et al. (1983)
11	Cordierite ($Mg_2Al_4Si_5O_{18}$)	Ring silicate	Predecki et al. (1987)
12	Lithium Disilicate ($Li_2Si_2O_5$)	Layer silicate	De Jong et al. (1998)
13	Fluorophlogopite ($KMg_3AlSi_3O_{10}F_2$)	Layer silicate	Mc Cauley et al. (1973)
14	Leucite ($KAlSi_2O_6$)	Framework silicate	Mazzi et al. (1976)
15	Nepheline ($KNa_3[AlSiO_4]_4$)	Framework silicate	Simmons and Peacor (1972)
16	Mullite ($3Al_2O_3$•$2SiO_2$)	Chain aluminosilicate	Sadanaga et al. (1962)
17	Spinel ($MgAl_2O_4$)	Oxide	Dowty (1999b)
18	Rutile (TiO_2)	Oxide	Dowty (1999c)
19	Fluoroapatite ($Ca_{10}(PO_4)_6F_2$)	Phosphate	Sänger and Kuhs (1992)
20	Monazite ($CePO_4$) for ($LaPO_4$)	Phosphate	Ueda (1953)
21	ZrO_2- crystals		
	a. Monoclinic modification	Oxide	Howard et al. (1988)
21	**b.** Tetragonal modification	Oxide	Howard et al. (1990)
21	**c.** Cubic modification	Oxide	Wang et al. (1999)

Figure II.9 - examples of crystalline structures and its structure type [08]

2.2.3. Crystal system

A crystal system consists of small unit cells, the smallest building block of the crystal structure. There are seven types of systems; cubic, tetragonal, orthorhombic, rhombohedral, hexagonal, monoclinic and triclinic. The seven crystal systems are based on the 3-dimensional arrangement of atoms, Figure II.10. Based on those 7 systems, 14 Bravais lattices are possible, Figure II.11. [43]

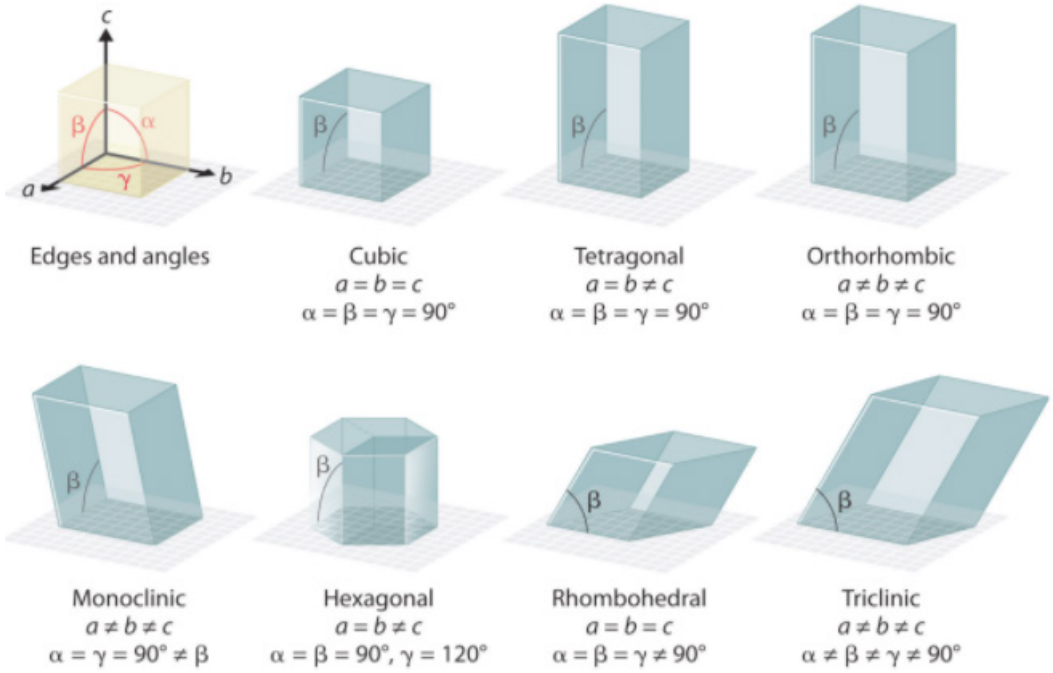

Figure II.10 - the seven crystal systems [46]

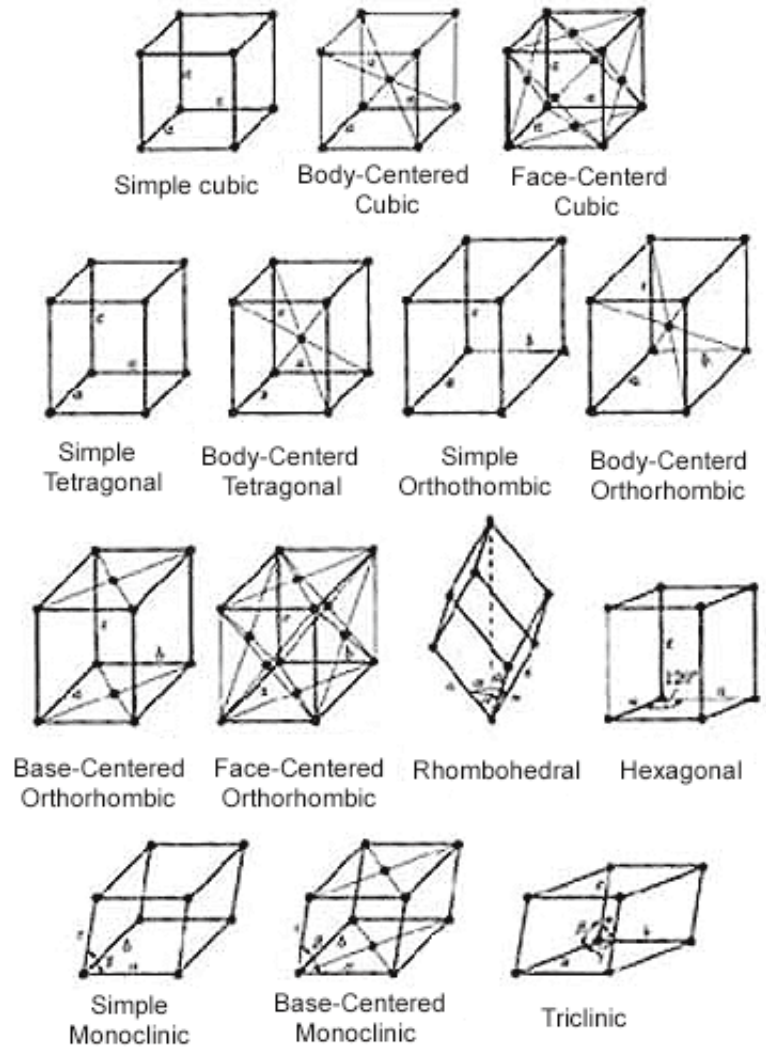

Figure II.11 - the 14 Bravais lattices [37]

2.3. Crystallization

Crystallization itself is a process dependent on a numerous of varying parameters, such as chemical parameters, biochemical parameters and physical parameters, see Figure II.12. Whereas for glass-ceramics in this research biochemical parameters are of less importance, but chemical and physical parameters are still applicable. However, the main parameters taken into account in this report are physical parameters as the temperature variation, time and viscosity.[36]

The crystallization performed for this report is based on transforming glass into glass-ceramics. Given Figure II.12, the raw materials are formed upon the melting process into glass. By reheating this glass at the right temperature, crystallization occurs and results into glass-ceramics.

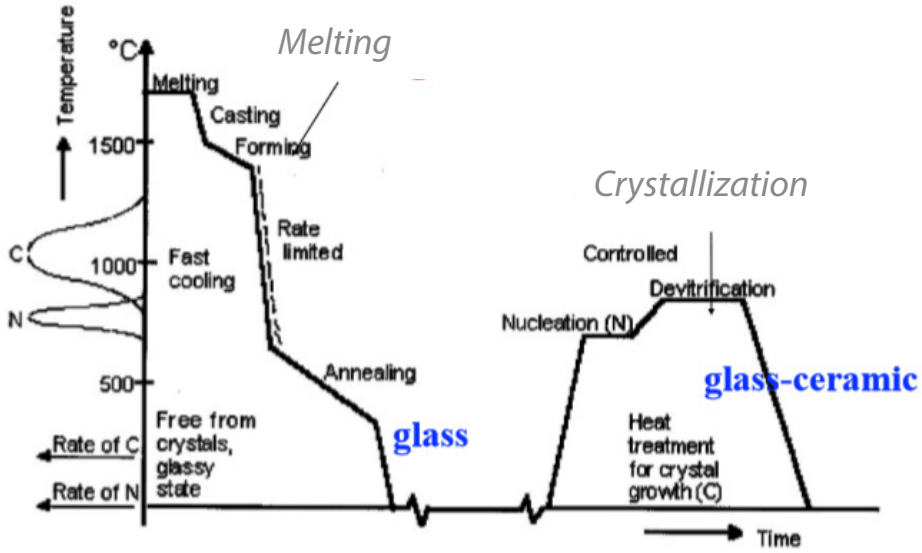

Figure II.13 - melting and crystallization curve [22]

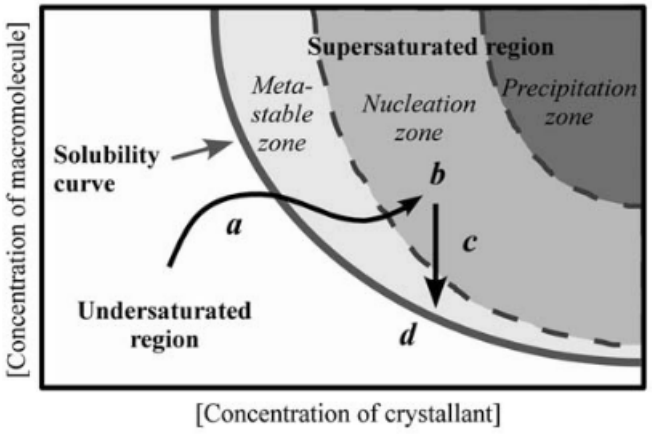

Biochemical parameters	Chemical parameters	Physical parameters
Purity of the macromolecule	pH	Temperature variation
Ligands, inhibitors, effectors	Crystallant type	Contact surfaces
Aggregation state of the macromolecule	Crystallant concentration	Methodology or approach to equilibrium
Post-translational modifications	Ionic strength	Gravity
Source of macromolecule	Specific ion effects	Pressure
Proteolysis or hydrolysis	Supersaturation	Time
Chemical modifications	Reductive or oxidative environment	Vibrations, sound or mechanical perturbations
Genetic variants	Concentration of the macromolecule	Electrostatic or magnetic fields
Inherent symmetry of the macromolecule	Metal ions	Dielectric properties of the medium
Stability of the macromolecule	Crosslinkers or polyions	Viscosity of the medium
Isoelectric point	Detergents, surfactants or amphophiles	Rate of equilibration
History of the sample	Non-macromolecular impurities	Homogeneous or heterogeneous nucleants

Figure II.12 - crystallization parameters [36]; biochemical, chemical and physical parameters

Crystallization is a two-step process of nucleation followed by crystal growth. Generally, nucleation occurs at low temperatures and growth occurs at higher temperatures, see Figure II.14. Nonetheless, both processes can occur simultaneously as long as the nucleation temperature curve and the growth temperature curve are intersecting Figure II.15. [39]

Through crystallization a glass becomes a glass-ceramic, whereby partially the random network of glass is re-arranged into a crystalline and thus well-ordered structure, as goes the opposite of Figure II.4.

In order to undergo crystallization, the cooling rate should be in the range of the crystalline curve, see Figure II.16. The cooling rate to obtain glass-ceramics should be lower than the cooling rate to obtain glasses. [21]

Many theories and expressions are developed to describe the crystallization process, divided into expressions for nucleation and crystal growth.

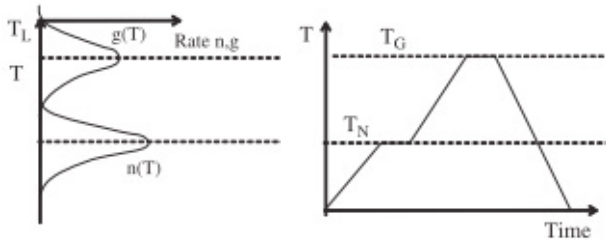

Figure II.14 - nucleation n(T) and growth g(T) curve [21]

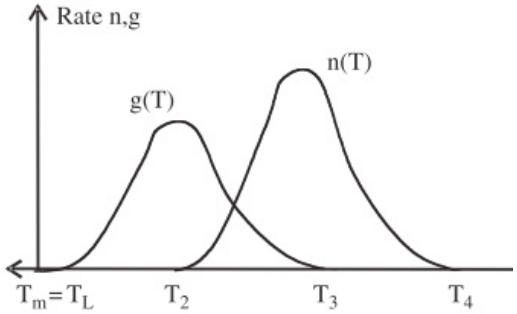

Figure II.15 - intersecting nucleation n(T) and growth g(T) curve [21]

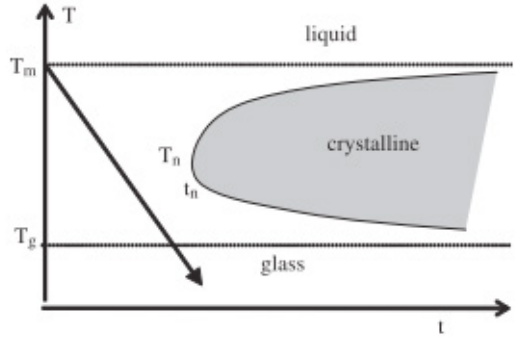

Figure II.16 - Temperature-Time-Transformation curve [22]

2.3.1. Nucleation

The general process of nucleation is given in Figure II.17. Whereby small nuclei start to form in a melt, liquid or solution. These nuclei then grow as particles from the melt are attaching to it and start growing till it reaches its critical size, where upon crystal growth will start.

Gibbs discovered in the 1920's that the formation of a new phase is built on small units of atoms or molecules in a supersatured ambient phase, as vapor, melt or solution. Whereby those small building units have the same properties as the parent phase, but in a much smaller size, given the increased surface to volume ratio and consequently enhances the drive of phase transition.[26]

Nucleation, therefore, is dependent on the free energy available from the driving force and the energy that is used to form a new interface. [03]

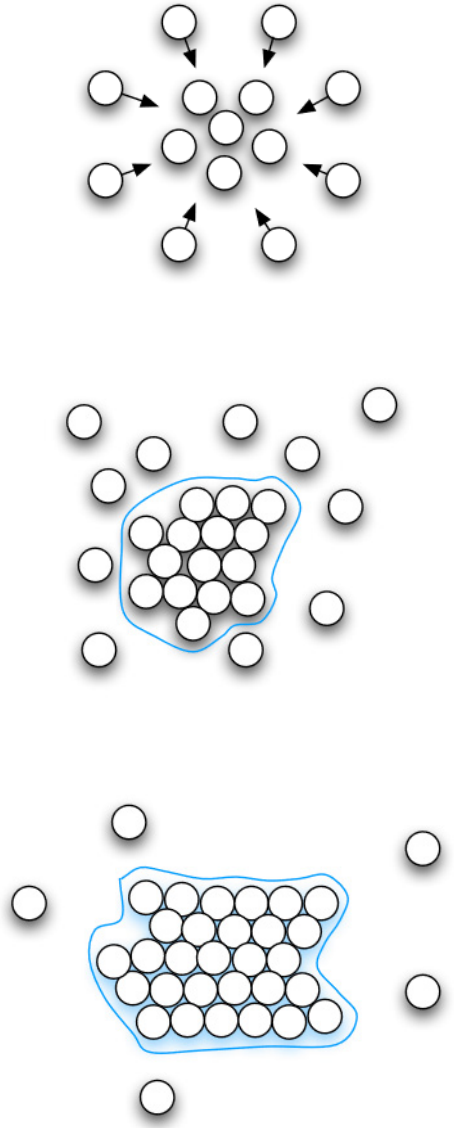

Figure II.17 - nucleation process [03]

Nucleation can be divided into two starting points, internal (volume) and surface nucleation, Figure II.18. Generally, controlled volume nucleation is performed to obtain glass-ceramics. However, if volume nucleation cannot be initiated for the base glass, surface crystallization will be used. Surface crystallization is less likely to be used in general situations through the toughened controllability compared to volume nucleation. Surface nucleation happens through the lower energy surface sites, giving crystallization the opportunity to start. [08]

Internal or volume nucleation occurs through homogeneous or heterogenous nucleation. Homogeneous nucleation is due to forming spontaneously and with equal probability throughout the melt. This spontaneous formation is the result of the absence of a foreign boundary which is caused through fluctuations in such as density and composition. Whereas heterogenous nucleation is formed at preferential surfaces such as impurities, bubbles, cracks or other surfaces in the melt. [08][39][52]

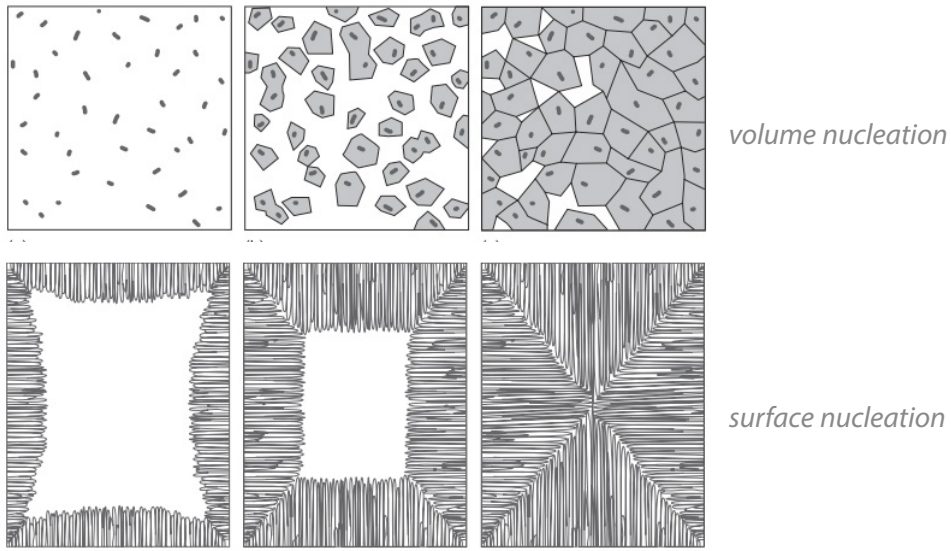

Figure II.18 - internal nucleation vs surface nucleation [08]

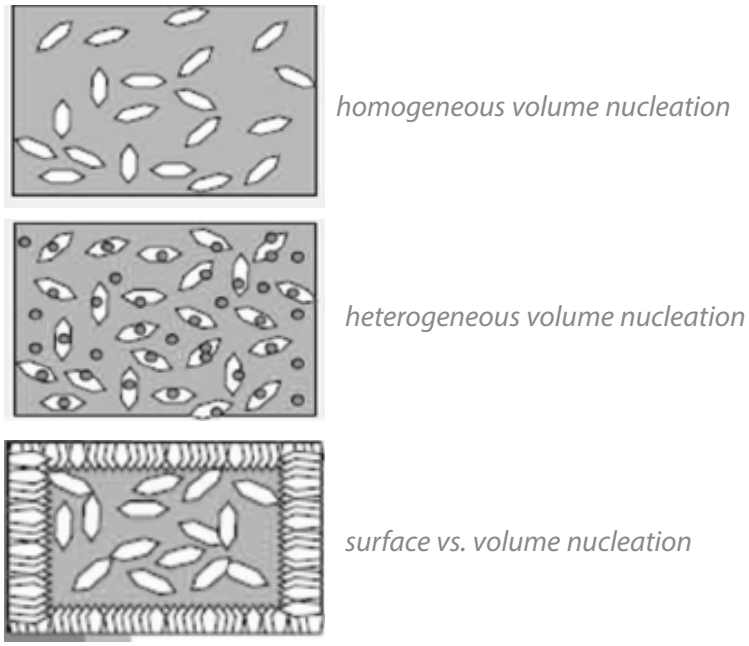

Figure II.19 - homogeneous vs heterogeneous nucleation and surface vs volume nucleation [33]

To form nuclei two barriers have to be overcome; a thermodynamic barrier followed by a kinetic barrier. The thermodynamic barrier is about the change in free energy through a system upon the formation of a nuclei. The kinetic barrier is the energy required for the movement and rearrangement of atoms and ions in the melt, allowing an ordered particle, the crystals, to grow in a disordered network, the melted glass. According to Shelby the overall process can be described as (1.1). Whereby the nucleation rate, I, defines the number of nuclei per unit volume formed per unit time. [39]

(1.1) $I = A\, e^{-\frac{W+\Delta G_D}{kT}}$

with
- A a constant
- W^* thermodynamic barrier with critical radius
- ΔG_D kinetic barrier
- k Boltzmann constant
- T absolute temperature (in K)

Despite the overall nucleation rate, nucleation is rather of homogeneous or heterogeneous nature, giving different theoretical approaches and a different Gibbs free energy (thermodynamic and kinetic barrier term), giving (1.9) and (1.11) respectively.

(1.2) $A = 2\, n_v\, V^{\frac{1}{3}} (\frac{k\,T}{h}) (\frac{\gamma}{k\,T})^{1/2}$

with
- n_v number of formula units of the crystallizing component phase per unit volume of the melt
- V volume per formula unit
- γ crystal-melt interfacial free energy per unit area
- h Planck's constant

(1.3) $A = n_v\, (\frac{k\,T}{h})$

simplified approximation of the constant

According to Shelby, the thermodynamic barrier is stated as (1.4).

With (1.5) the critical radius of a nuclei is determined. By reaching the size of the critical radius the nuclei become stable. By substituting (1.5) in (1.4), the critical value of the thermodynamic barrier can be determined.

(1.4) $W = \frac{4}{3}\pi r^3 \Delta g_v + 4\pi r^2 \gamma$

with
- Δg_v change in volume free energy per unit volume
- r radius of nuclei

(1.5) $r^* = -\frac{2\gamma}{\Delta g_v}$

(1.6) $W^* = -\frac{16\pi\gamma^3}{3(\Delta g_v)^2}$

And the kinetic barrier is dependent on the diffusion rate, D, (1.7). Whereby (1.8) is the diffusion rate based on the Stokes-Einstein relation.

(1.7) $$D = \left(\frac{k\,T\,\lambda^2}{h}\right) e^{-\frac{\Delta G_D}{k\,T}}$$

with λ atomic jump distance (generally, twice the radius)

η viscosity

(1.8) $$D = \frac{k\,T}{3\,\pi\,\lambda\,\eta}$$

Substituting the unknown terms (1.3), (1.7) and (1.8) into the overall formula (1.1), results in (1.9), the overall process of homogenous nucleation.

(1.9) $$I = \frac{n_v\,k\,T}{3\,\pi\,\lambda^3\,\eta}\, e^{-\frac{W^*}{k\,T}}$$

To obtain the nucleation rate for heterogeneous nucleation, the unknown terms simply have to be adjusted to the heterogeneous terms, to obtain (1.11).

(1.10) $$A_{het} = n_s \left(\frac{k\,T}{h}\right)$$

with n_s number of formula units of the melt in contact with the substrate per unit area

(1.11) $$I_{het} = \frac{n_s\,k\,T}{3\,\pi\,\lambda^3\,\eta}\, e^{-\frac{W_{het}^*}{k\,T}}$$

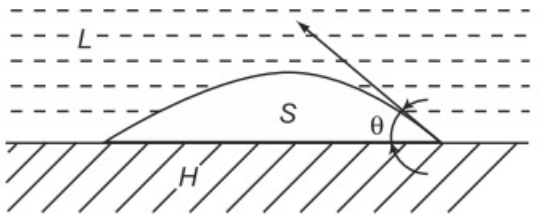

Figure II.20 - heterogeneous nucleation set-up, with H for heterogeneous substrate/catalyst, S for nucleus/formed crystal, L for the parent phase/liquid/ melt and θ for contact angle. [08]

In addition to the simplified formula of (1.11), heterogeneous nucleation has to take into account the contact between two phases. Other than homogeneous nucleation, heterogeneous nucleation arises from differences between the parent phase and the forming phase, such as phase boundaries, special catalysts and foreign substrates, whereby the contact angle between the two phases are of importance, Figure II.20. Given the (1.12) for the critical Gibbs free energy for heterogenous nucleation.

(1.12) $\Delta G_H^* = \Delta G * f(\theta)$ with $f(\theta) = \frac{(2+cos\theta)(1-cos\theta)^2}{4}$

Based on the Gibbs free energy and Figure II.20, three situations can occur.
• $\theta = 180^{\circ}$, thus $f(\theta)=1$, surface of H is not wetted, homogeneous nucleation will occur.
• $\theta \approx 0^{\circ}$, thus $f(\theta)\geq 0$, surface of H is completely wetted, ΔG_H^* is very small.
• $\theta < 180^{\circ}$, therefore, heterogeneous nucleation rather than homogenous nucleation will occur.

Other than the contact angle, the relation between the different phases (forming crystal, heterogeneous substrate and melt), several criteria for determining the effectiveness of the nucleating agent, such as the following three desirable criteria, which are based on (1.13).

(1.13) $\gamma_{HL} = \gamma_{SH} + \gamma_{SL} cos\theta$

• small γ_{SH}, a low interface energy between the heterogeneous substrate and the forming crystal.
• large γ_{HL}, indicates a large discrepancy of the thermal expansion coefficient compared with SH.
• Similar lattice parameters between the heterogeneous crystal and the forming crystal permits the determination of solid-state reactions based on epitaxy, the growth of crystals on a crystalline substrate.

2.3.2. Crystal growth

Theoretically, crystal growth occurs at any temperature below the melting temperature, there is no energy barrier to overcome for growth as of for nucleation. The involved nuclei do not have to have the same composition as the growing crystal, which is especially common for heterogenous nucleation. [39] Thereby, generally controlled crystal growth does not result in only one type of crystal phase, but it creates different types of crystals. [08][21]

Crystal growth only starts once a nucleus has reached the critical size r* (1.5). The crystallization rate is dependent on the extent of movement of molecules to the interface between nuclei and the glassy phase. Uhlmann (1982) examined crystallization in different glass compositions, Uhlmann thereby demonstrated that the different glass composition resulted in different crystal growth rates. Which Uhlmann described into three growth models; normal growth, screw dislocation growth and surface crystallization. [08]

The normal growth model considers a microscopically rough interface, given (1.14). The screw dislocation growth model is similar as the normal growth model, but with an additional factor for its preferential site, (1.15). The surface crystallization model is other than the previous models, based on a rather smooth surface and based on surface nucleation.

(1.14) $V = v\,a\,(1 - e^{-\frac{\Delta G}{kT}})$ with v frequency factor of material transport to the interface

a interatomic separation distance

ΔG Gibbs free energy

(1.15) $V = v\,a\,f\,(1 - e^{-\frac{\Delta G}{kT}})$ with f fraction of preferred growth site at the dislocation point

(1.16) $V = C\,v\,e^{-\frac{B}{T\,\Delta T}}$ with C, B function of time for the formation of nucleus relative to that required for its propagation across interface

2.3.3. Crystallization methods

The crystallization process is of a highly complex nature. Upon controlled crystallization various types of crystals can be formed, resulting in the special properties of a glass-ceramic product. However, there is no comprehensive mathematical theory describing the exact processes of the creation of those different crystal phases. According to Höland and Beall [08], with current knowledge of glass-ceramics production, nucleation is rather assumed to be influenced by two general factors:

- the selection of the appropriate base glass, with or without the addition of nucleating agents.
- controlled heat treatment of the base glass, with time and temperature as main parameters.

However, to create a glass-ceramics several methods are possible, different heat treatment processes are developed throughout the years. Whereby the most common methods are the conventional method (two-stage), the modified conventional method (single-stage), petrurgic method and the powder method. [34]

The conventional method consists of two-stages with limited overlap between the nucleation and the growth rate curve, Figure II.21. The first stage is a lower temperature treatment at a temperature that gives a high nucleation rate, to form enough nuclei. Whereas the second stage consists of a higher temperature heat treatment, which temperature gives a reasonable crystal growth rate. To achieve this phenomenon, it is possible to add nucleating agents, which can be metallic (Au, Cu, Ag, Pt, Pd) as well as non-metallic (TiO_2, P_2O_5 and fluorides). [21]

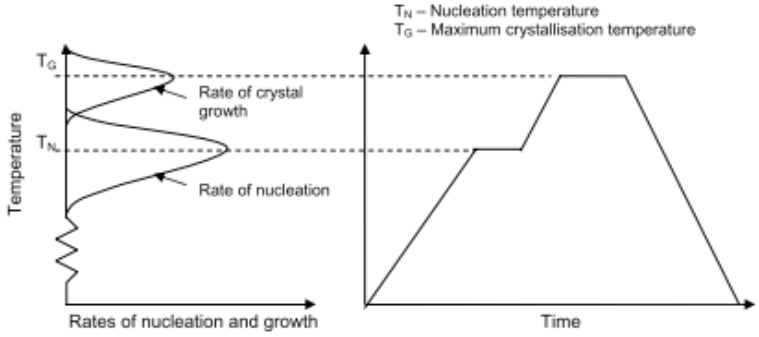

Figure II.21 - nucleation and growth curve - conventional method [34]

The modified conventional method consists of only one stage. If the nucleation and growth curve are overlapping enough, one stage is sufficient to perform crystallization. With the requirement that the nucleation and growth rate curves are extensively overlapped, Figure II.22. Resulting in simultaneous processes of nucleation and crystal growth during a single heat treatment. As well as for this method it is possible to add nucleating agents to favour the possibility and ability of crystallization. [34]

The petrurgic method has its nucleation and crystal growth during cooling. This method was found in a certain glass-ceramic (Silceram CaO-MgO-Al_2O_3-SiO_2), whereby heating up to the T_{ng} (optimal nucleation and growth temperature) as for the conventional method and cooling down to T_{ng} made little difference in the crystallized end product. The discovery led to the petrurgic method where the crystallization occurs during the cooling of the melt. It uses a shorter dwell time at the optimal nucleation and crystallization temperature, followed with a controlled low cooling rate. [34]

Both the petrurgic and modified conventional method are more economical than the conventional method. [34]

The powder method is by shaping through cold-compacting and heat treated at a high temperature to sinter the powder into a glass-ceramic. A high level of control is required to perform this method, if the crystallization rate is too high it will hinder the low temperature sintering, resulting in an undesirable porous final product. Thereby, if the sintering is completed before crystallization, the final product will not differ from glass-ceramics obtained through the other methods. Therefore, to create a dense glass-ceramic product it is required to have a controlled sintering process where both densification and crystallization are occurring at the right temperature. This method is rarely used in practice due to its limitations in shape and size, the required high temperature for sintering and the costs of producing a powder, whereas the powder method would not be considered further on in this thesis report. [34]

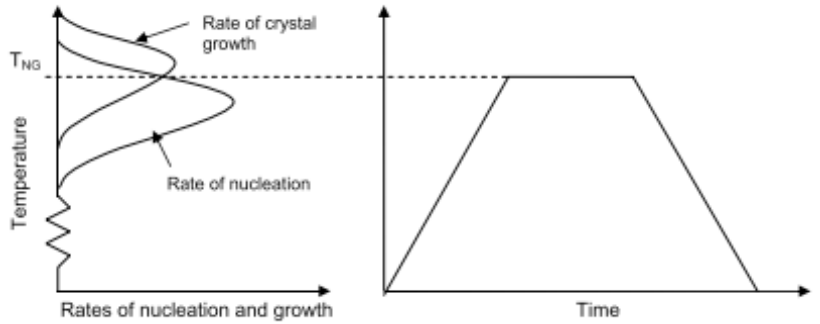

Figure II.22 - nucleation and growth curve - modified conventional method [34]

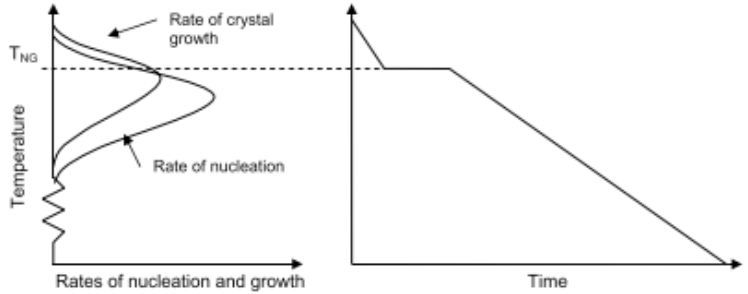

Figure II.23 - nucleation and growth curve - petrurgic method [34]

2.4. Parameters of influence

Based on the theory behind nucleation and crystal growth, the formulas and the crystallization methods given in previous subchapters, influencing parameters can be determined. The parameters given below are not all influencing parameters, but only parameters which are selected for this research.

According to the nucleation theory, a thermal and kinetic barrier have to be overcome in order to start forming nuclei, as (1.1). Given the parameters temperature and viscosity as variable for both homogeneous and heterogeneous nucleation. In addition to heterogenous nucleation, preferential sites have to be taken into account as well, which contact angle is crucial to the nucleation process, as (1.13).

Crystal growth relies mainly on the availability of required compounds (and thus relying on the composition of the parent glass) for the growth and time, see (1.13) and (1.14).

The theory behind the diverse crystallization methods confirm the above-mentioned parameters, which will also be the main parameters for this research:

- Composition of parent glass
  - glass type and glass size
- Viscosity
  - application of additional flux
- Temperature
  - melting and crystallization temperature
- Time

The following chapter discusses the composition (parent glass and flux) and temperatures. The parameter glass size and time are neglected. Both parameter time will be determined through the melting experiments.

Chapter 3 Parameters

According to Höland and Beall [08], glass-ceramics is a multicomponent material, yet it is possible to control the properties. The first step is to select the chemical system, thereafter the desired material properties have to be determined and the right composition has to be developed through trials.

As mentioned in Chapter 2.3 many parameters are of influence of the crystallization, whereby in this chapter the most important parameters of this research are discussed, which are the glass composition (parent glass and flux) and the temperatures.

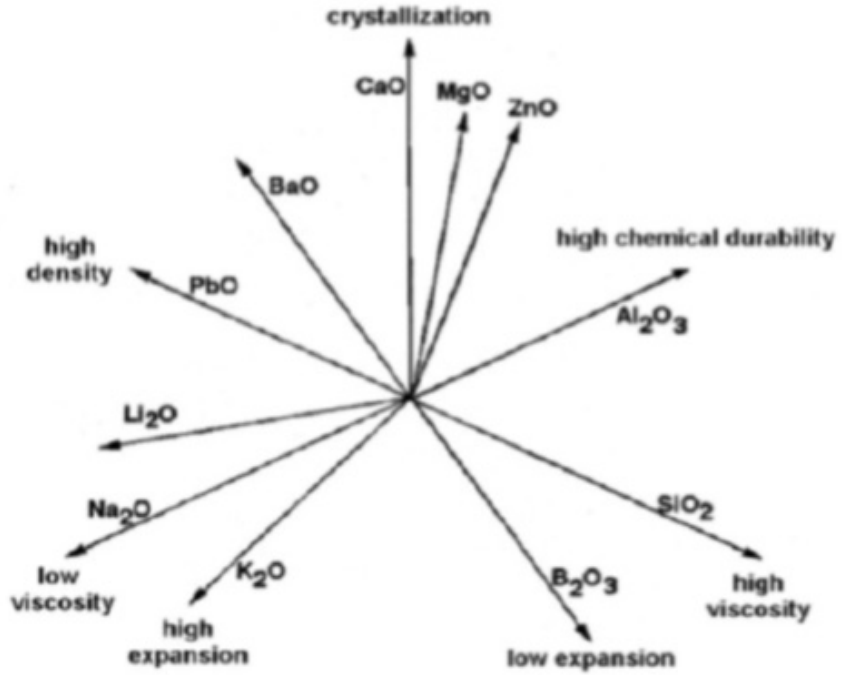

Figure II.24 - the effect on properties of certain elements [33]

3.1. Glass type

3.1.1. Parent glass

As mentioned earlier in Chapter 1, only silica-based glasses are used in this research, whereas only silica-based glass compositions are discussed. The definition of a soda-lime silica glass is as defined as in Table II.1.

Certain compounds are beneficial towards crystallization, such as CaO, see Figure II.24. In accordance with the theory in Chapter 2.1.2, stating the fact that an excess amount of CaO enhances the probability of crystallization. In addition, the results of the paper of Bristiogianni et al. [01], showed that most test subjects with circa 10% CaO have crystallized. Based on aforementioned facts can be determined that the amount of CaO is of influence for crystallization, confirming the use of soda-lime silica glass as the initial material for the upcoming melting experiments in Chapter 4.

3.1.2. Flux

Fluxes are molecule compounds that upon adding to the melt it will modify the network. The addition of the fluxes changes the average number of oxygen-silicon bonds forming bridges. The principal use of a flux is to decrease the viscosity, whereby the melting and melting/working temperatures will decrease along, as mentioned in Chapter 2.1.2. A certain amount of excess fluxes will break down the network into very simple and mobile units, where after crystallization is a more favourable process than the formation of glass. [21]

For this project, Na_2O will be used as a flux, based on previous experiments done by Telesilla Bristiogianni and Giulia Anagni in the TU Delft glass lab. By adding Na_2O to the composition, network bonds will be broken, it will modify the Si-O network of a tetrahedra by breaking the O-O bonds. The negatively charged oxide ion of the Na_2O group, will be attached to the network while the positively charged sodium ion will be mobile, yet part of the structure, Figure II.2. Electrostatic interactions between the broken O-O bonds and the sodium ions are present. [21][27]. New bonds will be formed in the form of crystallization.

Through the studies performed by Telesilla Bristiogianni and Giulia Anagni, an initial amount of flux is set at 10wt%, see Appendix A.

3.2. Temperatures

From Figure II.21, Figure II.22 and Figure II.23 can be concluded that not all material configurations lead to the same nucleation and crystal growth curves. Each glass type consists of different compounds and different concentrations, whereas for each glass type another temperature curve is present, Figure II.25 shows the different temperature-viscosity curve of several silica-based glasses. [09] Theoretically, different crystalline phases can be created or decomposed at different temperatures.

To create a glass or obtain crystallization it is important to know the temperature curve of the corresponding glass. The most important temperatures for this thesis are the glass transition temperature (T_g), the crystallization temperature (T_c) and the melting temperature (T_m), Figure II.26. Those temperatures can be obtained through thermal analysis such as Differential Thermal Analysis or Differential Scanning Calorimetry. [10][27]

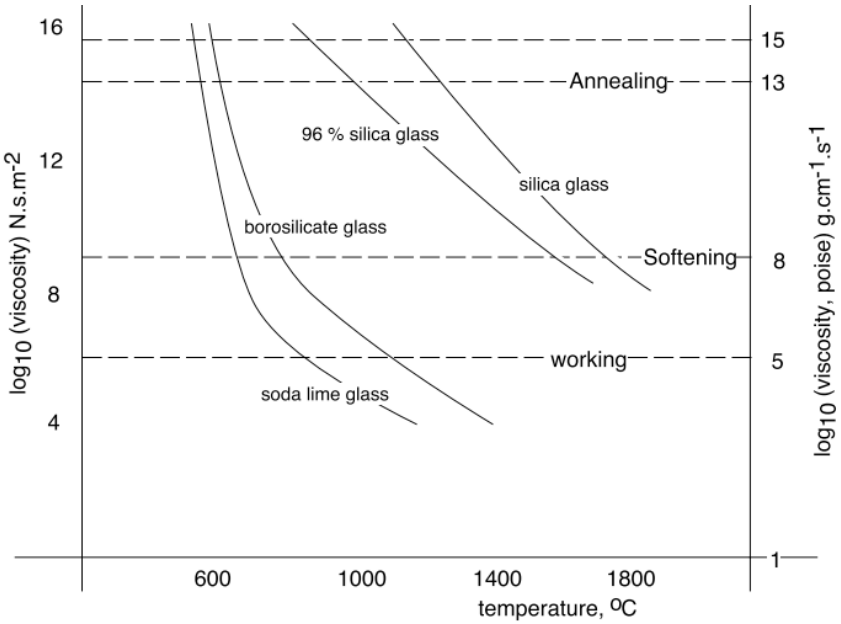

Figure II.25 - temperature curves of silicate glasses [27]

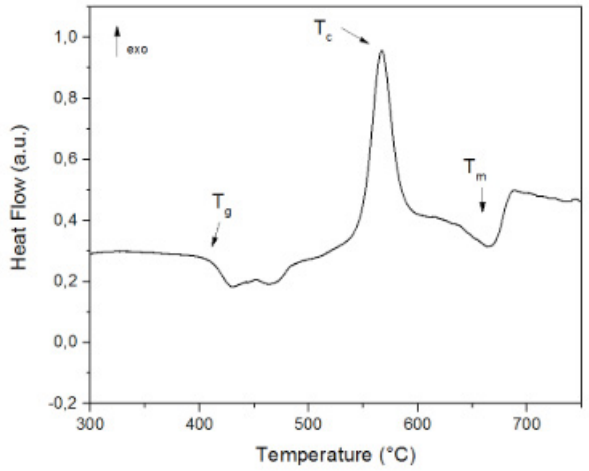

Figure II.26 - important temperatures; Tg, Tc and Tm [13]

- The glass transition temperature, T_g, the temperature where a supercooled liquid becomes a glass, Figure II.1. The glass transition occurs over a temperature range, whereby the median is taken as the T_g. For temperatures below T_g, the activity of the rearrangement of atoms and molecules are stagnated. However, the value of T_g is dependent on the cooling rate. A slow cooling rate allows more time for structural rearranging, resulting in a lower T_g and a denser glass. [10][27]
- The crystallization temperature, T_c, at some temperatures above the glass transition temperature the atomic network can arrange itself into an ordered structure. As T_g the crystallization temperature is in a range of a peak, whereby the maximum of the peak is where the maximum crystallization rate occurs. The peak is a result of the exothermic nature of crystallization, whereby heat is being released. [10][27]
- The melting temperature, T_m, at some temperature all material will liquidify and become a melt. The melting temperature of glass is highly dependent on its glass composition, whereby network modifiers are beneficially lowering the melting temperature. [10][27]

Through Figure II.27, Figure II.28 and Figure II.29 can be noticed that even for soda-lime-silica glass there are different crystallization temperatures. Taken from these figures, the optimal crystallization temperature is varying between 670 to 740 °C for soda-lime-silica glass. Whereby the study by Xiaojie et al. [50], showed that different glass size and heat treatment, resulted in different crystallization peaks, Figure II.29. [01][50]

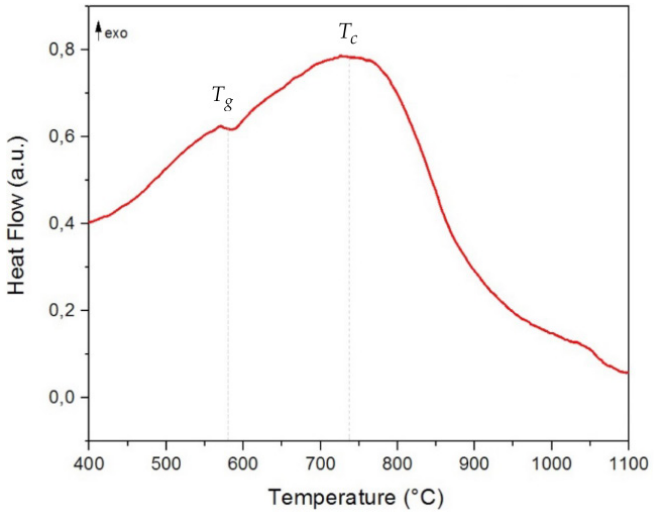

Figure II.27 - DSC analysis with Tg and Tc of PPG Starphire [01]

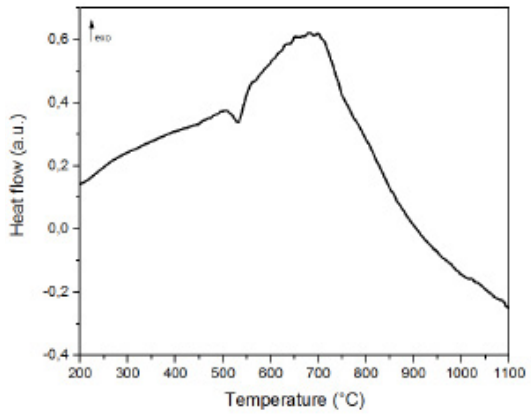

Figure II.28 - DSC analysis of Spruce Pine transparant clear glass [01]

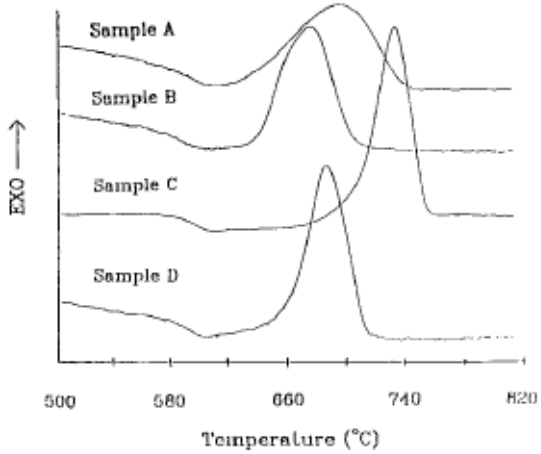

Figure II.29 - DTA analysis of Na_2-2CaO-3SiO_2 glass [50]

Summary part II - LITERATURE STUDY

SQ 1. What is crystallization?

Crystallization is the process of turning an amorphous glassy structure into a well-ordered crystalline structure. Upon this thermal treatment of crystallization, molecule bonds in the random network of glass are broken and atoms are re-arranged into a new structure. Crystallization consists of two steps: (low temperature) nucleation and (high temperature) crystal growth. During nucleation nuclei are formed spontaneously (homogeneous volume nucleation) or formed upon a preferential site (heterogeneous volume and surface nucleation). Once a nucleus reached its critical size, crystal growth starts.

SQ 2. What is a glass-ceramic?

A glass-ceramic used to be defined as a glassy yet crystalline material of inorganic and non-metallic compounds, with the requirement of 50 to 95vol% crystalline phases. However, new definitions of glass-ceramic are suggested, whereby glass-ceramics are inorganic, non-metallic materials which are obtained through controlled crystallization of glasses via different processing methods. The volume fraction of crystals may vary from ppm to almost 100vol%, but it has to contain at least one crystalline phase and a residual glass. A glass-ceramic can consist of different crystalline silica structures; nesosilicates, sorosilicates, cyclosilicates, inosilicates, phyllosilicates and tectosilicates, with nesosilicates as the lowest polymerization and least important mineral group and tectosilicates as the major mineral group respectively. Zooming in even further, the crystalline phases of a glass-ceramic can be built of 7 different crystal systems and 14 Bravais lattices are possible, giving different composition possibilities and properties for glass-ceramics.

SQ3. How to control crystallization?

Crystallization has many parameters of influence, whereby in this research only glass type (glass composition, glass size and flux), temperatures and dwell time are taken into account. Certain molecule compounds are beneficial towards the occurrence of crystallization, such as lime (CaO) and soda (Na_2O). Excessing a certain amount of lime makes glasses more prone for crystallization. Soda influences the viscosity of the melt, it makes the glass more soluble, whereas atoms can more easily move and re-arrange. Using appropriate melting temperatures, crystallization temperatures and the dwell times allows nucleation and crystal growth to occur.

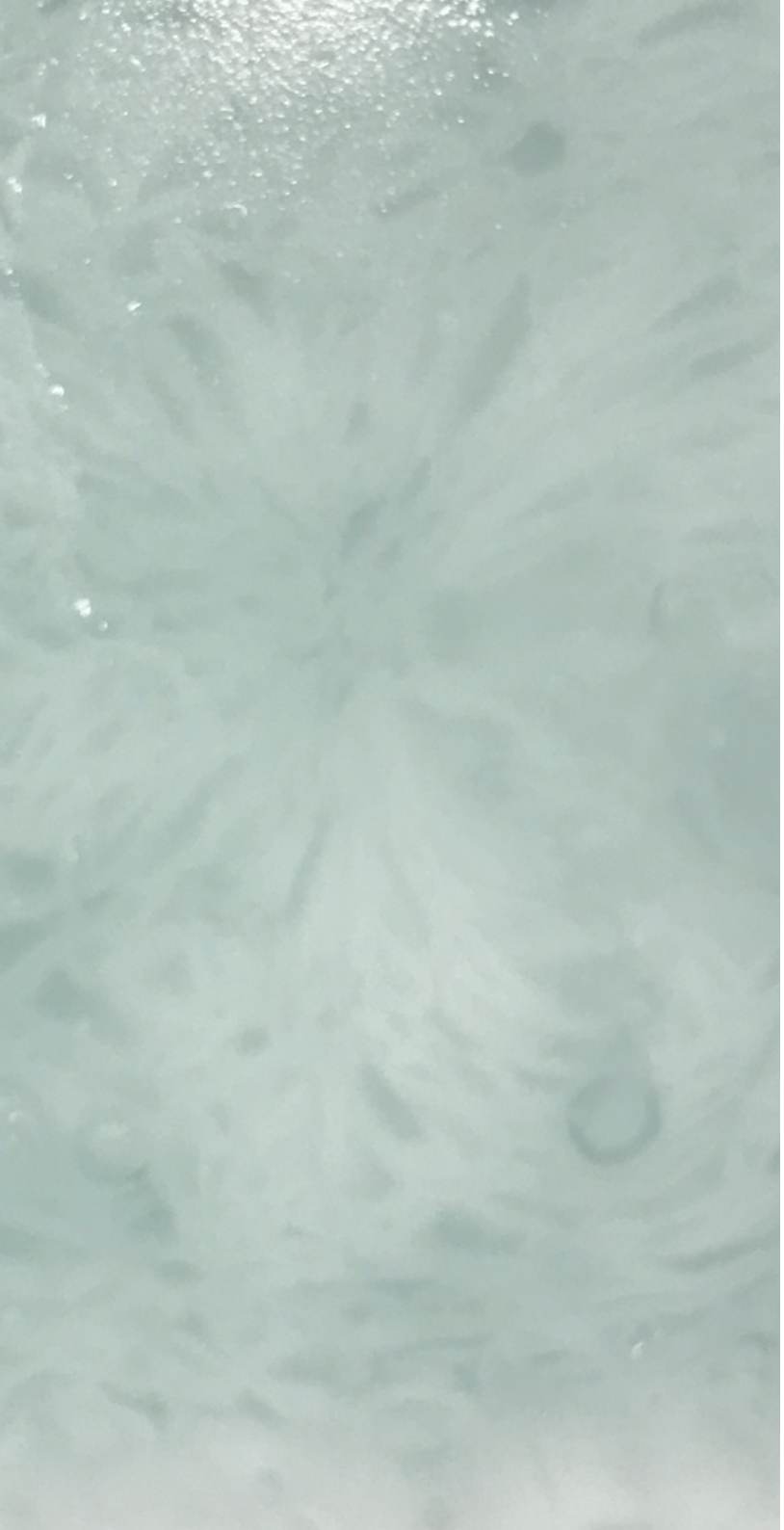

PART III - LABORATORY TEST

Chapter 4 Melting experiments

The first step and thus the object of the first melting experiments are to get familiar with the different parameters in order to produce crystallized samples. The melting experiments function as a base and reference for the following property experiments. During the melting experiments the different parameters will be determined and examined on the effect of crystallization in order to produce glass-ceramic samples.

All samples are 5x5x5cm cubes, produced by casting glass in crystalcast moulds. The glass sizes used in this research are glass shards, cullet (1,4-5mm) and powder (<1.4mm), to fill up one mould approximate 400gram of glass is required. Glass shards are prepared by simply breaking the glass with a hammer, while glass cullet and powder are prepared by using a disc mill. Figure III.1 gives an overview of the melting experiments process.

Figure III.2 gives an overview of all melting experiments, whereas chapter 4.1 to chapter 4.8 explain the goal and result per experiment and chapter 4.9 discusses the findings through the melting experiments.

Note: Two different ovens are used for the melting experiments, whereby melting experiment 1, 5, 6, 7 and 8 are done in a small oven, which fits two moulds. And melting experiment 2, 3 and 4 are done in a relatively larger oven, which could fit approximately 12 moulds.

For more imagery see Appendix B.

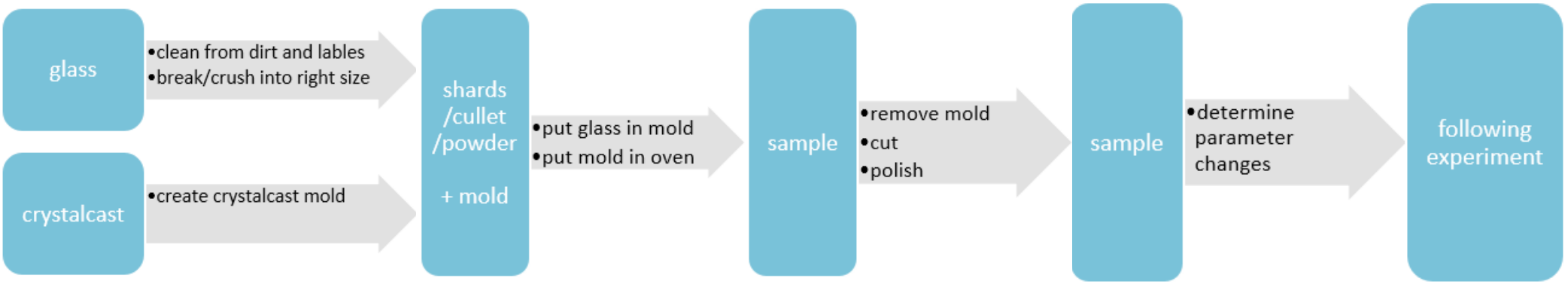

Figure III.1 - melting experiment process overview

Melting experiment 1

First firing:

Dwell	Temp
3h	1050°C
10h	860°C

Second firing:

Dwell	Temp
10h	840°C

Melting experiment 2

First firing:

Dwell	Temp
10h	1120°C

Second firing:

Dwell	Temp
10h	840°C

Melting experiment 3

Dwell	Temp
3h	1050°C
5h	840°C
5h	860°C

Melting experiment 4

Dwell	Temp
3h	1070°C
5h	780°C
10h	860°C

Melting experiment 5

Dwell	Temp
3h	1050°C
5h	760°C
10h	890°C

Melting experiment 6

Dwell	Temp
3h	1050°C
5h	500°C
10h	650°C

Melting experiment 7

Dwell	Temp
3h	1070°C
5h	760°C
10h	890°C

Melting experiment 8

Dwell	Temp
3h	1070°C

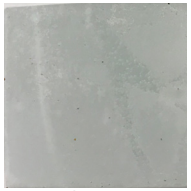

1A • flat glass

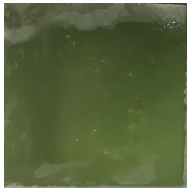

2A • bottle shards

3A • bottle cullet

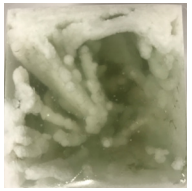

4A • bottle shards

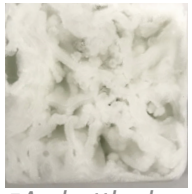

5A • bottle shards

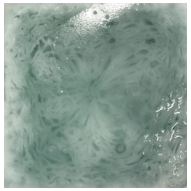

6A • bottle cullet (water bottle)

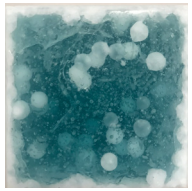

7A • as 5B

8A • as 5B

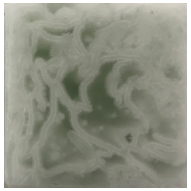

1B • bottle glass

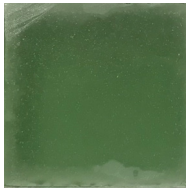

2B • bottle cullet

3B • as 3A + 10wt% flux

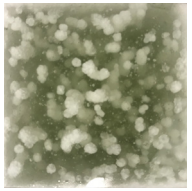

4B • bottle cullet

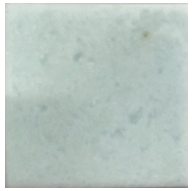

5B • bottle cullet (wine bottle)

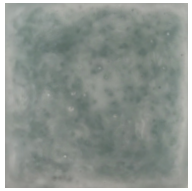

7B • as 6A

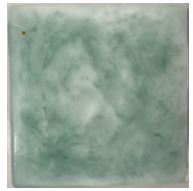

8B • as 6A

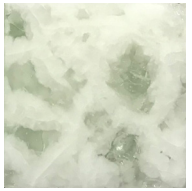

2C • as 2B+10wt% flux

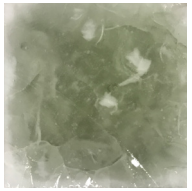

4C • as 4B+ 5wt% flux

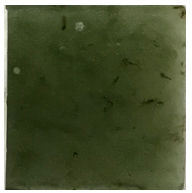

2D • bottle powder

Figure III.2 - overview all melting experiments (Dwell = dwell time, Temp = temperature)

4.1. Melting experiment 1

Melting experiment 1 is to determine what glass is more prone to crystallization, based on the experiments done by Bristogianni et al. [01] and Chapter 3, soda-lime-silica glasses are tested. Suspecting that the lime in soda-lime-silica glass is beneficial towards the crystallization mechanism.

4.1.1. Parameters

Material

Soda-lime silica glass

- 1A • Flat glass
- 1B • Bottle glass

Temperature and cooling rate

First firing:

Temperature °C	Dwell time
1050	3h
860	10h

Second firing:

Temperature °C	Dwell time
840	10h

4.1.2. Results

After first firing	No significant crystallization could be observed from the top, whereas a second firing was decided upon. But, since the samples were only externally observed, it is not possible to conclude whether crystallization has occurred or not internally.
After second firing, see Figure III.3	1A - The flat glass of sample 1A is fully melted with visible lines of the glass shards at the surface, which can be caused through some reaction with the mould leaving marks behind. After cutting it is visible that the glass is hazier and less transparent than its parent glass. Also, air bubbles are visible throughout the cube, but no visible crystallization can be observed. 1B - Sample 1B has many cracks at the surfaces, probably through stresses along shrinkage. After cutting visible lines of crystallization can be observed. Most likely the crystallization started at the surface boundaries between the glass pieces, whereby the parent glass was not totally melted and homogenized, leaving preferential sites for crystallization.
Conclusion	Based on sample 1A and 1B, it can be determined that bottle glass is more prone to crystallization under the applied melting temperature and thermal treatment compared to flat glass. Whereas the following melting experiments are based on bottle glass.

1A - flat glass *1B - bottle glass*

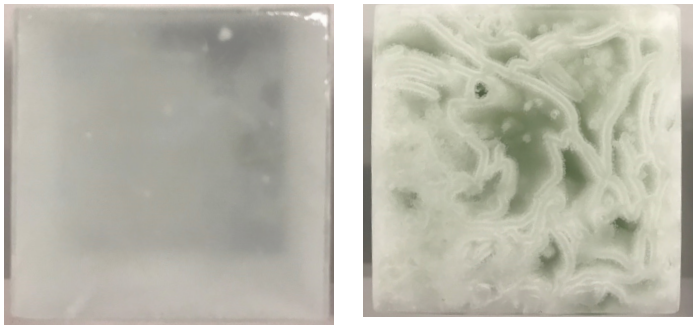

Figure III.3 - samples melting experiment 1, after cutting and polishing

4.2. Melting experiment 2

Melting experiment 2 is used to determine several factors:

- The size of the parent glass, whether a certain size is more beneficial towards the occurrence and effectiveness of crystallization. Three sizes are used; shards (as melting experiment 1), cullet of 1,4-5mm and powder of 1,4mm and smaller.
- The effect of the fluxing agent Na_2CO_3 is tested.
- A higher melting temperature is used, since in melting experiment 1 sample 1B did not fully melt and homogenize. Whereby the first firing is used to simply melt and homogenize the sample and the second firing is for the heat treatment of crystallization.

4.2.1. Parameters

Material

Soda-lime silica glass from bottle glass

2A • Bottle glass	shards
2B • Bottle glass	1,4-5mm cullet
2C • Bottle glass	as 2B + 10w% flux
2D • Bottle glass	<1,4mm powder

Temperature and cooling rate

First firing

Temperature °C	Dwell time
1120	10h

Second firing

Temperature °C	Dwell time
840	10h

4.2.2. Results

After first firing	The external surfaces seem to have undergone some reaction/crystallization.
After second firing, see Figure III.3	The result of the second firing is visible through colour changes on the top surface. After cutting it is visible that all samples have a small layer of surface crystallization on its external surfaces. 2A, 2B- Both samples are relatively similar. Other than the reactions visible on the external surfaces, no visible reactions can be observed in the core of the sample other than small air bubbles. 2B consists of a larger amount of air bubbles. 2C - Crystallization can be clearly observed. Patches of crystallization are connected and forming a pattern. The formed crystallization can be a result of the fluxing agent and the formed cracks during the first firing, which created possible surfaces for crystallization during the second firing. 2D - Also for this sample the outer surface has gotten through visible reactions. Through the core of this sample it can be clearly observed that bubbles and contaminations are present, however, visible crystallization is not observed.
Conclusion	Based on this experiment can be concluded that using high melting temperatures have been unfavourable in terms of crystallization, whereby all samples homogenized and no visible crystallization occurred no matter its size (sample 2A, 2B and 2D). Sample 2C on the other hand did crystallize, but with large amounts of cracking.

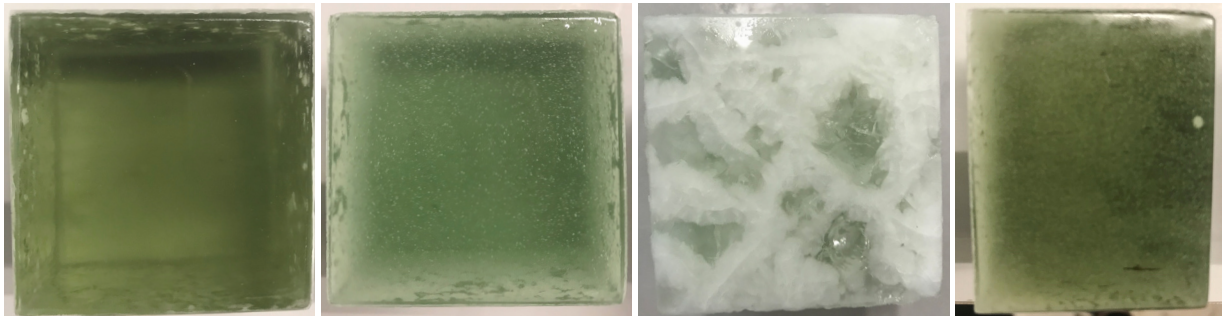

Figure III.4 - samples melting experiment 2, after cutting and polishing

4.3. Melting experiment 3

Melting experiment 3 is to determine the crystallization temperature and the dwell duration, based on the previous experiments:

Parameter	Melting experiment 1	Melting Experiment 2
Melting temperature	1050 °C	1120 °C
Melting duration	3h	10h
Number of firings	2	2
Total crystallization dwell duration	20h (2x 10h)	10h
Crystallization temperature	860, 840 °C	840 °C

First of all, one firing is tried instead of two, out of simplicity and economic value. Based on the theory of low temperature nucleation and high temperature crystal growth, the samples will dwell in two different temperatures.

4.3.1. Parameters

Material

Soda-lime silica glass from bottle glass

3A • Bottle glass	1,4-5mm cullet
3B • Bottle glass	as 3A + 10wt% flux

Temperature and cooling rate

Temperature °C	Dwell time
1050	3h
840	5h
860	5h

4.3.2. Results

After firing, see Figure III.5	3A - the sample did not fully melt, instead it mainly fused together, resulting in the cullet being still visible. However, from the colour of the outer surface of the sample can be reasoned that crystallization has occurred. After cutting and polishing, both crystalline and glassy phases are visible. By observing only single cullet pieces, it is visible that crystallization started both from the external surface and centre. 3B - the sample shows visible cracks over the outer surface, the effect of the fluxing agent is obvious present. After removing the mould, the sample did break, from the broken corner the crystalline phase is visible.
Conclusion	However, melting experiment 3 could not verify the mentioned parameters. Possible hypothesis of the obtained samples: • Lack of insulation of the oven, resulting in possibly lower temperatures than planned. • Too low melting temperature, resulting in fusing in sample 3A instead of a homogenized melted sample. • Too much fluxing agent, resulting in cracks in sample 3B through reaction with the mould. The melt being attached to the mould results in undesired stresses upon cooling through different thermal expansion coefficients. • Wrong annealing temperature and/or duration, resulting in cracks in sample 3B.

3A - cullet *3B - cullet + 10w% flux*

Figure III.5 - samples melting experiment 3, after cutting and polishing (3A), after removing mould (3B)

4.4. Melting experiment 4

Melting experiment 4 is taking a step back.

- By comparing shards, cullet and cullet with a lower amount of fluxing agent. 5wt% of fluxing agent will be used instead of 10wt%, in response to the cracking of sample 2C and 3B.
- Small adaptations are made for the oven program. With regard to overcome the loss due to insulation leakage, a slightly higher melting temperature will be used.
- Nucleation at a lower temperature and a longer duration for crystal growth at a higher temperature will be implemented.

4.4.1. Parameters

Material

Soda-lime silica glass from bottle glass

4A • Bottle glass	shards
4B • Bottle glass	1,4-5mm cullet
4C • Bottle glass	as 4B + 5wt% flux

Temperature and cooling rate

Temperature °C	Dwell time
1070	3h
780	5h
860	10h

4.4.2. Results

After firing, see Figure III.6

Based on the top surface of the samples after firing, surface crystallization is noticeable for all three samples.

4A - after cutting and polishing crystallization can be observed throughout the sample. The crystals are adjacent in a form of lines, whereby the density of crystallization differs over the volume. Few bubbles are noticeable in the sample.

4B - crystallization can be observed throughout the sample after cutting and polishing. The crystal size and form look similar as 4A, but less connected to adjacent crystals compared to sample 4A. The crystals are like dots well spread over the volume. Lots of bubbles are visible throughout the sample.

4C - during polishing the edges broke off. It is less visible what happened throughout the volume of the sample, the sample is less transparent through the many cracks and its hazy nature.

Conclusion

- Samples 4A and 4B have a different crystallization distribution compared to samples 1B and 2C, which could be a result of the different glass sizes.
- The samples with fluxing agents are still not performed successfully. This could be a result of the amount of fluxing agent used and/or the wrong temperatures (e.g. different annealing temperature required through the flux).
- The applied temperatures and durations seem to be favourable towards crystallization, but yet the amount of visible crystallization (3A and 3B) is limited.

4A - shards *4B - cullet* *4C - cullet + 5w% flux*

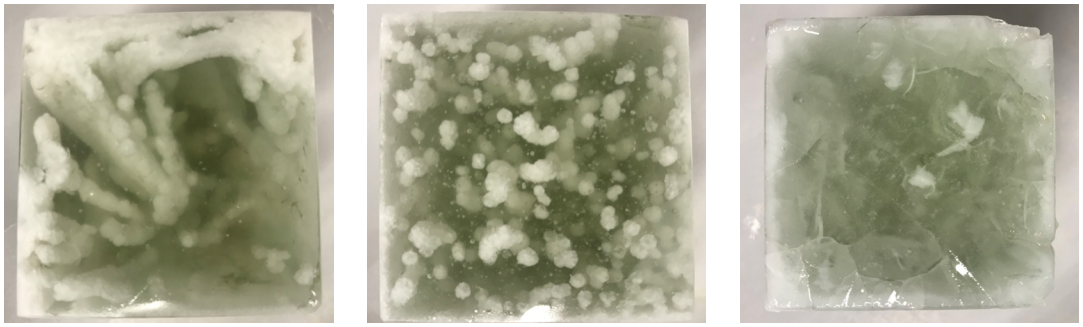

Figure III.6 - samples melting experiment 4, after cutting and polishing

4.5. Melting experiment 5

Based on the positive results of melting experiment 4, only the nucleation temperature and crystal growth temperature are adjusted to create a larger range. By doing so, a larger temperature range is covered through slow heating and its influence can be determined.

4.5.1. Parameters

Material

Soda-lime silica glass from bottle glass

5A • Bottle glass	shards
5B • Bottle glass*	1,4-5mm cullet

*(blue wine bottles are used, resulting in bluish sample)

Temperature and cooling rate

Temperature °C	Dwell time
1050	3h
760	5h
890	10h

4.5.2. Results

After firing, see Figure III.7	5A - from the outer surface of sample 5A, crystallization is observable, an opaque white cover. After cutting sample 5A, it shows a similar crystallization pattern as sample 1B, 2C and 4A, crystals are lined up. Based on visual inspection, it seems like sample 5A is having a higher percentage of crystallization then the aforementioned samples. 5B - from the outer surface it looks like the cullet is only fused, but after cutting sample 5B it is visible that the cullet did melt and homogenize fairly well. After cutting sample 5B, it shows a majority of crystallized phases, with fewer spots of glassy phases. It looks relatively well homogenized and with few very small bubbles through the sample.
Conclusion	Sample 5B has a higher amount of crystallization compared to sample 5A. Which could be the result of the glass size, shards versus cullet. The cullet has compared to glass shards more surface, whereas more locations for nuclei to start forming and growing. Whereas it might be possible if sample 5A would have more time during the crystal growth phase, it might be crystallized in a higher volume percentage.

5A - shards *5B - cullet*

Figure III.7 - samples melting experiment 5, after cutting and polishing

4.6. Melting experiment 6

Melting experiment 6 is performed to verify the DSC analysis of bottle glass (water bottle in this case, Figure III.9). Which showed a fairly low glass transition temperature and crystallization temperature. The DSC analysis shows a glass transition temperature around 430 °C and the optimum crystallization temperature at 560 °C. Based on those given temperatures from the DSC analysis, the temperatures of melting experiment 6 are set. A slightly lower nucleation temperature and a higher crystal growth temperature are set.

4.6.1. Parameters

Material

Soda-lime silica glass from bottle glass

6A • Bottle glass* 1,4-5mm cullet

*(blue greenish water bottles are used, resulting in bluish sample)

Temperature and cooling rate

Temperature °C	Dwell time
1050	3h
500	5h
650	10h

4.6.2. Results

After firing, see Figure III.8	At first glance, from the outer surface it does look crystallized. Where after upon cutting, several fractures occurred. However, after polishing, it is visible that the cullet is partially melted and fused, which could have resulted in some weaker bonds and therefore the fractures upon cutting. The outer surfaces/edges of each cullet, the light-coloured exterior, seems to be crystallized.
Conclusion	From the DSC analysis the melting temperature is measured at 1070°C, though, 1050°C was used, which could explain the result of a not fully melted and homogenized sample. Yet, if a longer crystallization duration was used, the sample might have a larger amount of crystallization.
Discussion	The glass transition and crystallization temperature are sceptically lower than expected, generally the glass transition temperature for soda-lime-silica glass is around 500-600 °C and its crystallization temperature around 700-800 °C. Whereas the performed DSC analysis will not be used for further research.

6A - cullet

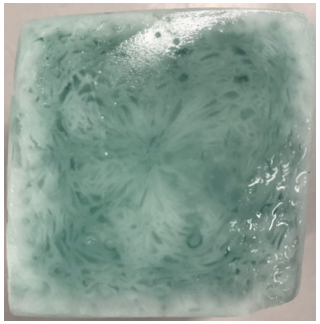

Figure III.8 - samples melting experiment 6, after cutting and polishing

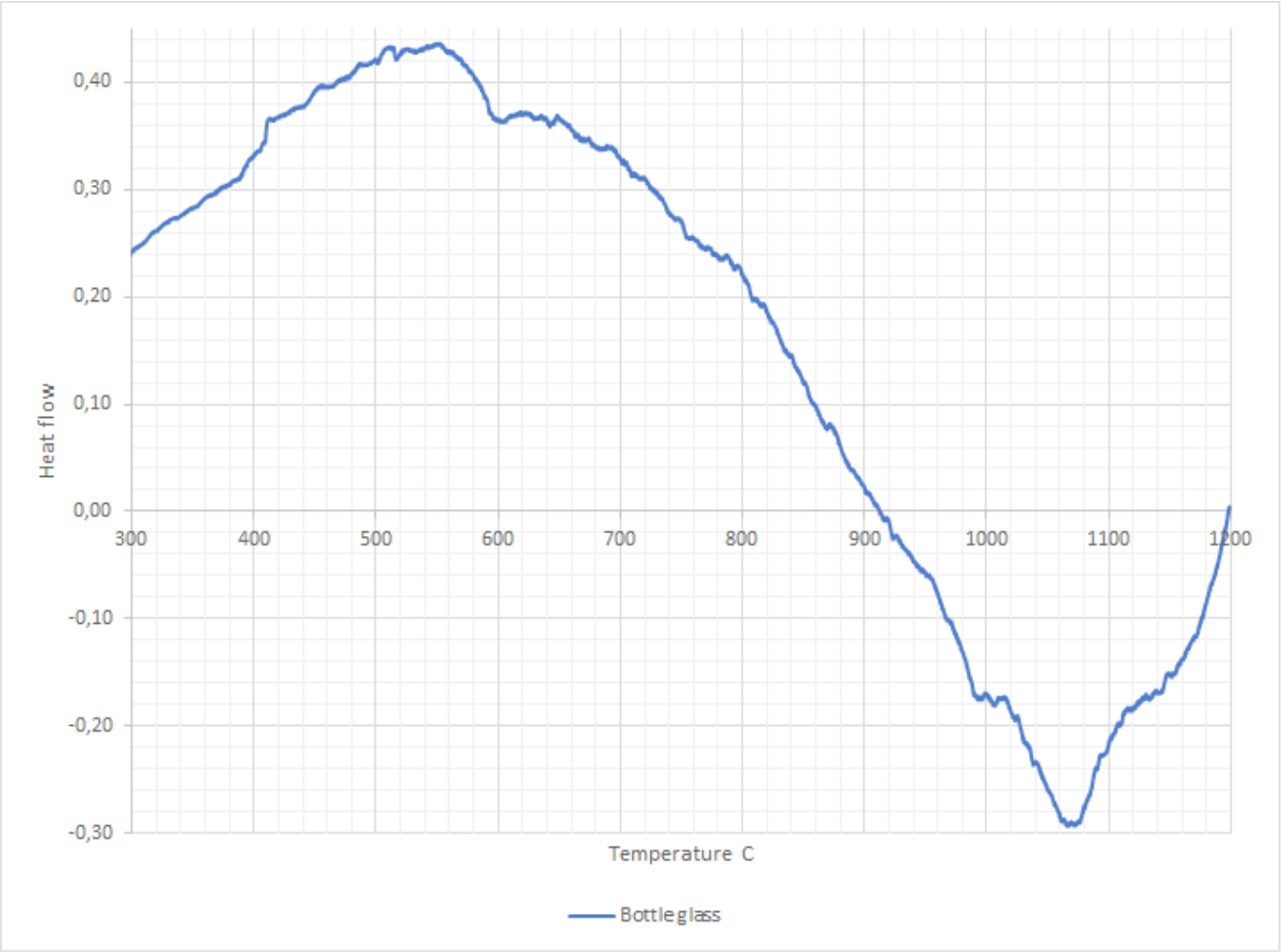

Figure III.9 - DSC analysis of the water bottle

4.7. Melting experiment 7

Melting experiment 7 is performed in order to verify melting experiment 5. Since sample 5B showed high percentage of crystallization, melting experiment 7 is re-doing the program to verify its results by using the same glass as 5B and 6A. But using a slightly higher melting temperature in order to try homogenizing the sample a bit more than sample 6A.

4.7.1. Parameters

Material

Soda-lime silica glass from bottle glass

7A • Bottle glass	1,4-5mm cullet (as 5B)
7B • Bottle glass	1,4-5mm cullet (as 6A)

Temperature and cooling rate

Temperature °C	Dwell time
1070	3h
760	5h
890	10h

4.7.2. Results

After firing, see Figure III.10	7A - visible surface crystallization can be observed, whereas after cutting less crystallization is observed as expected. The core is mainly glassy with large dots of crystals spread over the volume. 7B- very similar as sample 6A, traces of crystallization and glass mixed throughout the sample.
Conclusion	• The addition of 20 °C for the melting phase seems to have influenced the result of sample 7A compared with 5B. Whereas a temperature getting too close to the liquidus point, seems to be disadvantageous towards crystallization. • Sample 7B and 6A on the other hand, look very similar despite the change in both melting temperature and thermal treatment. Whereby the addition of 20 °C did not seem to reach its liquidus point yet and/or the crystallization range is very large.

7A - cullet (as 5B, wine) *7B - cullet (as 6A, water)*

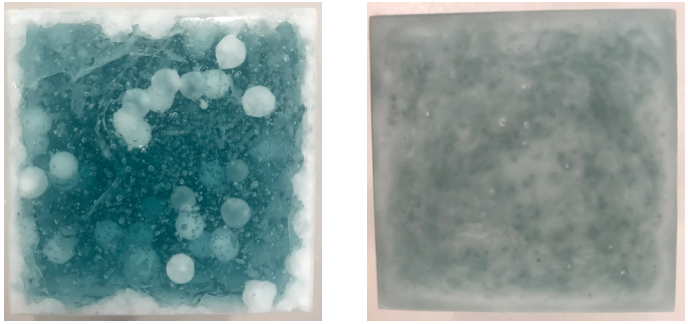

Figure III.10 - samples melting experiment 7, after cutting and polishing

4.8. Melting experiment 8

Melting experiment 8 is performed to confirm the conclusion made for melting experiment 7. Hereby this experiment will not include any heat treatment for crystallization, but only melting and annealing, in order to see the influence of no heat treatment, but purely the effect of the melting temperature.

4.8.1. Parameters

Material

Soda-lime silica glass from bottle glass

8A • Bottle glass	1,4-5mm cullet (as 5B)
8B • Bottle glass	1,4-5mm cullet (as 6A)

Temperature and cooling rate

Temperature °C	Dwell time
1070	3h

4.8.2. Results

After firing, see Figure III.11	8A- very glassy, no visible crystallization, lots of air bubbles. 8B- very similar as sample 6A and 7B, traces of crystallization and glass mixed throughout the sample.
Conclusion	• Logically, sample 8A did not crystallize since it did not undergo any heat treatment. Besides, the melting temperature has gotten too near or over to the liquidus point, which results in less or no crystallization. • Sample 6A, 7B and 8B all look very similar even though the thermal treatment is totally different. Whereas it can be assumed that the thermal treatment has been of less influence compared to the applied melting temperature, which has been below the liquidus point and therefore favourable towards crystallization.

8A - cullet (as 5B, wine) *8B - cullet (as 6A, water)*

Figure III.11 - samples melting experiment 8, after cutting and polishing

4.9. Conclusion melting experiments

Based on the melting experiments, several crucial findings can be determined.

Flux

The addition of flux did not succeed throughout the melting experiments, all samples with additional flux cracked, Figure III.12. The addition of flux results in a lower viscosity and therefore a lower forming temperature and a higher solubility. Whereby the melt and mould are undergoing some reaction, resulting the melt to be attached to the mould. Upon cooling both materials are shrinking with a different thermal expansion, resulting in stresses and thereupon cracking. However, if the right amount of flux is being used, it might result in more positive results.

First firing:

Dwell	Temp
10h	1120°C

Second firing:

Dwell	Temp
10h	840°C

Dwell	Temp
3h	1050°C
5h	840°C
5h	860°C

Dwell	Temp
3h	1070°C
5h	780°C
10h	860°C

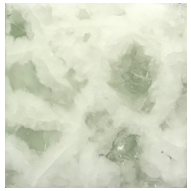

2C • as 2B + 10wt% flux

3B • as 3A + 10wt% flux

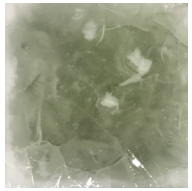

4C • as 4B + 5wt% flux

Figure III.12 - influence of flux

Glass size

The influence of the glass size towards crystallization is shown in Figure III.13. The two different glass sizes result in different preferential sites for nucleation and thereupon crystal growth to occur. Both glass sizes give preferential sites along its external surface, whereas for sample 4A pieces are bigger and preferential sites are larger but the total surface is smaller. For sample 4B the total surface is larger due to its small cullet size and thus throughout the volume preferential sites are better distributed. Therefore, sample 4A has crystallization formed along lines, all small dots connected along the preferential surface. While for sample 4B the crystallization seems more loosely but well distributed over the volume.

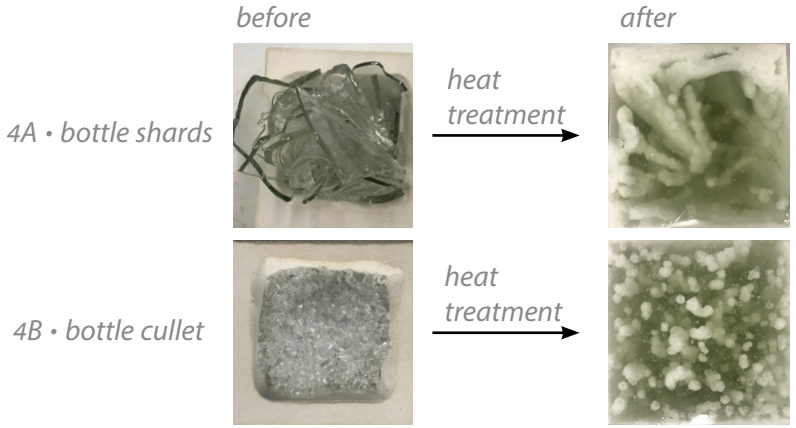

Figure III.13 - influence of glass size

Glass composition

The difference of glass composition between different samples, which result in a different reaction to the applied temperatures is shown in Figure III.14. For both melting experiment 7 and 8 all parameters were aligned, the same cullet size and the same heat treatment has been used per experiment, but a different glass bottle. Whereas during the different heat treatments, the amount of crystallization is very diverse. The samples from water bottles seem always to crystallize under the applied temperatures, while the wine bottle is dependent on the heat treatment in these experiments. In the following chapter an XRF analysis is performed to analyse the difference in glass compositions.

Melting temperature

The next finding is the importance of the melting temperature, which can be clearly observed through the results of the samples using the wine bottle, see Figure III.14. The only difference between sample 5B and 7A is the melting temperature, 1050°C and 1070°C respectively. The increase of 20 degrees resulted in much lower amounts of crystallization, which could possibly be through the decomposition of preferential sites when reaching the liquidus point. However, there do still is some crystallization. In comparison to sample 8A, sample 7A shows that the heat treatment still works, but less effective.

Thermal treatment

The last finding is the difference in thermal treatment, throughout the melting experiments one-step and two-step processes are used. Melting experiments 1 and 2 used two firings, whereby the first firing was to homogenize and melt the glass and the second firing applied the modified conventional crystallization method (Chapter 2.3.3). Melting experiments 3 to 8 on the other hand uses only one firing. Within this firing the glass melts and homogenizes, whereupon the conventional crystallization method is applied. The temperature drops to a lower temperature for nucleation and rises to a temperature favourable to crystal growth. Throughout the melting experiments the application of the conventional method seems to be favourable for the used soda-lime-silica glass.

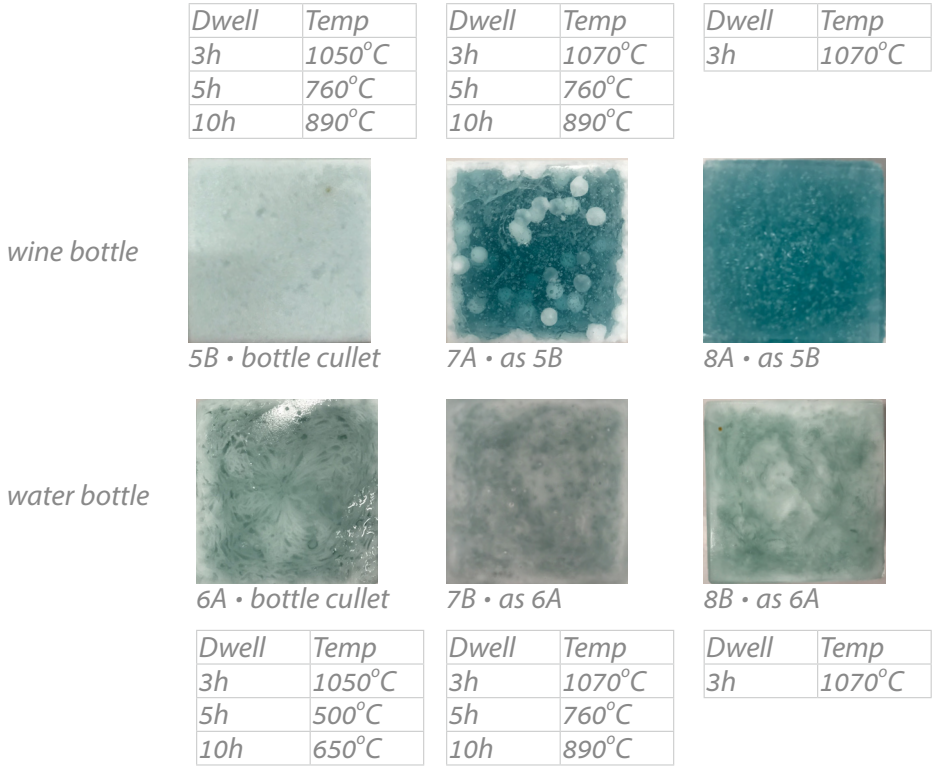

Figure III.14 - influence of glass composition, melting temperature and heat treatment

Chapter 5 X-ray Fluorescence

Based on the differences in the samples in melting experiment 5, 6, 7 and 8. An X-ray fluorescence (XRF) analysis is performed for the wine bottle glass used for samples 5B, 7A and 8A, and the water bottle glass used for samples 6A, 7B and 8B (Appendix C).

5.1. XRF results

The obtained XRF results are relatively in line with the composition of soda-lime-silica glass as given in Table II.1. The two glass bottles are in main compounds relatively similar, yet differences in concentration and number of compounds are present. Table III.1 shows the results of the XRF results and categorization of each compound.

5.2. XRF conclusions

The composition of both materials differs in small amounts per compound. The property modifiers are generally contributing to a higher viscosity and can contribute to the occurrence of crystallization, while a flux is lowering the viscosity.

The concentration of main modifiers and main flux are given in Table III.2. The other modifiers and fluxes are not taken into account due to their fairly small amount and will only be seen as traces rather than influencing compounds. The concentration of main fluxes is very similar, but the concentration of modifiers is about 1,5wt% different.

The presence of a higher amount of modifiers in the water bottle explains the higher melting point and the susceptibility of crystallization in melting experiment 6 to 8 compared to the wine bottle.

Table III.1 - XRF result of the glass of the wine bottle and water bottle

#	Compound name	Concentration (wt%) wine bottle	Concentration (wt%) water bottle	Category [21][27][33][39]
1	SiO_2	74,296	72,714	Glass former
2	Na_2O	12,478	11,947	Flux
3	CaO	10,906	9,986	Property modifier
4	Al_2O_3	1,570	1,329	Property modifier
5	MgO	0,249	2,951	Property modifier
6	Fe_2O_3	0,214	0,165	Colorant
7	SO_3	0,095	0,180	Fining agent
8	K_2O	0,089	0,507	Flux
9	TiO_2	0,034	0,045	Property modifier
10	Cl	0,023	0,039	Fining agent
11	P_2O_5	0,019	0,028	Property modifier
12	ZrO_2	0,016	0,013	Property modifier
13	SrO	0,008	0,007	Property modifier
14	ZnO	0,005	0,017	Property modifier
15	BaO		0,023	Property modifier
16	Cr_2O_3		0,015	Colorant
17	MnO		0,014	Colorant
18	CuO		0,007	Colorant
19	NiO		0,006	Colorant
20	PbO		0,005	Flux
21	Rb_2O		0,002	Property modifier

Table III.2 - concentration of modifiers and fluxes in wine and water bottle

	Compounds	Concentration (wt%) wine bottle	Concentration (wt%) water bottle
main modifiers	$CaO + MgO + Al_2O_3$	12,725	14,266
main fluxes	$Na_2O + K_2O$	12,567	12,454

Chapter 6 Splitting experiments

The splitting experiment is done for all samples of melting experiment 1 to 5, excluding sample 2C, 3A and 3B, due to cracking or fusing of the glass.

Figure III.15 shows the process of the splitting experiment.
Each sample has to be polished at the two surfaces which will be touching the set up. These surfaces have to be as flat as possible in order to obtain good contact with the set-up and the surfaces in contact with the set-up should be smooth without flaws. Flaws can cause localized stress points and result in an undesired early failure.
The sample will be attached to the set-up by taping two opposite sides of the sample to the upper piece of the set-up, whereupon the splitting experiment can start.
Once the sample fails, the splitting experiment stops.

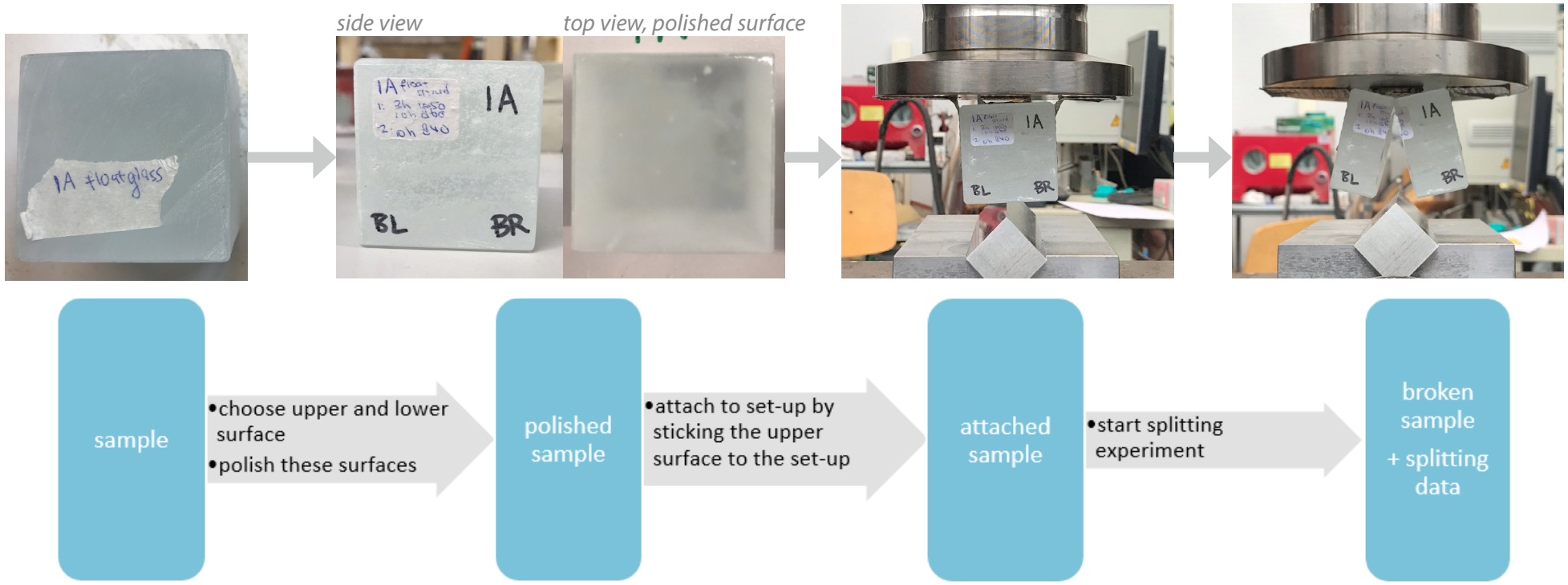

Figure III.15 - splitting experiment process overview

The results of the splitting experiments are given in Table III.3 and Figure III.16. Figure III.16 has ranked the samples based on their performance during the splitting experiments, where the results will be given in chapter 6.5.

The following sub chapters describe the results of each split sample, for a better look of the figures and pictures of the set-up, Appendix D can be consulted.

*Table III.3 - splitting experiments data and results (*bad contact)*

Sample	LxWxH [mm]	Program oven	Visual observation	Force maximum [N]	Force break [N]	Deformation max [mm]	Deformation break [mm]
1A	51x49x51	1: 3h 1050°C 10h 860°C 2: 10h 840°C	no crystals visible	26.317	25.069	0,7	0,7
1B*	50x49x51		thin crystalline lines, glassy phase predominant	13.315	10.900	1,0	0,8
2A*	50x50x47	1: 10h 1120°C 2: 10h 840°C	crystalline outer surface, internal no crystals visible	7.443	7.163	0,5	0,6
2B*	50x51x48		crystalline outer surface, internal no crystals visible	11.010	11.003	0,7	0,7
2D	50x40x46		crystalline outer surface, internal no crystals visible, lots of bubbles	17.961	17.945	0,7	0,7
4A*	50x50x48	3h 1070°C 5h 780°C 10h 860°C	lines	7.434	6.949	0,4	0,5
4B	51x51x49		crystalline dots, but glassy phase predominant	12.890	12.715	0,5	0,5
5A	50x50x48	3h 1050°C 5h 780°C 10h 860°C	crystalline lines, crystalline phase predominant	21.740	20.483	0,7	0,7
5B	51x50x50		bulk crystallization, crystalline phase predominant	30.185	29.579	1,0	1,0

6.1. Splitting experiment 1

Sample 1A has had good contact with the set-up, resulting in a good split of the sample. The sample broke at roughly 25kN, which resulted in that sample 1A withstood the highest force.

The inside of the sample is very glassy, showing no visible crystallization.

Sample 1B underwent some cracking before breaking, referring to bad contact of the sample and the set-up. After the initial crack at 13kN, the force dropped back to 7,7kN and the loading of the sample continued. After more cracking the sample broke at approximate 11kN.

The crystallized lines seem powdery/splintery, through cracking.

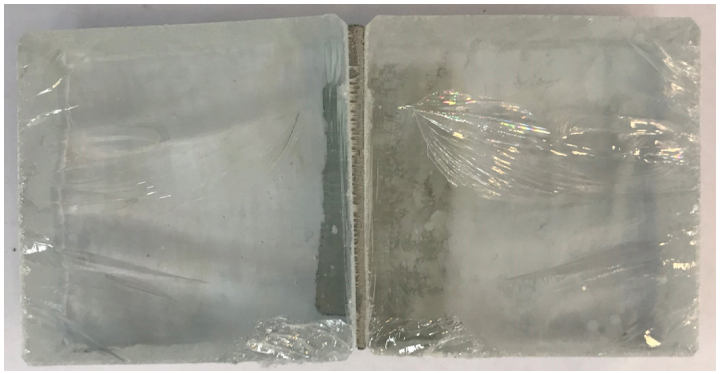

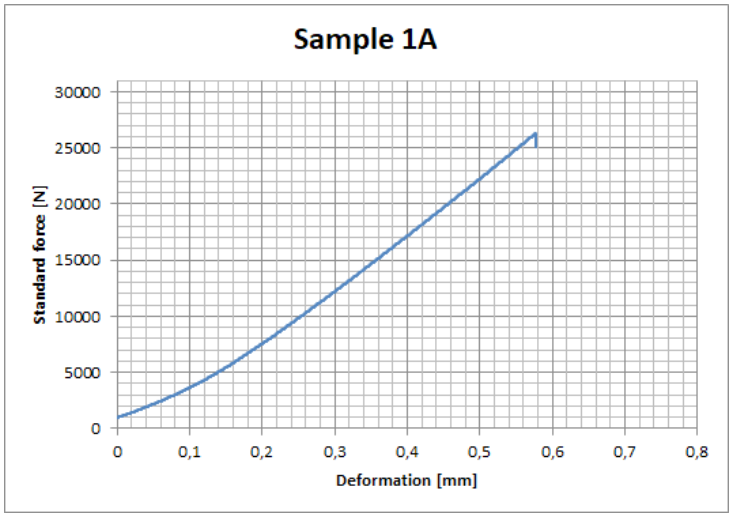

Figure III.16 - splitting experiment result sample 1A

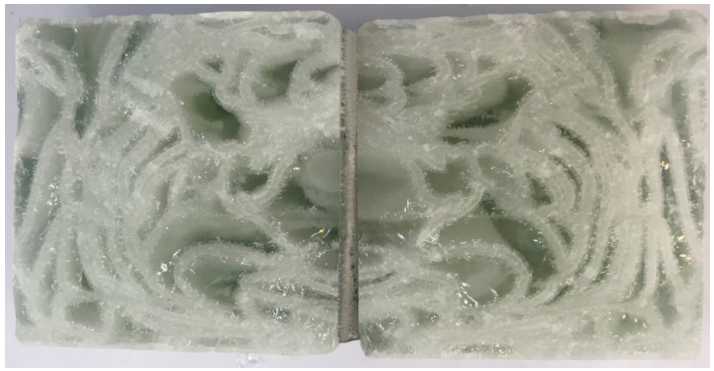

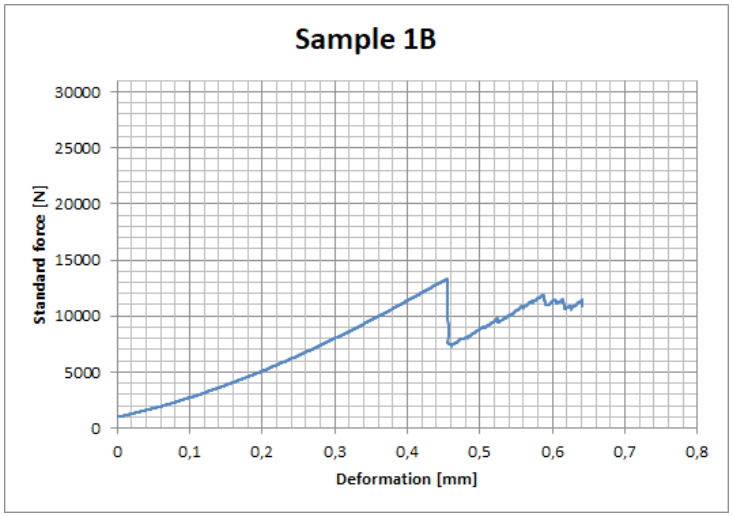

Figure III.17 - splitting experiment result sample 1B

6.2. Splitting experiment 2

Comparable to sample 1B, sample 2A underwent some cracking before breaking at 7kN and therefore the contact of the sample and the set-up was not well. Through the split of sample 2A can be observed that the split initiated at the corner, whereby the sample split, but remained as a cube after the break (see Appendix D), through some extra force the sample could be rip apart.

The inside of the sample is very glassy.

Likewise, sample 2B did not have good contact with the set-up, resulting in cracking (initial at 10kN) before breaking at 11kN.

The inside is very glassy.

Sample 2D shows that there are two obvious initiations of splitting at the corners. During the experiment an initial cracking sound was right before the break occurred, explaining the two cornered initiations of splitting.

The inside is very glassy, lots of bubbles and contamination is visible.

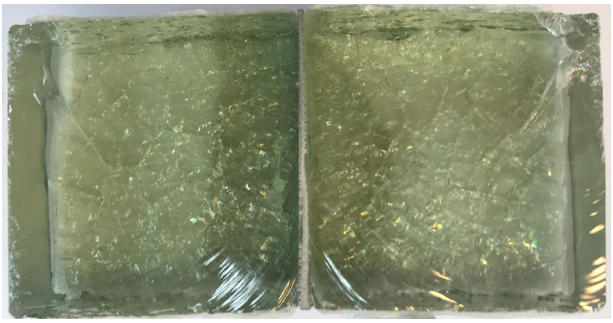

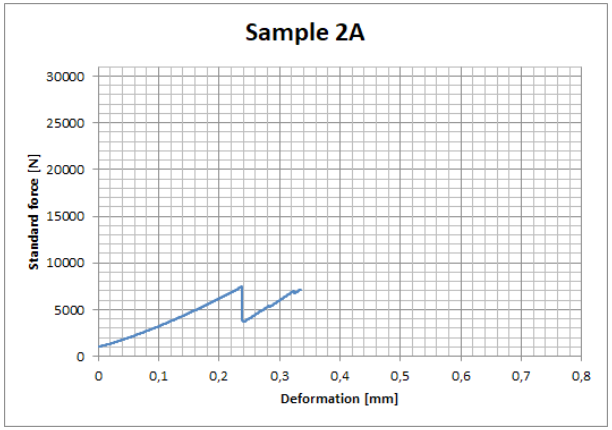

Figure III.18 - splitting experiment result sample 2A

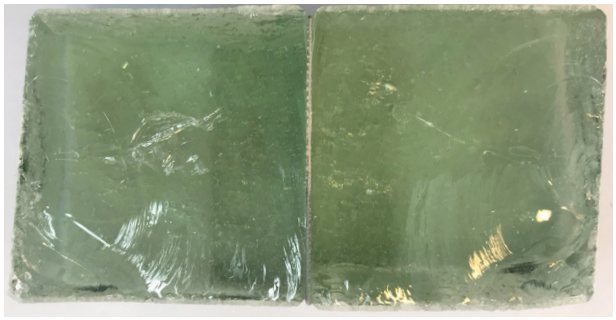

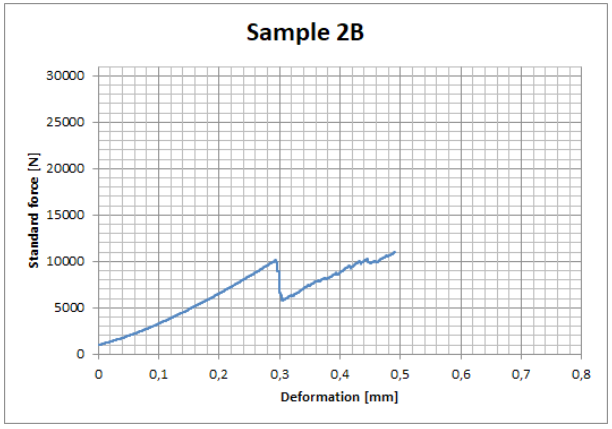

Figure III.19 - splitting experiment result sample 2B

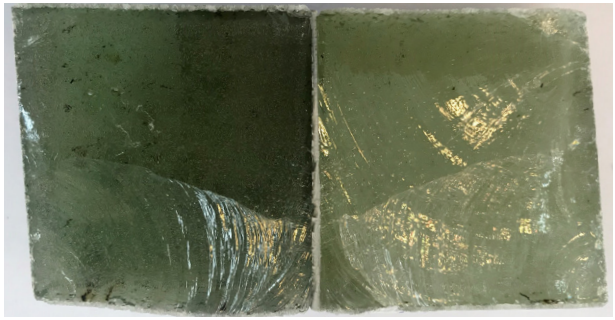

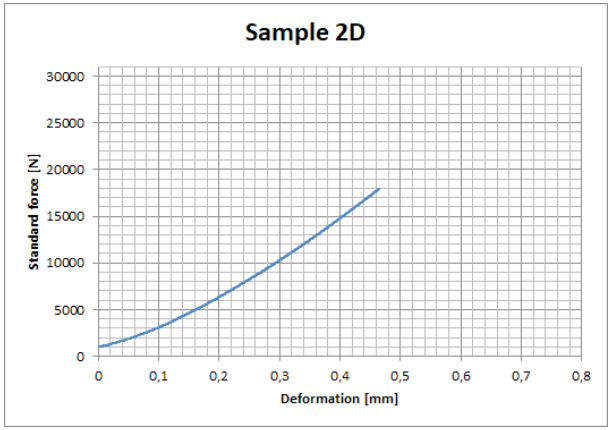

Figure III.20 - splitting experiment result sample 2D

6.3. Splitting experiment 4

Sample 4A already showed cracks at the upper right corner before the splitting experiment.

Before breaking, some minor cracks occurred but without a large drop in loading. However, the sample did not split thoroughly, the crack line does not go all around, whereas the sample could not be ripped apart to observe the inside.

Sample 4B had good contact with the set-up, the sample broke well, showing a clean crack at first glance.

Inside is very glassy with visible dots of crystallization.

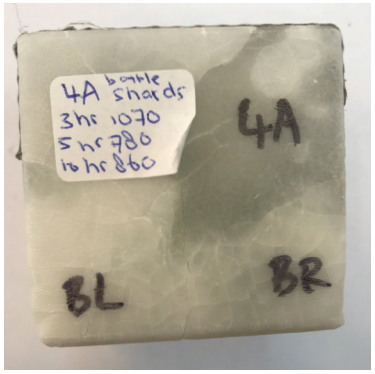

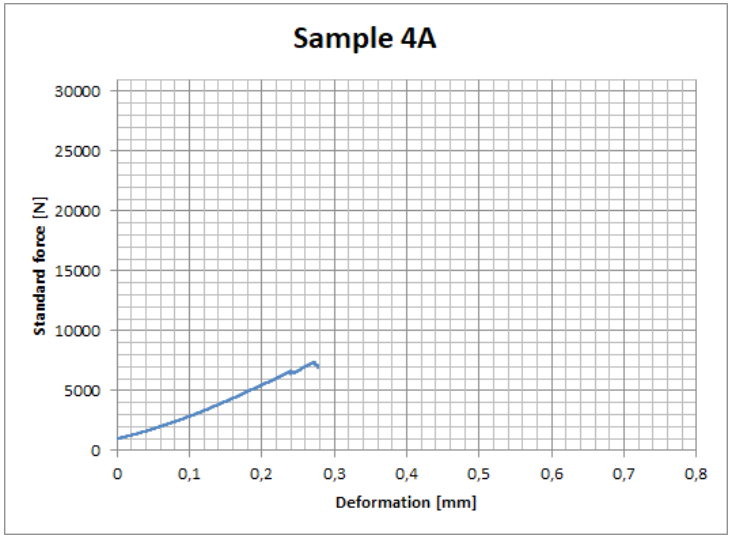

Figure III.21 - splitting experiment result sample 4A

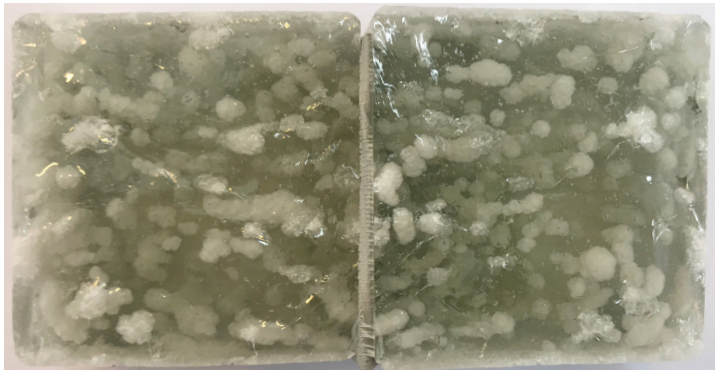

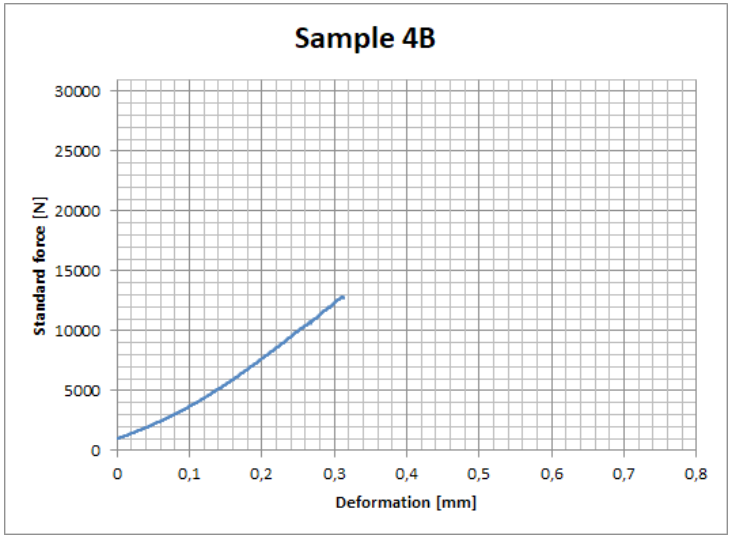

Figure III.22 - splitting experiment result sample 4B

6.4. Splitting experiment 5

Sample 5 had its initial cracking right before breaking at 20kN, which can be recalled in the graph, the slight drop in force right before breaking.

The sample did not split totally, remained as cube with crack line all around, had to be ripped apart.

Mainly crystalline inside, crystals formed along lines with similar line thickness, few glassy phases.

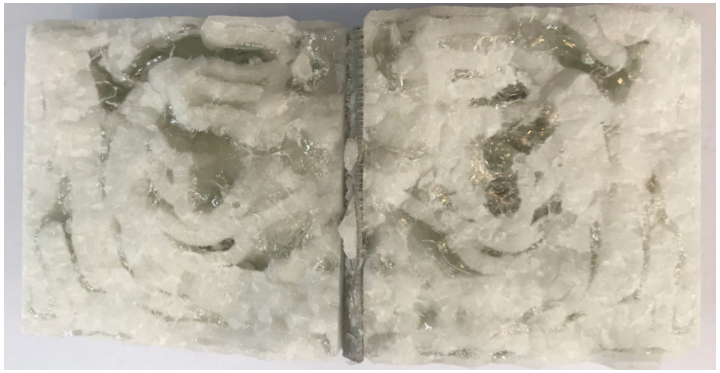

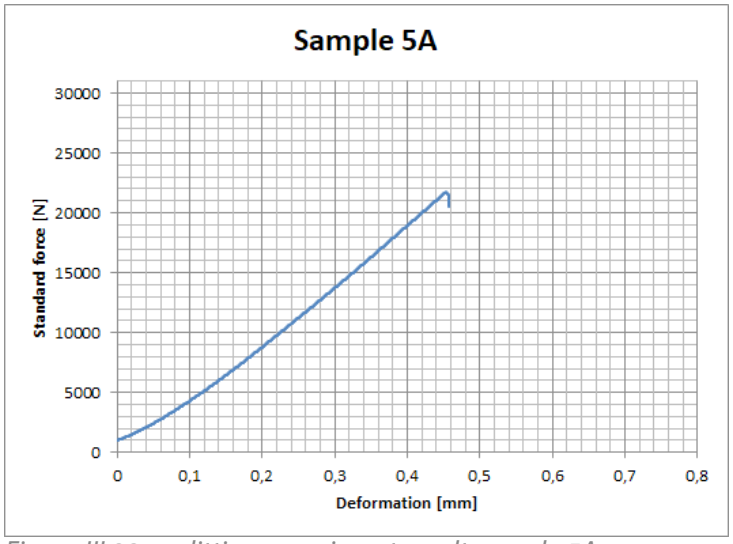

Figure III.23 - splitting experiment result sample 5A

As sample 5A, sample 5B underwent an initial crack at 28kN right before breaking at 29,5kN.

The inside of 5B is very solid, visibly about fully crystallized.

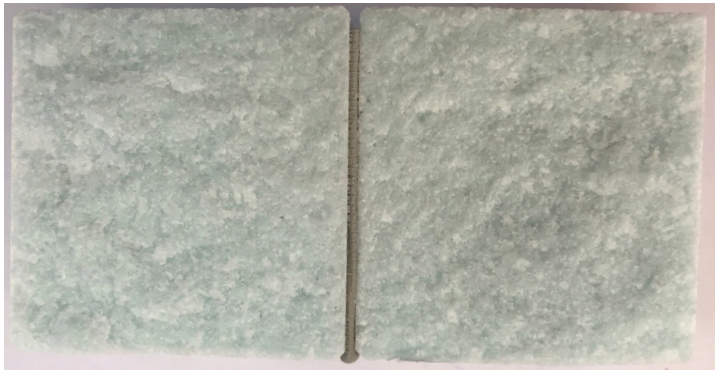

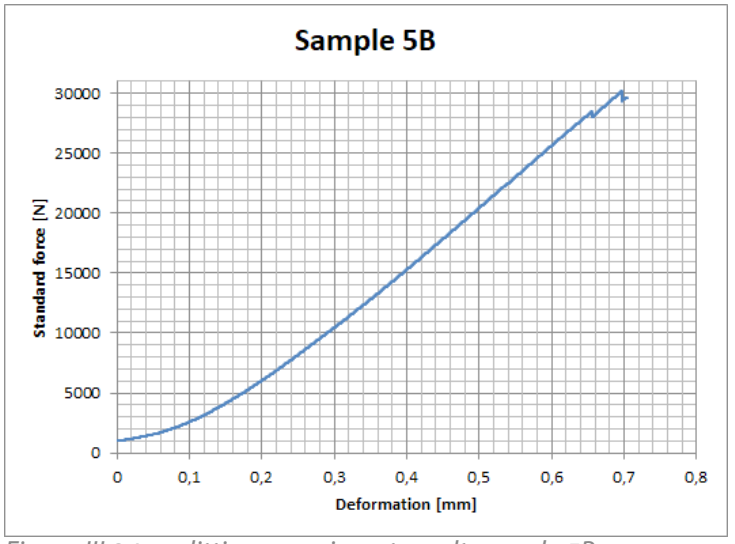

Figure III.24 - splitting experiment result sample 5B

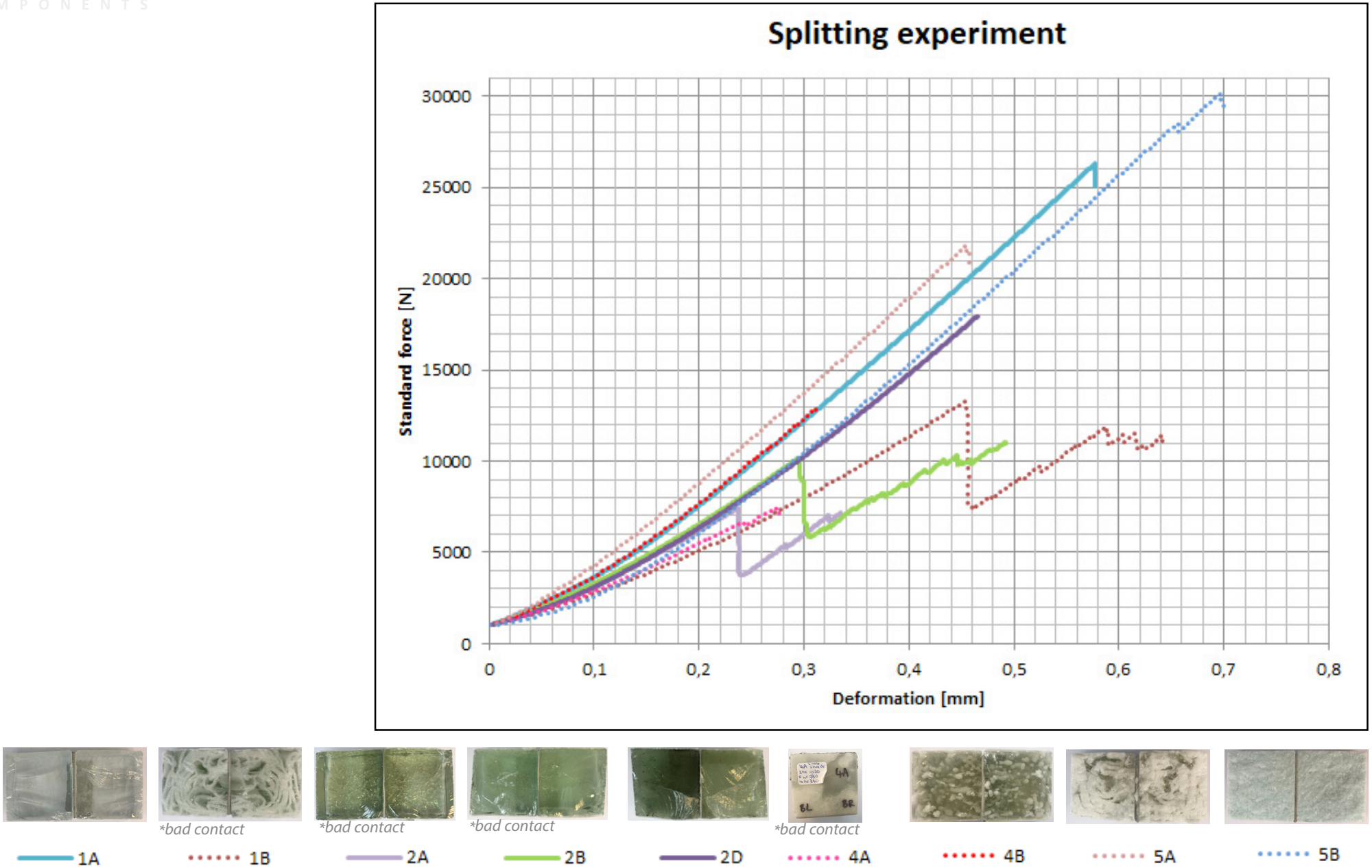

Figure III.25 - graph of all the splitting experiments (dotted lines are samples with visible crystallization)

6.5. Conclusion splitting experiments

Based on the flaws of the splitting experiment (see 'flaws'), the results of the splitting experiment will not be quantitively used to take conclusions, but rather observations between the different samples will be used for analysis. Figure III.25 shows an overview of all split samples.

Comparing based on force upon failure

The samples that withstood the highest force before failure are sample 1A, 2D, 5A and 5B (Table III.3). Remarkable is that these four samples are either mainly crystallized or glassy with no visible crystallization. Indicating that samples consisting of visibly mainly one phase, glassy or crystalline, are having a better structural capacity since it mostly behaves as one material and therefore not resulting in critical weak spots within the material. However, there is no absolute from those splitting experiments to set a conclusion about its structural capacities.

Comparing based on force-deformation relation

By comparing all samples through Figure III.25 and not including the samples which had bad contact (samples 1B, 2A and 2B), a relation can be found. All samples show a similar deformation pattern upon loading, the increase in force and deformation are all in a similar range. Whereas the assumption can be made that a glass-ceramic has the same structural behaviour as a glass upon loading. Hereby no difference is to be found in the amount of crystallization, for as well glassy, more glassy than crystalline or more crystalline than glassy samples the deformation upon loading relation appears similar. Whereas it is possible to use cast glass components as a reference for the usage of structural cast glass-ceramic components.

Comparing crystallized samples

By comparing the samples with visible crystallization; sample 4B, 5A and 5B, a rough conclusion can be taken about the visible crystallized samples. Samples 4B, 5A and 5B showed a rather similar behaviour upon breaking, some initial cracking right before breaking. Sample 1B and 4A are not included in this comparison due to the bad contact during the splitting experiment. Even so, it can be determined that the amount of crystallization is beneficial in terms of strength. Sample 5B, which is mainly crystallized was able to withstand the highest amount of force during these splitting experiments, followed by sample 5A and 4B.

Flaws

The first flaw to notice of these splitting experiments is the contact between the sample and the set-up, which for a few samples the contact was not optimal and therefore possibly might have influenced the result of the splitting experiment. The samples with bad contact are sample 1B, 2A, 2B and 4A.

Moreover, the size of the different samples is not exactly similar. This will not change the results abruptly but it does is another factor which should be taken into account.

Sample 4A is not included in the results comparison through the existing crack before the splitting experiment and a bad splitting result, whereby the interior could not be analysed.

Chapter 7 X-ray Diffraction

7.1. XRD results

X-ray diffraction (XRD) is used to obtain information about the atomic structure of materials and hereby used to differentiate the crystal structures. Table III.4 and Figure III.26 show the results of the XRD analysis, the XRD reports can be found in Appendix E.

Table III.4 - XRD result of sample 1B, 2A, 4B and 5B

Sample	Oven program	Compound/polymorph	Formula	Prcentage of crystallinity
1B- bottle shards 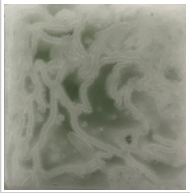	1: 3h 1050°C 10h 860°C 2: 10h 840°C	Wollastonite- 2M Cristobalite low	$CaSiO_3$ SiO_2	9%
2A- bottle shards 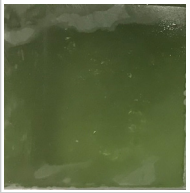	1: 10h 1120°C 2: 10h 840°C	Quartz low (alpha) Mullite	SiO_2 $Al_2.26SiO.74O4.87$	0%
4B- bottle cullet 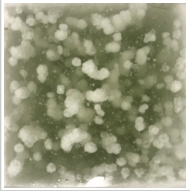	3h 1070°C 5h 780°C 10h 860°C	Wollastonite- 2M Cristobalite low	$CaSiO_3$ SiO_2	5%
5B- bottle cullet 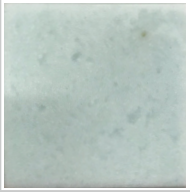	3h 1070°C 5h 760°C 10h 890°C	Cristobalite Coesite Sodium Calcium Silicate	SiO_2 SiO_2 $Na_2Ca_3Si_6O_{16}$	40%

7.2. The detected polymorphs

Based on the XRD result of the four samples (Figure III.26), seven different polymorphs are detected. Wollastonite-2M and cristobalite low were found in sample 1B and 4B, while quartz low and mullite are found in sample 2A and cristobalite, sodium calcium silicate and coesite are found in sample 5B. Table III.5 on the following page gives an overview of the characteristics of the different polymorphs.

Since wollastonite-2M is the main appearing crystal in samples 1B and 4B, a bit more research is done for this polymorph. Wollastonite-2M is a low temperature polytype of β-wollastonite, also named parawollastonite. β-wollastonite consists of 6 polytypes, 1T, 2M, 3T, 4T, 5T and 7T. The number indicates the number of subcells in each unit cell of the sub polytype, while M and T indicates the crystal system, either monoclinic or triclinic. β-wollastonite is formed below approximately 1120°C. For soda-lime-silica glasses β-wollastonite is a generic devitrification product. It arises through locally high concentration of lime. [54]

Cristobalite, mullite and coesite have the same molecule composition, but a different crystal structure, resulting in different material characteristics. Cristobalite consists of two types, cristobalite low and cristobalite high, which difference is mainly through the occurrence at a different temperature.

Since sodium calclium silicate is no crystal polymorph, based on its molecule formula it is assumed that it is the crystal polymorph devitrite. Devitrite is often confused with wollastonite because of its similar appearance and characteristics. However, limited information about devitrite is available, whereas Table III.5 does not give a complete overview.

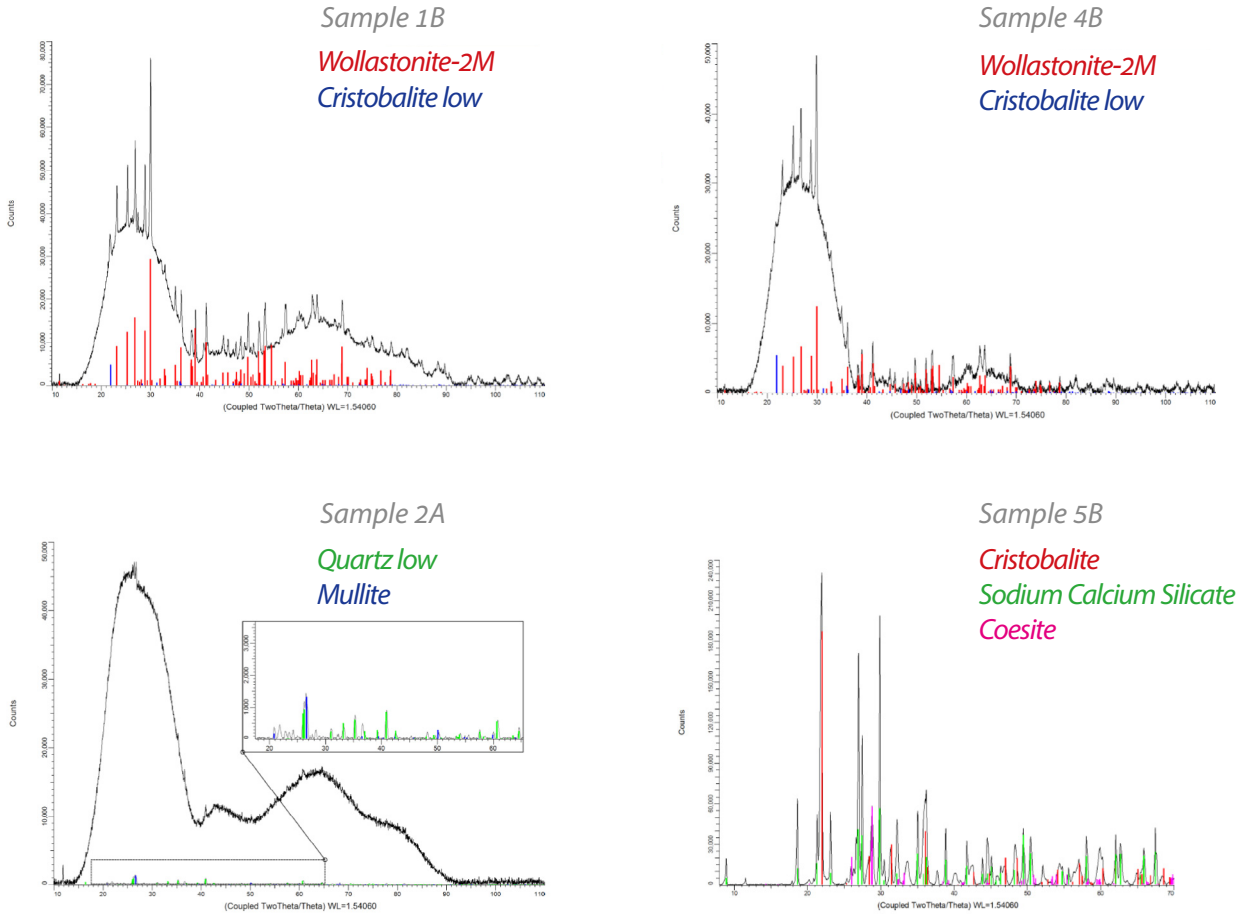

Figure III.26 - XRD graphs of samples 1B, 2A, 4B and 5B

7.3. Conclusions XRD

Based on the graphs of Figure III.26 can be concluded that, as expected, sample 2A has much more glassy phases than crystalline phases through its obvious amorphous halos and little crystalline spikes compared to the other samples. Whereby the crystalline traces are negligible small, its amount of crystallinity is rounded as 0%.

From the XRD analysis appears that the samples 1B and 4B consist of mainly wollastonite-2M. Glass has a hardness of 5,4 to 6,6 on Mohs hardness scale (chapter 2.1.1), while wollastonite-2M has a hardness of 4,5 to 5. In terms of hardness, wollastonite is less favourable compared to glass. However, the hardness does not seem to be a drawback. Theoretically the strength of crystalline material is generally stronger compared to glass (chapter 2.2) and in combination with the obtained fracture toughness of samples (chapter 6.5), the crystallinity does seem to have its structural advantage.

Sample 5B on the other hand consists of different crystal polymorphs than sample 1B and 4B. According to the XRD analysis there are slender glassy halos and multiple crystalline peaks. The detected crystal polymorphs are of a higher hardness compared to the other samples. Sample 5B showed a better failure toughness during the splitting experiment, which could be a result of the amount of crystallinity and the higher quality crystal polymorphs.

Table III.5 - characteristics of the detected crystal polymorphs

	wollastonite-2M [20][32]	cristobalite (low) [17][29]	quartz low [19][31]	mullite [18][30]	coesite [16][28]	devitrite [14][15]
Formula	$CaSiO_3$	SiO_2	SiO_2	$Al_{4+2x}Si_{2-2x}O_{10-x}$	SiO_2	$Na_2Ca_3Si_6O_{16}$
Refractive indices	1,616-1,631	1,484-1,487	1,54-1,55	1,63-1,69	1,593-1604	1,564-1,579
Crystal system	Monoclinic	Tetragonal	Trigonal	Orthorhombic	Monoclinic	Triclinic
Silica structure	Inosilicate, chain silicate	Tectosilicate, framework silicate	Tectosilicate, framework silicate	Nesosubsilicate, chain aluminosilicate	Tectosilicate, framework silicate	Inosilicate, chain silicate
Shape	Fibrous or needle-like growths or laths	Dendritic form, normally 90 degree branching, but sporadically occuring at 55 degree branching	-	-	-	Needle-like
Lustre	Vitreous, silky	Vitreous, greasy	Vitreous, greasy, waxy, unpolished	Vitreous	Vitreous	-
Break	Splintery	Conchoidal	Conchoidal, irregular, splintery	-	Sub-conchoidal	Splintery
Colour	White	Colourless, white, blue grey, brown, grey	Colorlesss, white, grey, yellow, violet, pink, brown, black, green, blue, red	Colorlesss, white, yellow, pink, red, gray	Colourless	-
Mohs hardness	4,5 - 5	6 - 7	7	6 - 7	7,5- 8	-

Chapter 8 Microscopy

After the splitting experiment samples 1B, 2A, 4B, 5A, 5B and 6A were observed under the microscope to see the crystalline structures (mainly wollastonite-2M), the glassy and crystalline interfaces and tracks of the failure mechanism. Digital microscope Keyence (VHX-5000) has been used for the microscopic imagery, Appendix F gives all retrieved microscopic material.

8.1. Sample 1B

Figure III.27 shows conchoidal cracks through the glassy phase till it meets a crystallized surface. The crystals seem to stop the crack from its continuity; however, it also seems that cracks start from the other side of the crystallized surface. Suggesting that a crystallized surface or line is detaining the failure, but not stopping the failure, whereas the energy of the crack still continues, showing a different crack pattern through the different phases.

Figure III.28 shows a crack that goes from a crystallized surface/line to an air bubble, however, the crack seems to have lost its energy and stopped at the air bubble. Zooming in on the air bubble, two fractures can be observed. The one visible of the crystal, whereby the last crystal is at the air bubble. The cracks through the crystal are following its acicular structure. The second fracture is the fracture wave going from right to left and stopping at the intersection with the cracked crystal line.

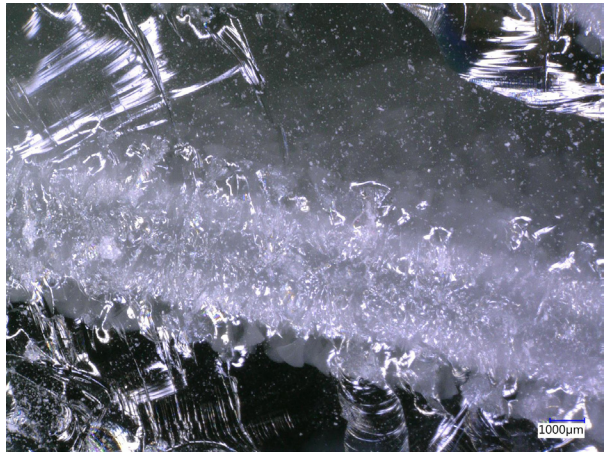

Figure III.27 - transition of crack from glassy to crystalline phase in sample 1B

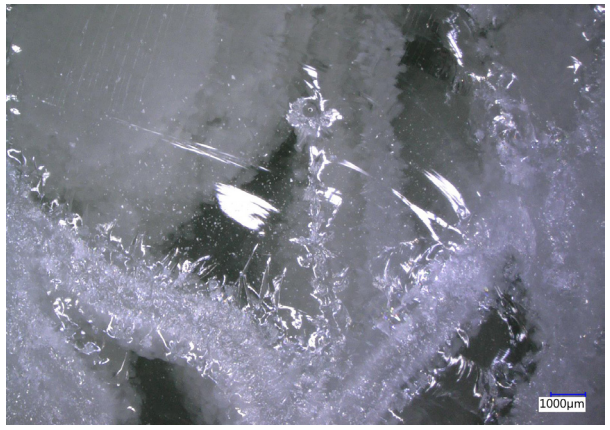

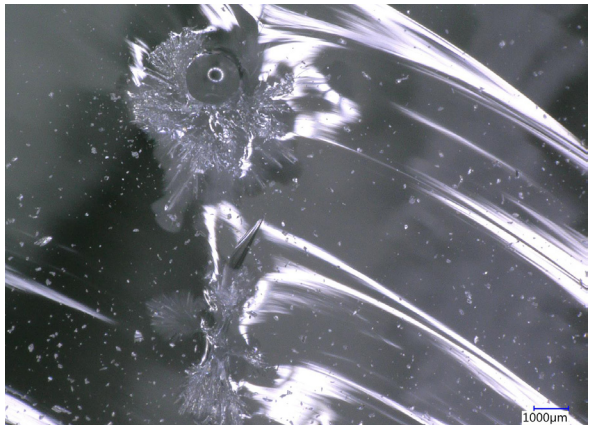

Figure III.28 - left: crack from crystals to air bubble in sample 1B. right: zoom of air bubble

From the edge and corner of sample 1B can be observed that there are multiple crack initiations, Figure III.29.

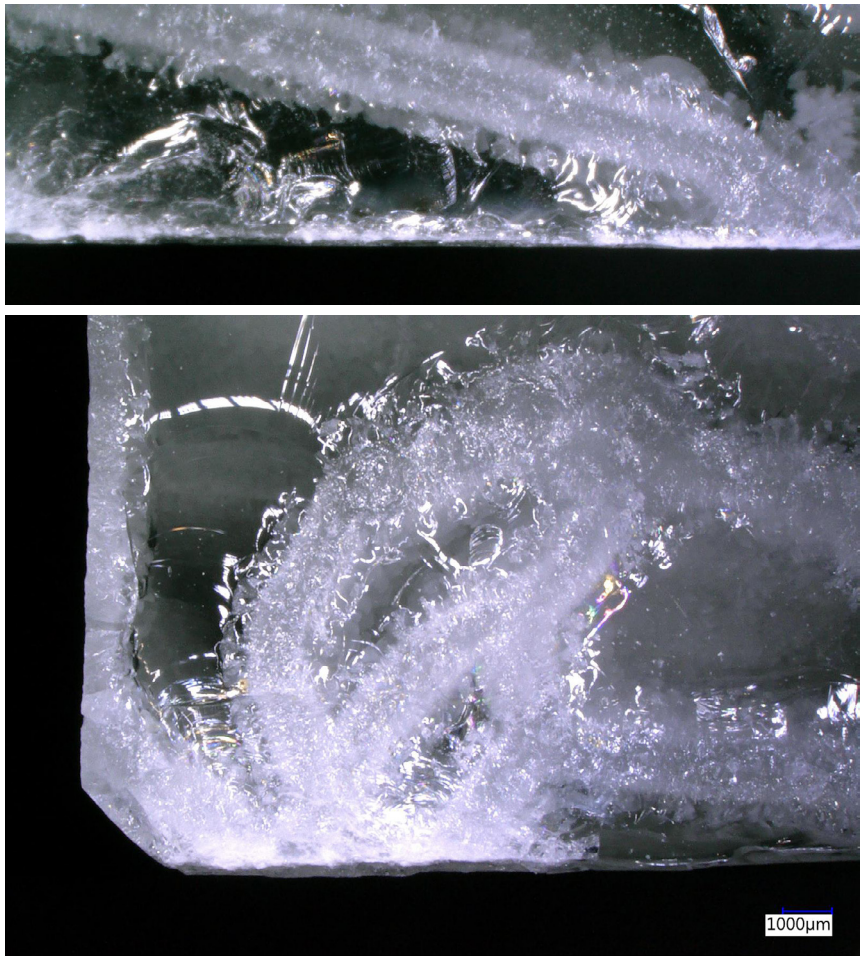

Figure III.29 - edge and corner of sample 1B

Figure III.30 shows the shape of the crystals, which are shaped like fans. Starting from a centric point and having acicular crystals going divergent into a fan shape, creating a flaky bed of crystals continuing in 3 dimensions. The white silky acicular shape corresponds to the shape of wollastonite-2M (white, silky, needle-like) rather than cristobalite low (white, greasy, dendritic), confirming that the (majority of the) visible crystals are wollastonite-2M.

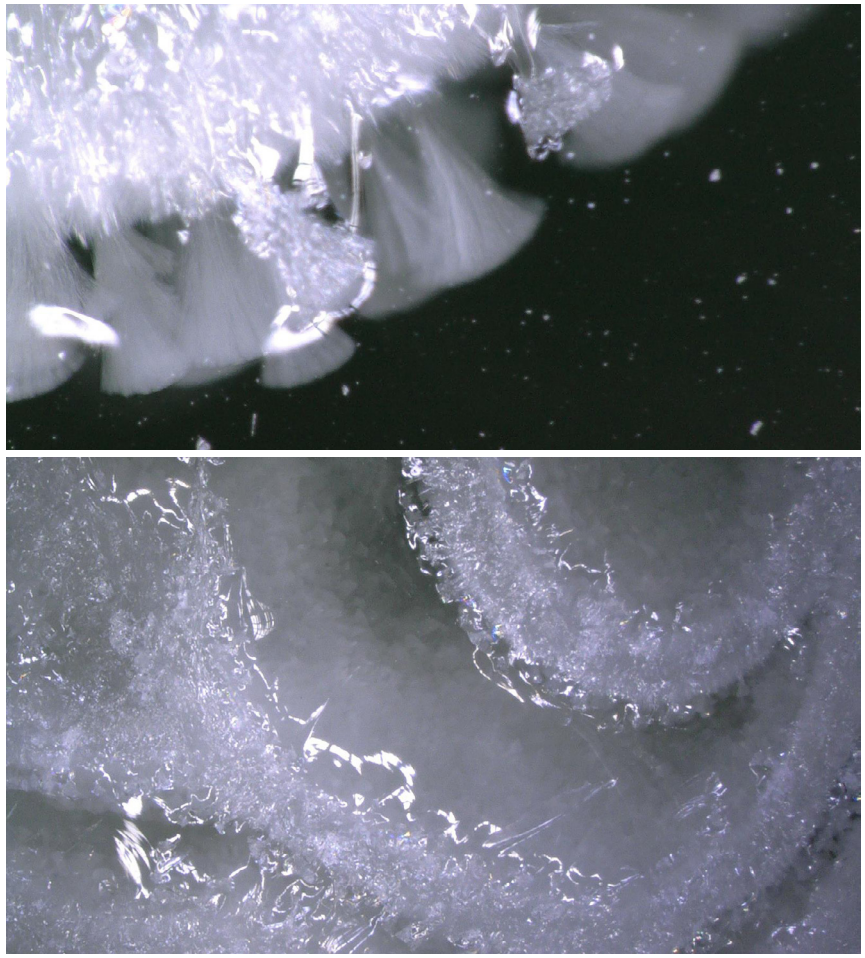

Figure III.30 - crystal shape and 3D continuity of crystals in sample 1B

8.2. Sample 2A

Figure III.31 shows that sample 2A has multiple failures along its edge, especially at its right corner, but the left picture shows the origin of the actual failure.

In Figure III.32 an arrest line can be observed. Visible lines can be observed going from the bottom right corner up to the top left corner. Those conchoidal movement of lines are the result of the origin of the crack in the left bottom corner (Figure III.31 left). These movement of lines are interrupted by an arrest line, which is showing another failure movement than the crack started from the bottom left corner.

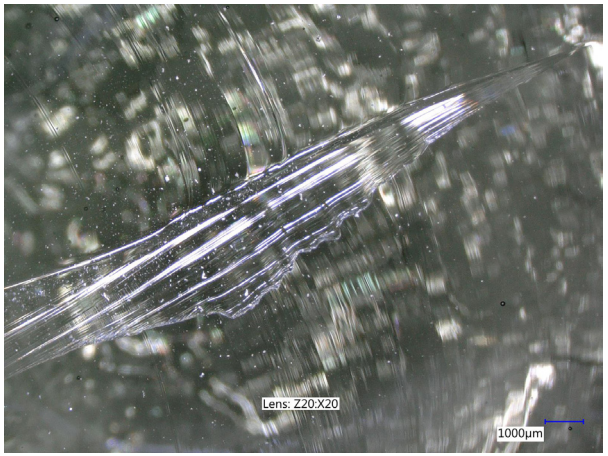

Figure III.32 - arrest line and crack propagation in sample 2A

Figure III.31 - multiple failure origins in sample 2A
left: failure original point at left corner
middle: zoom of Left picture (note: different lighting)
right: minor origins, non critical

At first glance, sample 2A looks very glassy and transparent, with no visible crystallization. However, through the XRD analysis from Chapter 7 it was defined that sample 2A does have crystals in the form of alpha-quartz and mullite. Whereas the small particles in Figure III.33 may possibly be nuclei or crystals, but it may also be contamination.

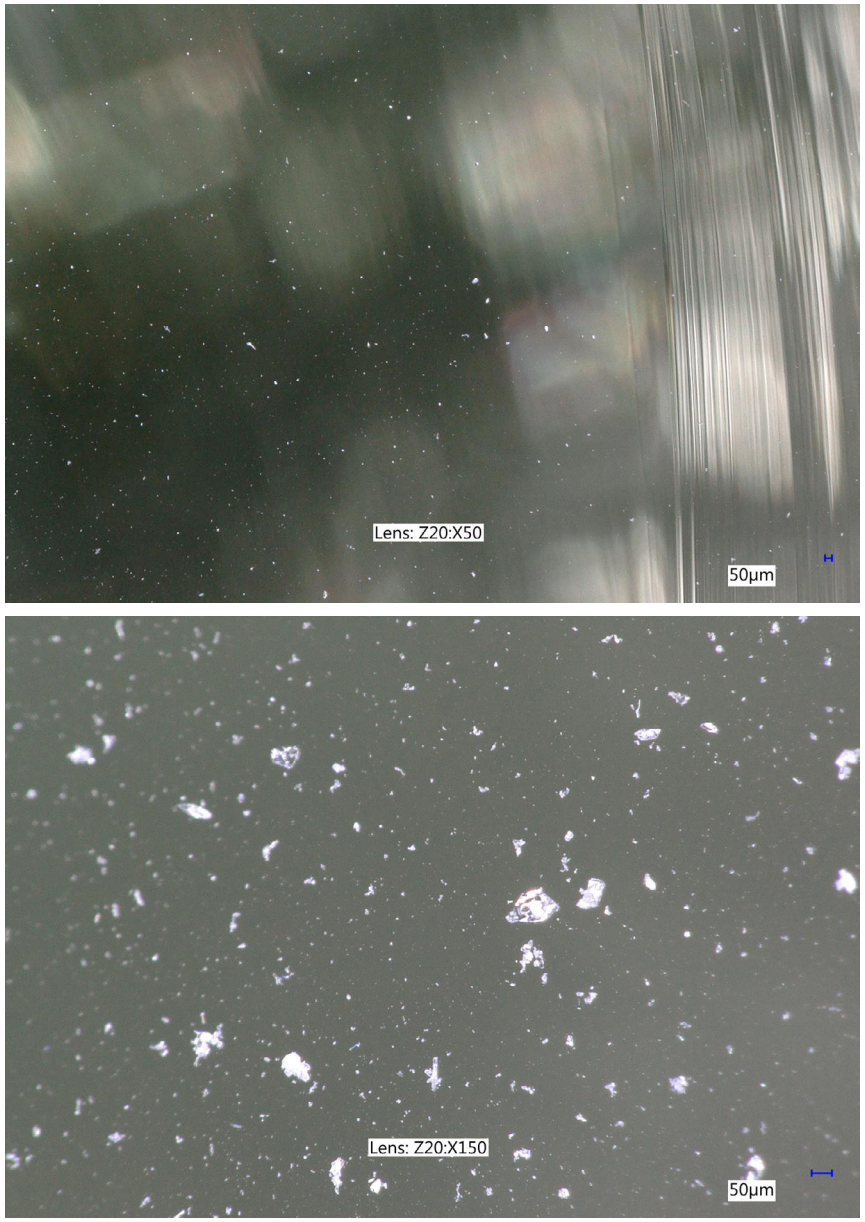

Figure III.33 - small particles in sample 2A

8.3. Sample 4B

Through Figure III.34 can be observed that multiple small cracks occurred along de corners and edges of sample 4B. Seemingly the crystals are withholding the cracks to continue its propagation. In both bottom corners, left and right, an origin of a failure can be found.

Through Figure III.35 several things can be observed. Through the microscope a lot more air bubbles are visible than by eye. Traces of failure propagation can be observed in both glassy phase and crystal. In the glassy phase lines are visible in the lower right corner, those lines are a propagation of the origin in the bottom right corner. The crystal on the cracked surface suggests a broken crystal through the split, where the energy of the failure seems to propagate through all its ends. The intersection of the glassy phase and the crystal seem to have stopped the original crack from the bottom right corner, on the left side of the crystal no visible lines of crack propagation are visible. Yet, at the middle part of the crystal an origin of a new crack seems to have occurred. The lines seem curving into the direction of the upper left corner.

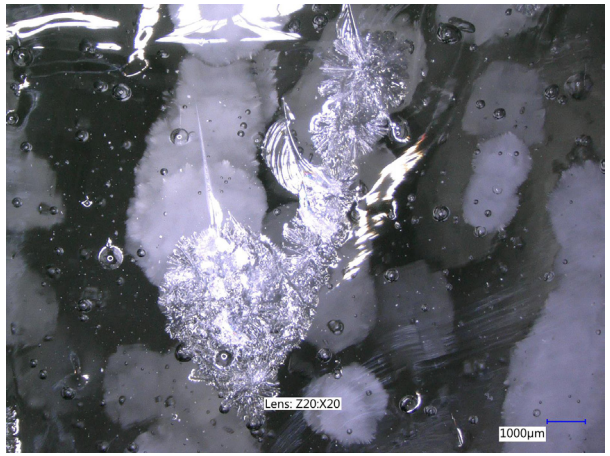

Figure III.35 - failure of a crystal in sample 4B

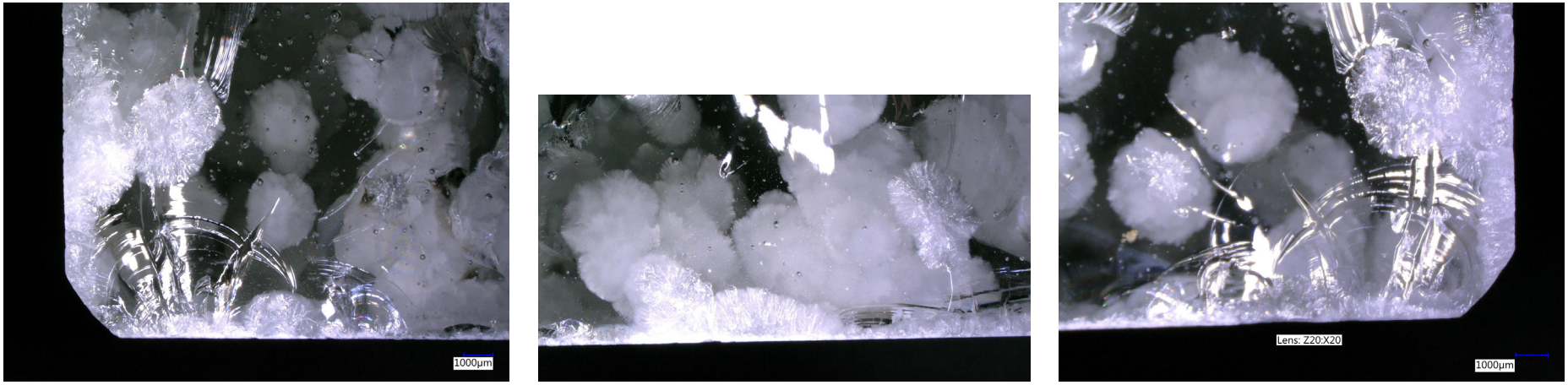

Figure III.34 - cracks along edge of sample 4B
left: left corner
middle: edge
right: right corner

The crystals have an acicular shape in the form of a dot, Figure III.36. It looks different than the fan-shape crystals in sample 1B, but are also wollastonite-2M crystals. These dots are randomly distributed throughout sample 4B and found in irregular sized clusters.

Figure III.36 - zoomed on crystals in sample 4B
top: focus on front
bottom: focus on back

By zooming in on a broken crystal, its acicular nature is visible, Figure III.37. Also notable is the failure starting somewhere in the crystal and reaches to the ends of its 'needles', but without necessarily propagation of the crack over to the glassy phase.

Another visible characteristic of wollastonite-2M is the splintery break, which is observable in Figure III.36 and Figure III.37, rather than the conchoidal break pattern of cristobalite low.

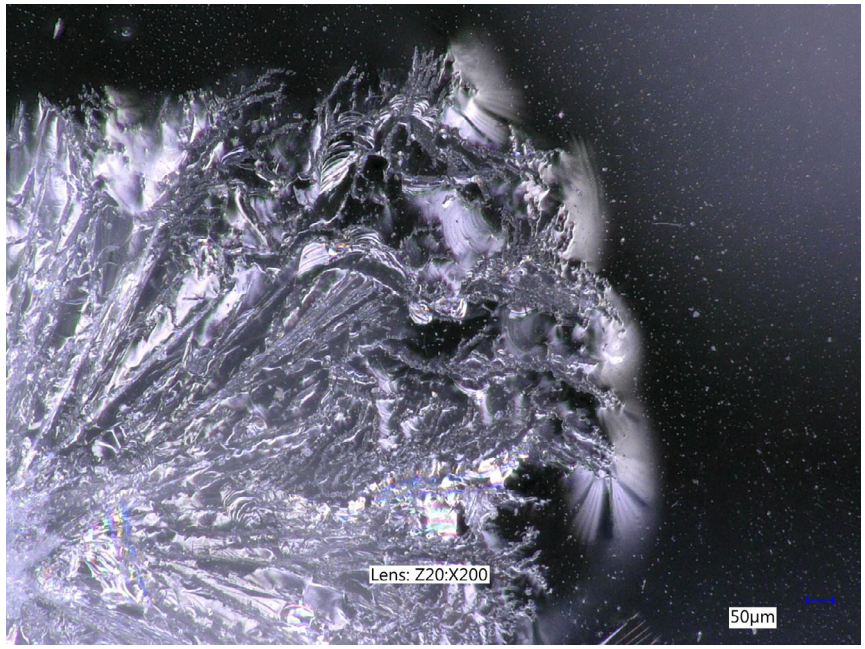

Figure III.37 - zoomed failure of a crystal in sample 4B

8.4. Sample 5A

Sample 5A has visibly more crystalline phases than glassy phases, which is recurring under the microscopic pictures, Figure III.38 and Figure III.39. The large amount of crystalline phases along the edge conceals the failure propagation.

The glassy phases do show visible cracks and failure patterns; however, those patterns cannot be tracked over the crystalline phases.

Other than that, the crystalline phases are like patched connected to each other. Comparing to sample 1B and 4B, sample 5A gives a more solid structure of the crystals.

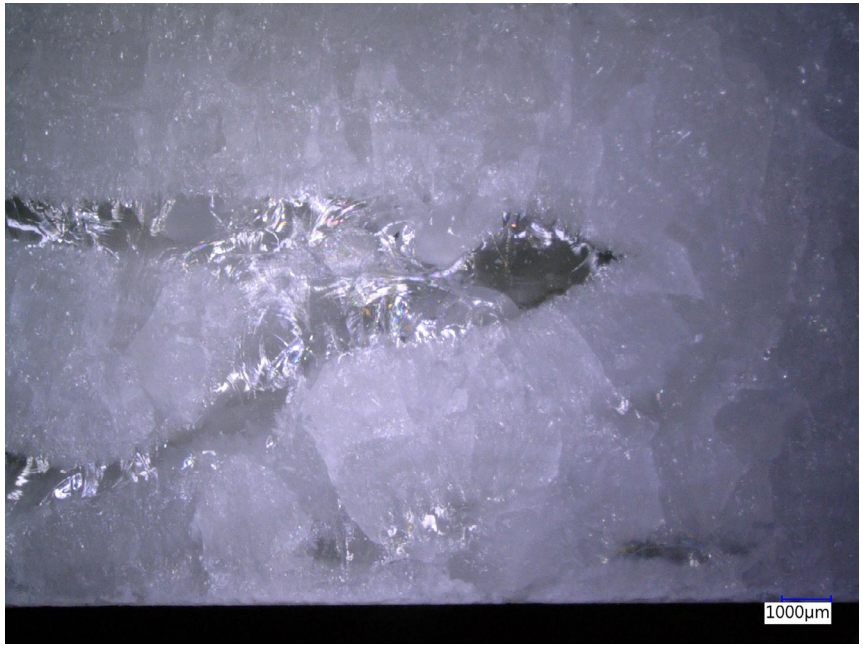

Figure III.38 - edge of sample 5A

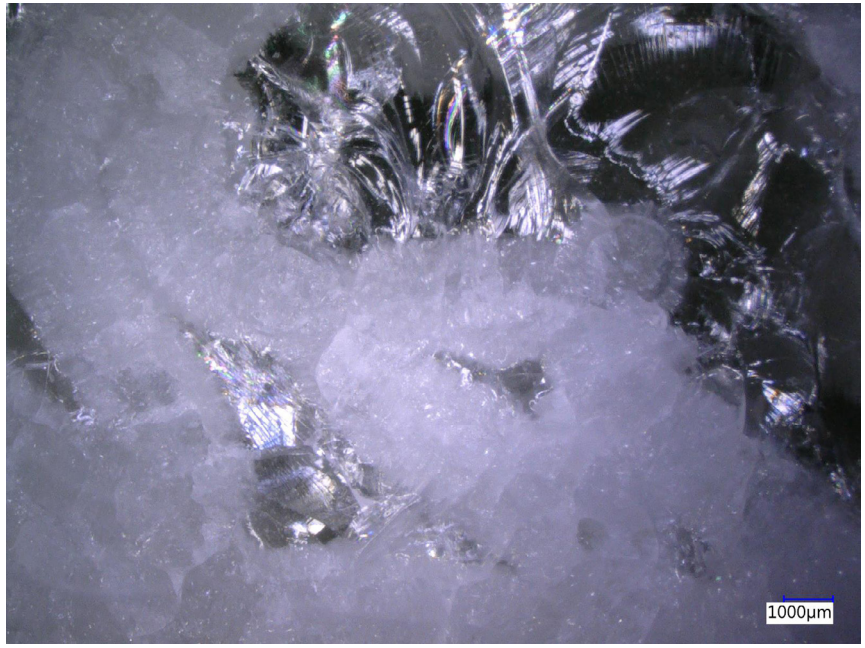

Figure III.39 - center of sample 5A

8.5. Sample 5B

Even under the microscope sample 5B looks rather crystalline. Through the crystallization the transparancy of the sample is largely reduced. Resulting in no visible aspects in terms of failure propagation, Figure III.40 and Figure III.41.

Figure III.40 - edge of sample 5B

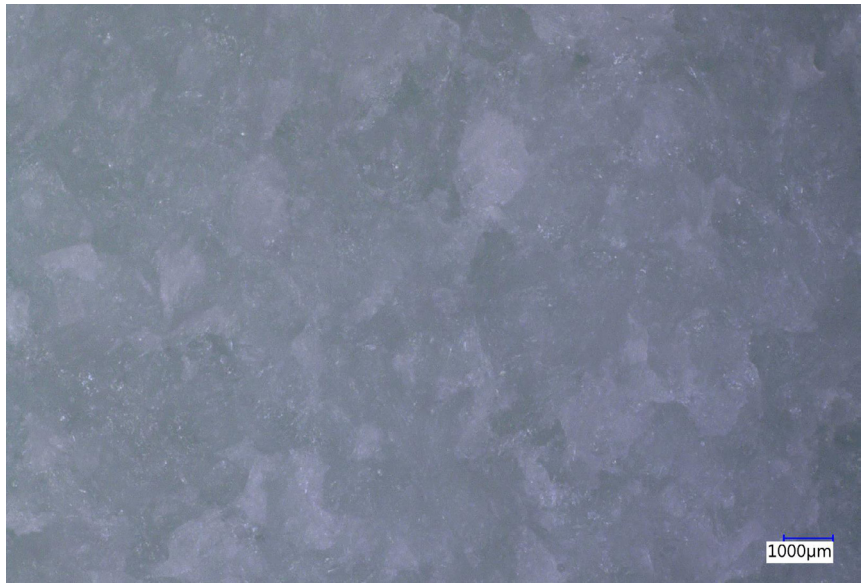

Figure III.41 - center of sample 5B

8.6. Sample 6A

Sample 6A did not go through the splitting test, however, the fractured corner upon cutting is used for observation under the microscope.

The surface of the broken corner looks very rough. As lots of thin crystallized lines are broken and cut.

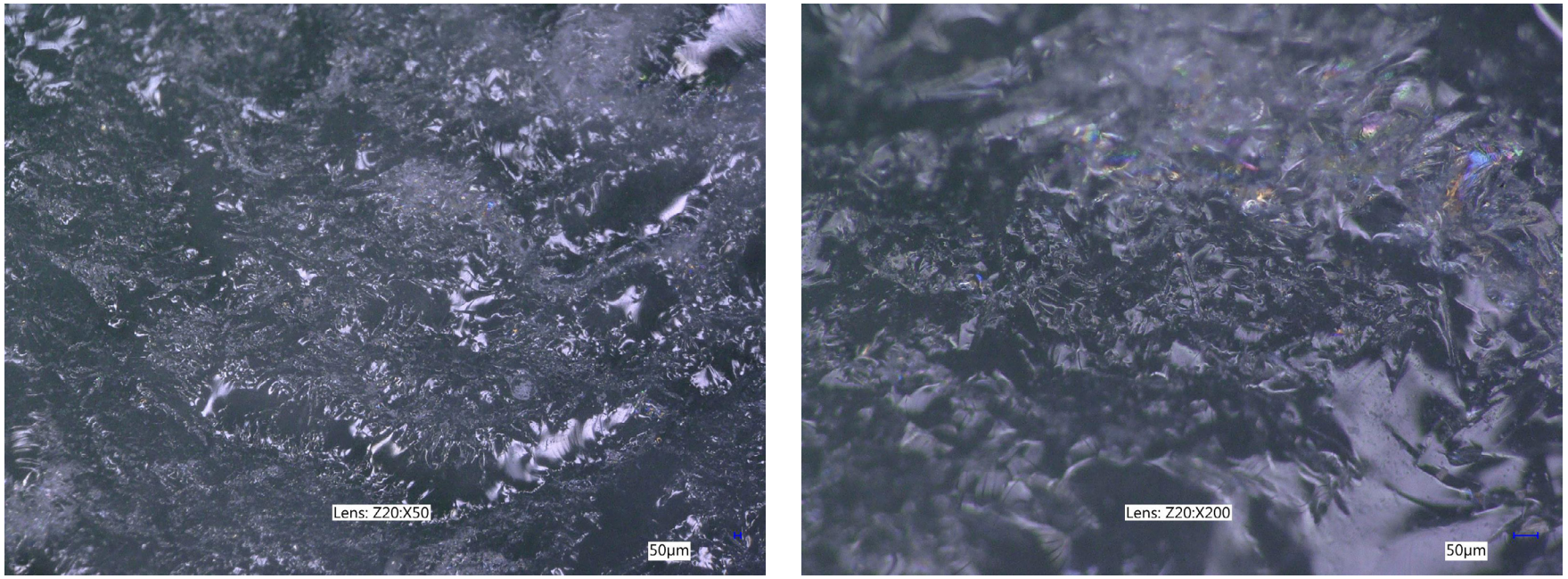

Figure III.42 - surface of broken corner of sample 6A
left: regular view
right: zoomed view

8.7. Conclusions microscopy

Based on the microscopic analysis, several crucial findings can be determined.

Wollastonite-2M

Through the microscopic images can be observed that the visible crystals are indeed wollastonite-2M crystals rather than cristobalite low crystals in samples 1B and 4B. The crystals are distinguished through their crystal appearance and the failure pattern.
The observed crystals are white, silky and acicular, as wollastonite-2M crystals. Cristobalite low crystals can be of more colours, as white, blue grey, brown, grey or even colourless, it looks greasy and has a more dendritic form (Table III.5). The acicular crystal in sample 1B are more fan shaped, while in sample 4B the acicular crystals are dot shaped. Even though this difference, the crystals in both samples are still the same.
The failure pattern of wollastonite-2M is more splintery-like as the samples show, while for cristobalite low the failure pattern is conchoidal.

Failure propagation through phase change

Through observing failure propagation from glassy phase to crystalline phase and back to glassy phase an interesting finding is observed. Through a glassy phase the failure propagates conchoidal, when reaching a crystal or crystalline surface, the crystal acts like an obstacle and delays the failure propagation. The failure thereupon does continue and follows the acicular shape of the crystal. Once reaching the ends of the crystals, the failure propagates from crystal to glassy phase, hereby the energy and direction is different compared to the propagation in the initial glassy phase. Concluding that the presence of a crystal or crystalline surface arrest the primary failure propagation.

Summary part III - LABORATORY TESTS

SQ 4. What is the relation between composition, forming temperature, thermal treatment and crystallization?

From part II- Literature study could be determined that different parameters are of influence. The glass type has been split into glass size, additional flux and glass composition. The glass size influences the amount and distribution of the crystals, through the distribution and amount of preferential sites. The usage of cullet results in a more well-distributed and uniform crystallization throughout the sample, whereas glass shards result in more localized crystallization dependent on the placement of the shards. The addition of flux could be favourable towards crystallization, since the flux lowers the viscosity and forming temperature, whereas compounds are more freely to move. However, the amount of flux used during the melting experiments did not result in a favourable result and are therefore neglected in this research. Through melting experiment 5 to 8 can be determined that small differences in composition (amount of property modifiers) results in different melting points and required heat treatment. Hereby the melting temperature should be lower than the liquidus point, to remain preferential sites in the sample for crystallization to occur, but high enough to melt the glass in order to avoid fusing. The temperatures applied for nucleation and crystal growth are a bit lower and higher than the optimum crystallization temperature, based on theory and trial and error.

SQ5. What is the influence of crystallization on the fracture toughness of a cast glass-ceramic component?

Due to the limited number of samples and the flaws through execution, no absolute answer can be given but rather an indication of the influence of crystallization towards the fracture toughness can be described. A sample consisting mainly of one phase (majority glassy or large amount of crystallinity, sample 1A, 2D, 5A and 5B) are structurally more enhanced compared to the more mixed samples (sample 1B and 4B). Besides the amount of crystallinity, the type of crystal polymorph also influences the structural capacity. Each crystal polymorph has its own mechanical characteristics, resulting in different failure toughnesses. In addition, the deformation behaviour upon loading is similar for all samples, indicating that a cast glass component can be used as structural reference for a cast glass-ceramic component.

SQ6. What is the influence of crystallization on the fracture behaviour of a cast glass-ceramic component?

Through the observation of the split samples, a clear difference can be observed through the fracture behaviour of glassy and crystalline phases. A fracture initiates at the edge of the sample, whereas in most samples its initial fail starts at a corner. Through the glassy phases the fracture propagation can be clearly observed through its conchoidal fracture marks. Once a fracture reaches a crystalline surface or a crystal, the crystallized part arrests the fracture and in most cases the fracture continues from the crystal over to the glassy phase, but its energy and direction changes. Therefore, a failure propagation through glassy and crystalline phases interact differently but yet there do is interaction between both phases.

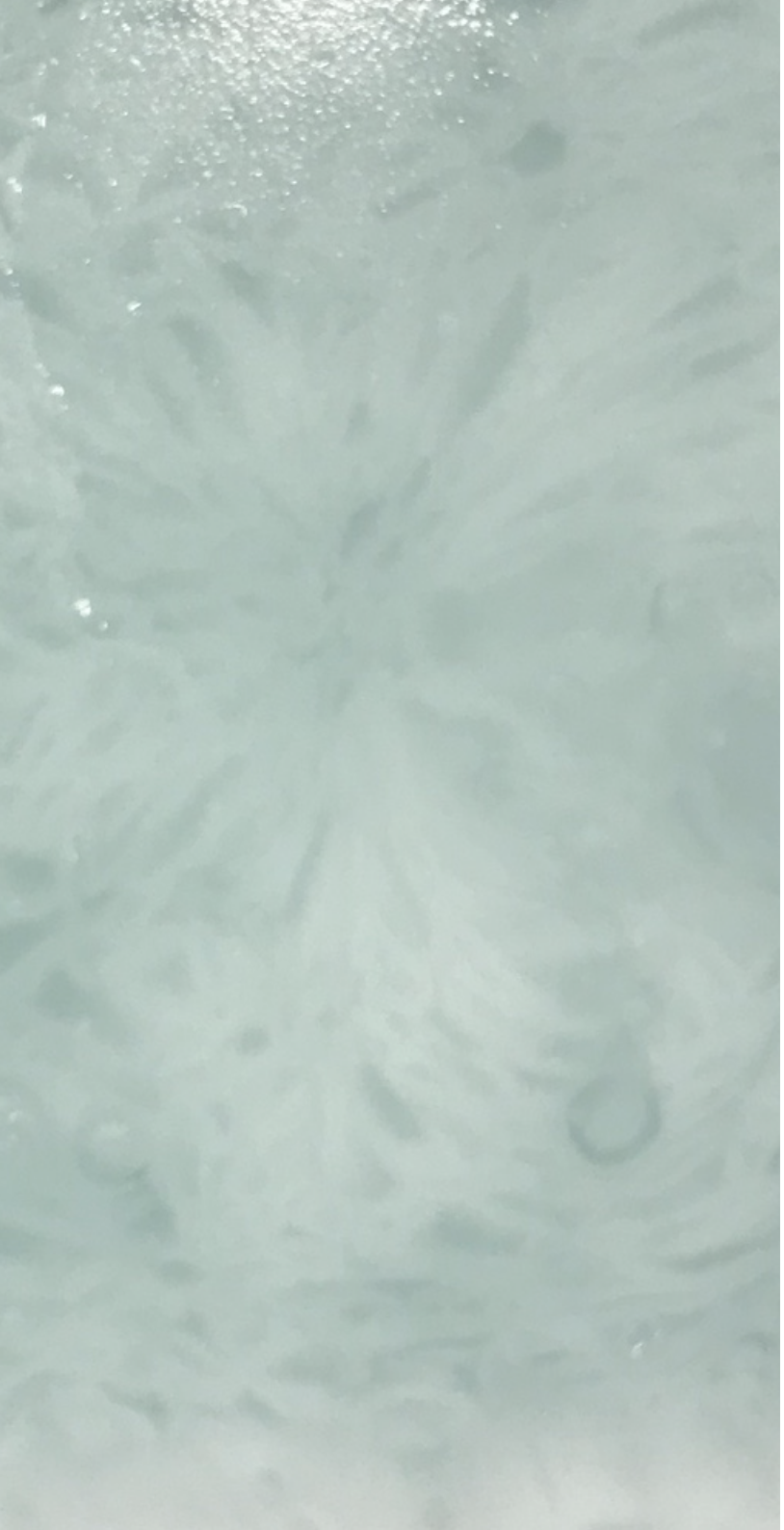

PART IV - FINAL REMARKS

Chapter 9 Discussions

The *melting experiments* have depicted the influences of the different applied temperatures on different glass compositions. From the melting experiments, and the DSC/DTA curves obtained from literature can be observed that each glass composition has a different crystallization temperature and melting temperature even though it all is soda-lime-silica glass.
Through the melting experiments could be observed that the applied melting temperature is crucial towards the crystallization in a sample. From melting experiment 1, 2 and 3 can be concluded that applying melting temperatures too low or too high are disadvantageous.
When the applied melting temperature is too low, the glass does not melt but rather fuse, e.g. sample 3A. Fused samples are taken as undesired in this research, due to increased unknown factors as porosity and bonding strength between fused particles.
High melting temperatures were expected to be advantageous since samples would get fully homogenized, whereupon homogeneous nucleation could create a consistent glass-ceramic. However, temperatures too high are getting too close or at the liquidus temperature, whereas samples are fully melted and homogenized, leaving no preferential sites for crystallization, e.g. sample 2A, 2B and 2D. Through the applied heat treatment sample 2A, 2B, 2D did not show any visible crystallization. Whereupon the focus was set to surface nucleation rather than homogeneous nucleation.
The crystallized samples (e.g. sample 1B, 4A, 4B, 5A) underwent heat treatment at a melting temperature high enough to melt and solidify as a volume, but without fully homogenizing and thus leaving preferential sites for nuclei to form.
The applied temperatures are therefore only an indication of applicable temperatures (and thermal treatment) ranges, but through the differences in glass size and glass composition, each sample has its own temperature curve and optimum temperatures.

After understanding the creation of crystallized samples, parameters were taken out, such as; different glass sizes, different glass bottles and the use of different ovens.
The difference in crystallization per sample of the same melting experiment, is depicted through melting experiments 7 and 8. These samples are all from soda-lime-silica (bottle) glass in the form of cullet and underwent the same heat treatment per melting experiment, yet the result is very different.
From the *XRF analysis* can be noticed that small differences are present in the composition. All soda, lime and silica are in a lower amount present in the water bottle (sample 7B) compared to the wine bottle (sample 7A). At which the water bottle consists of more property modifiers and colorants.
The most significant difference is in the amount of main modifiers (CaO, MgO and Al_2O_3), the water bottle consists of about 1.5wt% more modifiers. These modifiers, among other things, make the melt less soluble, explaining the higher liquidus point of the water bottles compared to the wine bottles.
The samples using wine bottles as cullet, crystallized when using a melting temperature of 1050°C (sample 5B), while using 1070°C and the same crystallization heat treatment (sample 7A) resulted in little crystallization, concluding that the temperature of 1070°C was getting around the liquidus point and thus being unfavourable in terms of crystallization. While for the water bottle the melting temperature of 1050 and 1070°C did not result in much differences in the glass-ceramic, whereas it can be concluded that the liquidus point of the water bottles is higher than the used melting temperatures.
Moreover, according to literature [33] the modifiers stimulate crystallization, which can explain the tendency of crystallization in all water bottles samples (sample 6A, 7B and 8B) under different heat treatments.

Through the *splitting experiments* an indication is given about the fracture toughness and fracture behaviour of the glass-ceramic samples. As a consequence of the limited samples and variations per sample, only observations are used and no quantitively conclusions.
In terms of fracture toughness can be observed that samples which are visibly mainly ceramic or mainly glassy are tougher to break compared to more equally mixed samples. Where the minority phase can result in localized stresses and therefor the cause to failure. The force-deformation relation between all samples seem similar, it deforms in a similar rate upon loading.
All by all, there is no clear or strict difference between the more glassy and more crystalline samples. According to expectations, the more glassy and more crystalline samples would behave differently throughout the splitting experiment, e.g. an abrupt failure or the occurrence of cracking before total failure, or a clear division in failure toughness, endurance and maximum deformation.
However, during the analysis of the performances of the splitting experiments, the flaws during the experiments have to be taken into account, which might be the reason of deviations of results. It should be considered that the samples are not of exact the same size, surfaces can be slightly inclined, which both can result in a contact between the sample and set-up that is not optimal. Thereby, the number of samples is very limited, whereas small flaws of samples or performances are of great influence towards the results, as no average can be taken or comparison can be done to normalize results.

Through *microscopic research* few samples are observed over its failure behaviour. Other than the performances of the splitting experiment, through these microscopic imageries can be clearly observed that glassy and crystalline phases are behaving in a different manner. Most fractures start from the corners and edge, whereby the most critical fracture is generally at one corner. The failure propagation through glassy phases can be clearly tracked. In samples with visible crystalline phases is visible that the crystalline phases act as an obstacle for the failure propagation. The failure propagation does continue going from glassy to crystalline phase and from crystalline to glassy phase, but a change in direction and energy is inevitable. However, in samples with a majority of crystalline phases, as sample 5A and 5B, it is hard to track failure propagations since the crystalline parts do not show any traces.
Nevertheless, the observation of crystals acting as an obstacle does not necessarily increase the fracture toughness, according to the splitting experiments. Samples 1B and 5A might have performed better due to the arrests of the failure propagation caused by the crystalline surfaces. Yet, the observation in sample 4B, does not seem beneficial for its performance, which however could be caused of its relatively lower amount of crystals.

Through the *XRD analysis* wollastonite-2M and cristobalite are found in sample 1B and 4B, while quarts low and mullite are found in sample 2A. Based on the XRD analysis and the microscopic research can be concluded that the visible crystals are wollastonite-2M. Yet, the according to Mohs scale of hardness, wollastanite-2M has a hardness of 4,5 to 5, cristobalite 6 to 7 and glass 5,4 to 6,6. Considering these numbers can be determined that the crystalline phases in these samples might not enhance the hardness of the sample, but it does enhance its performance upon splitting.
The detected traces of crystal polymorphs in sample 2A on the other hand are questioned. Since these polymorphs are not common to occur at the applied temperatures and only little amounts are mentioned. Whereas the detected polymorphs might be a result of contamination from the crystalcast mould, rather than a product created based on the parent glass.
Other than expected, sample 5B resulted in different crystal polymorphs than the aforementioned. In sample 5B cristobalite, coesite and devitrite are detected and no wollastonite. These crystal polymorph are of a higher toughness (>6) compared to glass, which might be one of the reasons of the better failure toughness. The different crystal polymorphs can be a result of the glass composition or the thermal treatment.

Chapter 10 Conclusions

Throughout the literature study (part II) and laboratory tests (part III) the main question has been systematically answered by finding answers for the sub-questions. Resulting in the main conclusion:

The influence of crystallization on the mechanical properties of a cast glass-ceramic component is found in its failure toughness and failure propagation, but which are highly dependent on the amount and distribution of crystalline and glassy phases.

This main conclusion is based on the following detailed conclusion:
Crystallization is a two-step process, consisting of nucleation and followed by crystal growth. Nucleation occurs spontaneously (homogeneous volume nucleation) or along preferential sites (heterogeneous volume nucleation and surface nucleation). Throughout the melting experiments preferential sites are noticed to be of great importance to allow crystallization to occur. Crystal growth occurs once the nuclei reaches its critical size and the crystal can start developing in size.

A *glass-ceramic* consist of amorphous glassy phases and ordered crystalline phases. It is an inorganic and non-metallic material, which arises from controlled crystallization of glasses. There are different crystallization methods possible, whereby in this research heat treatment on casted components are applied. A glass-ceramic used to have crystalline phases of 50 to 95vol%, whereas recent suggestions are to vary the crystallinity from ppm to almost 100vol%. There are different types of crystals possible based on the composition of the parent glass and the applied heat treatment. Whereas for this research the main crystals formed are of wollastonite-2M or a mixture of coesite, cristobalite and devitrite.

Throughout this research, crystallization is mainly *controlled* through melting and crystallization temperature and dwell time. Another parameter of influence is the glass type, consisting of the glass composition, glass size and additional fluxes. There are many factors of influence towards crystallization, but only glass type, temperatures and dwell times are taken into account in this research. From the beginning is decided to use a glass type prone to crystallization, soda-lime-silica glass, whereas crystallization is easier to obtain. The glass size has shown a difference in crystallization amount and distribution, through the difference in preferential sites. The use of glass cullet resulted in more well distributed crystallization, while the use of glass shards resulted in more localized crystallization dependent on the placement of the glass pieces. Na_2O has been used as flux, but due to undesired results no further research has been done. Through literature study and trial and error, the useful temperatures and dwell times are found. An adequate dwell time under an appropriate melting and crystallization temperature are crucial to allow crystallization to occur. According to this research, generally 3 hours at 1050°C for melting, 5 hours at 760°C for nucleation and 10 hours 890°C for crystal growth appeared to be contributing to obtain crystallized samples.

However, the previous mentioned program does not apply for all glasses, since the different *parameters* are affecting each other. Some glass compositions require lower or higher melting and crystallization temperatures through the different amounts of glass formers, modifiers and fluxes in the composition. For the melting temperature has to be considered that the temperature is high enough to melt the parent glass to avoid having a fused sample, but on the other hand the temperature should not exceed its liquidus point in order to keep preferential sites within the melt for nucleation. The preferential sites are based on the external surfaces of a glass shard or cullet, whereas the amount and distribution of crystallization is also dependent on the used glass size.

After the creation of crystallized samples, the samples have been used for a splitting experiment in order to analyse its *fracture toughness* and fracture behaviour. Through the results of the splitting experiment can be determined that a sample consisting mainly of one phase, glassy or crystalline, is structurally more enhanced compared to a more equally mixed sample. Thereby, glassy, mixed and more crystalline samples all show the same deformation pattern upon loading. This appearance indicates that glass-ceramic has a similar structural behaviour compared to a glass.

Through microscopy analysis of the split samples, the *fracture behaviour* can be traced. From the microscopic imagery a clear difference can be observed between glassy and crystalline phases. Generally, the critical failure origin starts at a corner of a sample, but multiple non critical failure origins can be found along the split bottom edge. From the critical failure origin the failure propagates, in glassy phases the propagation is clearly observable through the conchoidal propagation marks. Once the failure propagation meets a crystal or crystal surface, the propagation undergoes a form of arrest and continues its propagation over the crystal through its needle like structure. Thereupon the failure propagates from crystalline to glassy phase, but its energy and direction is different than before.

Chapter 11 Recommendations

The results of this research indicate that there do are possibilities creating cast glass-ceramic components through recycling (or upcycling) of soda-lime-silica bottle glass and these glass-ceramic components do have its structural potential. Yet, many aspects are still unknown or to be optimized, whereas the following recommendations and suggestions are made for future research.

Glass

Throughout this research only soda-lime-silica glass is used, from the first melting experiment has been decided to use soda-lime-silica bottle glass because of its prone nature towards crystallization. The object of this research is to find new possibilities for waste glass, whereby not only soda-lime-silica glass should be considered but also other glass types.
Another factor to be considered is the cleanliness of glass, during the experiments in this research the glass has been properly cleaned from dirt and labels. But to increase the recyclability of waste glass, the effect of contaminated glass should be looked into since the problematic part of collected waste glass is the amount that is too contaminated to be recycled.

Temperatures

The melting experiments have shown temperature ranges and dwell times favourable to crystallization of soda-lime-silica bottle glass. However, it also showed diverse useful ranges per parameter per glass composition, whereas the applied parameters in this research may not work for a glass with a different glass composition. Yet, through thermal analysis, trial and error and/or using the applied parameters of this research as an indication (if soda-lime-silica bottle glass is applied) the right temperatures and dwell times can be found in order to create crystallized samples in further research.

Cooling rates

The cooling rate used on a melt to go back to ambient temperature is an important factor, however, neglected throughout this research in order to limit unknown parameters. Cooling rates play an important role, a melt becomes a glass under an appropriate cooling rate, whereby no/limited nuclei can be formed. Whereas the other way around, a cooling rate disadvantageous for forming a glass, should be advantageous for forming a glass-ceramic. Therefore, applying the right cooling rate may be advantageous in terms of crystallization and might for example also affect dwell times positively (as the petrurgic crystallization method).

Mechanical properties

This research only indicated on the fracture toughness and fracture behaviour of the samples, whereas a qualitative analysis is lacking. The number of samples and the execution faults during the splitting experiment were limiting the reliability and accuracy of the results. For further research it may be possible to perform a qualitative analysis by creating and testing more samples.

Crystal polymorphs

The majority of the crystals were wollastonite-2M or a mixture of coesite, cristobalite and devitrite. It would be more interesting if the forming crystals can be manipulated to enhance the structural value of the glass-ceramic components. Yet, this aspect was not taken into account in this research, but can be of interest for the creation of structural cast glass-ceramic components.

Chapter 12 References

[01] Bristogianni, T., Oikonomopoulou, F., De Lima, C., Veer, F., & Nijsse, R. (2018). Structural cast glass components manufactured from waste glass: Diverting everyday discarded glass from the landfill to the building industry. *Heron, 63*(1-2), 57-102.

[02] Buckett, J., Marsch, J., & Torr, A. (2002). *International Publication Number WO 02/16277 A1*.

[03] Darwish, M. S. (2006). Nucleation an Growth. American University of Beirut.

[04] Deubener, J., Allix, M., Davis, M., Duran, A., Höche, T., Honma, T., . . . Zhou, S. (2018). Updated definition of glass-ceramics. *Journal of Non-Crystalline Solids, 501*(February), 3-10.

[05] European Commission. (2014). *European Commission.* Retrieved from New use for glass recycled into dust: https://ec.europa.eu/easme/en/news/new-use-glass-recycled-dust

[06] Facilitair Bedrijf Utrecht. (2010). *Afval scheiden is de moeite waard*. Utrecht: University of Utrecht.

[07] Hasanuzzaman, M., Rafferty, A., Sajjia, M., & Olabi, A.-g. (2016). Properties of Glass Materials. R*eference Module in Materials Science and Materials Engineering*, 1-12.

[08] Höland, W., & Beall, G. (2012). *Glass-ceramic technology* (2 ed.).

[09] Höland, W., Rheinberger, V., Schweiger, M., Kelton, K., & Haywood, B. (2003). Control of nucleation in glass ceramics. *Philosophical Transactions of the Royal Society A: Mathematical, Physical and Engineering Sciences, 361*(1804), 575-589.

[10] Humboldt Universitat zu Berlin. (n.d.). Investigation of Polymers with Differential Scanning Calorimetry. 1-17. Berlin.

[11] Hunt, K. (2018). *A Rwandan Engineer Is Recycling Glass Bottles Into Bricks*. Retrieved from Green Matters: https://www.greenmatters.com/renewables/2018/08/16/Z1pR3pt/recycled-glass-bottle-bricks

[12] HVC. (2016). *Wat hoort waar?*.

[13] Justino De Lima, C. (2018). *Innovative low-melting glass compositions containing fly ash and blast furnace slag.*

[14] Kahlenberg, V., Tobbens, D. M., Arroyabe, E., Kaindl, R., & Girtler, D. (2010). Devitrite (Na2Ca3Si6O16)—Structural, Spectroscopic and Computational Investigations on a Crystalline Impurity Phase in Industrial Soda-Lime Glasses. *Mineralogy and Petrology*, 1-9.

[15] Knowles, K. M., & Thompson, R. P. (2014). *Growth of Devitrite, Na2Ca3Si6O16, in Soda-Lime-Silica Glas*. University of Cambridge.

[16] Lapaire, J. (1997). *Coesite*. Retrieved from EUROMIN project: http://euromin.w3sites.net/mineraux/COESITE.html

[17] Lapaire, J. (1997). *Cristobalite*. Retrieved from EUROMIN project: http://euromin.w3sites.net/mineraux/CRISTOBALITE.html

[18] Lapaire, J. (1997). *Mullite*. Retrieved from EUROMIN project: http://euromin.w3sites.net/mineraux/MULLITE.html

[19] Lapaire, J. (1997). *Quartz alpha (low)*. Retrieved from EUROMIN project: http://euromin.w3sites.net/mineraux/QUARTZalphalow.html

[20] Lapaire, J. (1997). *Wollastonite-2M*. Retrieved from EUROMIN project: http://euromin.w3sites.net/mineraux/WOLLASTONITE-2M.html

[21] Le Bourhis, E. (2014). *Glass: Mechanics and Technology* (2 ed.). Wiley-VCH Verlag GmbH & Co. KGaA.

[22] Lutterotti, L. (2006). Crystallization of Glass. 1-30.

[23] Magna Glaskeramik. (2019). *Sustainable production*. Retrieved from Magna Glaskeramik: https://www.magna-glaskeramik.com/material/sustainable-production/

[24] Maltha Groep BV. (2014). Flat glass: conditions of acceptance. 1-5.

[25] Maltha Groep BV. (2014). Packaging glass: conditions of acceptance. 1-2.

[26] Markov, I. (1995). *Crystal Growth for Beginners*.

[27] Massachusetts Institute of Technology. (2010). 3.091 – Introduction to Solid State Chemistry Lecture Notes No. 7. (7), 1-20.

[28] Mindat.org. (n.d.). *Coesite*. Retrieved from Mindat.org: https://www.mindat.org/min-1104.html

[29] Mindat.org. (n.d.). *Cristobalite*. Retrieved from Mindat.org: https://www.mindat.org/min-1155.html

[30] Mindat.org. (n.d.). *Mullite*. Retrieved from Mindat.org: https://www.mindat.org/min-2806.html

[31] Mindat.org. (n.d.). *Quartz*. Retrieved from Mindat.org: https://www.mindat.org/min-3337.html

[32] Mindat.org. (n.d.). *Wollastonite-2M*. Retrieved from Mindat.org: https://www.mindat.org/min-4306.html

[33] Pascual, M. (2015). Glasses and Glass-ceramics : a general overview. (*June*), 1-87.

[34] Rawlings, R., Wu, J., & Boccaccini, A. (2006). *Glass-ceramics: Their production from wastes. A Review.*

[35] Realm of Design. (2013). *The Growth of Greenstone*. Retrieved from Realm of Design: https://realmofdesign.com/the-growth-of-greenstone/

[36] Sauter, C., Lorber, B., McPherson, A., & Giege, R. (2012). Crystallization – General Methods PART 4 . CRYSTALLIZATION. *International Tables for Crystallography, F*(October 2016), 99-121.

[37] School work helper. (2018). Crystallography & Types of crystals. Retrieved from School work helper: https://schoolworkhelper.net/crystallography-types-of-crystals/

[38] Schott. (2019). NEXTREMA: Glass-ceramics engineered and designed for extreme conditions. 1-24.

[39] Shelby, J. (2005). *Introduction to Glass Science and Technology* (2 ed.).

[40] Stichting Duurzaam Verpakkingsglas. (2018). Retrieved from Duurzaamglas.nl: http://www.duurzaamglas.nl/file/view/MVP-Glas-SDV-def.pdf

[41] TGP America. (n.d.). Crystallized Glass Ceramic Panels–The Superior Alternative To Stone. 1-2.

[42] University of Groningen. (2015, December). *Glas*. Retrieved from University of Groningen: https://www.rug.nl/about-us/who-are-we/sustainability/practices/afvalstromen/standaard-afval/glas

[43] University of Washington. (2016). *Crystalline Structure*. Retrieved from Material Science & Engineering: https://depts.washington.edu/matseed/ces_guide/crystalline.htm

[44] Vallet-Regi, M., & Salinas, A. J. (2019). Ceramics as bone repair materials. In *Bone Repair Biomaterials* (pp. 141-178). Elsevier.

[45] Varshneya, A. K. (2016). *Industrial glass.* Retrieved from Encyclopedia Britannica: https://www.britannica.com/topic/glass-properties-composition-and-industrial-production-234890/Properties-of-glass#ref608298

[46] Vitz, E., Moore, J. W., Shorb, J., Prat-Resina, X., Wendorff, T., & Hanh, A. (2019). Crystal Systems. Retrieved from Chemistry LibreTexts: https://chem.libretexts.org/Bookshelves/General_Chemistry/Book%3A_ChemPRIME_(Moore_et_al.)/10Solids%2C_Liquids_and_Solutions/10.03%3A_Crystal_Systems

[47] Vlakglas Recycling Nederland. (2017). *Jaarverslag 2017*.

[48] Vlakglas Recycling Nederland. (n.d.). *Geschiedenis en organisatie*. Retrieved from Vlakglas Recycling Nederland: https://www.vlakglasrecycling.nl/index.php?page=onze-geschiedenis-nl

[49] Vogel, W. (1971). *Structure and Crystallization of Glasses.*

[50] Xiaojie, J., Chandra, S., & Delbert, E. (1991). Nucleation and Crystallization of Na2O. 2CaO. 3Si02 Glass by Differential Thermal Analysis. *Journal of the American Ceramic Society, 14*, 909-914.

[51] Zanotto, E. (2010). Synthesis, characterisation and kinetic study of a glassy material in the BaO-TiO2-Ta2O5-B2O 3-Al2O3 system obtained by a traditional glass fusion-casting method. *American Ceramic Society Bulletin, 89*(8), 19-27.

[52] Zanotto, E. (2017). *From glass to crystal.* (D. Neuville, L. Cormier, D. Caurant, & L. Montagne, Eds.)

[53] Zanotto, E. D. (2006). A bright future for glass-ceramics. *American Ceramic Society*, *89*, 19-27.

[54] Zhu, L., & Sohn, H. (2012). Growth of 2M-wollastonite polycrystals by a partial melting and recrystallization process for the preparation of high-aspect-ratio particles. *Journal of Ceramic Science and Technology, 3(4),* 169-180.

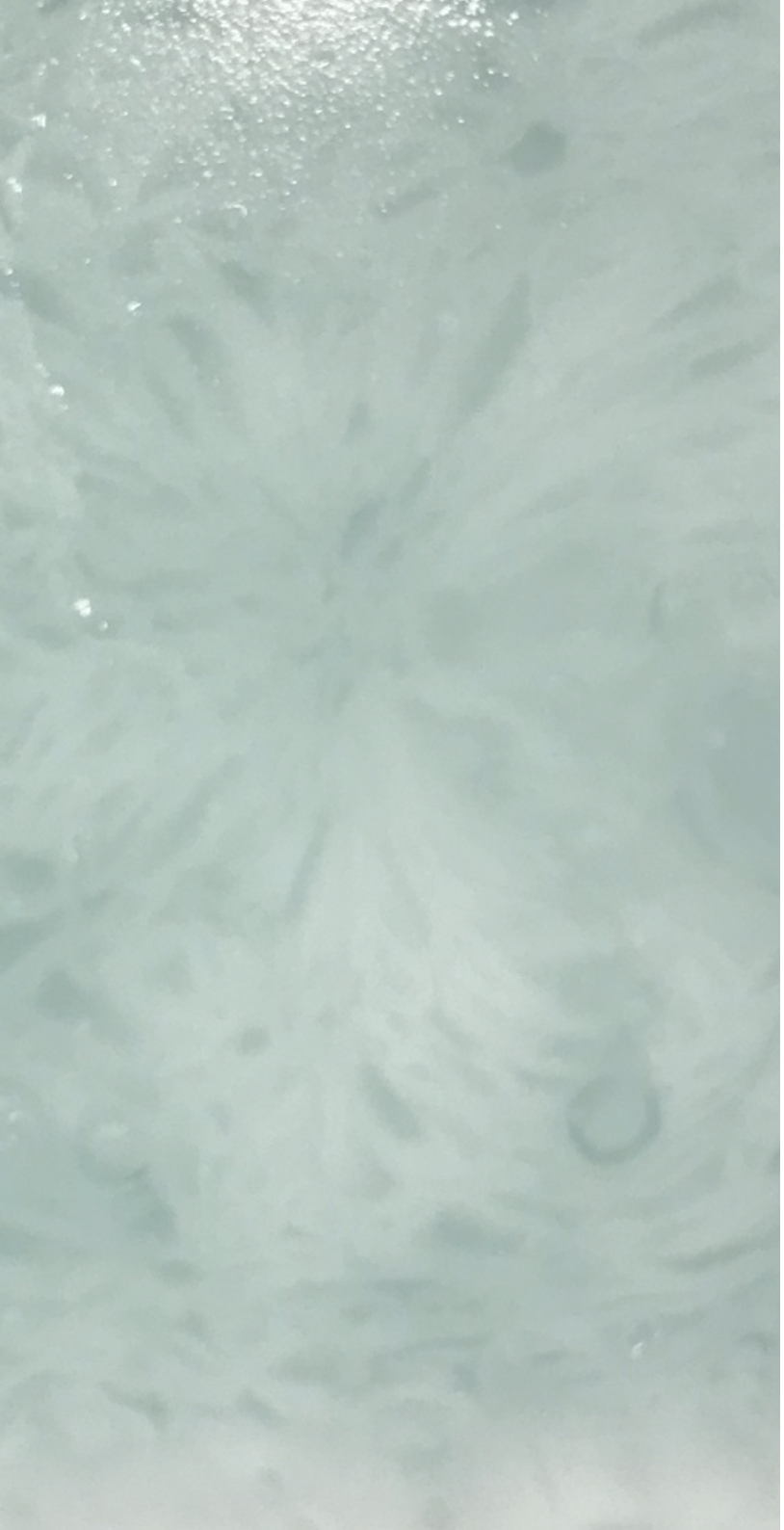

PART V - APPENDIX

Appendix A: Flux

Na_2O is already in the composition of a soda-lime-silica glass as a flux. To add additional flux, Na_2CO_3 can be used. Based on previous experiments done by Telesilla Bristiogianni and Giulia Anagni in the TU Delft glass lab, 10% of the weight of the cullet (parent glass) is required of the component Na_2O. Hereby, 10wt% of the flux is taken as the initial amount for the melting experiments.

Based on the molar masses and the below formula, it is possible to recalculate how much Na_2CO_3 is required.

Formula:	Na_2CO_3	->	Na_2O	+	CO_2,
Molar mass:	105,98		61,97		44,01

Example:

Weight parent glass:	400 gram
Weight Na_2O:	40 gram
Weight Na_2CO_3:	68,4 gram

Appendix B: Melting experiments

The following tables show the oven program of each melting experiment. The programs are based on trial and errors of each melting experiment.

Melting experiment 1
First firing

Date	Heating/ cooling rate °C/h	Temperature °C	Dwell time
Tu May 14th	-	20	-
-	+60	1050	3h
-	-30	860	10h
-	-30	560	10h
-	?	20	-

Second firing

Date	Heating/ cooling rate °C/h	Temperature °C	Dwell time
Mo May 27th	-	20	-
-	+60	840	10h
-	-30	560	10h
-	?	20	-

Melting experiment 2
First firing

Date	Heating/ cooling rate °C/h	Temperature °C	Dwell time
Tu Jul 2nd	-	20	-
-	+50	1120	10h
-	-160	560	10h
-	-6	505	-
-	?	20	-

Second firing

Date	Heating/ cooling rate	Temperature °C	Dwell time
Tu Jul 9th	-	20	-
-	?	840	10h
-	?	20	-

Melting experiment 3

Date	Heating/ cooling rate °C/h	Temperature °C	Dwell time
Tu Jul 16th	-	20	-
-	+50	780	24h
-	+50	780	-
-	+40	1050	3h
-	-30	840	5h
-	+3	860	5h
-	-100	560	8h
-	-3	505	-
-	-8	450	-
-	?	20	-

Melting experiment 4

Date	Heating/ cooling rate °C/h	Temperature °C	Dwell time
Tu Jul 30th	-	20	-
-	+50	160	24h
-	+50	780	-
-	+40	1070	3h
-	-30	780	5h
-	+3	860	10h
-	-100	560	8h
-	-3	505	-
-	-8	450	-
-	?	20	-

Melting experiment 5

Date	Heating/ cooling rate °C/h	Temperature °C	Dwell time
Wo Sep 18th	-	20	-
-	+60	1050	3h
-	-120	760	5h
-	+30	890	10h
-	-156	560	10h
-	-6	505	-
-	?	20	-

Melting experiment 6

Date	Heating/ cooling rate °C/h	Temperature °C	Dwell time
Th Oct 3rd	-	20	-
-	+60	1050	3h
-	-120	500	5h
-	+30	650	10h
-	-156	560	10h
-	-6 C/h	505	-
-	?	20	-

Melting experiment 7

Date	Heating/ cooling rate °C/h	Temperature °C	Dwell time
Th Oct 17th	-	20	-
-	+60	1070	3h
-	-120	760	5h
-	+30	890	10h
-	-156	560	10h
-	-6	505	-
-	?	20	-

Melting experiment 8

Date	Heating/ cooling rate °C/h	Temperature °C	Dwell time
Tu Oct 29th	-	20	-
-	+60	1070	3h
-	-60	560	10h
-	- 3	480	-
-	?	20	-

B.1. Melting experiment 1

Material

Soda-lime-silica glass

1A • Flat glass	476gram
1B • Bottle glass	430gram

Temperature and cooling rate

First firing

Date	Heating/ cooling rate °C/h	Temp. °C	Dwell time
Tu May 14th	-	20	-
-	+60	1050	3h
-	-30	860	10h
-	-30	560	10h
-	?	20	-

Second firing

Date	Heating/ cooling rate °C/h	Temp. °C	Dwell time
Mo May 27th	-	20	-
-	+60	840	10h
-	-30	560	10h
-	?	20	-

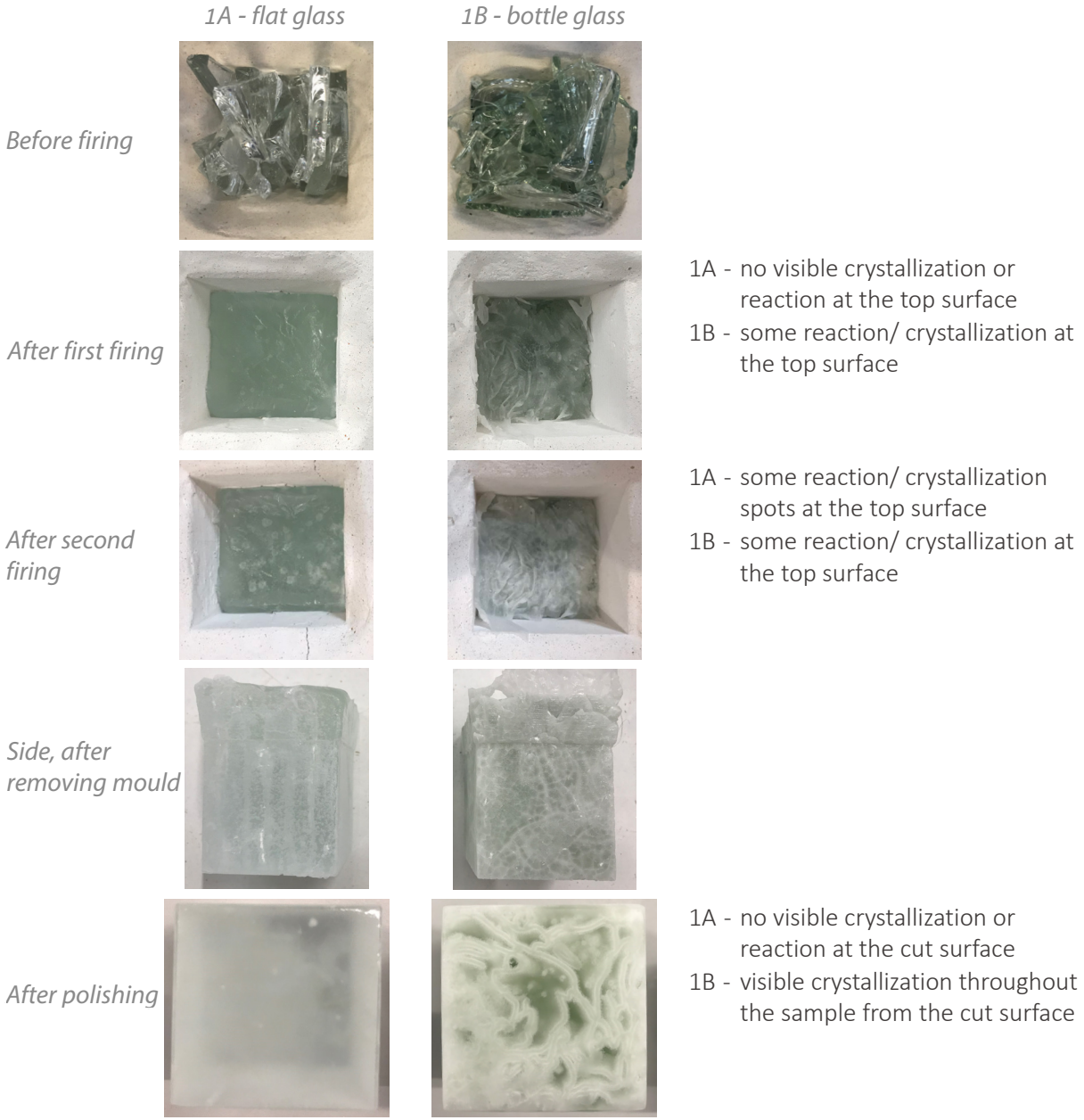

Figure B1 - melting experiment 1, top surface, at different stages with comment

B.2. Melting experiment 2

Material

Soda-lime silica glass from bottle glass

2A • shards	425gram
2B • cullet	354gram
2C • cullet+10w%flux	344+59gram
2D • powder	271gram

Temperature and cooling rate

First firing

Date	Heating/ cooling rate °C/h	Temp. °C	Dwell time
Tu Jul 2nd	-	20	-
-	+50	1120	10h
-	-160	560	10h
-	-6	505	-
-	?	20	-

Second firing

Date	Heating/ cooling rate	Temp. °C	Duration
Tu Jul 9th	-	20	-
-	?	840	10h
-	?	20	-

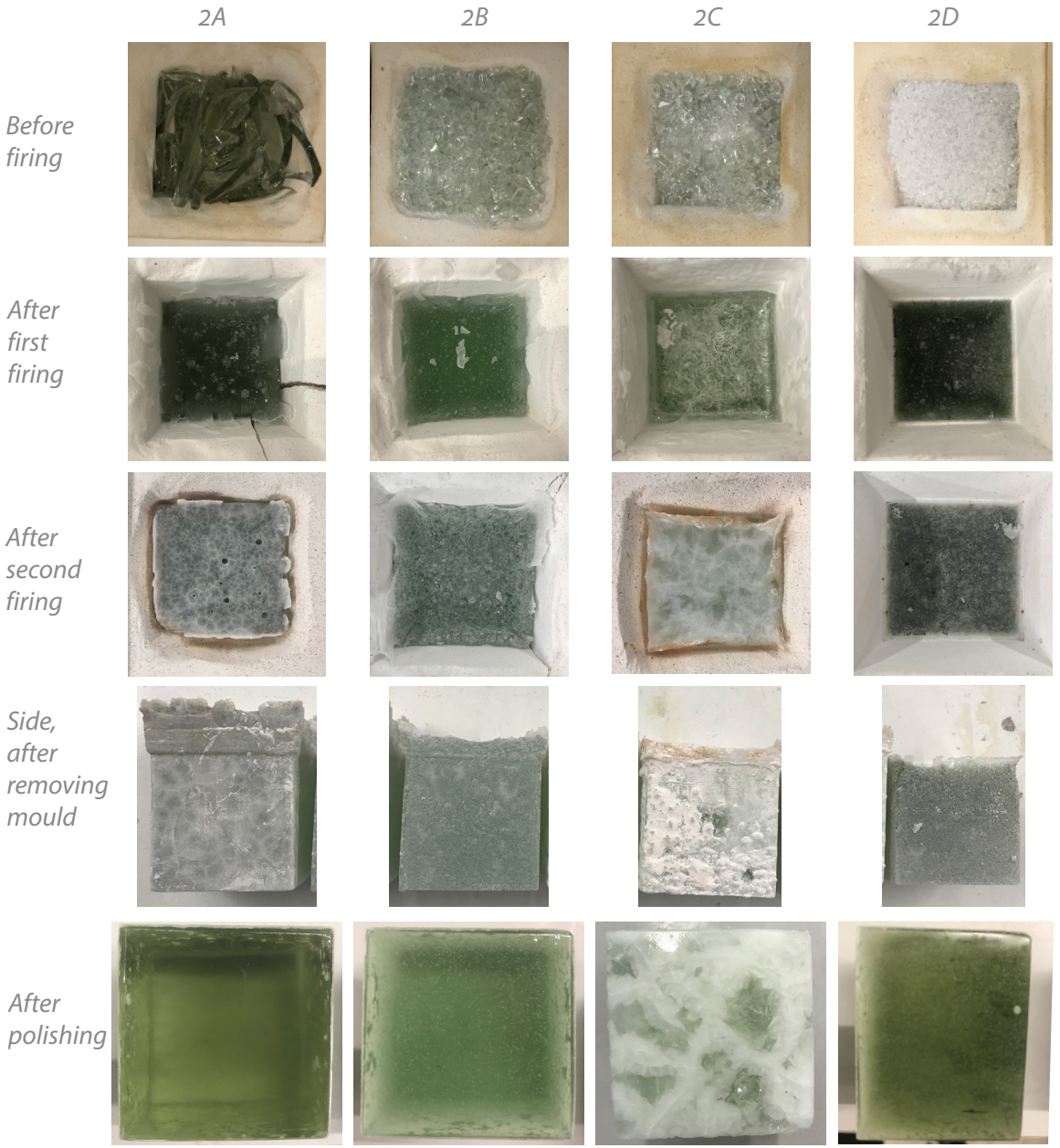

2A, 2B, 2D- no visible crystallization or reaction at the top surface

2C - no visible crystallization, many small cracks

2A, 2B, 2D- some reaction/ crystallization at the top surface

2C - possibly lines of crystallization, less cracks than before

2A - no visible crystallization

2B - no visible crystallization, but visible air bubbles

2C - patches of crystallization and many cracks

2D - no visible crystallization, but visible air bubbles and contamination

Figure B2 - melting experiment 2, top surface, at different stages with comment

B.3. Melting experiment 3

Material

Soda-lime silica glass from bottle glass

3A • cullet 338gram

3B • cullet+10w%flux 369+63gram

Temperature and cooling rate

Date	Heating/ cooling rate °C/h	Temp. °C	Dwell time
Tu Jul 16th	-	20	-
-	+50	780	24h
-	+50	780	-
-	+40	1050	3h
-	-30	840	5h
-	+3	860	5h
-	-100	560	8h
-	-3	505	-
-	-8	450	-
-	?	20	-

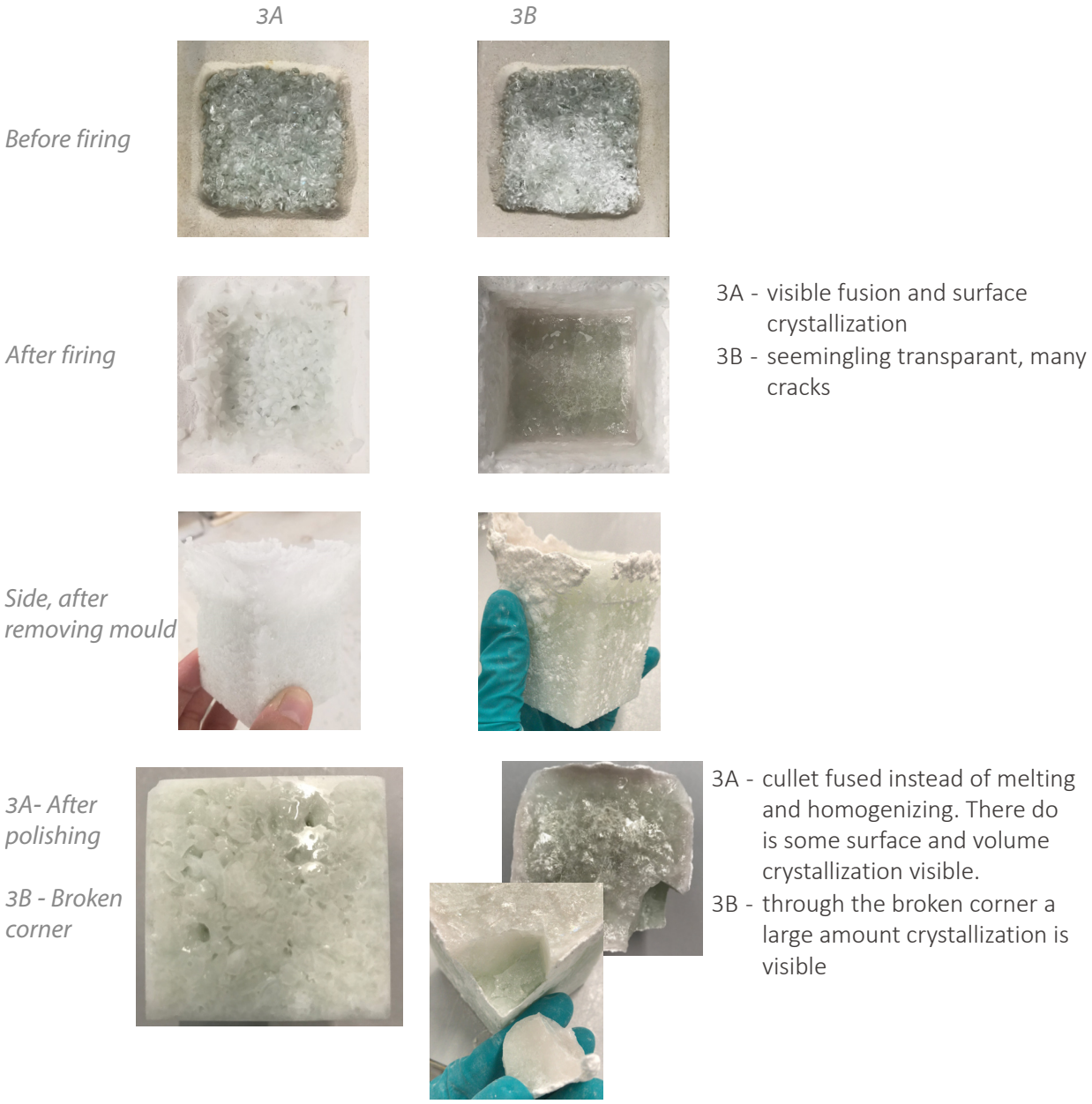

Figure B3 - melting experiment 3, top surface, at different stages with comment

B.4. Melting experiment 4

Material

Soda-lime silica glass from bottle glass

4A • shards	402gram
4B • cullet	400gram
4C• cullet+5w%flux	395+34gram

Temperature and cooling rate

Date	Heating/ cooling rate °C/h	Temp. °C	Dwell time
Tu Jul 30th	-	20	-
-	+50	160	24h
-	+50	780	-
-	+40	1070	3h
-	-30	780	5h
-	+3	860	10h
-	-100	560	8h
-	-3	505	-
-	-8	450	-
-	?	20	-

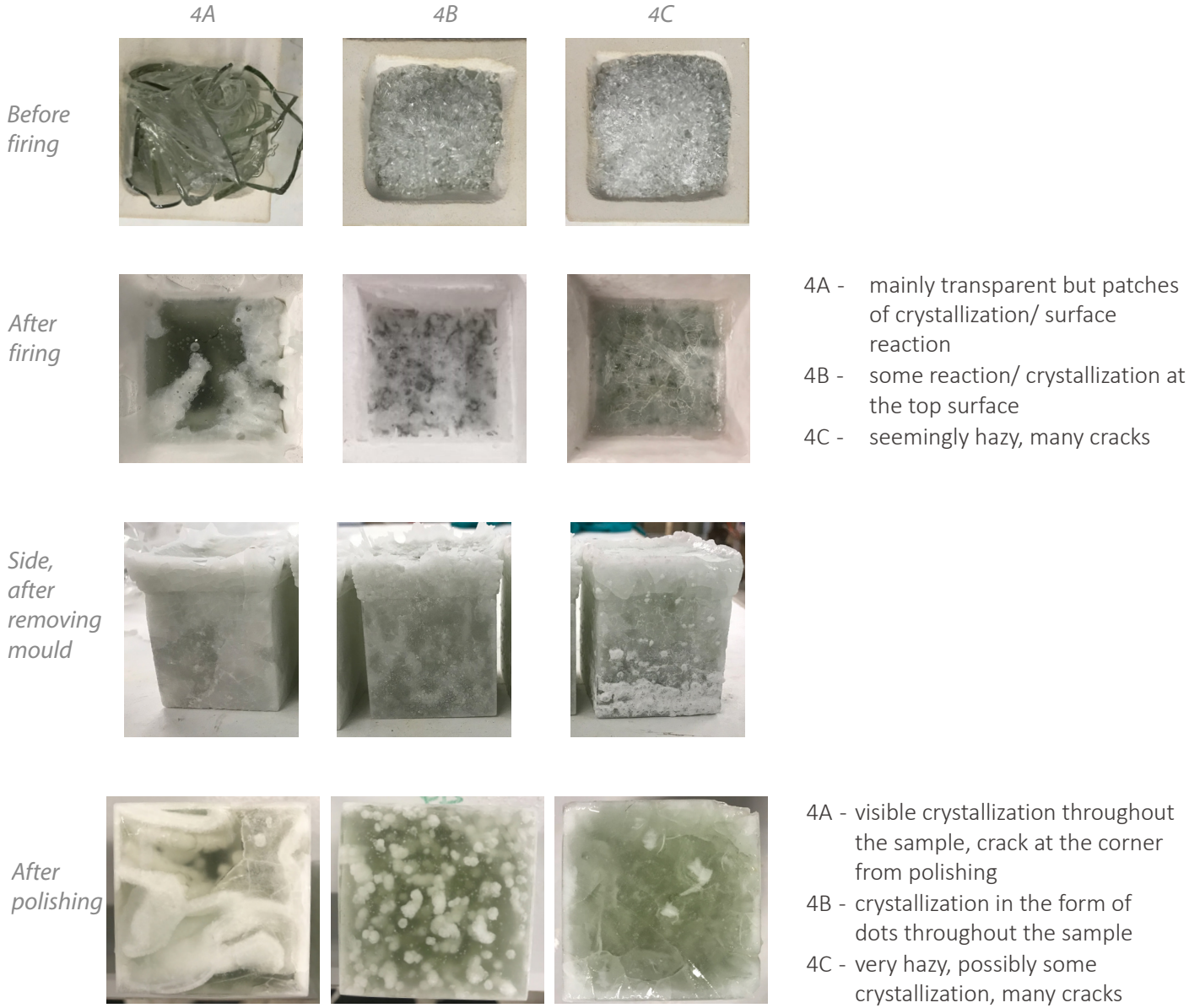

4A - mainly transparent but patches of crystallization/ surface reaction
4B - some reaction/ crystallization at the top surface
4C - seemingly hazy, many cracks

4A - visible crystallization throughout the sample, crack at the corner from polishing
4B - crystallization in the form of dots throughout the sample
4C - very hazy, possibly some crystallization, many cracks

Figure B4 - melting experiment 4, top surface, at different stages with comment

B.5. Melting experiment 5

Material

Soda-lime silica glass from bottle glass

5A • shard	390gram
5B • cullet	388gram

Temperature and cooling rate

Date	Heating/ cooling rate °C/h	Temp. °C	Dwell time
Wo Sep 18th	-	20	-
-	+60	1050	3h
-	-120	760	5h
-	+30	890	10h
-	-156	560	10h
-	-6	505	-
-	?	20	-

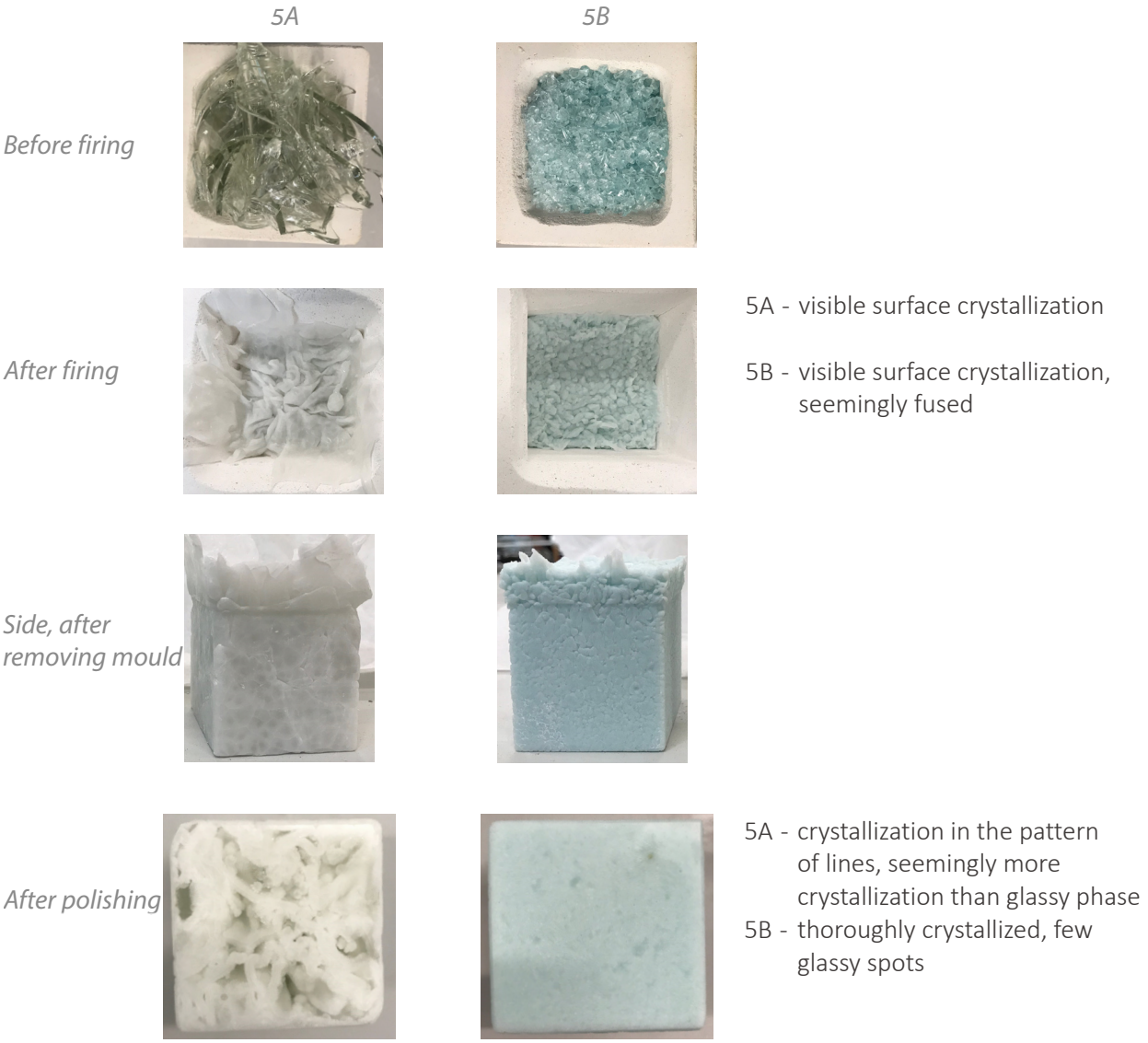

Figure B5 - melting experiment 5, top surface, at different stages with comment

B.6. Melting experiment 6

Material

Soda-lime silica glass from bottle glass
6A • cullet 381gram

Temperature and cooling rate

Date	Heating/ cooling rate °C/h	Temp. °C	Dwell time
Th Oct 3rd	-	20	-
-	+60	1050	3h
-	-120	500	5h
-	+30	650	10h
-	-156	560	10h
-	-6 C/h	505	-
-	?	20	-

6A

Before firing

After firing

6A - no visible surface crystallization

Side, after removing mould

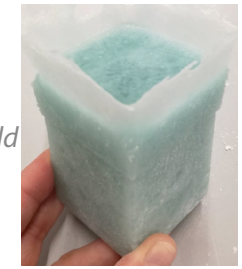

After polishing

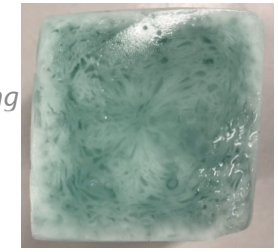

6A - cullet did not fully melt and homogenize, but fused. Along the fused boundaries crystallization is found.

Figure B6 - melting experiment 6, top surface, at different stages with comment

B.7 Melting experiment 7

Material

Soda-lime silica glass from bottle glass

7A • cullet	389gram
7B • cullet	500gram

Temperature and cooling rate

Date	Heating/ cooling rate °C/h	Temp. °C	Dwell time
Th Oct 17th	-	20	-
-	+60	1070	3h
-	-120	760	5h
-	+30	890	10h
-	-156	560	10h
-	-6	505	-
-	?	20	-

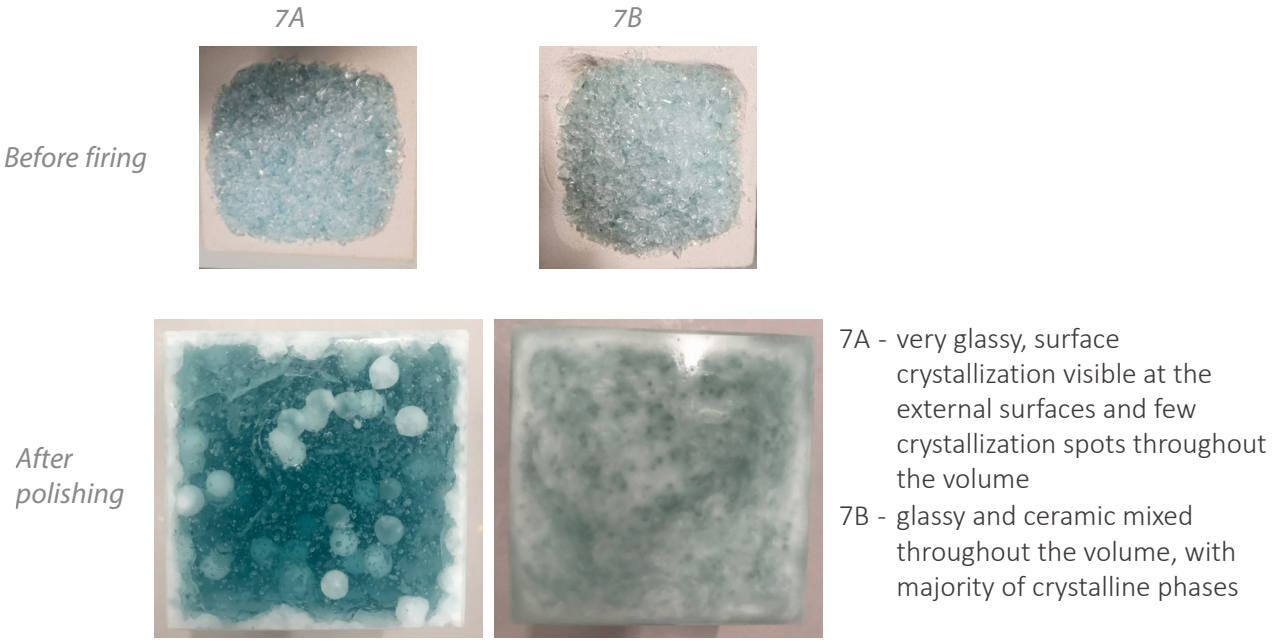

Figure B7 - melting experiment 7, top surface, at different stages with comment. Pictures of stages in between are not available.

B.8. Melting experiment 8

Material

Soda-lime silica glass from bottle glass

8A • cullet	329gram
8B • cullet	400gram

Temperature and cooling rate

Date	Heating/ cooling rate °C/h	Temp. °C	Dwell time
Tu Oct 29th	-	20	-
-	+60	1070	3h
-	-60	560	10h
-	- 3	480	-
-	?	20	-

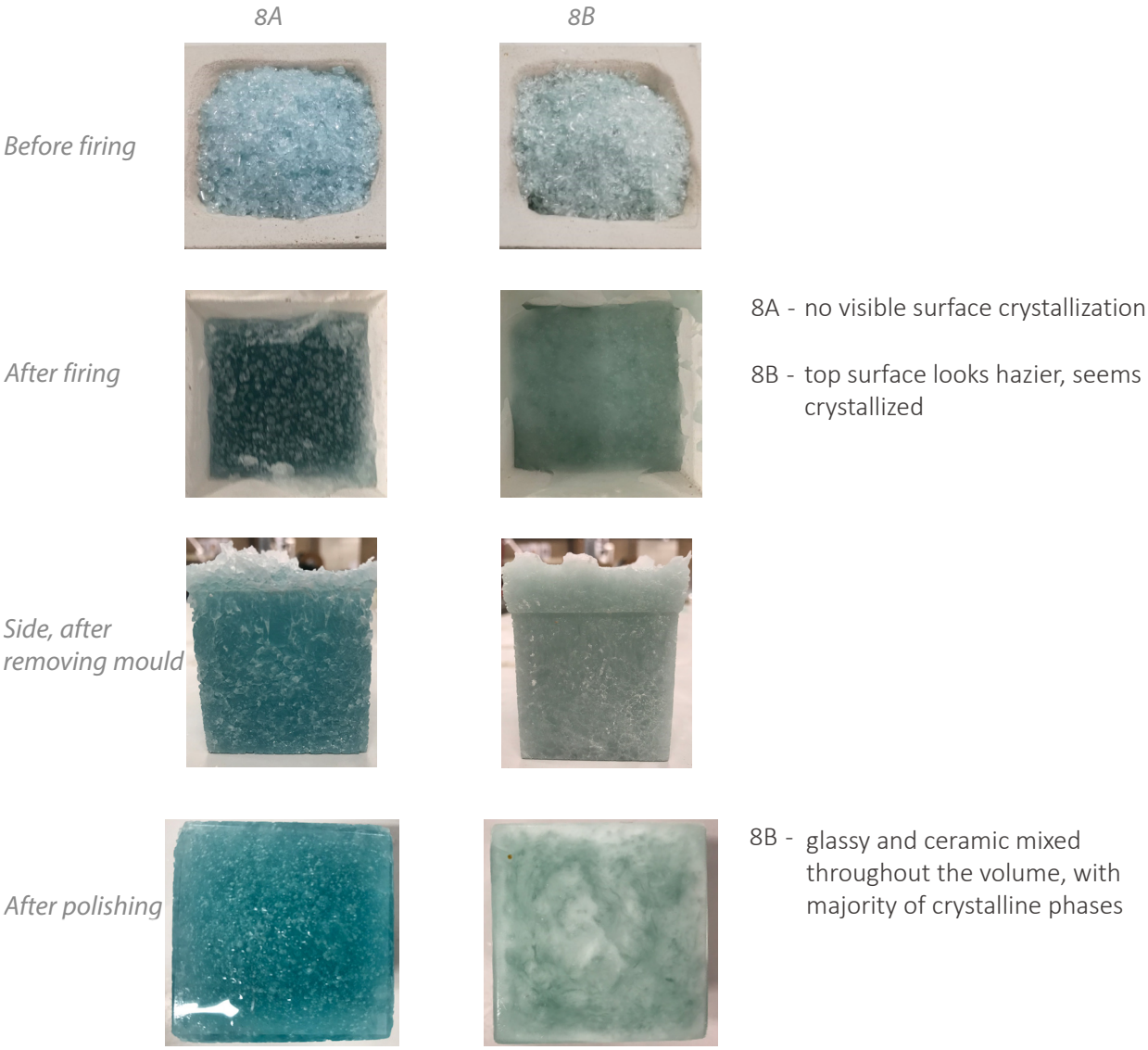

Figure B8 - melting experiment 7, top surface, at different stages with comment

Appendix C: X-ray fluorescence

The X-ray fluorescence (XRF) analysis is used primarily to distinguish the compositions of the parent glass. For this XRF analysis the wine bottle used for sample 5B, 7A and 8A and the water bottle used for sample 6A, 7B, and 8B are analyzed. The different results between those samples of the two different glasses makes it interesiting to know its exact composition and find the causes of its differences.

Experimental conditions:

For XRF analysis the measurements were performed with a Panalytical Axios Max WD-XRF spectrometer and data evaluation was done with SuperQ5.0i/Omnian software. 18/12/2015 09:37:03

31/10/2019 08:51:49

PANalytical

Quantification of sample Telesilla, sample "Cindy wine bottle", 31oct19

Sum before normalization: 93.8 wt%

Normalised to: 100.0 wt%

Sample type: Solid

Correction applied for medium: No

Correction applied for film: No

Used Compound list: Oxides

Results database: omnian 4kw 20mm

Results database in: c:\panalytical\superq\userdata

	Compound Name	Conc. (wt%)	Absolute Error (wt%)
1	SiO2	74.296	0.1
2	Na2O	12.478	0.1
3	CaO	10.906	0.09
4	Al2O3	1.57	0.04
5	MgO	0.249	0.01
6	Fe2O3	0.214	0.01
7	SO3	0.095	0.009
8	K2O	0.089	0.009
9	TiO2	0.034	0.006
10	Cl	0.023	0.005
11	P2O5	0.019	0.004
12	ZrO2	0.016	0.004
13	SrO	0.008	0.003
14	ZnO	0.005	0.002

31/10/2019 11:04:11

PANalytical

Quantification of sample Telesilla, sample "Cindy water bottle", 31oct19

Sum before normalization: 89.9 wt%

Normalised to: 100.0 wt%

Sample type: Solid

Correction applied for medium: No

Correction applied for film: No

Used Compound list: Oxides

Results database: omnian 4kw 20mm

Results database in: c:\panalytical\superq\userdata

	Compound Name	Conc. (wt%)	Absolute Error (wt%)
1	SiO2	72.714	0.1
2	Na2O	11.947	0.1
3	CaO	9.986	0.09
4	MgO	2.951	0.05
5	Al2O3	1.329	0.03
6	K2O	0.507	0.02
7	SO3	0.18	0.01
8	Fe2O3	0.165	0.01
9	TiO2	0.045	0.006
10	Cl	0.039	0.006
11	P2O5	0.028	0.005
12	BaO	0.023	0.005
13	ZnO	0.017	0.004
14	Cr2O3	0.015	0.004
15	MnO	0.014	0.004
16	ZrO2	0.013	0.003
17	CuO	0.007	0.002
18	SrO	0.007	0.002
19	NiO	0.006	0.002
20	PbO	0.005	0.002
21	Rb2O	0.002	0.001

Appendix D: Splitting experiments

For each sample, the state before and after the splitting test in the set-up, the surface of the interior after the split and the force-deformation graph are shown. The splitting tests are performed on the same day, but clustered according to the melting experiments.

D.1. Splitting experiment 1 - sample 1A and 1B

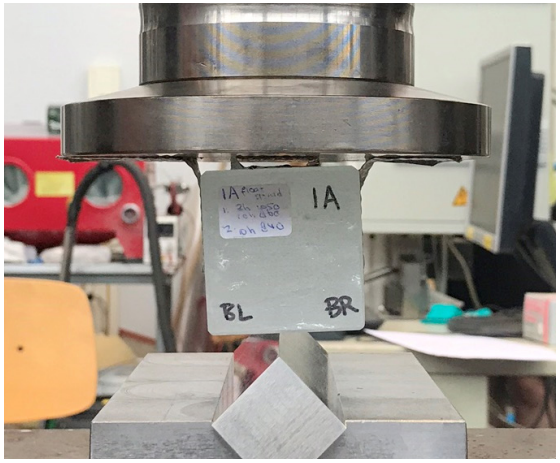

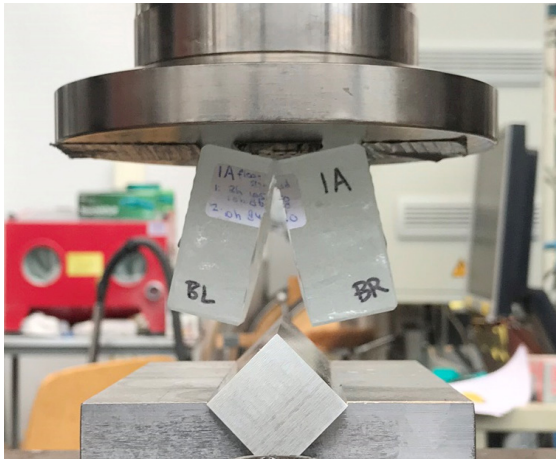

Figure D1 - sample 1A; left: set-up before and after splitting test. right: split surface

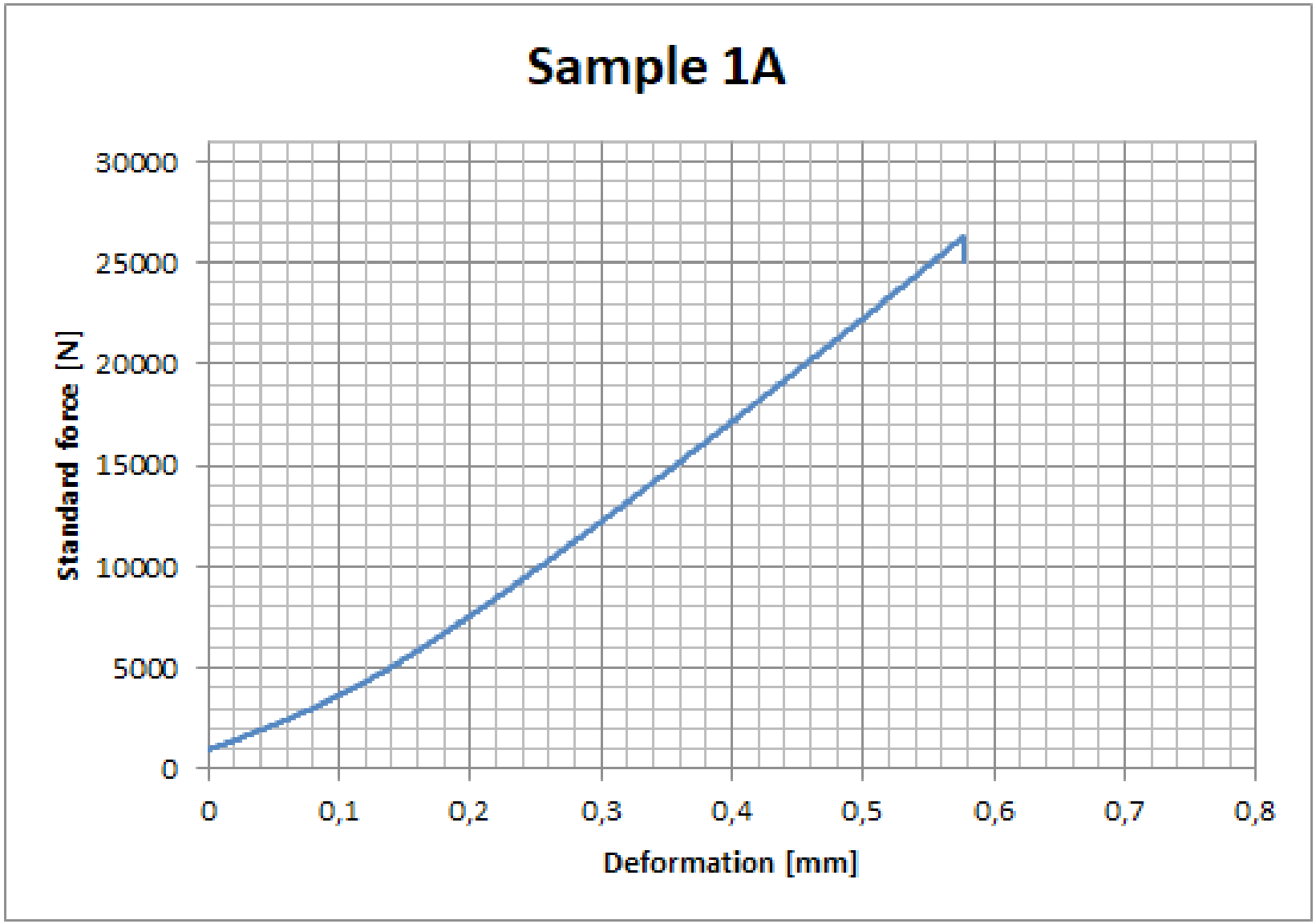

Figure D2 - sample 1A; deformation-force curve

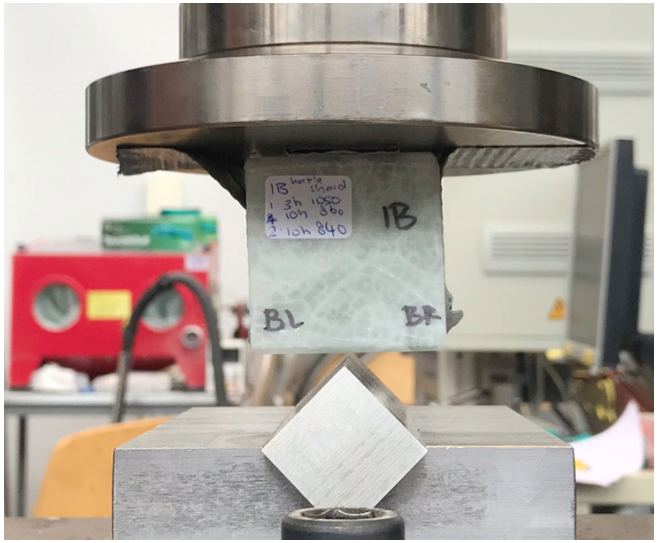

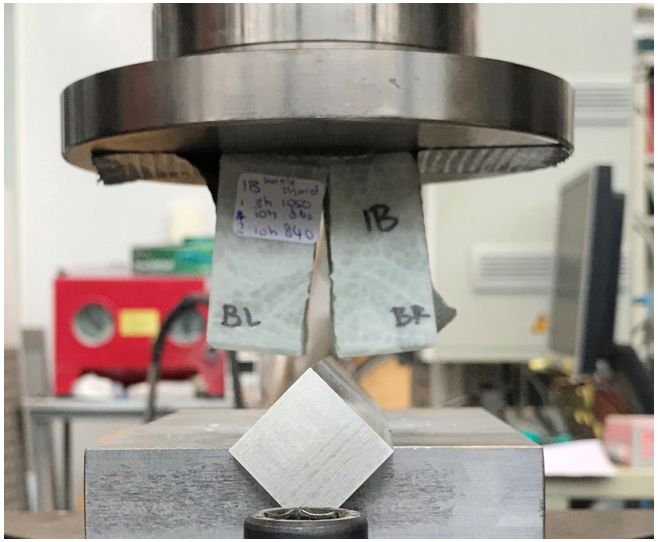

Figure D3 - sample 1B; left: set-up before and after splitting test. right: split surface

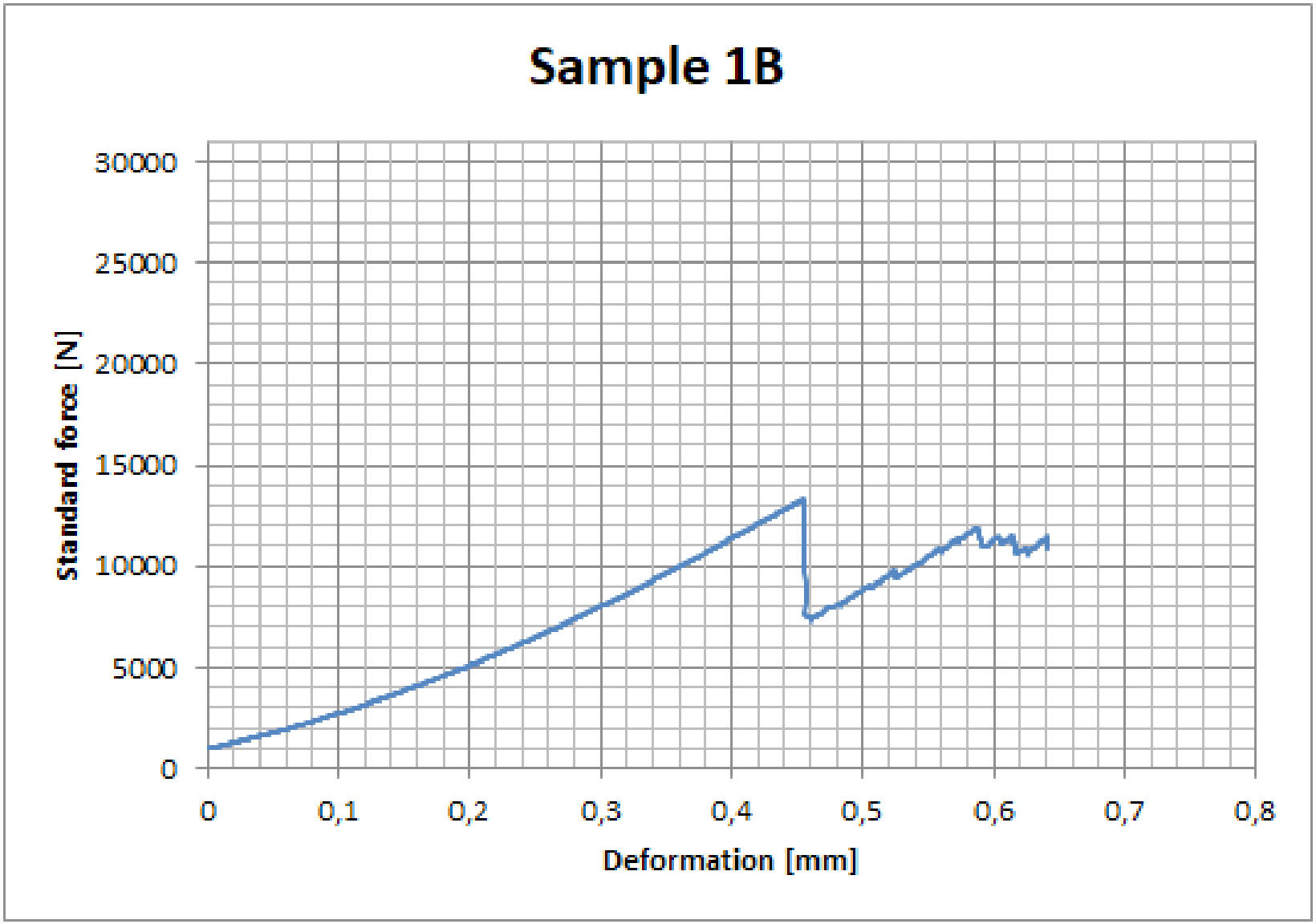

Figure D4 - sample 1B; deformation-force curve

D.2. Splitting experiment 2 - sample 2A, 2B and 2D

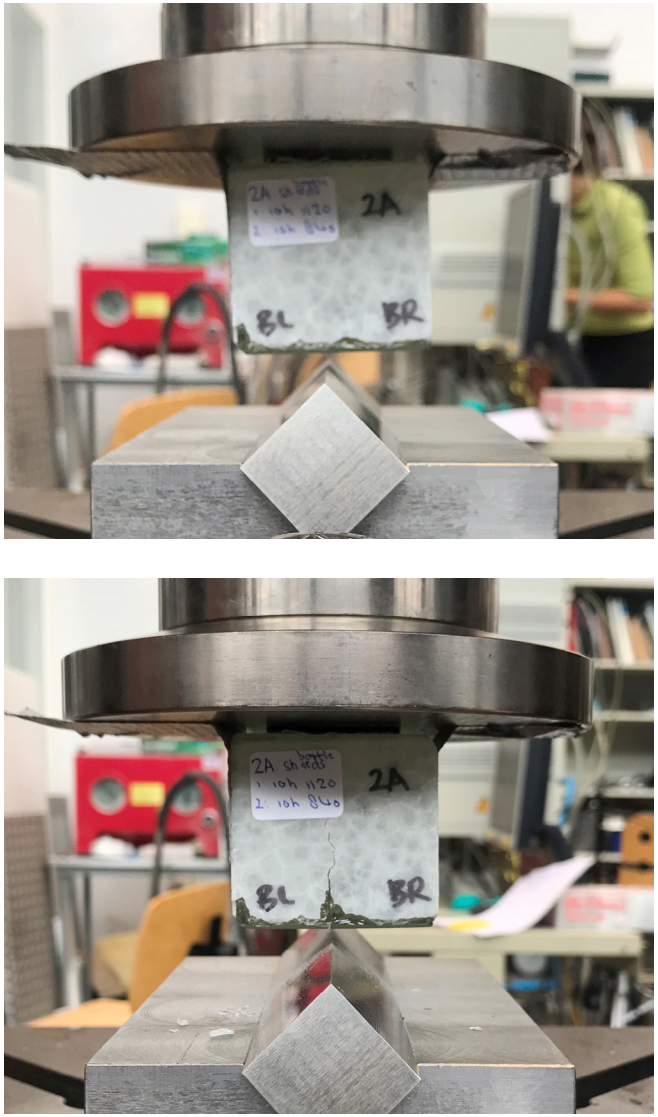

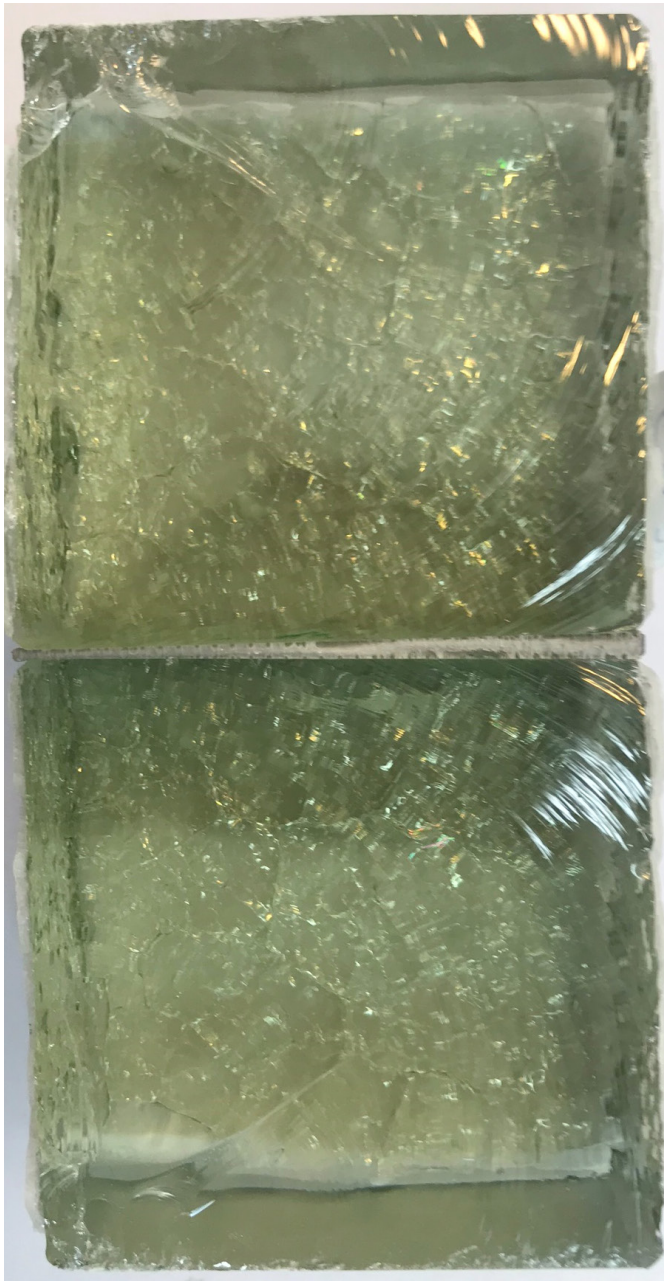

Figure D5 - sample 2A; left: set-up before and after splitting test. right: split surface

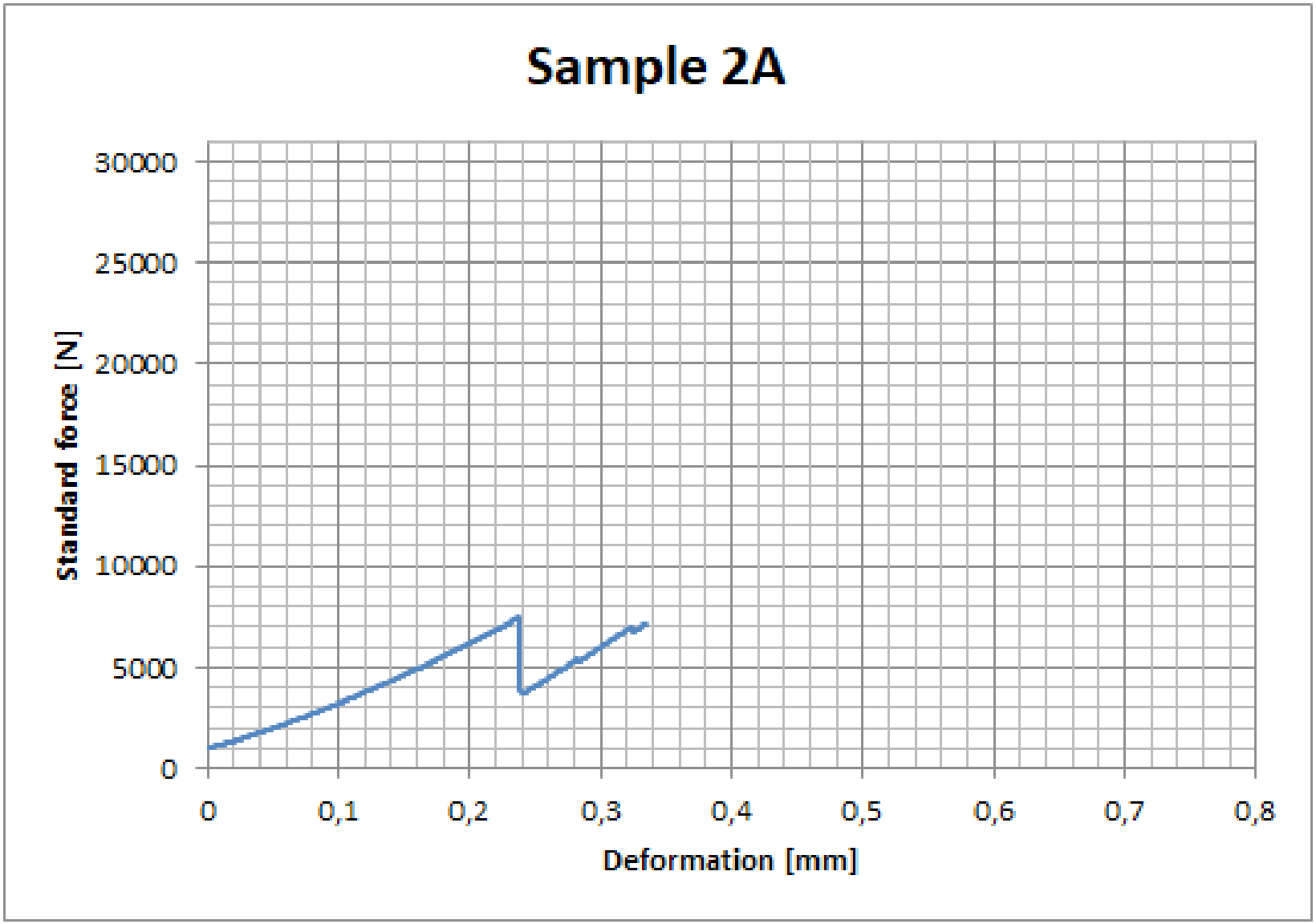

Figure D6 - sample 2A; deformation-force curve

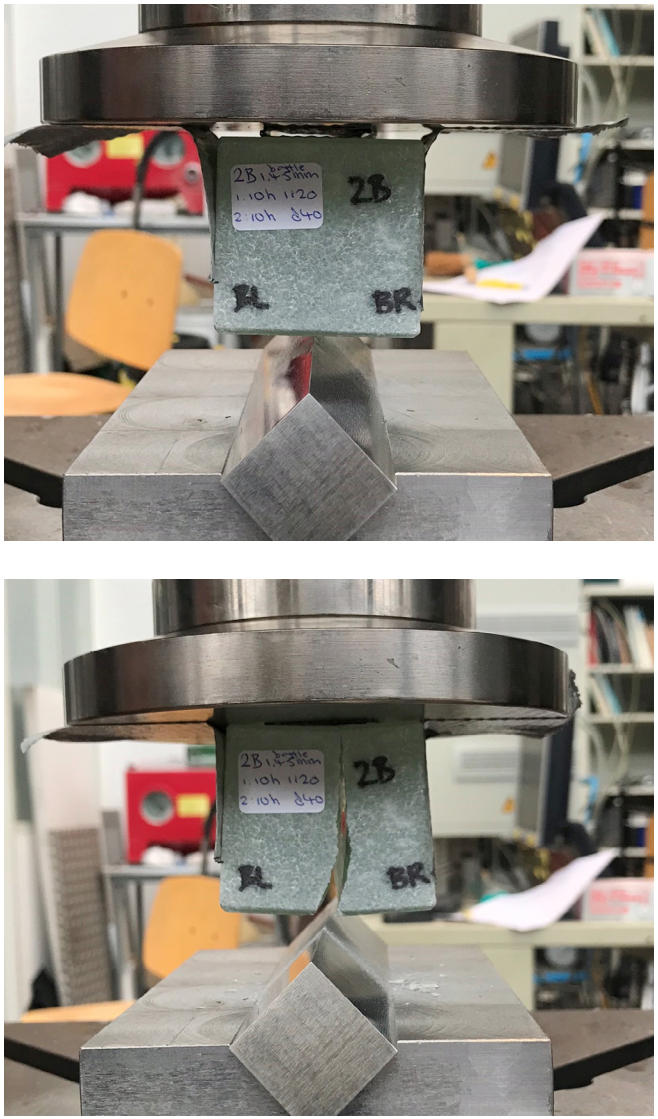

Figure D7 - sample 2B; left: set-up before and after splitting test. right: split surface

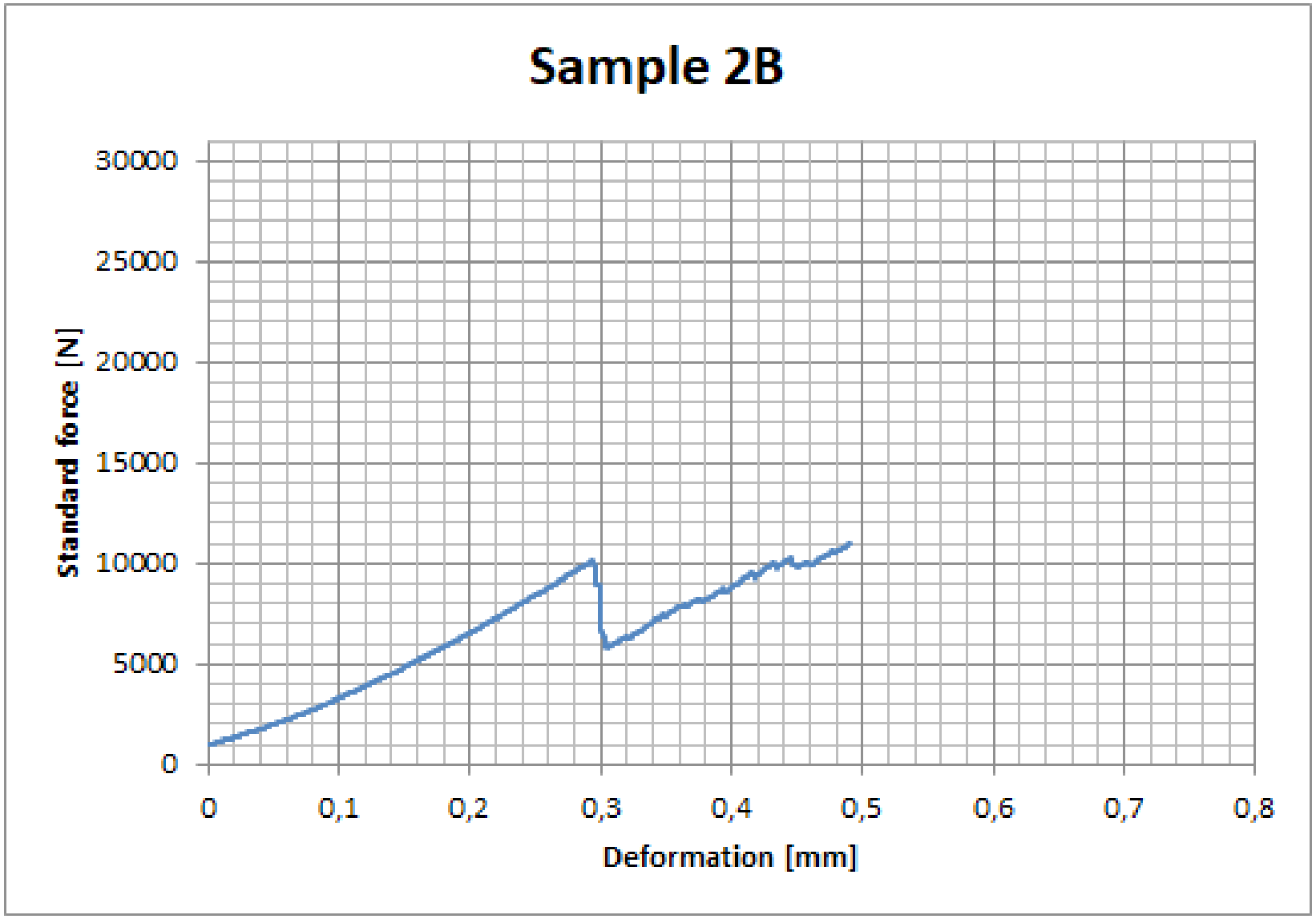

Figure D8 - sample 2B; deformation-force curve

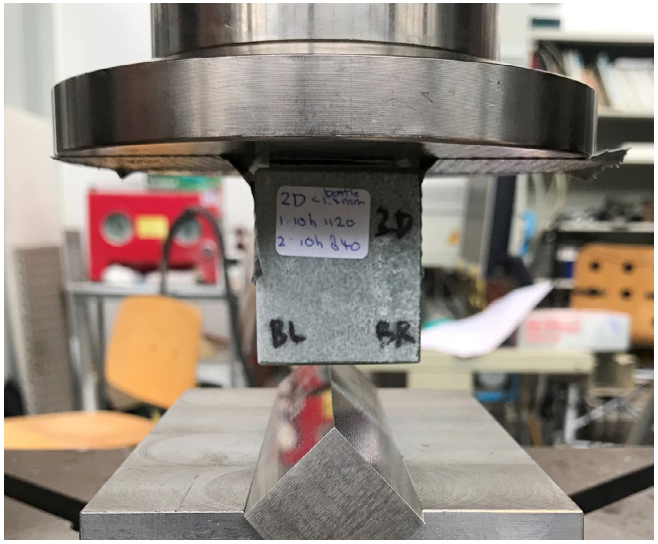

Figure D9 - sample 2D; left: set-up before and after splitting test. right: split surface

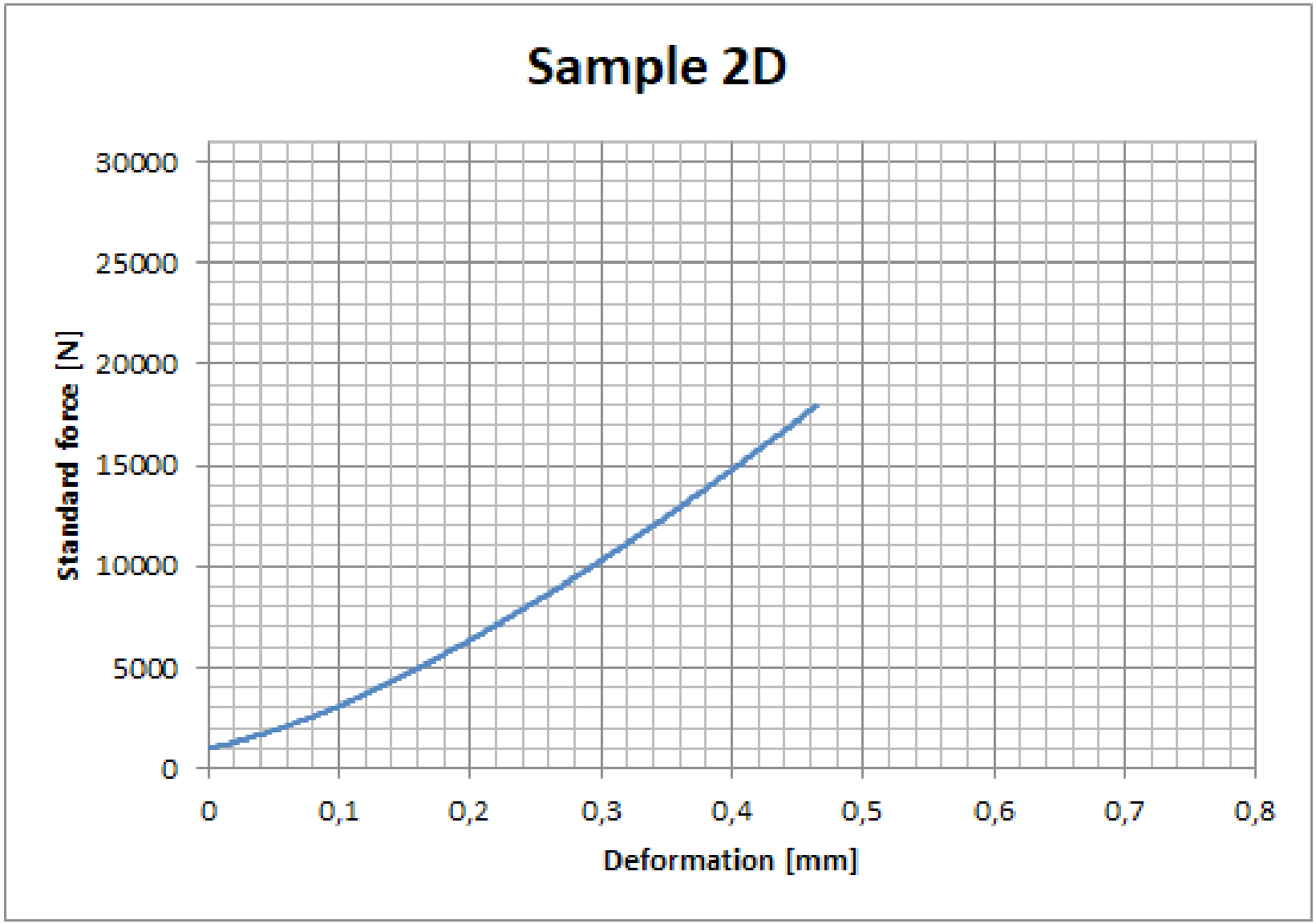

Figure D10 - sample 2D; deformation-force curve

D.3. Splitting experiment 4 - sample 4A and 4B

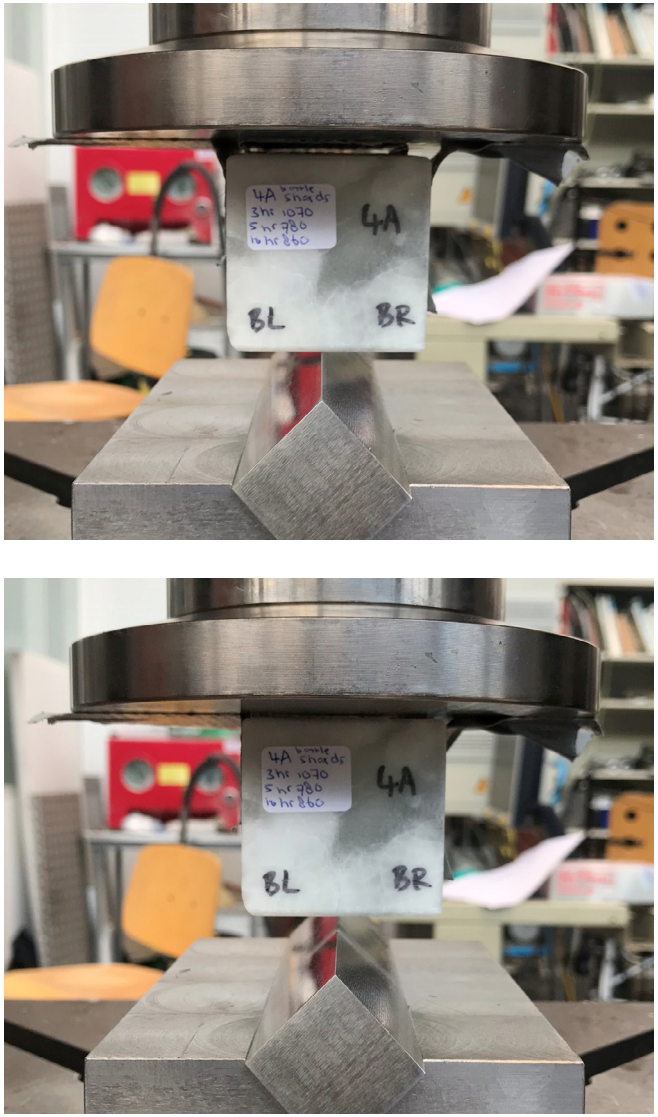

Figure D11 - sample 4A; left: set-up before and after splitting test

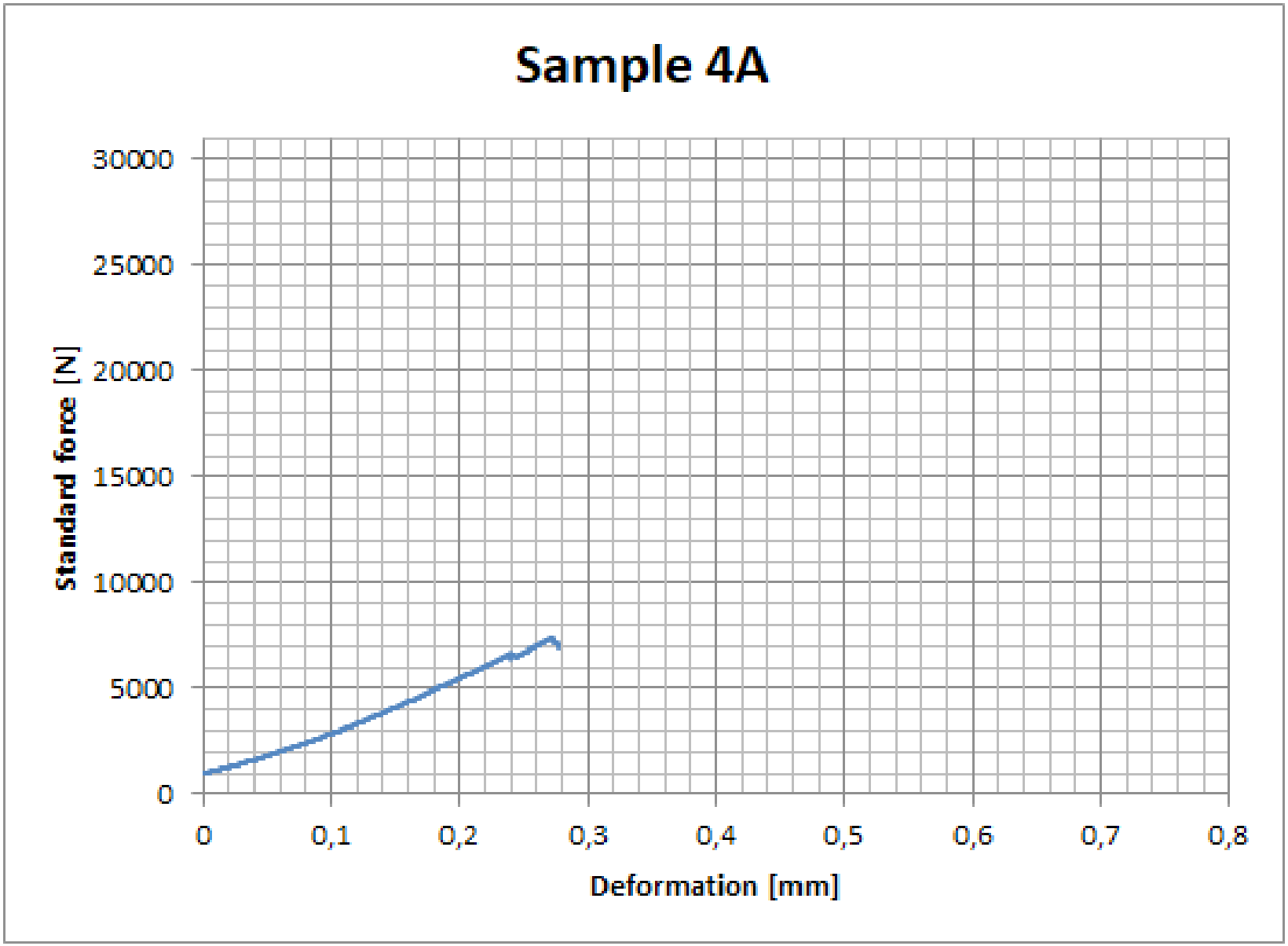

Figure D12 - sample 4A; deformation-force curve

Figure D13 - sample 4B; left: set-up before and after splitting test. right: split surface

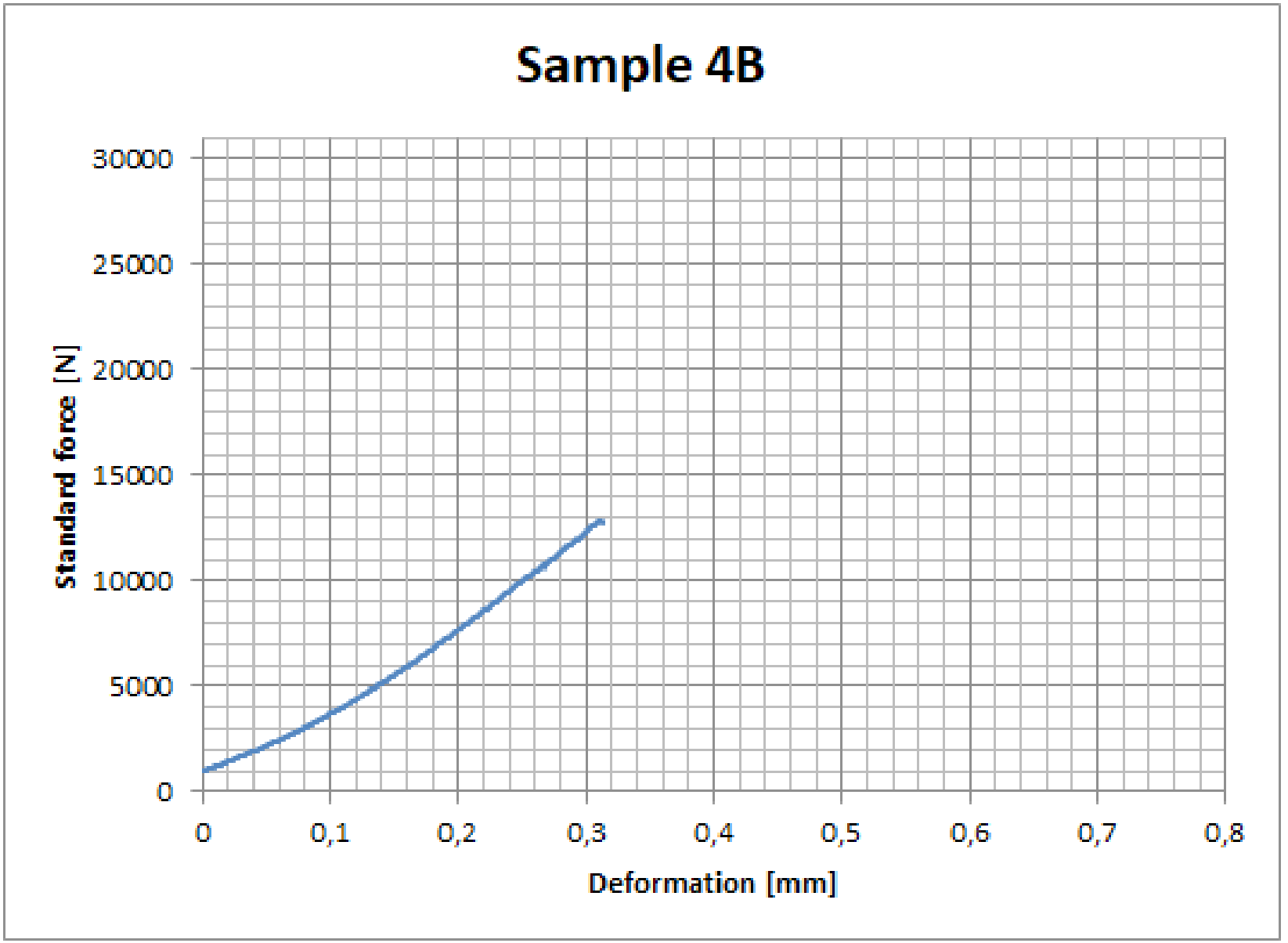

Figure D14 - sample 4B; deformation-force curve

D.4. Splitting experiment 5 - sample 5A and 5B

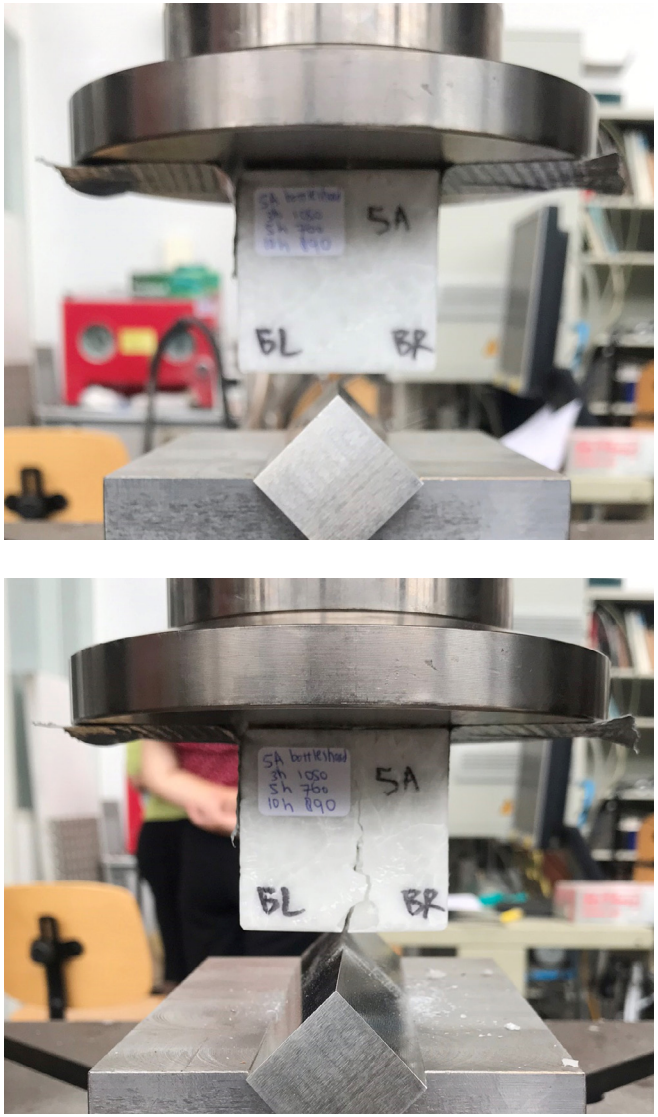

Figure D15 - sample 5A; left: set-up before and after splitting test. right: split surface

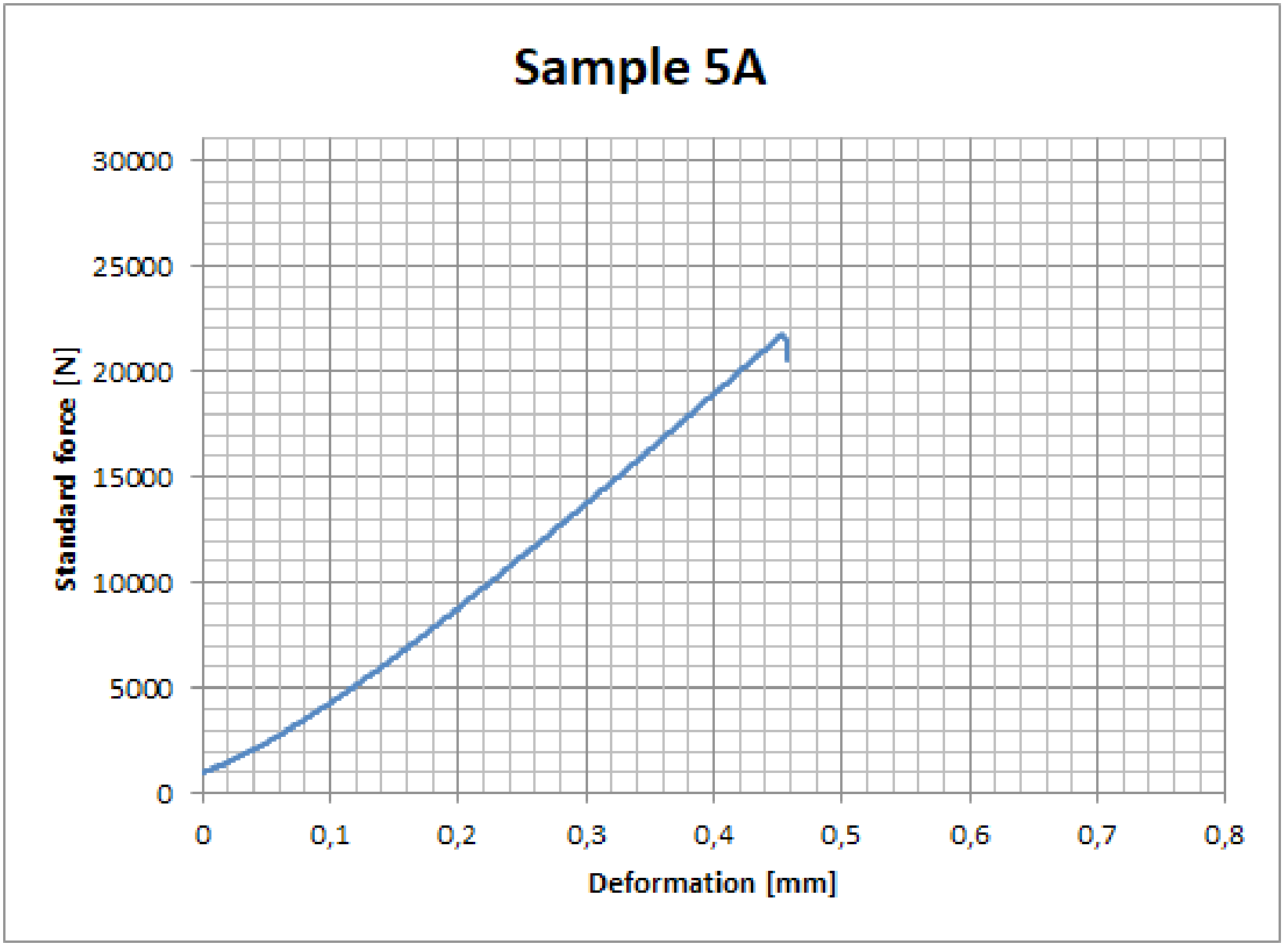

Figure D16 - sample 5A; deformation-force curve

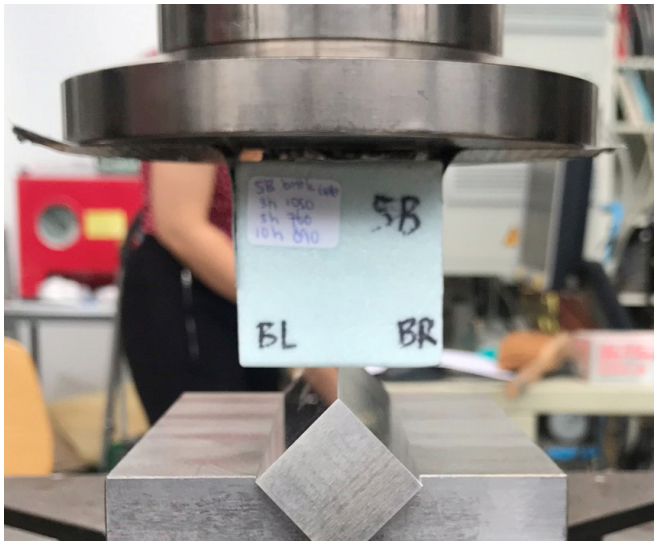

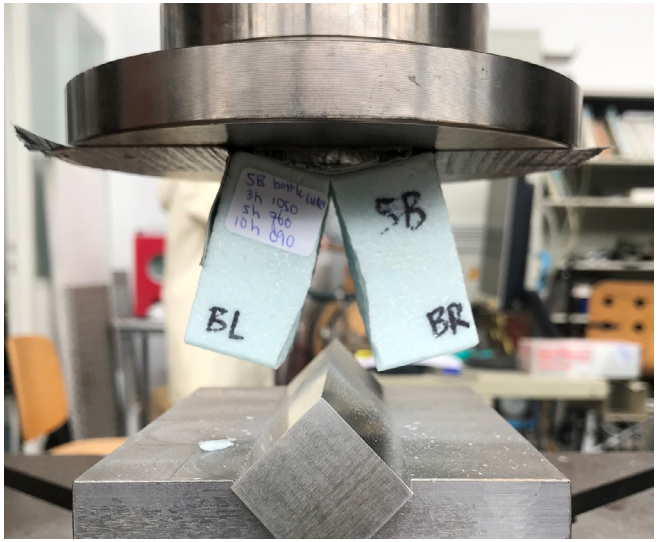

Figure D17 - sample 5B; left: set-up before and after splitting test. right: split surface

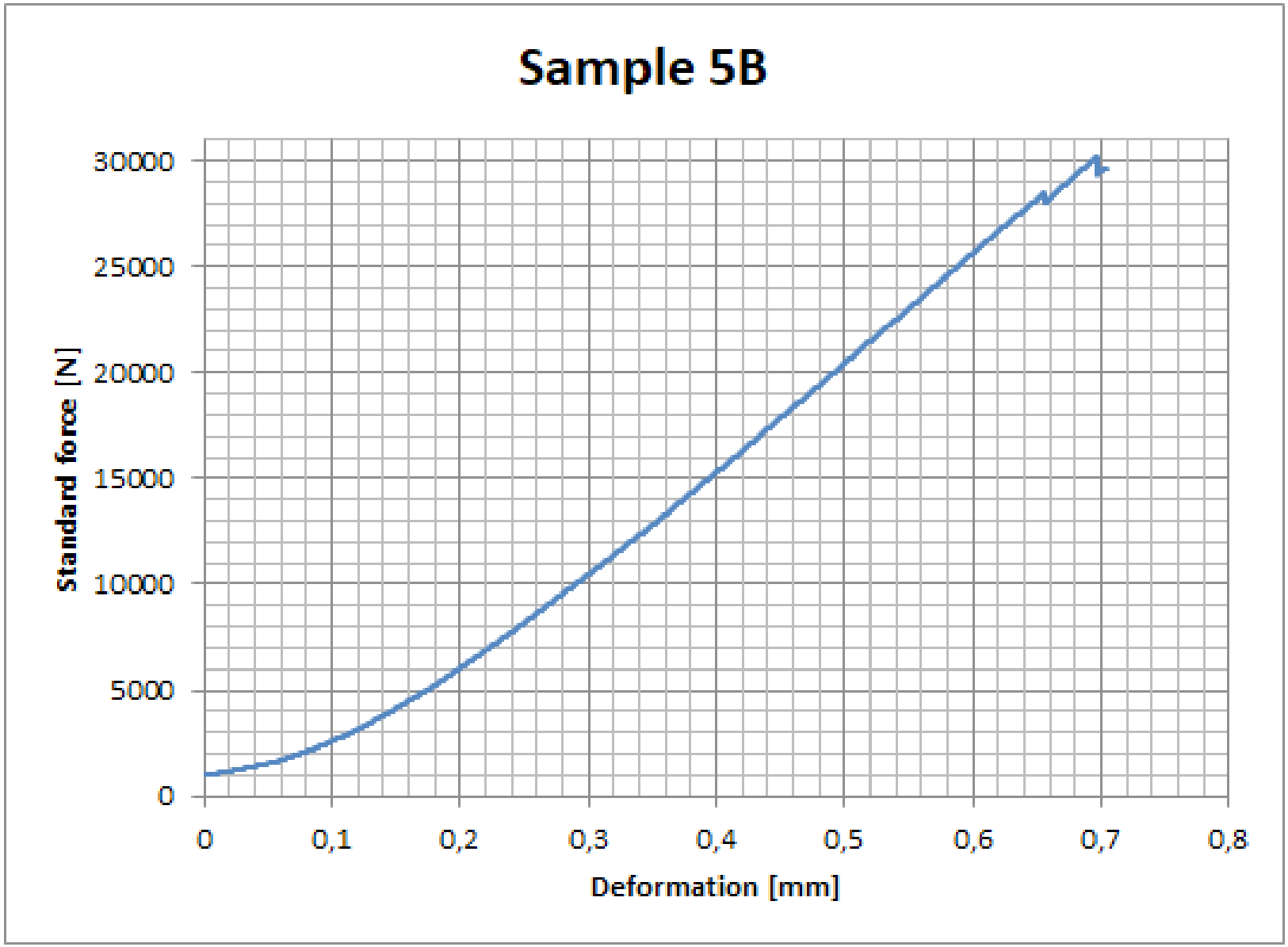

Figure D18 - sample 5B; deformation-force curve

Appendix E: X-ray diffraction

The X-ray diffraction (XRD) analysis is primarily used for the phase identification of crystalline materials, given the following XRD reports.

X-RAY FACILITIES GROUP

Dr. Amarante Böttger *A.J.Bottger@tudelft.nl*
phone +31(0)1527·82243
Dhr. Ruud Hendrikx *R.W.A.Hendrikx@tudelft.nl*
Drs. Richard Huizenga *R.M.Huizenga@tudelft.nl*

Delft University of Technology, Faculty of 3mE
Department of Materials Science and Engineering
Mekelweg 2, NL-2628 CD Delft, the Netherlands, phone +31(0)1527·82255/89459

XRD analysis of glass powders

Author : Ruud Hendrikx
Date : 19 sep 2019
Researcher : Rong Yu, Telesilla Bristogianni, BK
Research question : Identification of crystalline phases

Samples
The sample are labeled: "1B ", "2A", "4B".

Specimens
A thin layer of sample powder was deposited in PMMA sample holder L25.

Experimental
Instrument: Bruker D8 Advance diffractometer Bragg-Brentano geometry and Lynxeye position sensitive detector. Cu Kα radiation. Divergence slit V12, scatter screen height 5 mm, 45 kV 40 mA. Sample spinning. Detector settings: LL 0.11, W 0.14.

Measurement:
Coupled θ -2θ scan 8° - 110°, step size 0.030° 2θ, counting time per step 2 s.

Data evaluation: Bruker software DiffracSuite.EVA vs 5.1.

Results
Figures 1 - 3 show the measured XRD patterns, after background subtraction. Observing the large "humps" between 10 and 80° 2θ, it is clear that major part of the sample is amorphous. However, some small crystalline peaks are present. The colored sticks give the peak positions and intensities of the identified crystalline phases, using the ICDD pdf4 database, see table 1.
For sample 2 the amorphous contribution was subtracted and the resulting pattern was smoothed prior to the identification procedure, see the picture-in-picture in figure 2.

Sample	*compound*	
1B	Wollastonite-2M	CaSiO3
	cristobalite low	SiO2
2A	Quartz low	SiO2
	Mullite	Al2.26Si0.74O4.87
4B	Wollastonite-2M	CaSiO3
	cristobalite low	SiO2

Table 1.

Use of our XRD or XRF analysis:
In a publication: 'PersonX at the Department of Materials Science and Engineering of the Delft University of Technology is acknowledged for the X-ray analysis. If it is an important part of the publication: a co-authorship is preferred. It is useful to involve us in the preparation of any presentation!

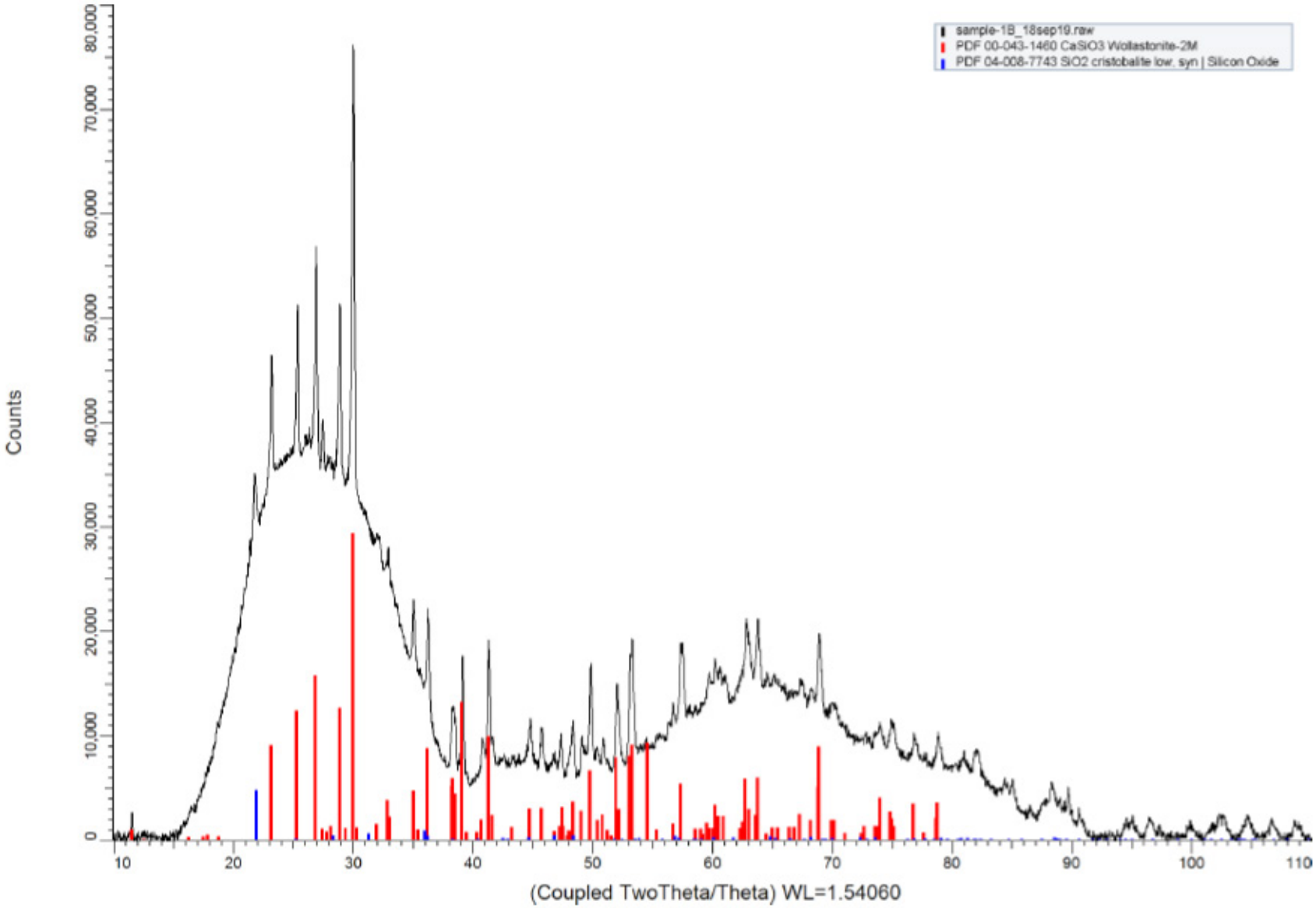

Figure E1 - XRD result sample 1B

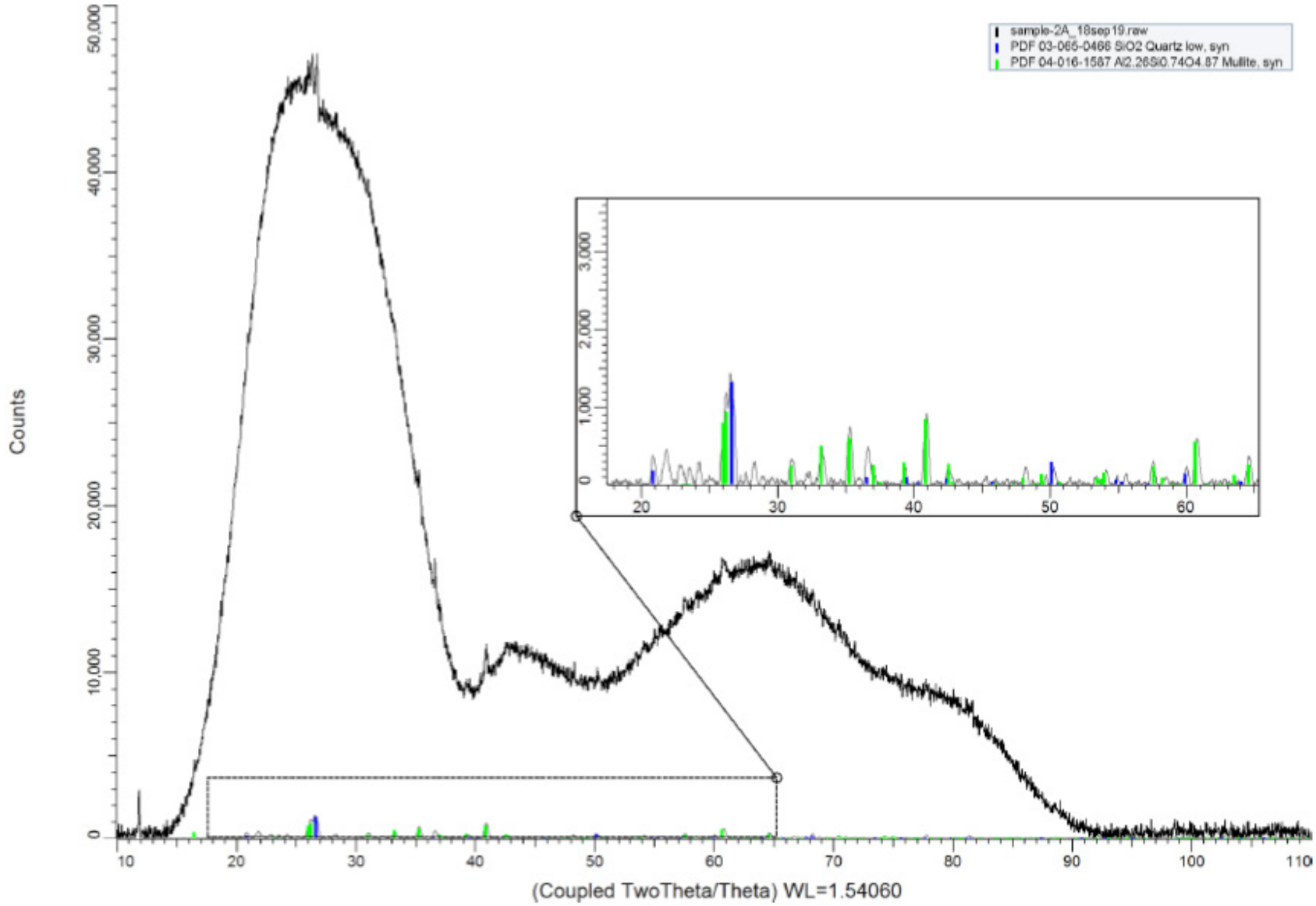

Figure E2 - XRD result sample 2A

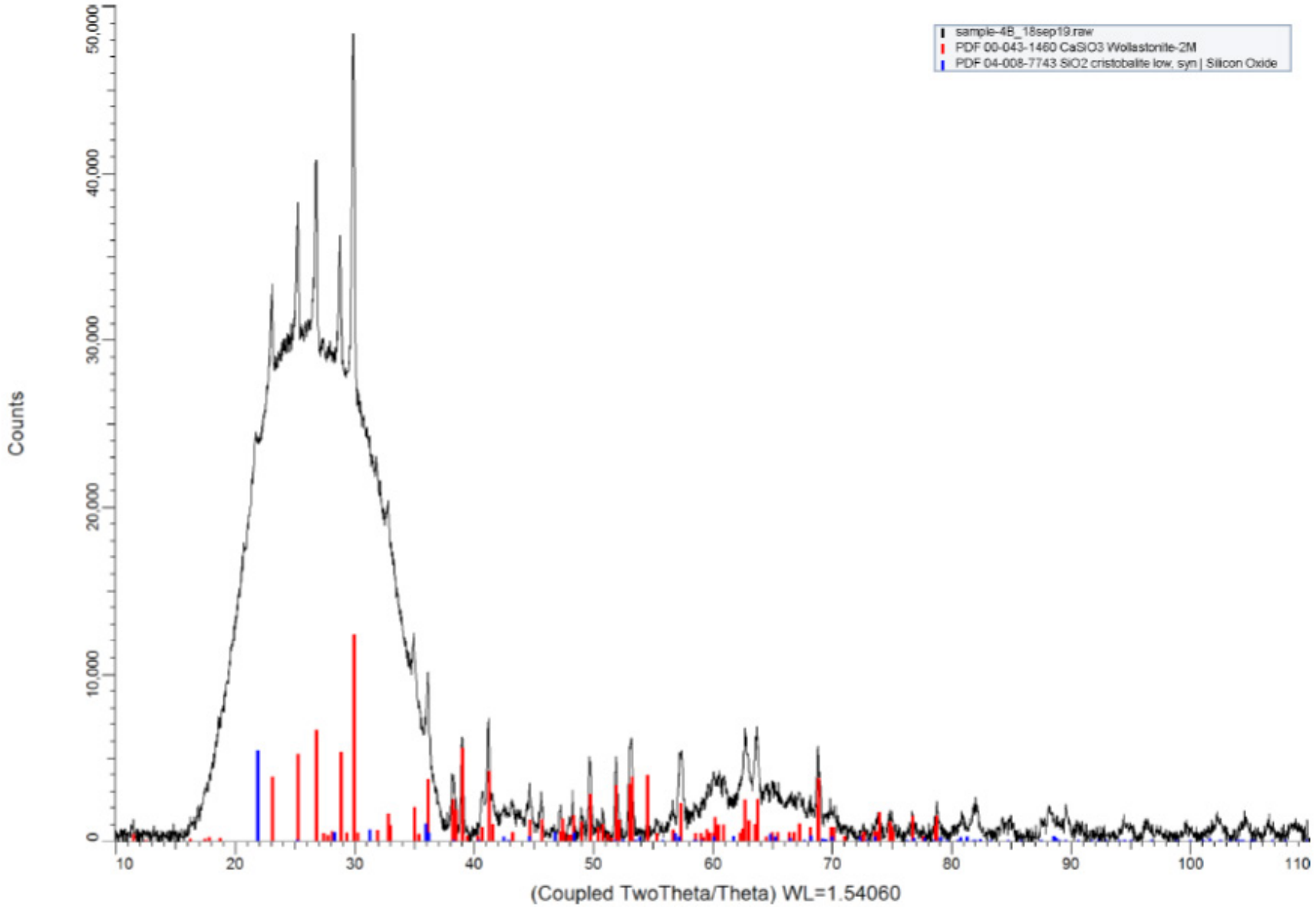

Figure E3 - XRD result sample 4B

X-RAY FACILITIES GROUP

Dr. Amarante Böttger *A.J.Bottger@tudelft.nl*
phone +31(0)1527·82243
Dhr. Ruud Hendrikx *R.W.A.Hendrikx@tudelft.nl*
Drs. Richard Huizenga *R.M.Huizenga@tudelft.nl*

Delft University of Technology, Faculty of 3mE
Department of Materials Science and Engineering
Mekelweg 2, NL-2628 CD Delft, the Netherlands, phone +31(0)1527·82255/89459

XRD analysis of glass powder

Author : Ruud Hendrikx
Date : 06 dec 2019
Researcher : Cindy Lei, BK
Research question : Identification of crystalline phases

Sample
The sample is labeled: "5B".

Specimen
A small amount of sample powder was deposited in PMMA holder l25.

Experimental
Instrument: Bruker D8 Advance diffractometer Bragg-Brentano geometry and Lynxeye position sensitive detector. Cu Kα radiation. Divergence slit V12, scatter screen height 5 mm, 45 kV 40 mA. Sample spinning. Detector settings: LL 0.11, W 0.14.

Measurement:
Coupled θ -2θ scan 8° - 110°, step size 0.030° 2θ, counting time per step 2 s.

Data evaluation: Bruker software DiffracSuite.EVA vs 5.1.

Results
Figure 1 shows the measured XRD pattern, after background subtraction. Observing the large "humps" between 10 and 90° 2θ, it is clear that a large part of the sample is amorphous. However, some crystalline peaks are present, figure 2 shows the zoomed-in view of those crystalline peaks.
The colored sticks give the peak positions and intensities of the possibly present crystalline phases, using the ICDD pdf4 database, see table 1.

Sample	*compound*	
5B	Cristobalite	SiO2
	Coesite	SiO2
	Sodium Calcium Silicate	Na2Ca3Si6O16

Table 1.

Crystallinity:
If we simply define the crystallinity as the integrated intensities of the crystalline peaks divided by the total of integrate intensities, then the crystallinity of this sample is 40%.

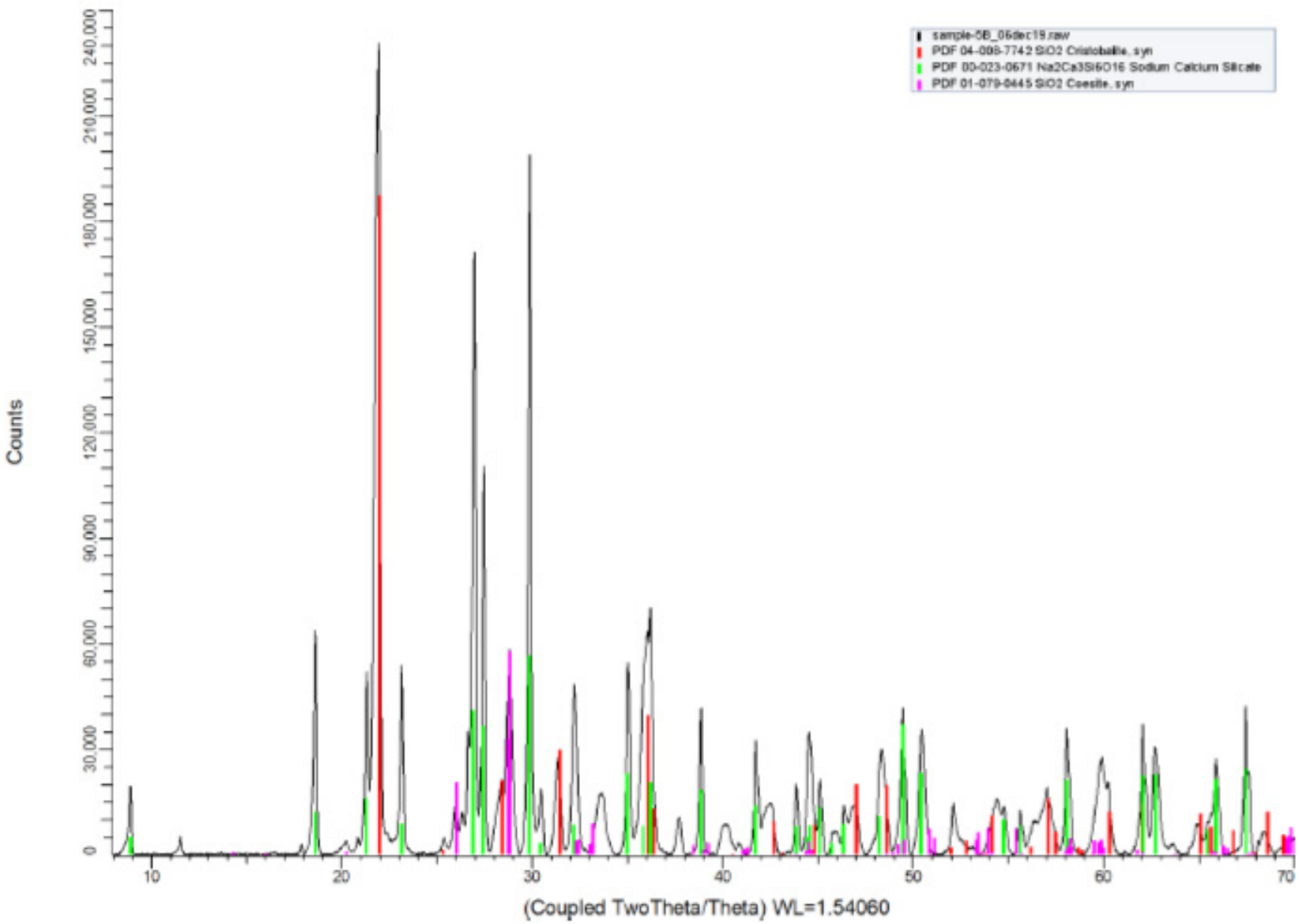

Figure E4 - XRD result sample 4B

Appendix F: Microscopy

F.1. Microscopic pictures sample 1B

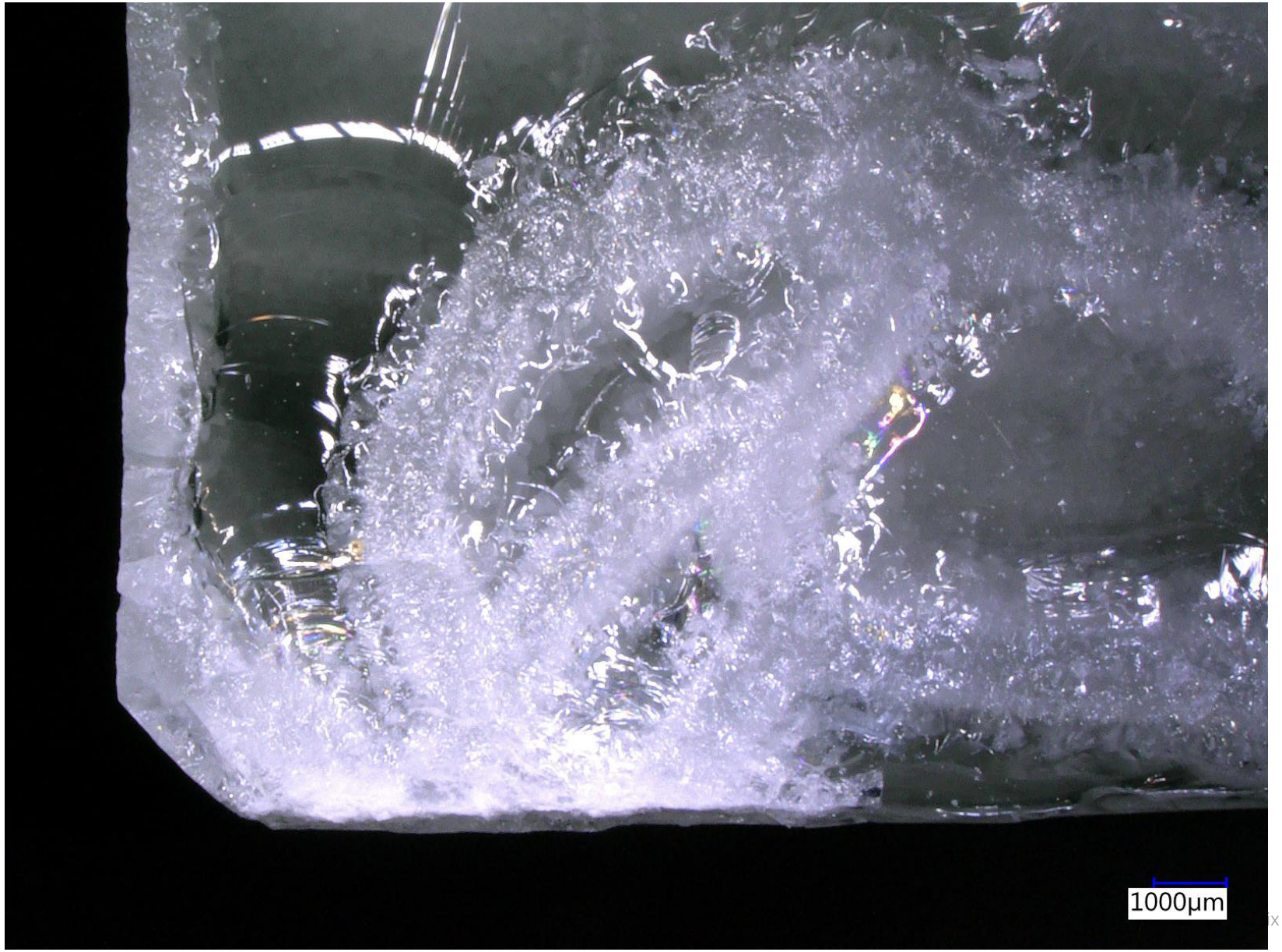

Figure F1 - sample 1B - Bottom right corner

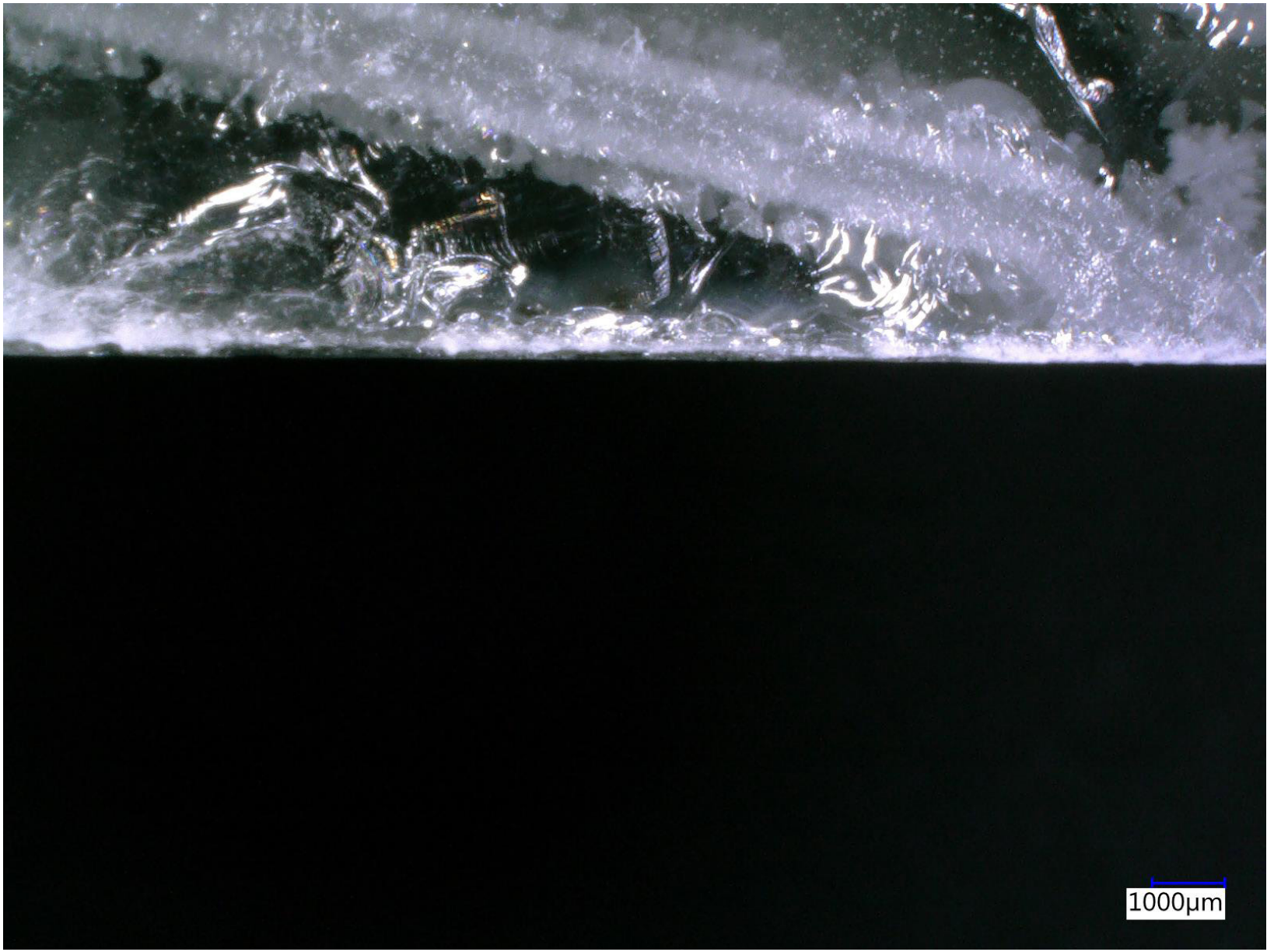

Figure F2 - sample 1B - Bottom crack

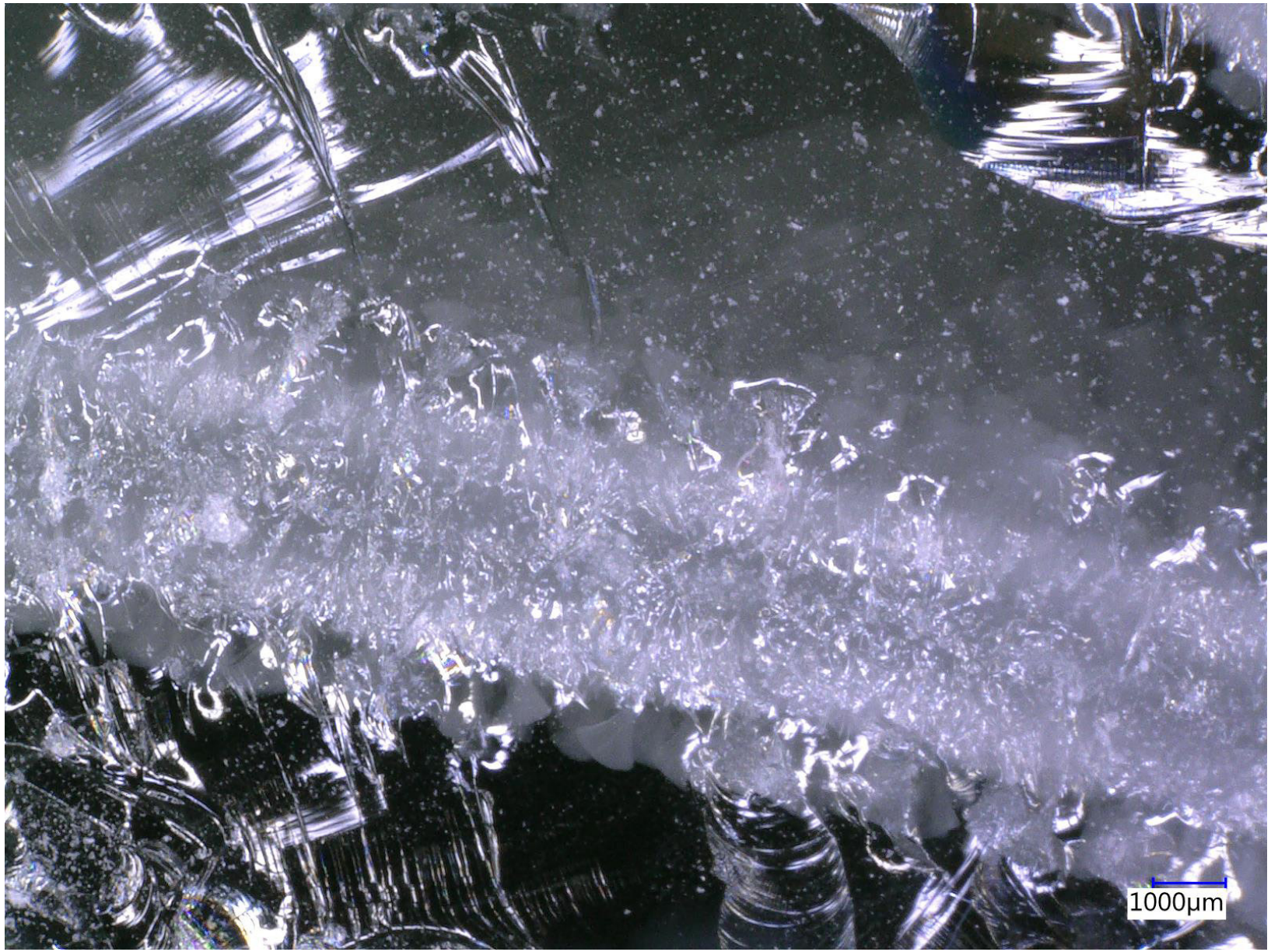

Figure F3 - sample 1B - Cracked crystal in between glassy phases

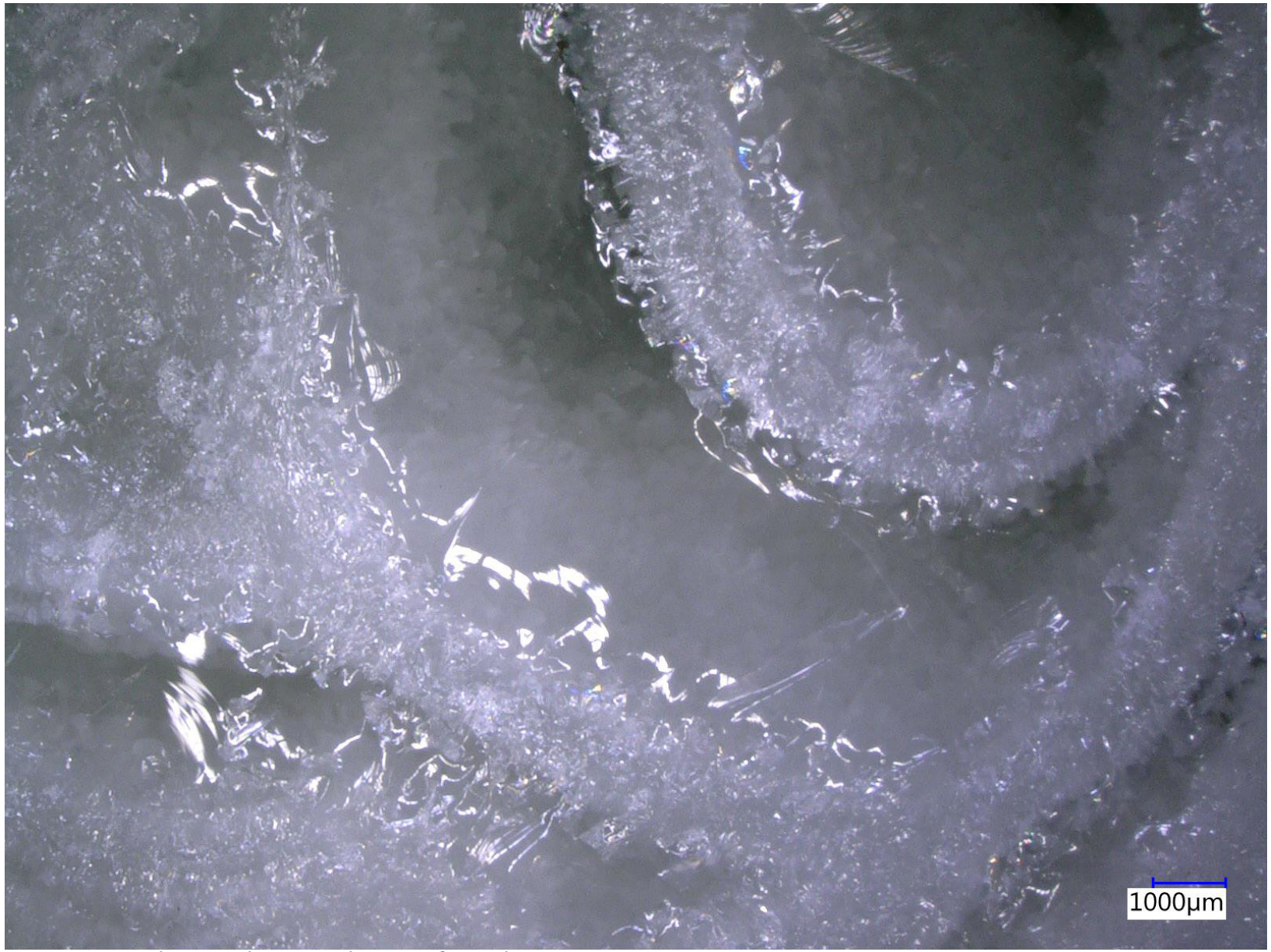

Figure F4 - sample 1B - 3 dimensional setting of crystals

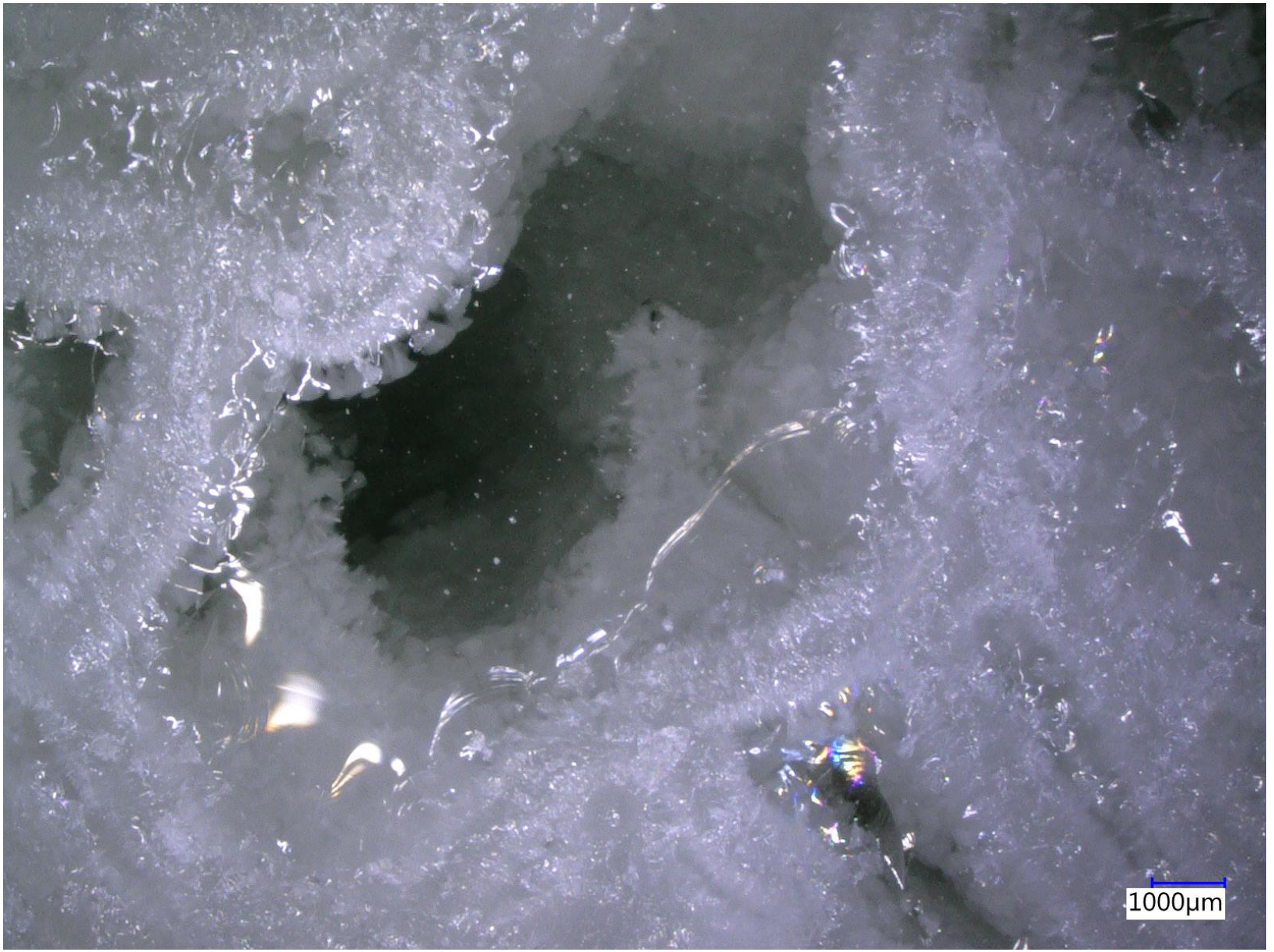

Figure F5 - sample 1B - 3 dimensional setting of crystals

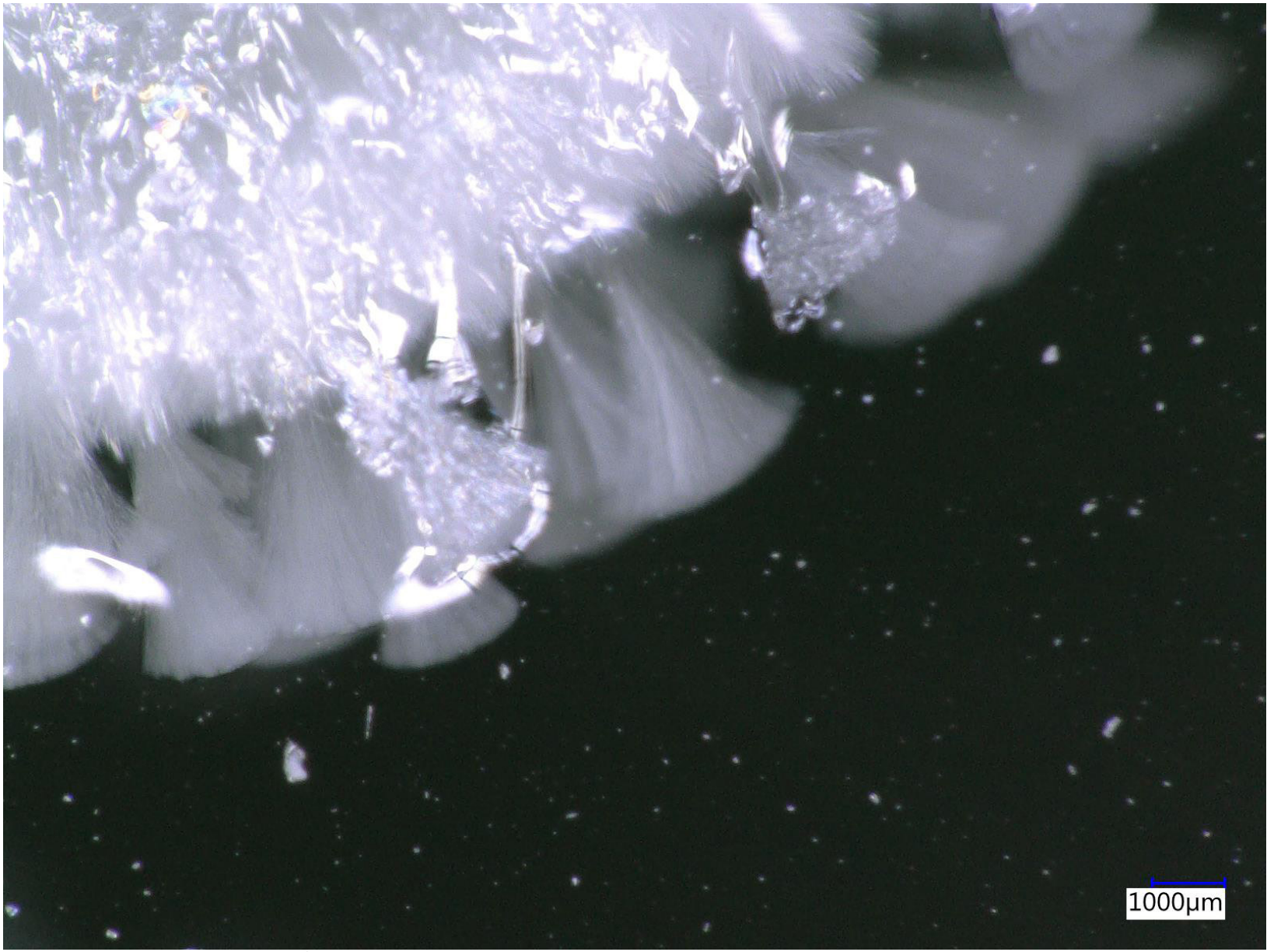

Figure F6 - sample 1B - Acicular fan shaped crystals

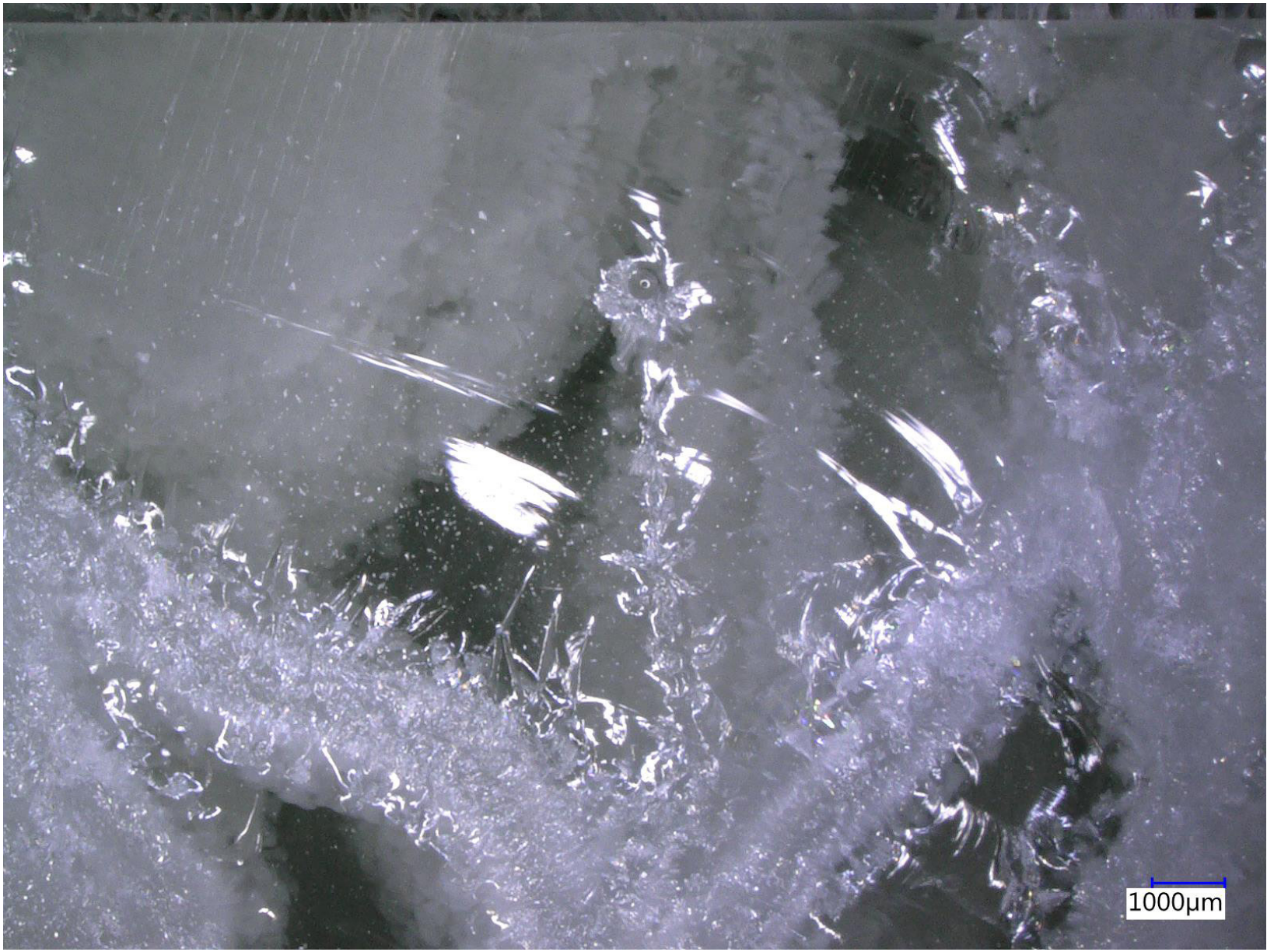

Figure F7 - sample 1B - Crack propagation from crystal to air bubble

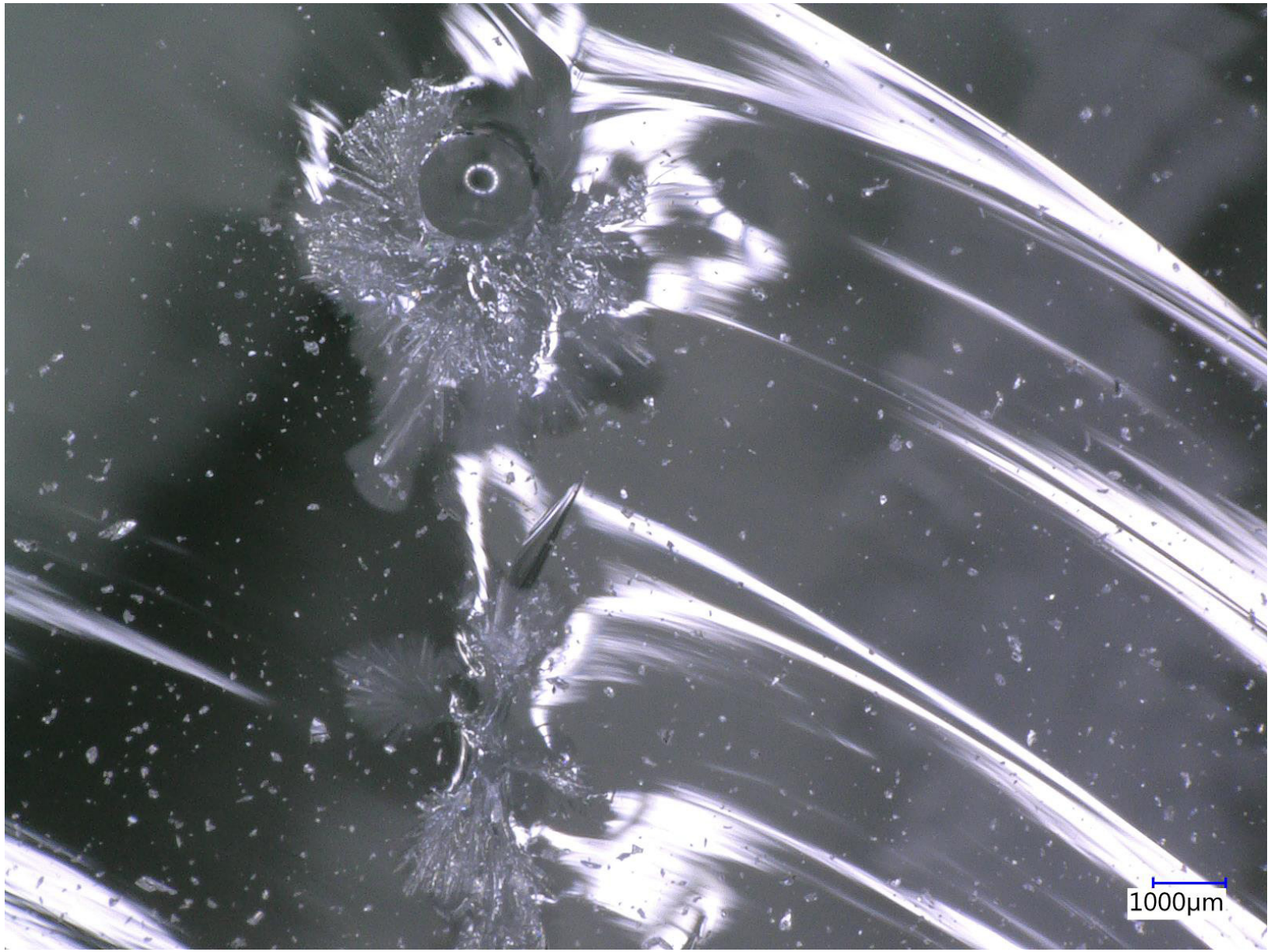

Figure F8 - sample 1B - Zoom of crack propagation to air bubble

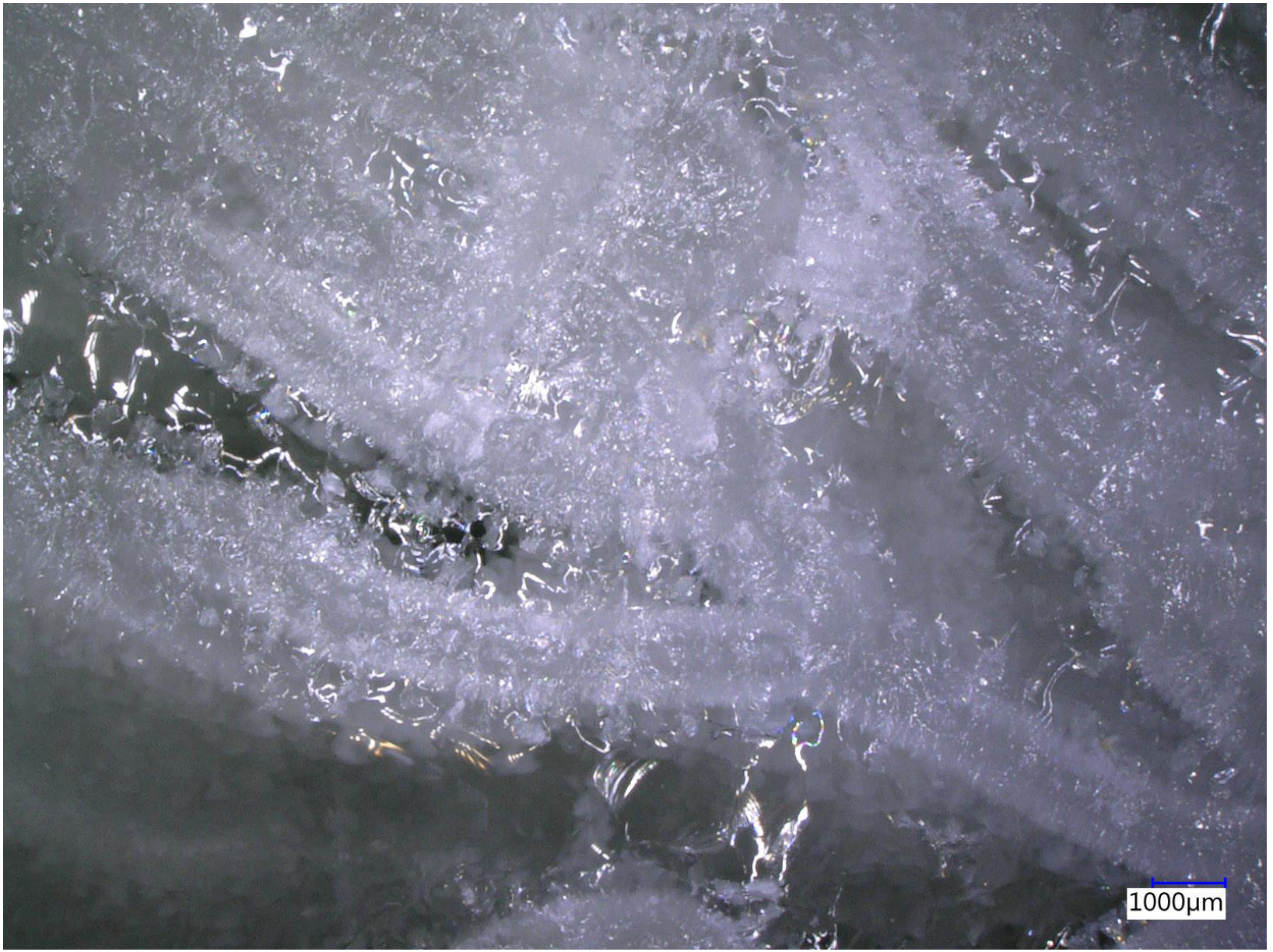

Figure F9 - sample 1B - Crystallized intersection

F.2. Microscopic pictures sample 2A

Figure F10 - sample 2A - Failure origin at bottom left corner

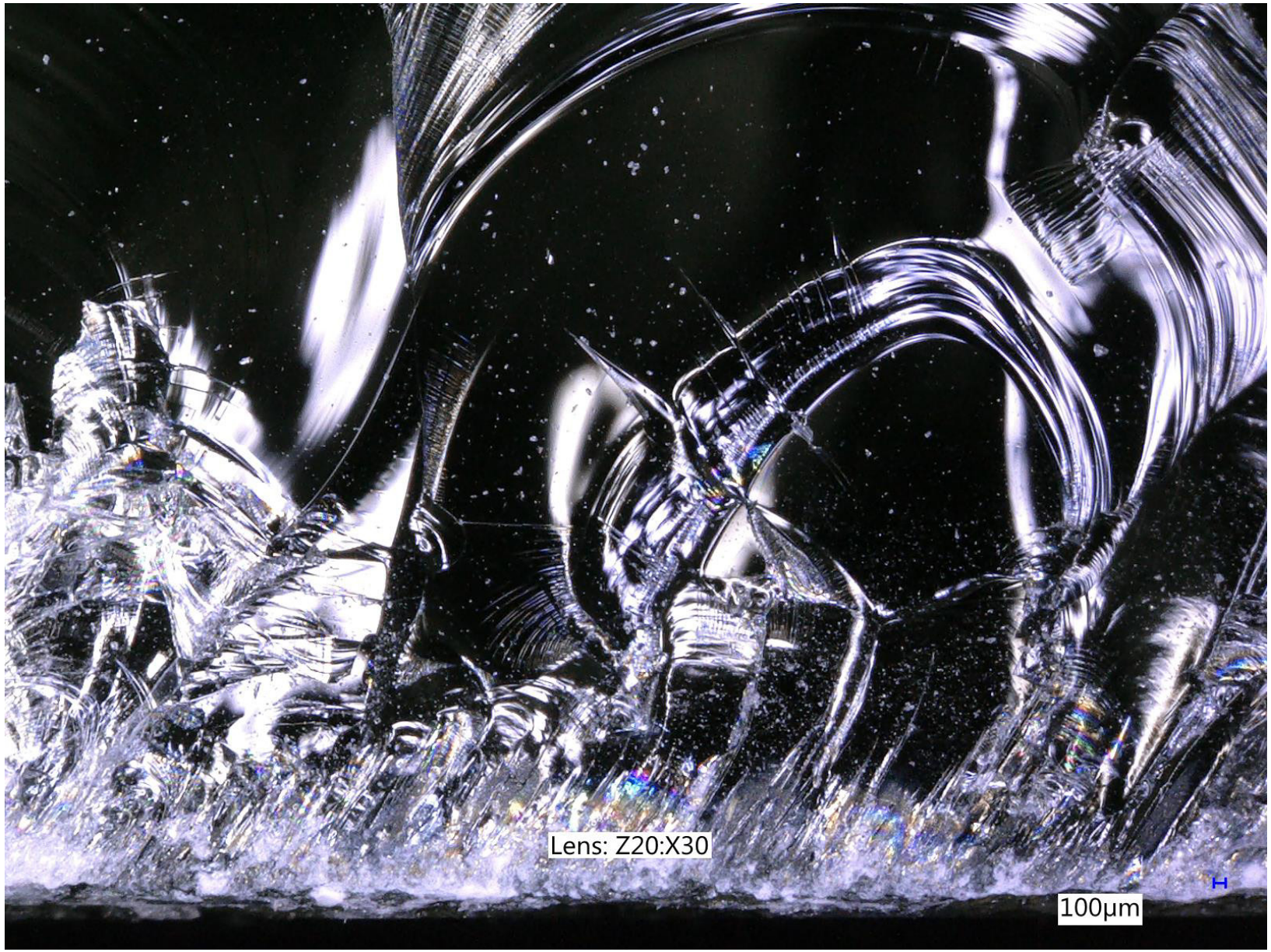

Figure F11 - sample 2A - Zoom of failure origin at bottom left corner

Figure F12 - sample 2A - Minor cracks at bottom right corner

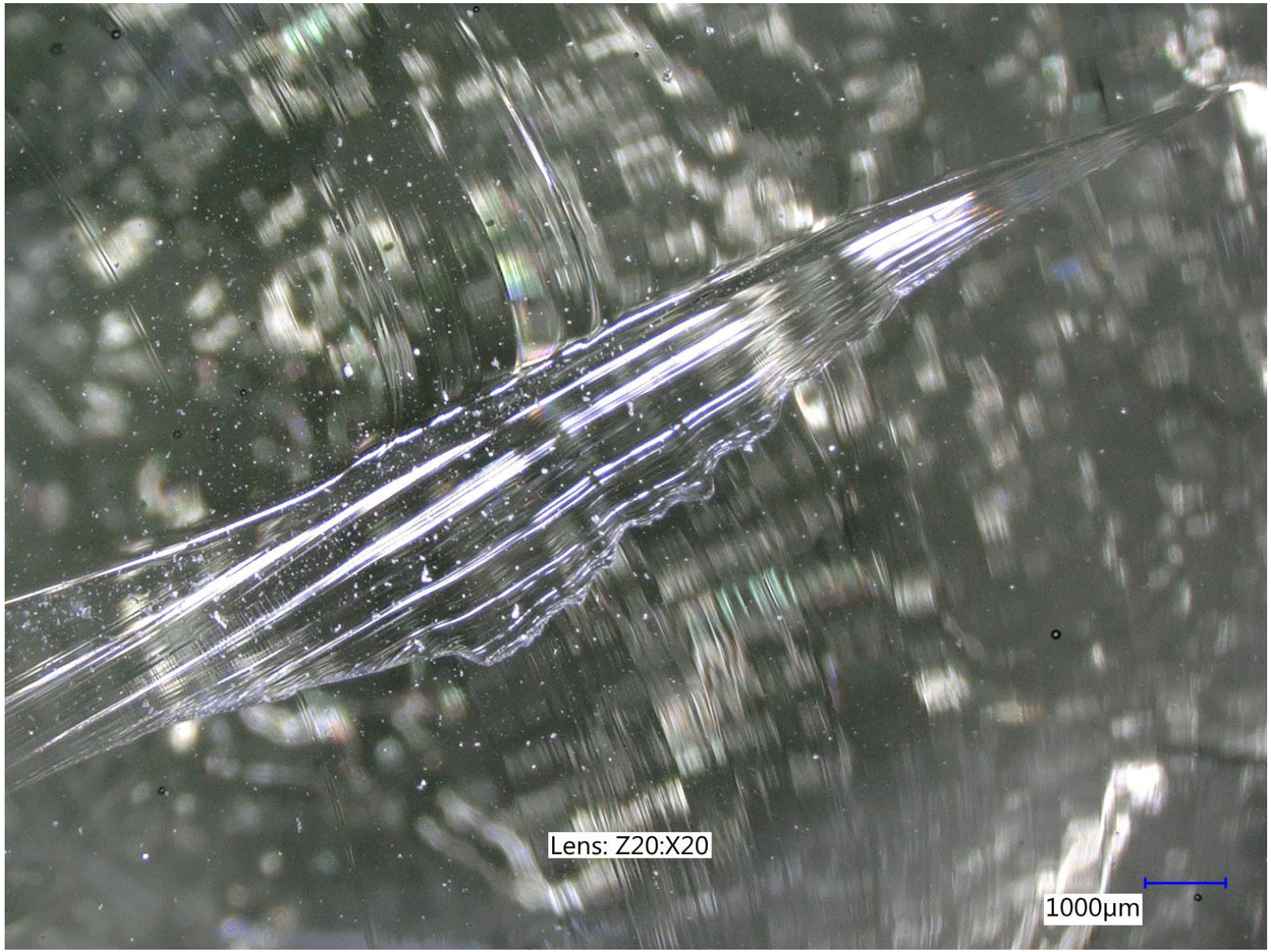

Figure F13 - sample 2A - Arrest line

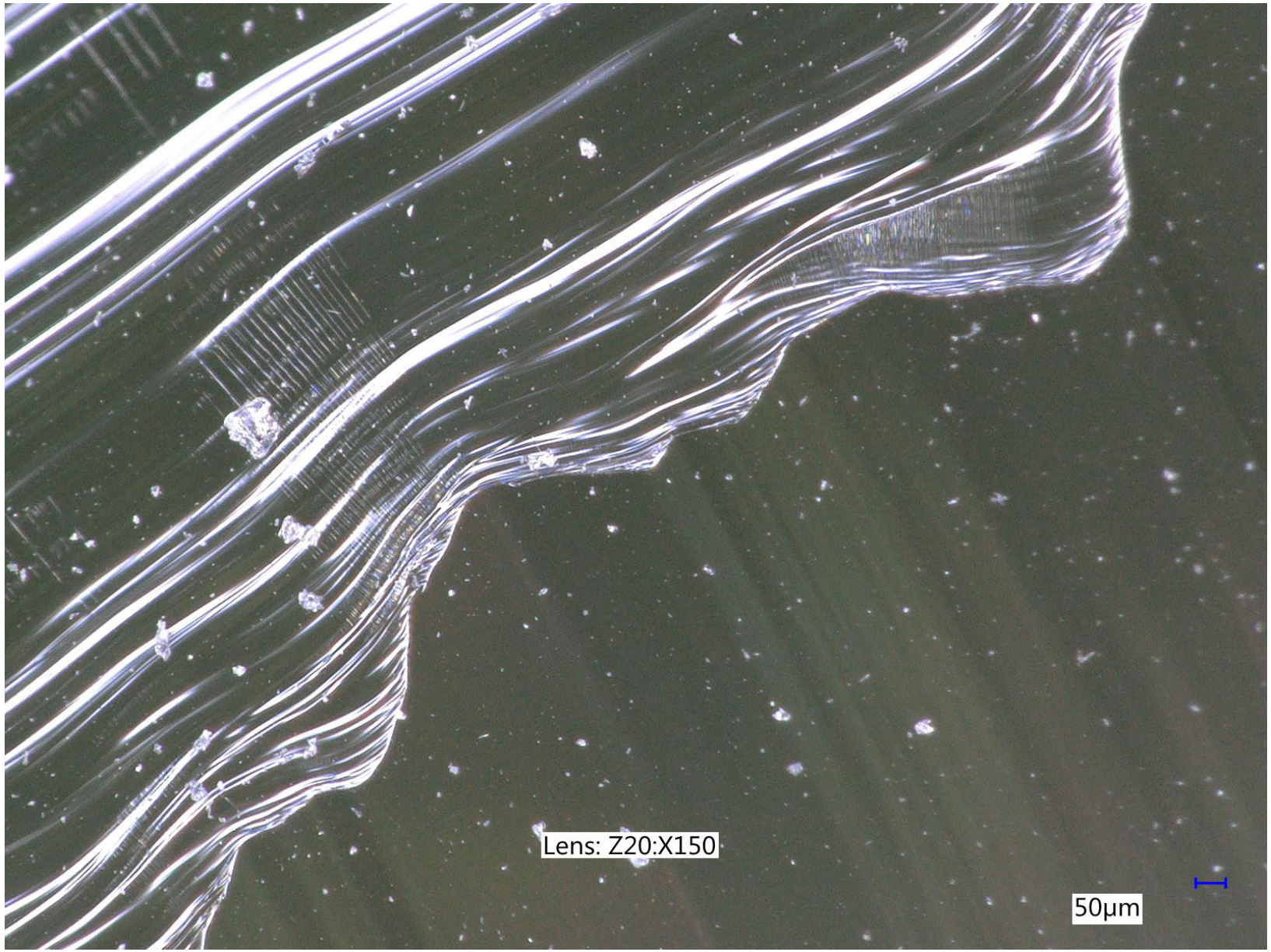

Figure F14 - sample 2A - Zoom of arrest line

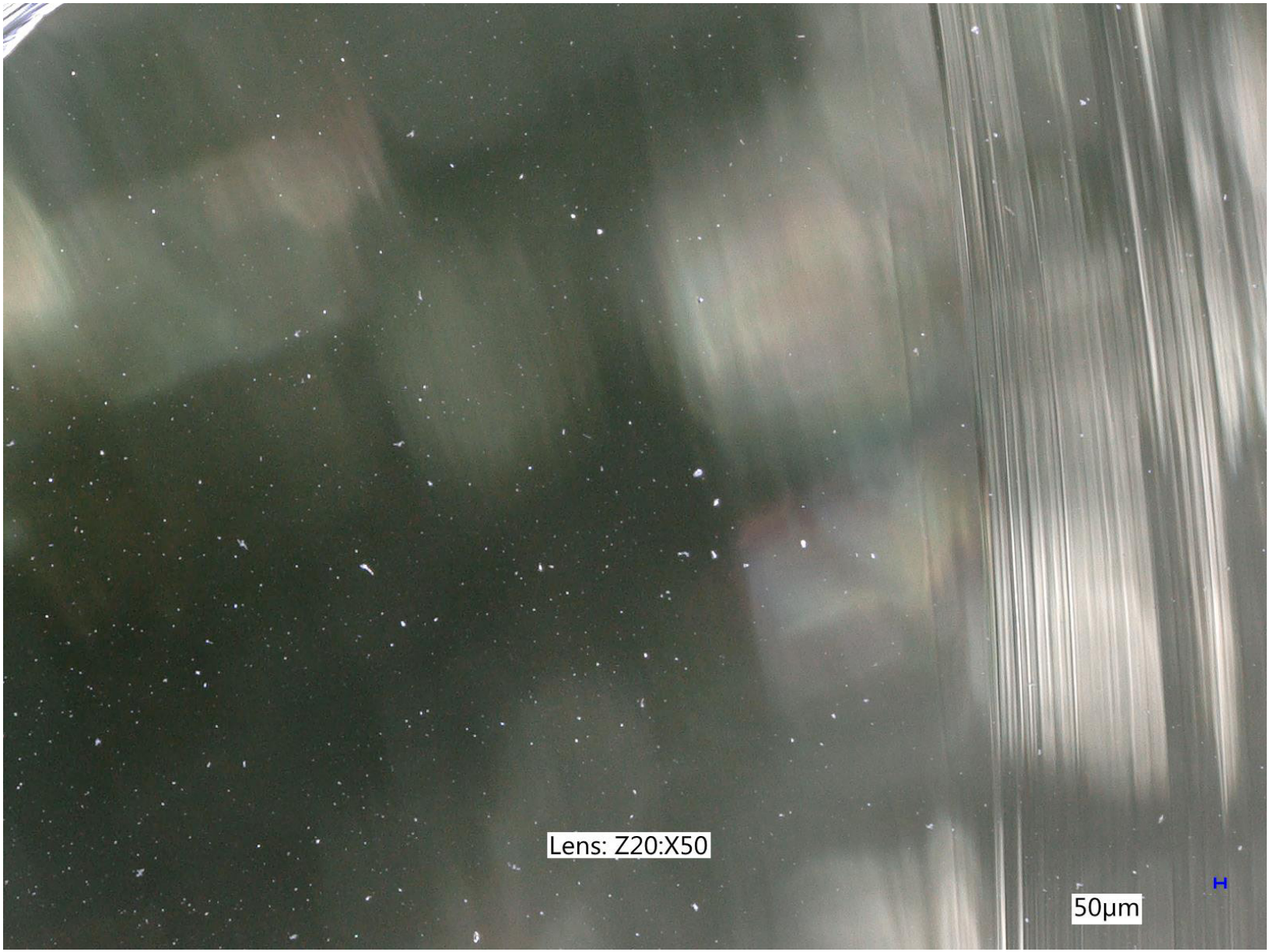

Figure F15 - sample 2A - Small particles throughout the sample, possibly nuclei

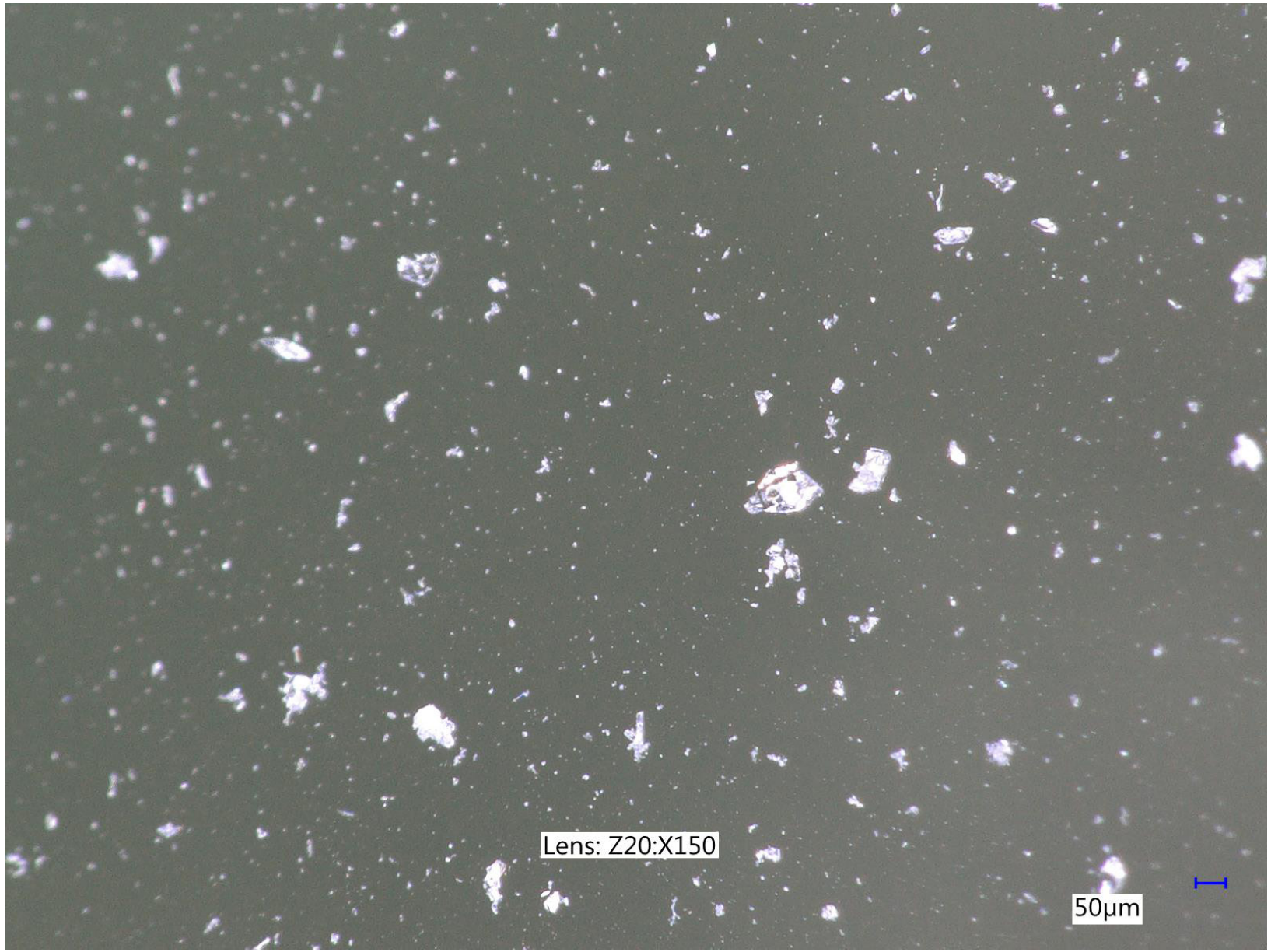

Figure F16 - sample 2A - Zoom on small particles throughout the sample, possibly nuclei

F3. Microscopic pictures sample 4B

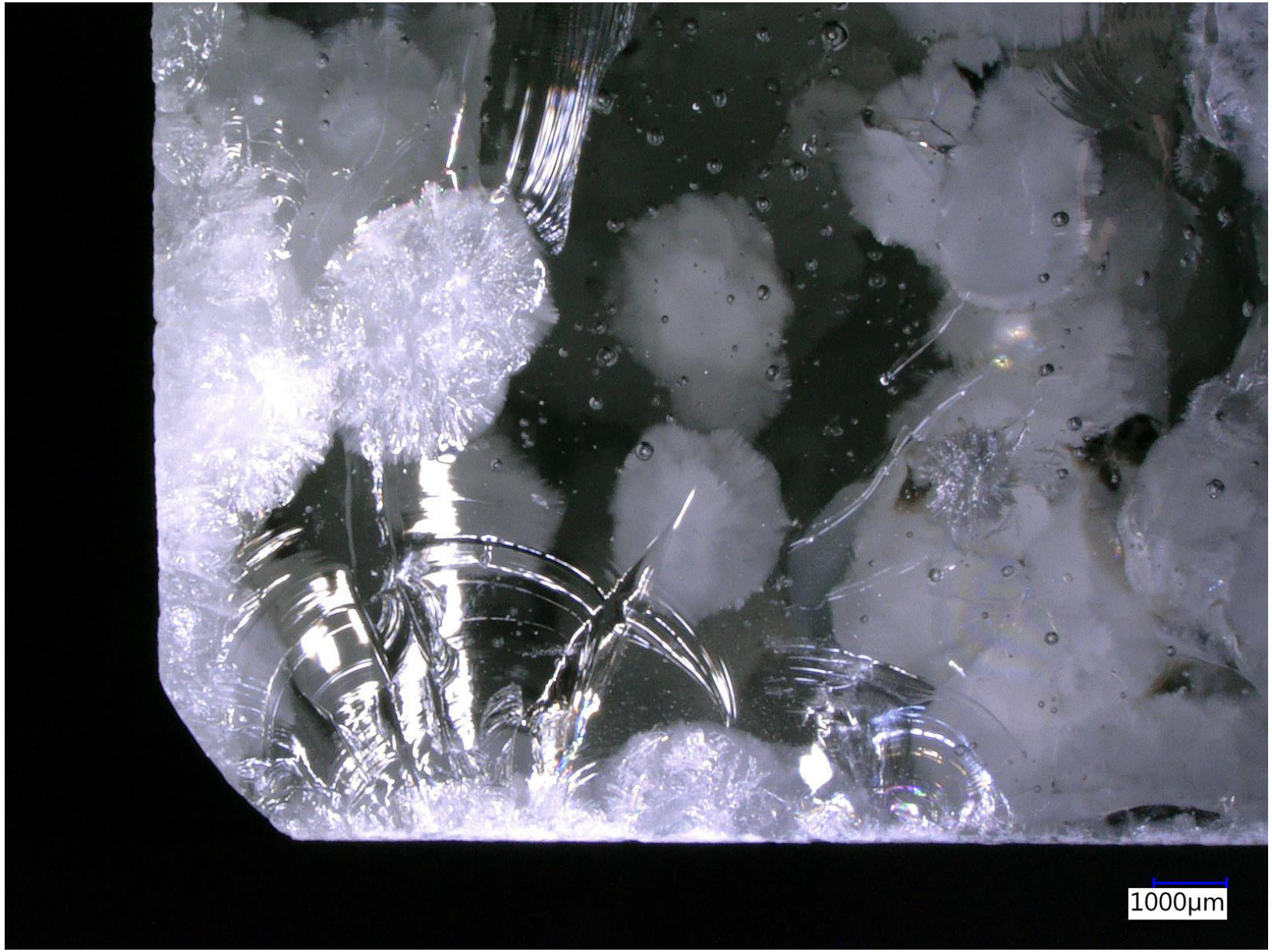

Figure F17 - sample 4B - Zoom of crack at bottom left corner

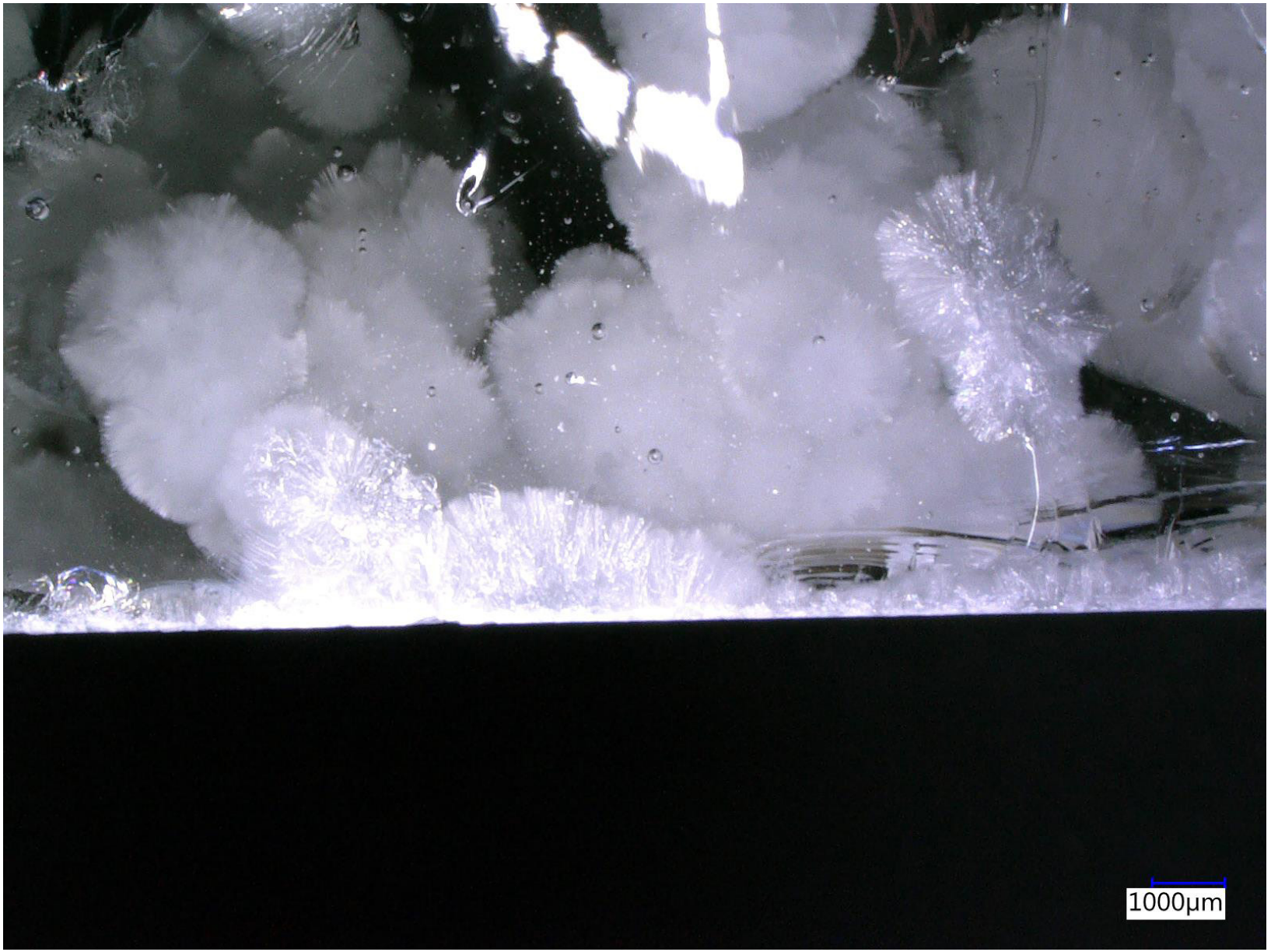

Figure F18 - sample 4B - Zoom of crack at bottom edge

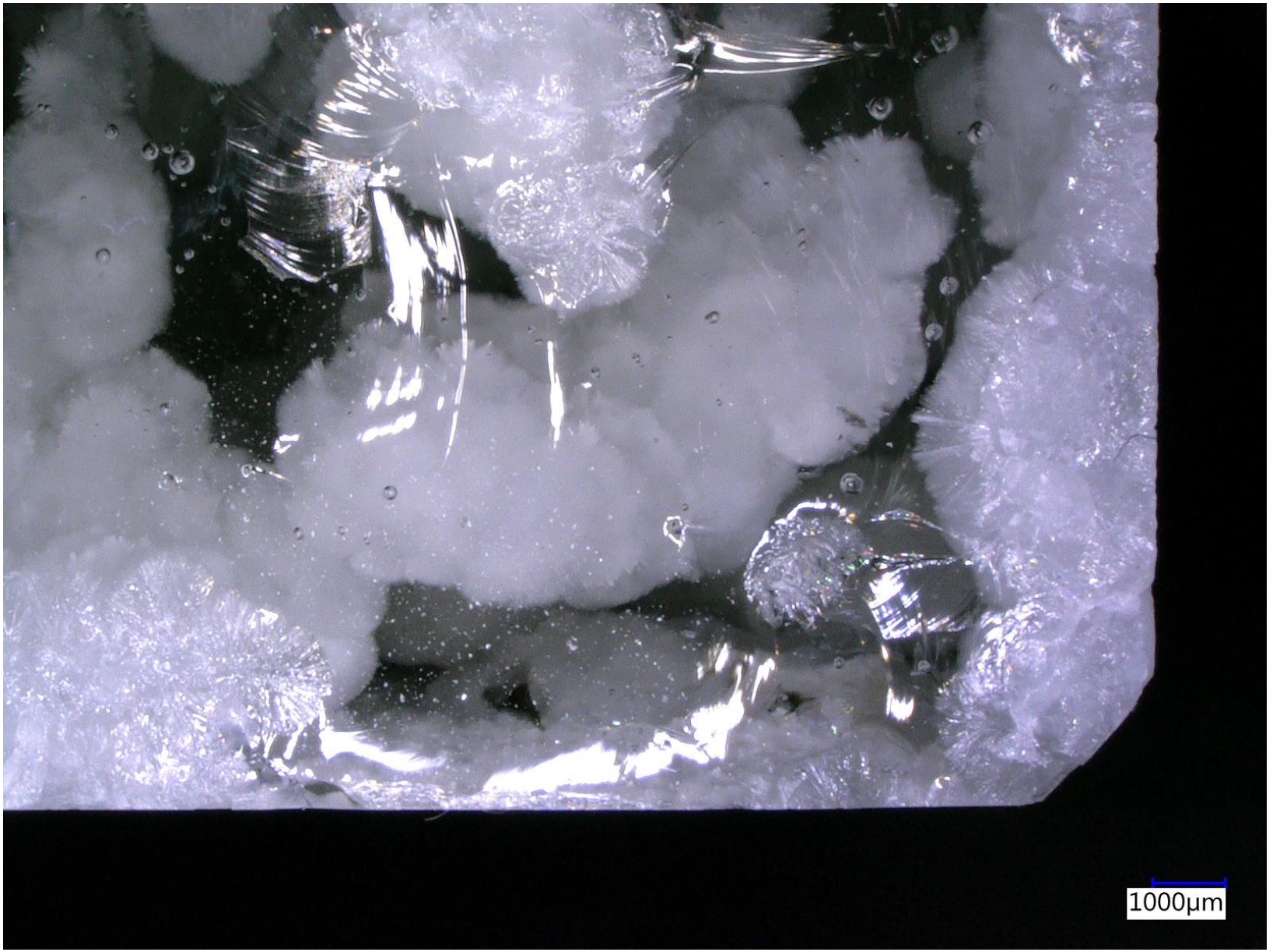

Figure F19 - sample 4B - Zoom of crack at bottom right corner

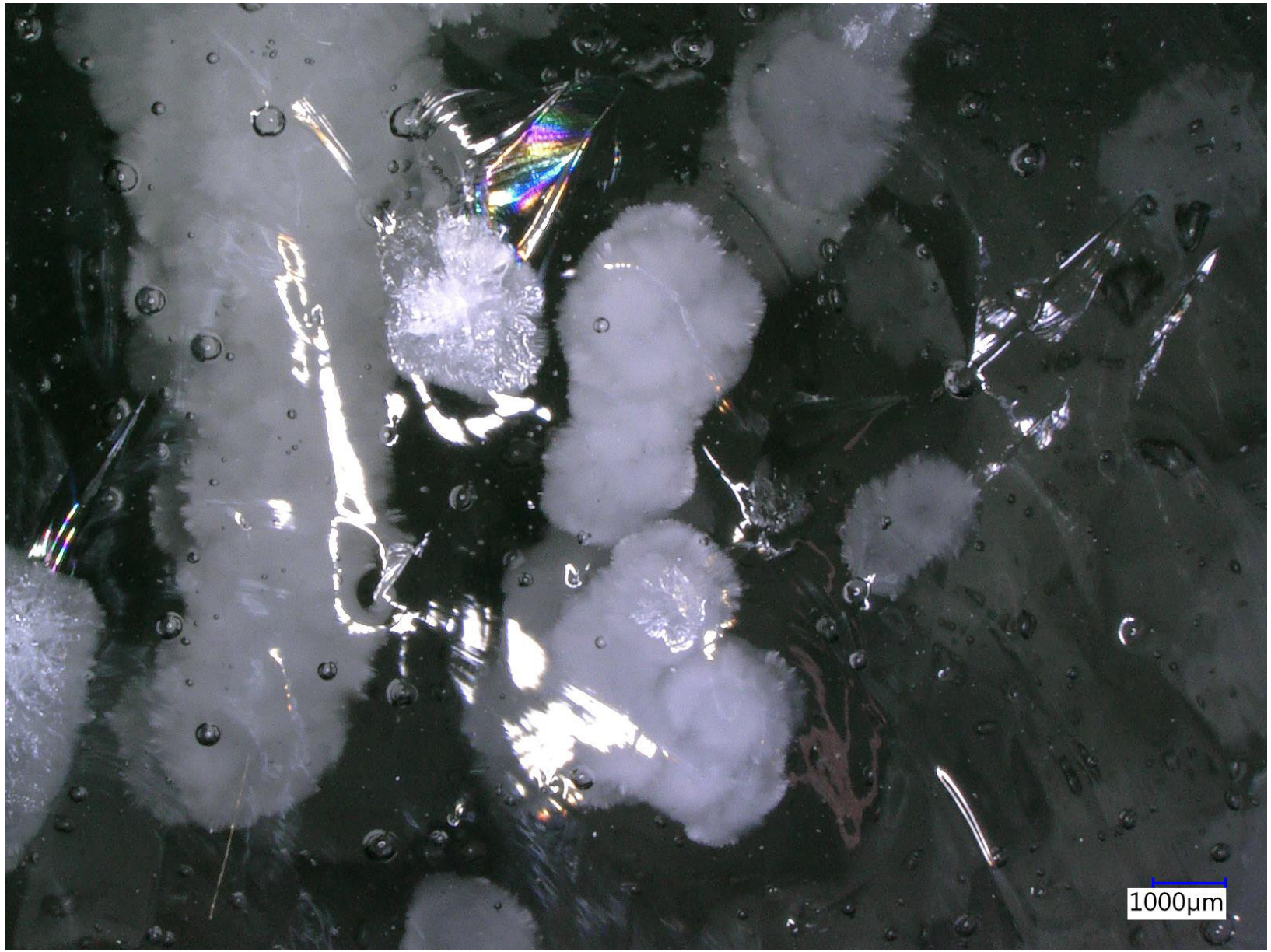

Figure F20 - sample 4B - Visible cracks in crystal and glassy phase

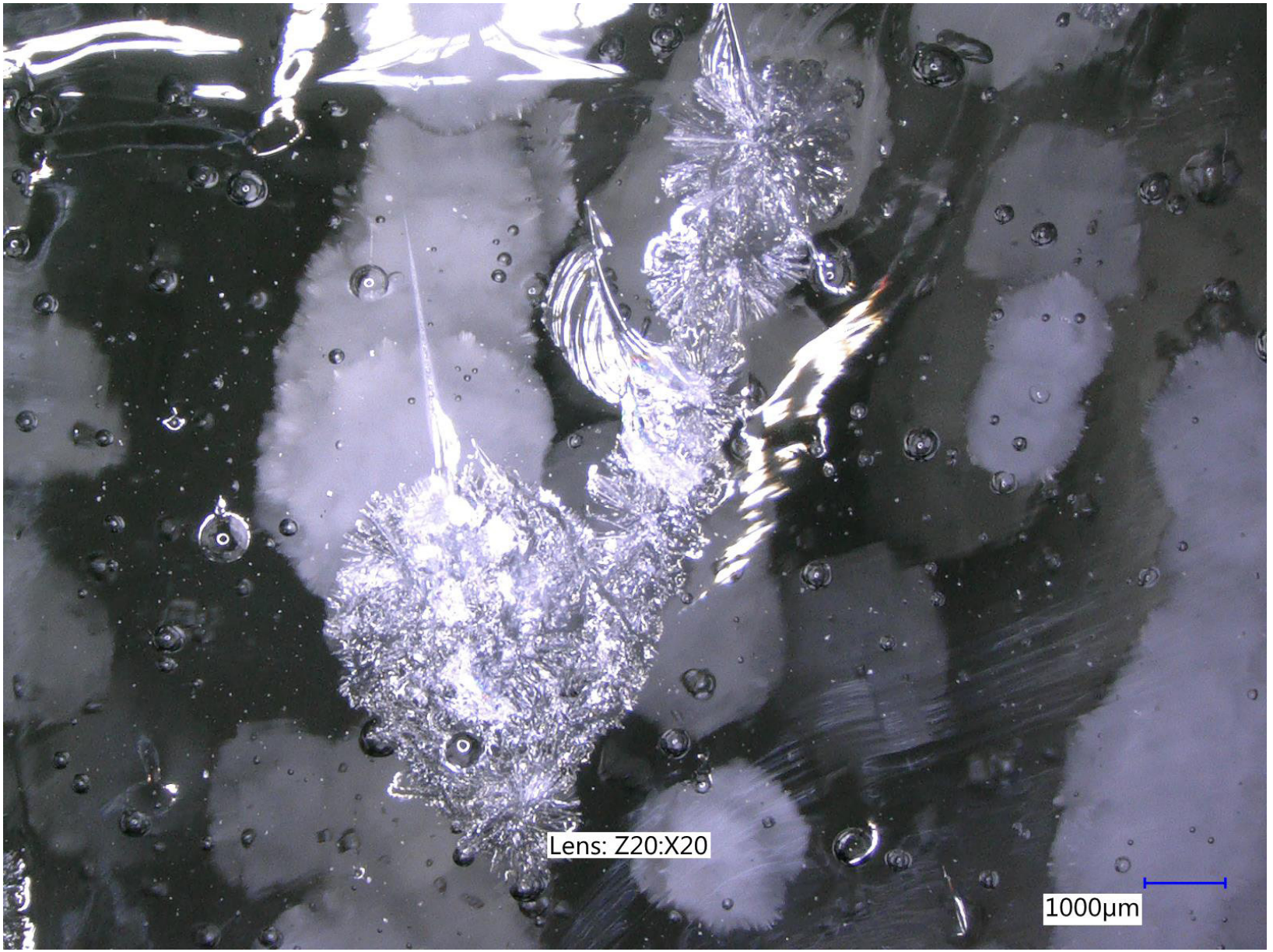

Figure F21 - sample 4B - Visible cracks in crystal and glassy phase

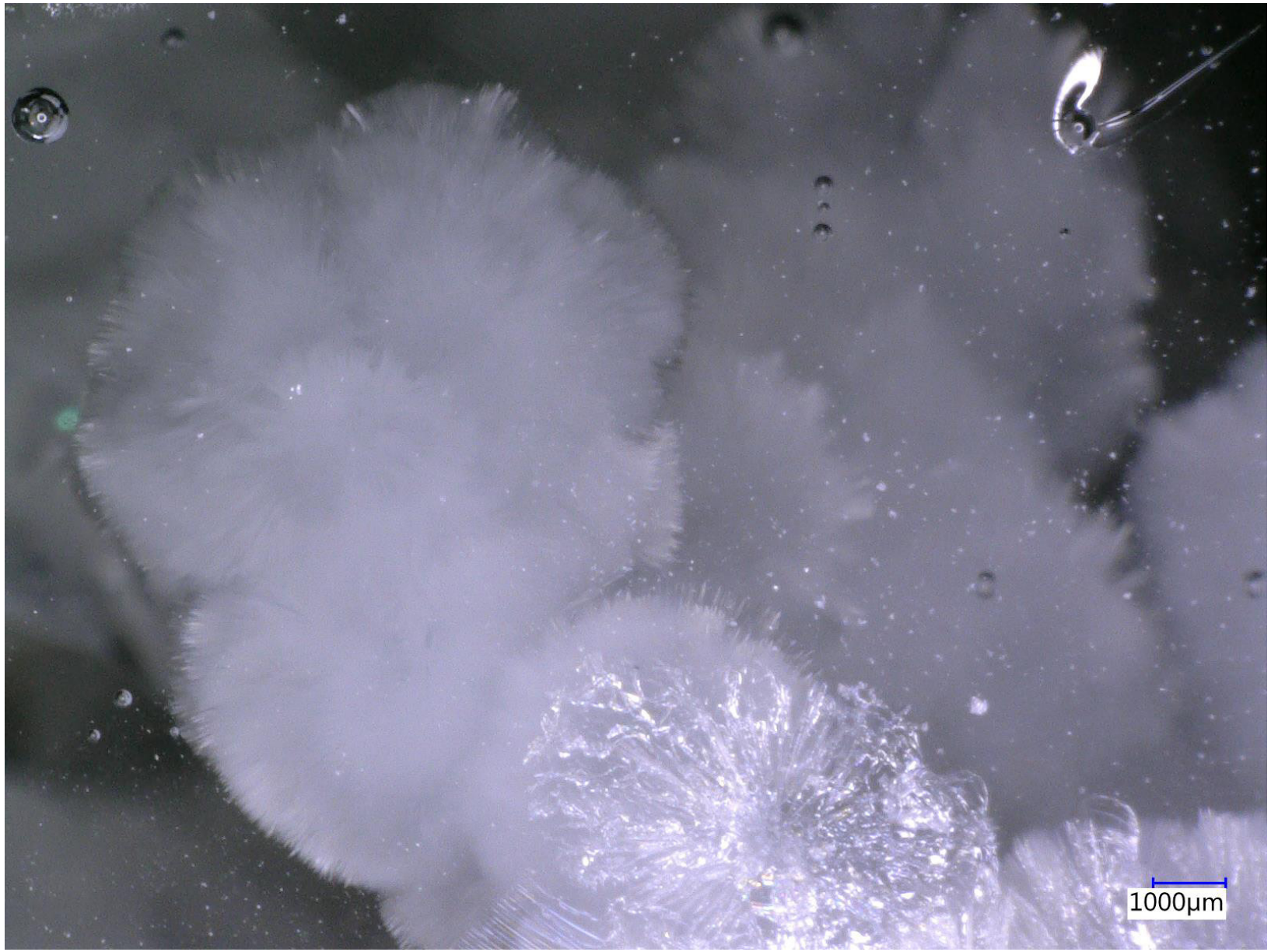

Figure F22 - sample 4B - Zoom on cluster of crystals

Figure F23 - sample 4B - Zoom on cluster of crystals, with focus on the foreground

Figure F24 - sample 4B - Zoom on cluster of crystals, with focus on the background

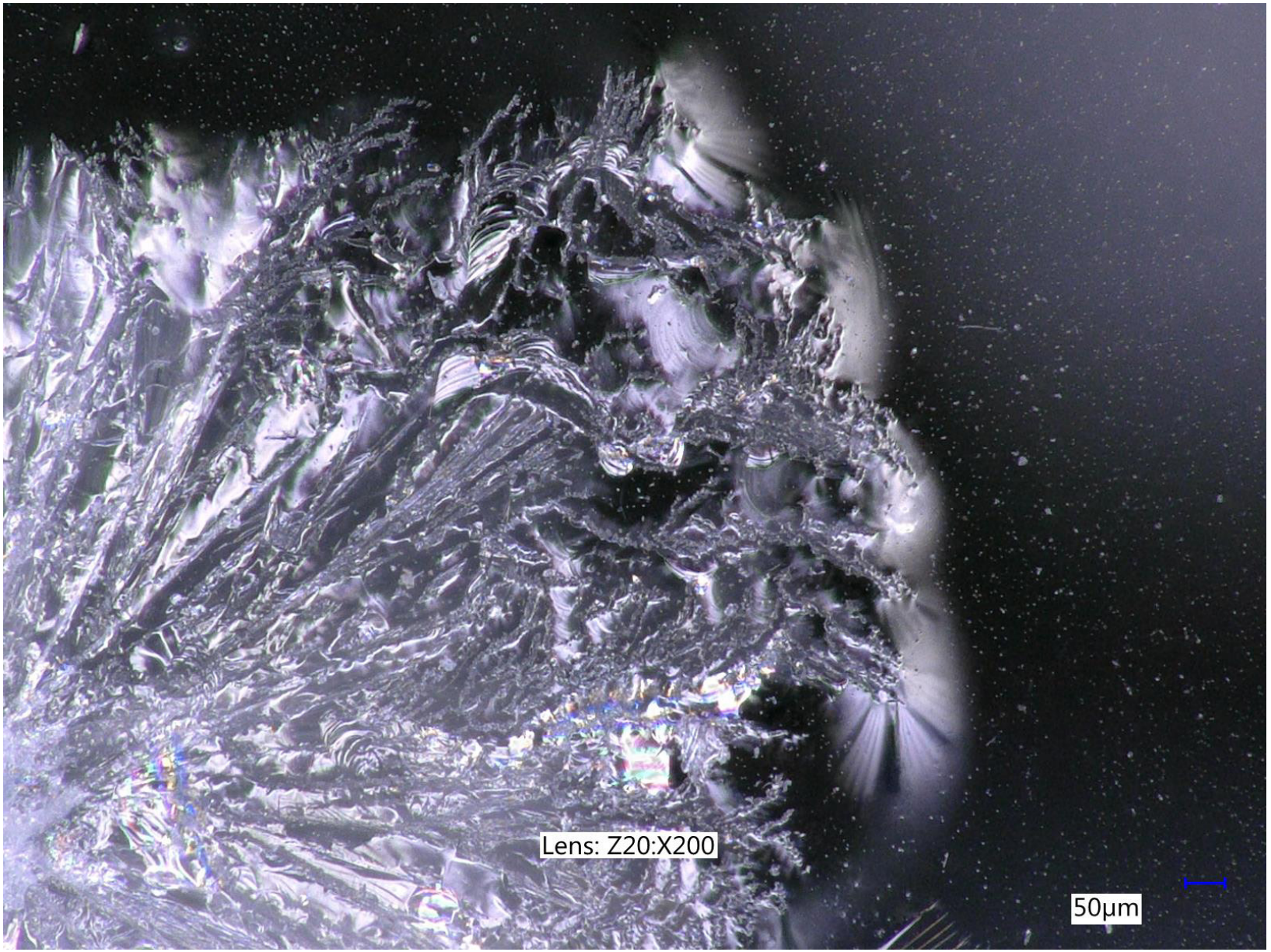

Figure F25 - sample 4B - Zoom on cracked crystal

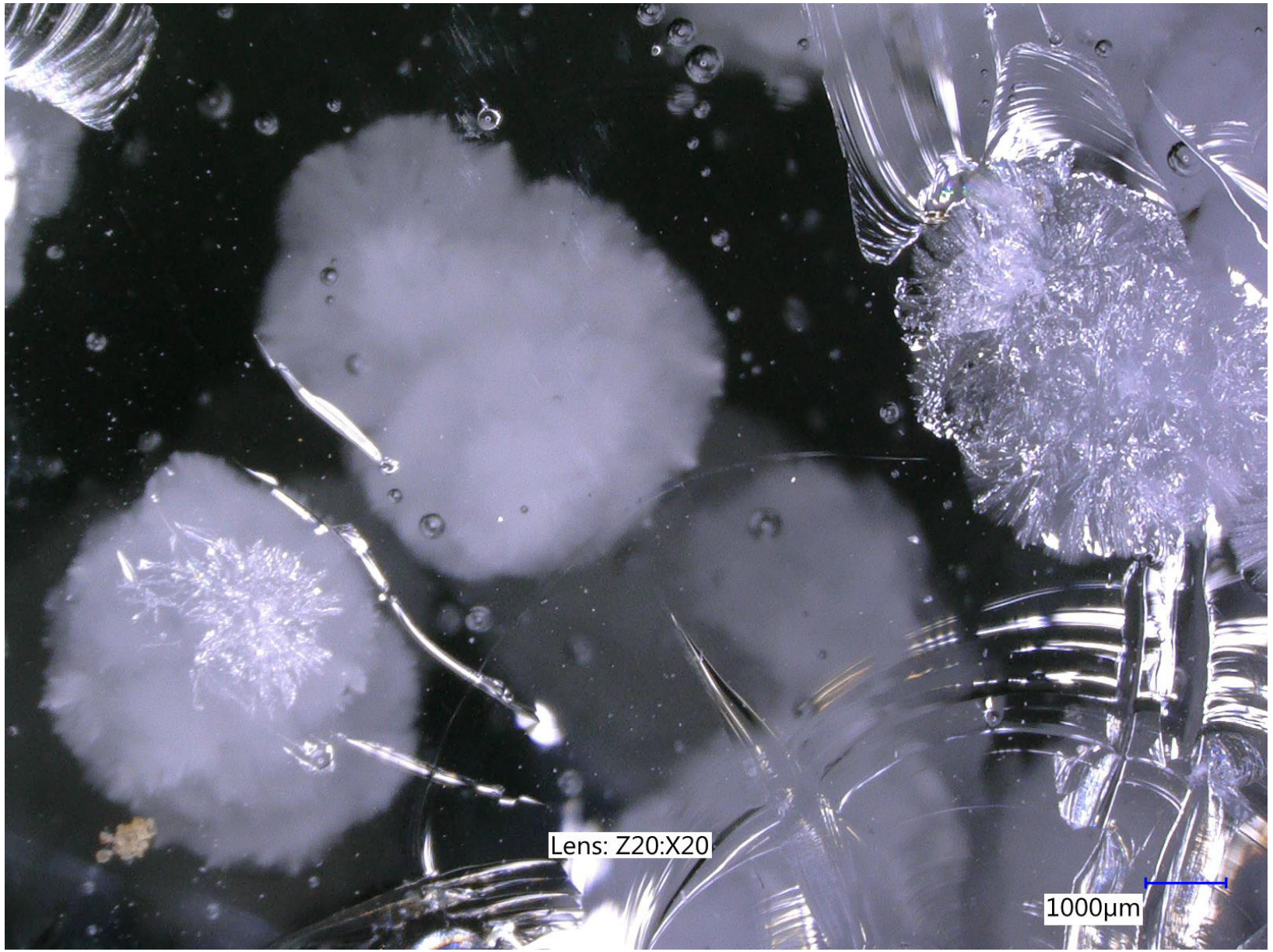

Figure F26 - sample 4B - Different cracking patterns of crystalline and glassy phase

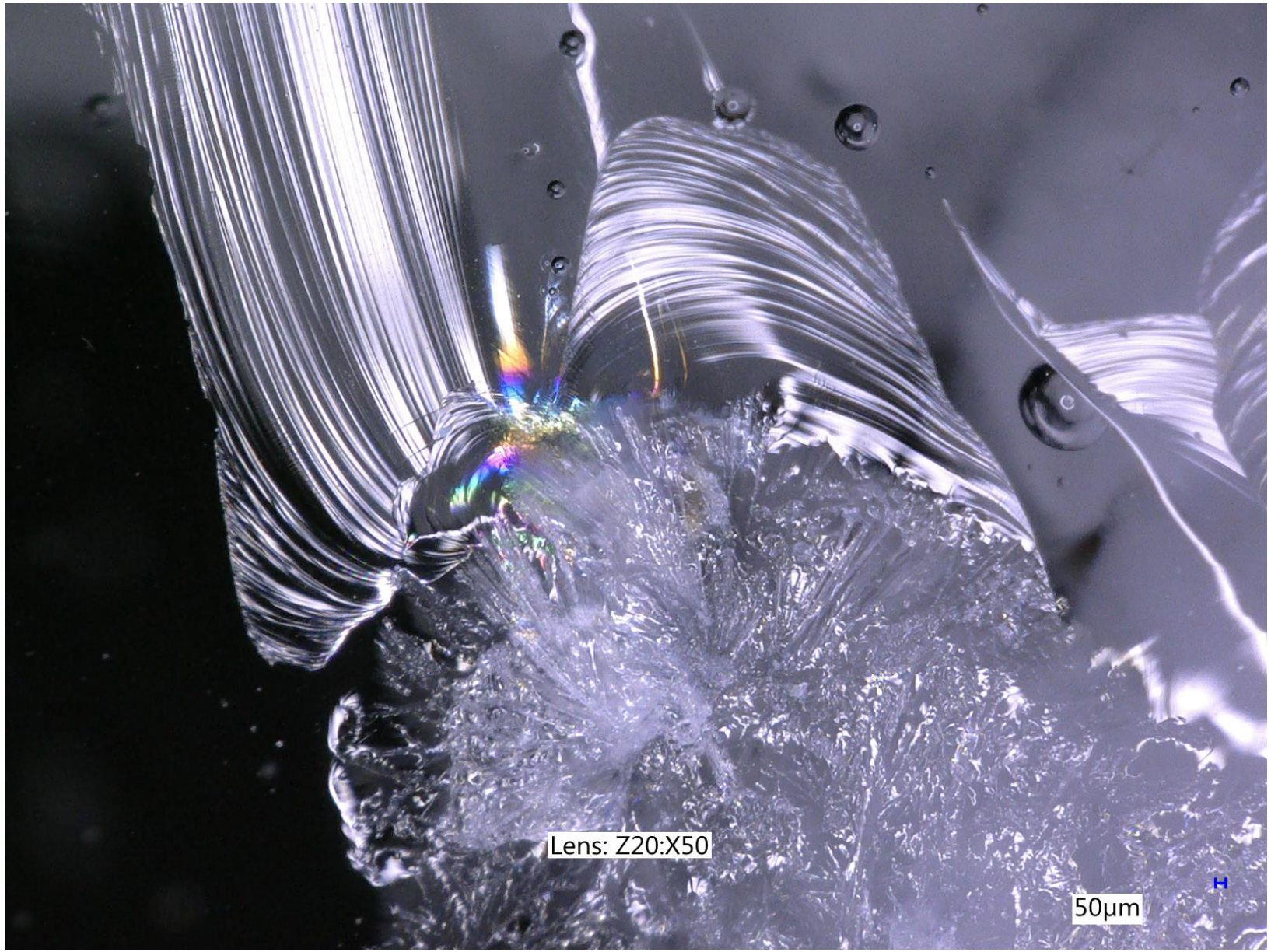

Figure F27 - sample 4B - Different cracking patterns of crystalline and glassy phase

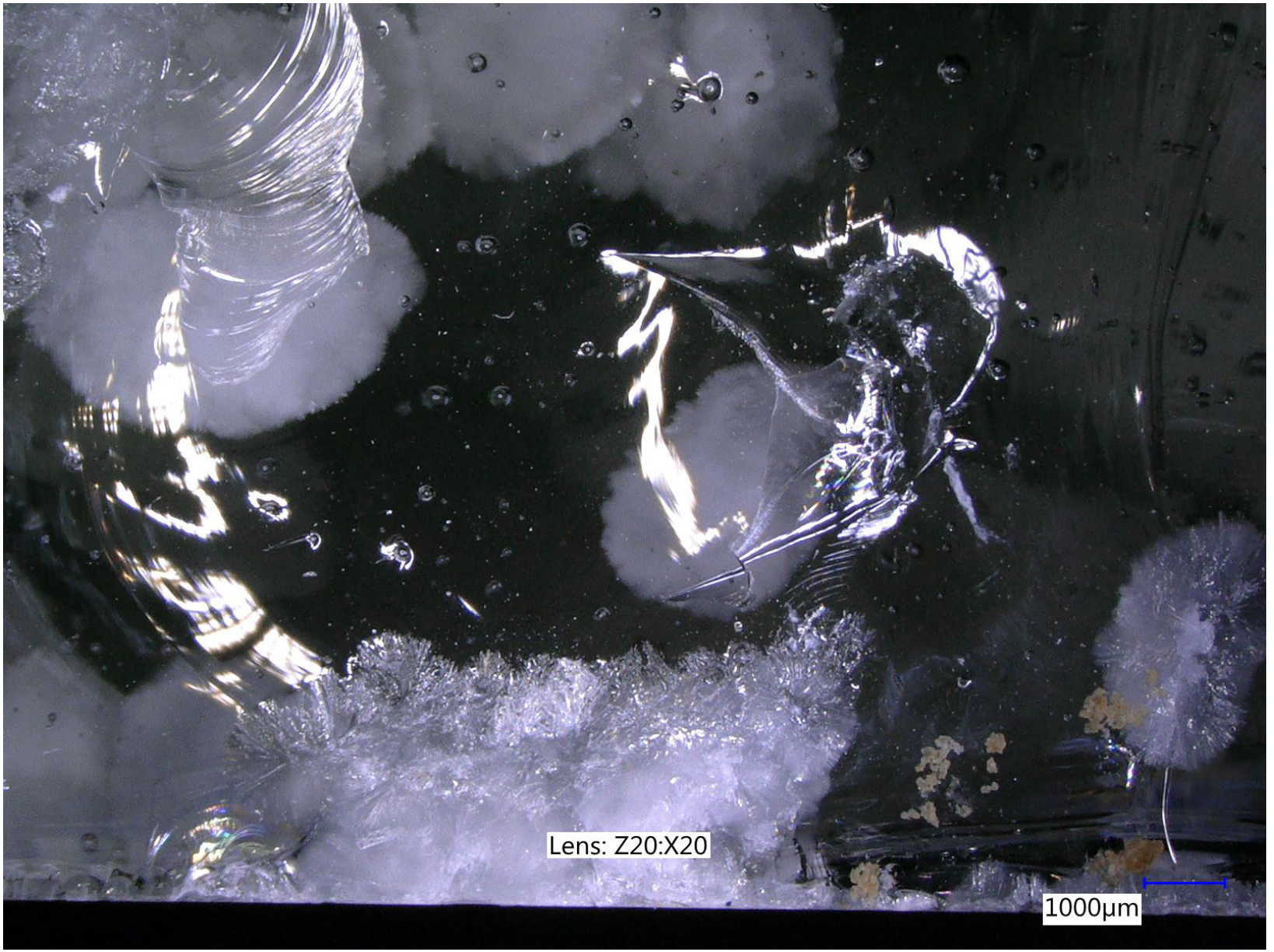

Figure F28 - sample 4B - Different cracking patterns of crystalline and glassy phase

F.4. Microscopic pictures sample 5A

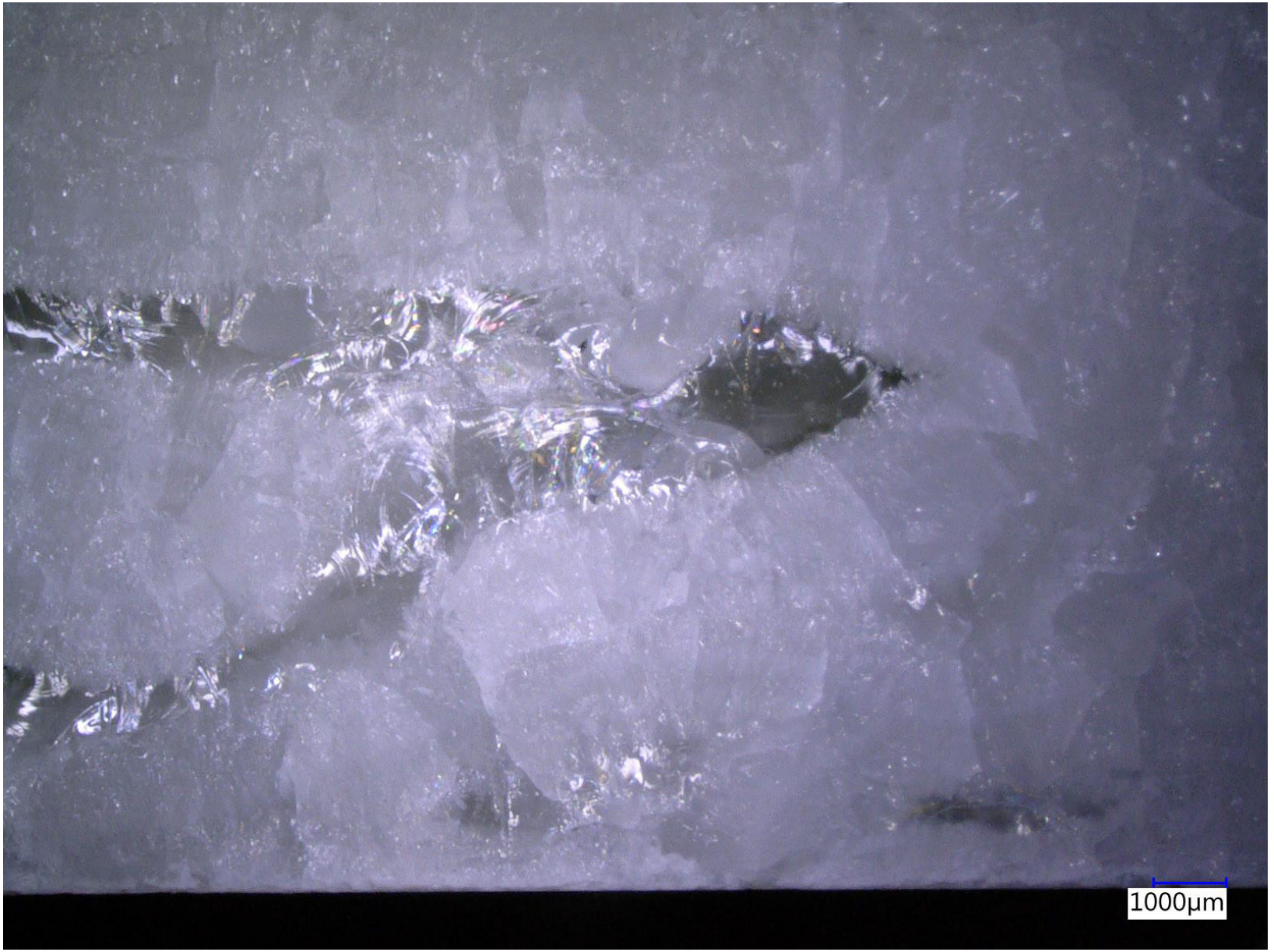

Figure F29 - sample 5A - Bottom edge

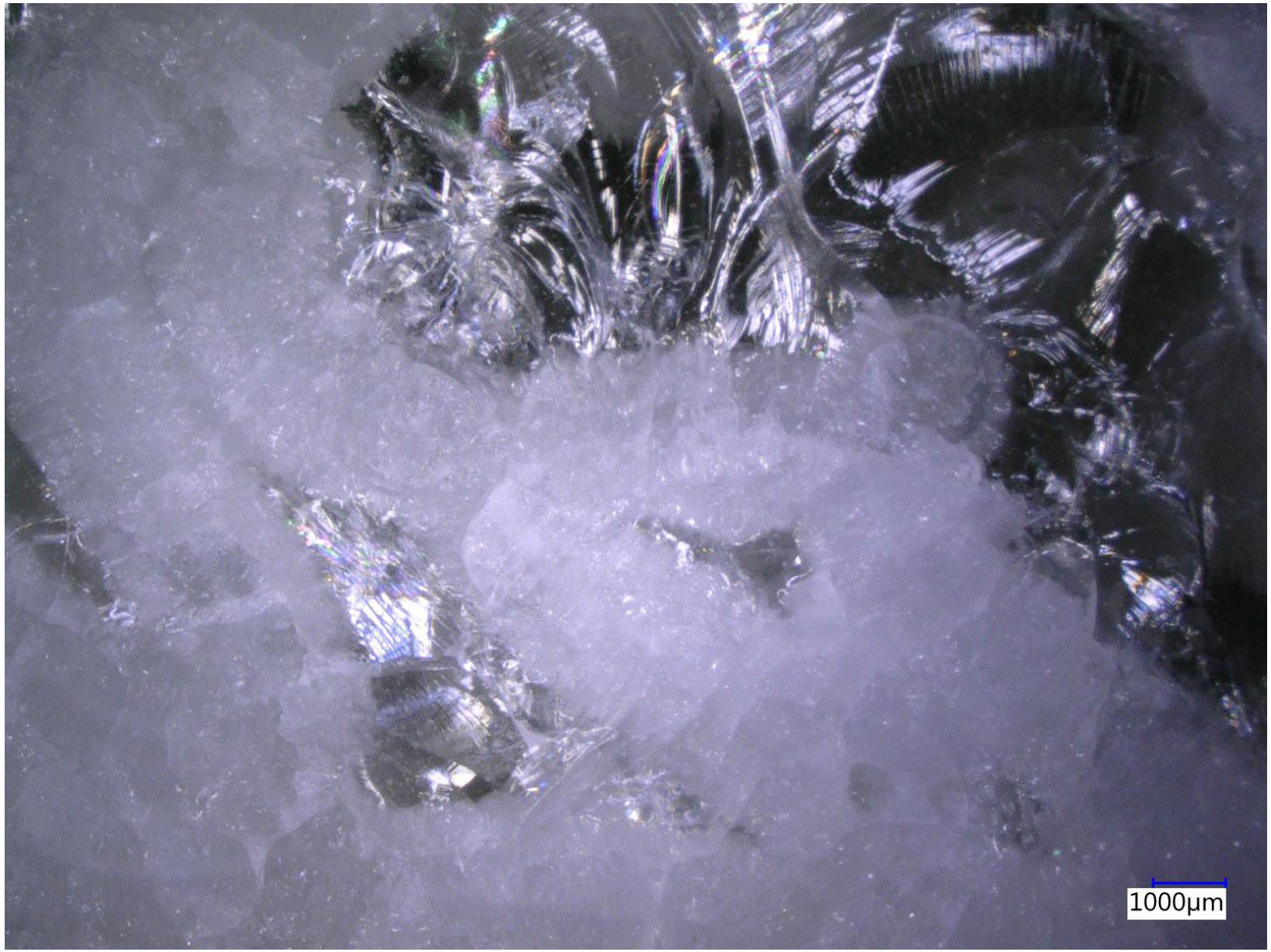

Figure F30 - sample 5A - Crystalline and glassy phase at the center

F.5. Microscopic pictures sample 5B

Figure F31 - sample 5B - Bottom left corner

Figure F32 - sample 5B - Center part

Figure F33 - sample 5B - Center part

F.6. Microscopic pictures sample 6A

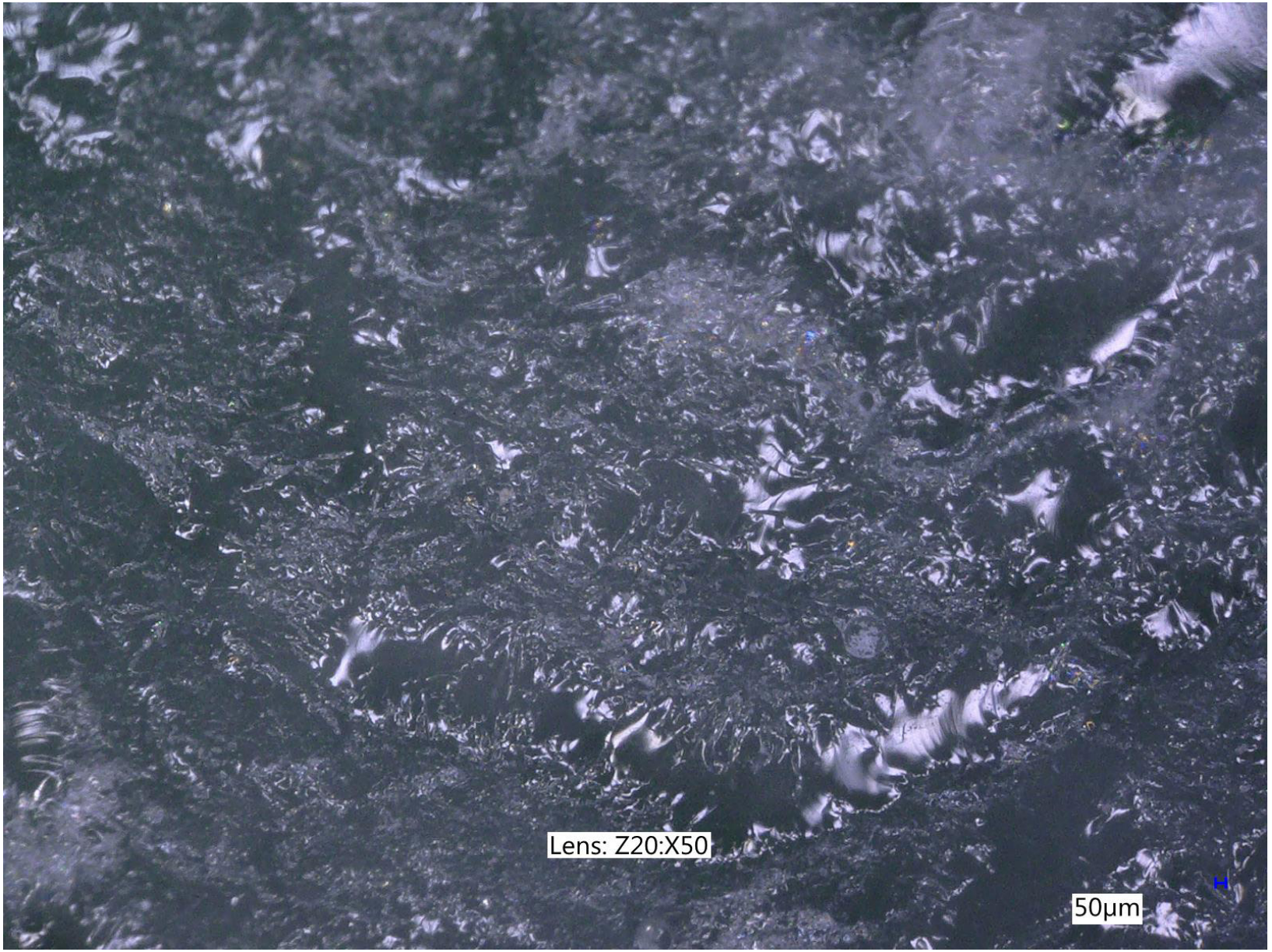

Figure F34 - sample 6A - Microscopic picture of broken corner

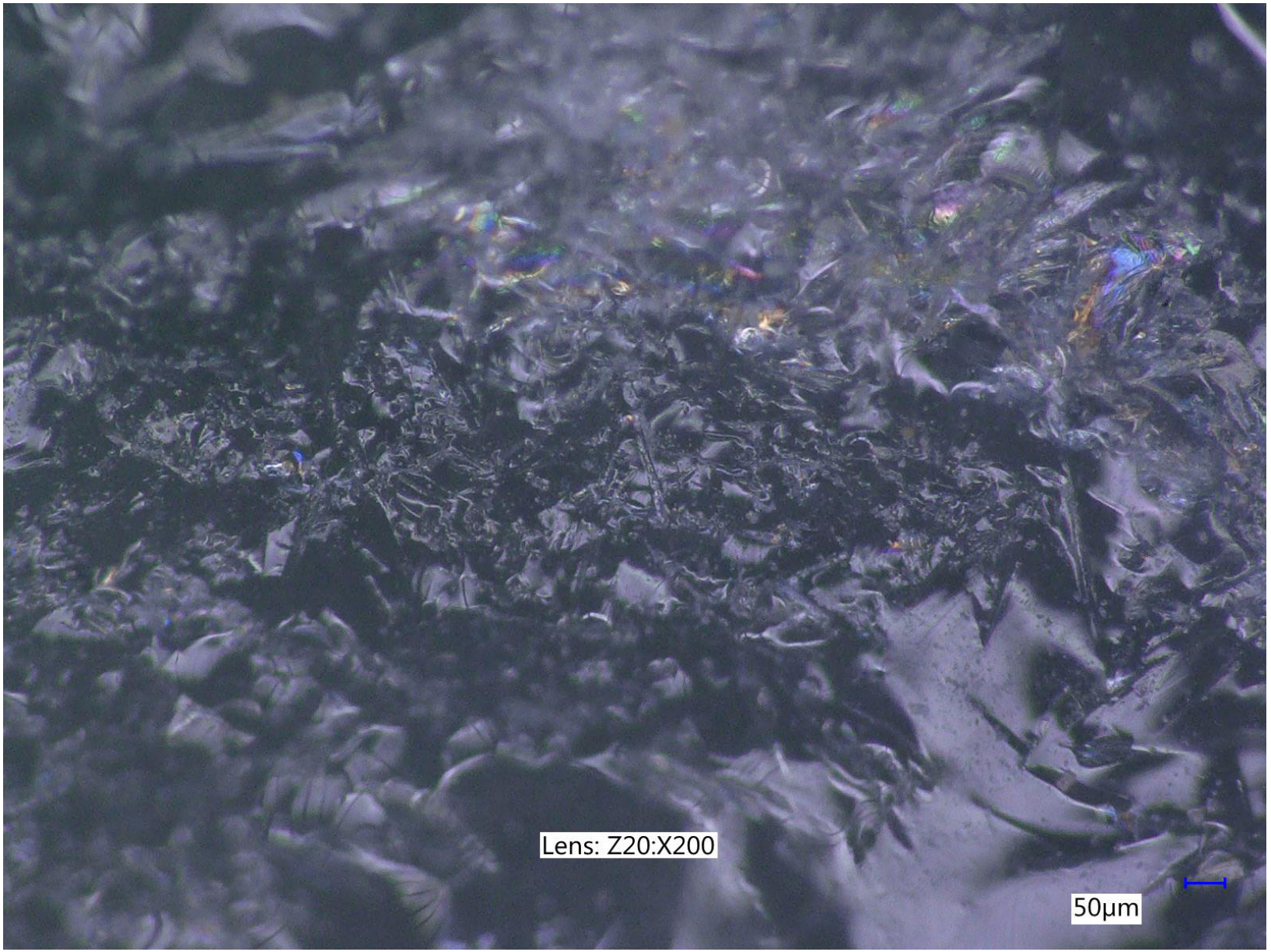

Figure F35 - sample 6A - Zoom of broken corner